

Antigenic variation of the malaria parasite counteracts the host immune system



Dissertation

with the aim to obtain a

Doctor rerum naturalium (Dr. rer. nat.)

of the Faculty of Mathematics, Informatics and Natural Sciences
Department of Biology, at the University of Hamburg

in collaboration with the Bernhard Nocht Institute for Tropical
Medicine (BNITM)

Submitted by

Yannick Daniel Höppner

Hamburg 2024

For visualization of the title image, the AI-based Microsoft image tool was used.

for my brother

Dissertationsgutachter: Prof. Tim-Wolf Gilberger
Prof. Ester Schnettler

Datum der Disputation: 29.11.2024

Eidesstattliche Versicherung:

Hiermit versichere ich, Yannick Daniel Höppner, an Eides statt, die vorliegende Dissertationsschrift selbst verfasst und keine anderen als die angegebenen Hilfsmittel und Quellen benutzt zu haben.

Sofern im Zuge der Erstellung der vorliegenden Dissertationsschrift generative Künstliche Intelligenz (gKI) basierte elektronische Hilfsmittel verwendet wurden, versichere ich, dass meine eigene Leistung im Vordergrund stand und dass eine vollständige Dokumentation aller verwendeten Hilfsmittel gemäß der Guten wissenschaftlichen Praxis vorliegt. Ich trage die Verantwortung für eventuell durch die gKI generierte fehlerhafte oder verzerrte Inhalte, fehlerhafte Referenzen, Verstöße gegen das Datenschutz- und Urheberrecht oder Plagiate.


Affidavit:

I, Yannick Daniel Höppner, hereby declare and affirm that this doctoral dissertation is my own work and that I have not used any aids and sources other than those indicated.

If electronic resources based on generative artificial intelligence (gAI) were used in the course of writing this dissertation, I confirm that my own work was the main and value-adding contribution and that complete documentation of all resources used is available in accordance with good scientific practice. I am responsible for any erroneous or distorted content, incorrect references, violations of data protection and copyright law or plagiarism that may have been generated by the gAI.

Hamburg, den 09.12.2024

Place, Date



Signature


Erklärung zur Abgabe der Dissertation

Ich, Yannick Daniel Höppner, versichere, dass dieses gebundene Exemplar der Dissertation und das in elektronischer Form eingereichte Dissertationsexemplar (über den Docata-Upload) sowie das bei der Fakultät (Studienbüro Biologie) zur Archivierung eingereichte gedruckte, gebundene Exemplar der Dissertationsschrift identisch sind.

I, Yannick Daniel Höppner, declare that this bound copy of the dissertation and the dissertation submitted in electronic form (via the Docata upload) and the printed bound copy the dissertation submitted to the faculty (Academic Office Biology) for archiving are identical.

Hamburg, den 09.12.2024

Place, Date



Signature

Acknowledgments

For this dissertation, there is a wide range of people to thank for who either directly or indirectly contributed to its completion. At first, I want to thank my supervisor Anna Bachmann who guided me through this project by providing an extensive and profound basic knowledge of the topic, was always available to answer questions and an empathetic boss who support people to reach their potential. I am very thankful to Heidrun von Thien who was always the greatest helping hand in the lab, a good mentor and great at given and receiving feedback. I always felt inspired by her being open about learning new concepts. Additionally, I am very thankful to Ralf and Thorsten who gave always great support for statistical and bioinformatic problems, which advanced the project enormously. A massive thank you also to the various study teams in Tübingen, Nijmegen and Lambaréné who did an excellent job conducting the study and providing the samples needed for the analysis and results presented here. Of course, the entire study would not have been successful without the volunteers in Gabon who decided to participate in the study and took a huge toll on being followed and monitored for such a long time and were willing to donate blood. Overall, the BNITM granted so many opportunities for which I will forever be grateful, e.g., a research trip to Madagascar or a conference meeting in Australia. Finally, I also want to thank Tim Gilberger who supervised my thesis and who I really appreciate for his critical eye.

Next, I also want to thank my colleagues who I initially met during the COVID-19 pandemic but still managed to develop great and strong friendships which I hope will be long lasting. I am so grateful for getting to know especially Barbara; who in my opinion is the most organized person I ever got to know and could always help with everything, Lenni; who is one of the kindest persons I ever met and for whom I wish that more people like him will shape the future of science, Clarissa; who was my “BNITM Bavarian”, Pilar; who I appreciate for always having time for coffee, handing out gifts to everyone and being just such a nice person to spend time with; Sheila, who is a great friend and from whom I learned to take life even less seriously, and finally Izzy who taught me to be a better scientist and who is a great role model for the next generation of researchers.

I also want to thank my family and friends, who supported me and without them I would have never been able to write this thesis. My dad, who laid the financial ground for me to be able to study and explore my talents. My mum who never put pressure on me and always gave the best advice to further develop and shape my plans or ideas for building my life. My brother who is likely the better scientist and without his help I would have already given up on science after the Bachelor. Furthermore, I admire my friend Marie for her critics, valuable input and loyalty and my friend Franzi who I know since before kindergarten and who still is my best friend on earth. Both of you always challenged me to never lose sight on other important, non-science related topics of life. Eventually, I want to thank my partner Jan, who I could always rely on in times of crisis and success, who is my source of energy and I admire for his ability to rationalize and providing a fresh perspective. Thank you all!

1. INTRODUCTION	10
1.1 MALARIA	10
1.1.1 Epidemiology and life cycle.....	10
1.1.2 Pathology of malaria	11
1.1.3 Vaccine and treatment strategies.....	13
1.2 ASYMPTOMATIC MALARIA	14
1.2.1 The role of asymptomatic malaria in transmission	14
1.2.2 Protection from disease via cross-reactive semi-immunity	15
1.3 IMMUNE EVASION.....	18
1.3.1 Var multicopy gene family	18
1.3.2 Sequestration	21
1.3.3 Immune evasion via other VSAs (STEVARs and RIFINs)	23
1.4 REGULATION OF VAR GENE EXPRESSION	24
1.5 CHMI STUDIES AS A TOOL FOR IN-DEPTH ANALYSIS OF VAR GENE EXPRESSION	27
1.6 AIM OF THE THESIS	31
2. MATERIAL AND METHODS.....	32
2.1 MATERIAL.....	32
2.1.1 Chemicals and reagents	32
2.1.2 Human blood and serum	33
2.1.3 Media.....	33
2.1.4 Buffers and Solutions	33
2.1.5 Enzymes and antibodies	34
2.1.6 DNA standards	34
2.1.7 Kits	34
2.1.8 Cell lines	34
2.1.9 Oligonucleotides for PCRs	34
2.1.10 Technical equipment and devices.....	35
2.1.11 Labware and disposables.....	36
2.1.12 Software, input files and databases.....	36
2.2 METHODS.....	37
2.2.1 Routine cell culture for NF54/7G8: Sanaria's master cell bank parasites	37
2.2.2 Synchronization of NF54/7G8: Sanaria's master cell bank parasites with D-Sorbitol.....	38
2.2.3 Controlled invasion of NF54/7G8: Sanaria's master cell bank parasites with Percoll	38
2.2.4 Inclusion criteria, samples processing and parasitemia quantification of ex vivo blood samples	39
2.2.5 Isolation of <i>P. falciparum</i> RNA	40
2.2.6 Control qPCR for residual genomic DNA in <i>P. falciparum</i> RNA samples.....	41
2.2.7 DNA digestion in solution	42
2.2.8 Determination of the specificity, efficiency and dynamic range of the var-qPCR.....	42
2.2.9 cDNA synthesis.....	42
2.2.10 var gene RT-qPCR for samples with an NF54 and 7G8 genotype.....	43
2.2.11 Sample inclusion criteria for var gene analysis following RT-qPCR.....	48
2.2.12 Genomic DNA isolation from <i>P. falciparum</i>	48
2.2.13 Genotyping	49
2.2.14 Luminex Assay	53
2.2.15 Processing of RNA-seq samples and bioinformatic analysis.....	55
2.2.16 DBL α -tag PCR for samples with a natural infection genotype	59
2.2.17 Purification of DBL α -tag RT-PCR products	61
2.2.18 Sequencing of DBL α -tag products.....	61

2.2.19 Bioinformatic processing and prediction of DBL α -tag	61
2.2.20 Visualization and statistical analysis of various datasets.....	62
3. RESULTS.....	64
3.1 OBJECTIVE AND SAMPLING OF THE LACHMI-002 LONGITUDINAL CLINICAL TRIAL	64
3.2 ANALYSIS OF VAR GENE PROFILES OF 7G8 PARASITES FROM LIFELONG-EXPOSED INDIVIDUALS.....	67
3.3 CLASSIFICATION OF VOLUNTEERS ACCORDING TO THEIR DEGREE OF SEMI-IMMUNITY INTO NON- CONTROLLERS AND CONTROLLERS.....	69
3.4 DEGREE OF SEMI-IMMUNITY AFFECTS THE VAR GENE EXPRESSION PATTERN	72
3.5 CHARACTERIZATION OF THE 1 ST PARASITIC WAVE.....	74
3.6 LONGITUDINAL ASSESSMENT OF PARASITEMIA AND INFECTION DURATION.....	76
3.7 LONGITUDINAL VAR GENE EXPRESSION PATTERN.....	78
3.7.1 Tracking of var gene entropy and anti-PfEMP1 immunity over time.....	78
3.7.2 Antigenic variation of the malaria parasite <i>P. falciparum</i>	80
3.8 CHARACTERIZATION OF PARASITES EXPRESSING C-TYPE VAR GENES	84
3.9 LONGITUDINAL ANALYSIS OF NATURALLY OCCURRING <i>P. FALCIPARUM</i> INFECTIONS (MOSQUITO BITE INFECTIONS)	92
3.9.1 Sample cohort characterization.....	92
3.9.2 Antigenic variation in naturally occurring <i>P. falciparum</i> infections.....	94
4. DISCUSSION.....	97
5. OUTLOOK.....	108
6. CONCLUSION.....	109
7. REFERENCES.....	110
8. PUBLICATION LIST AND CONFERENCES.....	126
9. SUPPLEMENTARY DATA.....	127

Malaria is one of the most infectious and deadliest infections disease worldwide. Human malaria is caused by unicellular, apicomplexan parasites of the genus *Plasmodium*, with *Plasmodium falciparum* being responsible for most lethal cases especially affecting children under the age of five. The pathogenesis of malaria is related to the expression of a highly polymorphic gene family known as *var*, which encodes the major variant surface antigen (VSA) *Plasmodium falciparum* erythrocyte membrane protein 1 (PfEMP1). With increasing age and exposure, people in endemic regions acquire immunity that leads to asymptomatic infections with chronic courses. These infections, which span periods of a few months up to several years, therefore represent the largest parasite reservoir for maintaining transmission. Long lasting infections are characterized by periodic peaks and troughs in peripheral parasitemia, thought to be caused by antigenic variation of the parasite's PfEMP1 surface expression, although this hypothesis has never been demonstrated in human infections. Thus, the main aims of this thesis are to a) accurately characterize the longitudinal infection dynamics of asymptomatic individuals with varying degrees of pre-acquired semi-immunity, b) evaluate the expression of the *P. falciparum* antigen repertoire during the course of human infections, and c) to correlate the occurrence of PfEMP1-specific antibodies with the change in *var* gene expression.

For this, we analyzed parasite gene expression in samples from a controlled human malaria infections (CHMI) study with 56 life-long malaria exposed Gabonese adults. We correlated a delayed onset of blood-stage infection with a less diverse *var* gene expression pattern, a lower peak parasitemia, a shorter duration of infection and a greater breadth of PfEMP1 sero-recognition in a group of volunteers termed 'controller'. With exception of the first wave of parasitemia at the infection onset in volunteers with limited immunity, in which parasites display a highly diverse *var* expression pattern consisting of subtelomeric located group B and severity-associated group A genes, we provide evidence that successive peaks of parasitemia are caused by parasites expressing distinct *var* gene variants. With increasing duration of infection and immunity, parasites from all longitudinally tracked volunteers show an expression shift towards a more homogenous expression of single variants and this pattern is dominated by *var* genes of the group B/C and C located in central regions of the parasite chromosomes. Preliminary data link the absence of expression of certain *var* genes with increased recognition of the encoded PfEMP1 by antibodies that were either pre-existing or gained during infection. Transcriptomic data from samples exhibiting a dominant C-type *var* expression indicate a higher proportion of circulating schizonts possibly as a consequence of weaker cytoadhesion. Simultaneously, *rif* genes, coding for another VSA family involved in immune evasion by targeting immune inhibitory receptors, were shown to be down-regulated in *var* C-type expressing parasites further suggesting a potential loss of parasite virulence over the course of infection.

With this *in vivo* study, we provide for the first-time mechanistic insights into the gradual exhaustion of the *var* gene repertoire over the course of *P. falciparum* infections, most likely driven by an increase of PfEMP1-specific antibodies. Parasitemia is dropping with increasing length of infection and rising strain-specific immunity, and parasites seem to be less adhesive by expressing C-type *var* and lower levels of *rif* genes. Overall, this suggest that chronicity of malaria is orchestrated by parasite and host specific factors mutually influencing each other over time.

Malaria ist eine der ansteckendsten und tödlichsten Infektionskrankheiten weltweit. Malaria beim Menschen wird durch einzellige Parasiten der Gattung *Plasmodium* verursacht, wobei *Plasmodium falciparum* für die meisten tödlichen Fälle verantwortlich ist, von denen vor allem junge Kinder unter fünf Jahren betroffen sind. Die Pathogenese der Malaria hängt mit der Expression einer stark polymorphen Genfamilie zusammen, die als *var* bezeichnet wird und die für das wichtigste Oberflächenantigen *Plasmodium falciparum* erythrocyte membrane protein 1 (PfEMP1) kodiert. Mit zunehmendem Alter und Exposition wird eine Immunität erworben, die zu mehr asymptomatischen und chronischen Infektionen führt. Diese Infektionen können sich über einen Zeitraum von einigen Monaten bis zu mehreren Jahren erstrecken und stellen damit das größte Reservoir an Parasiten dar, durch das die Übertragung der Erkrankung aufrecht erhalten bleibt. Diese chronischen Infektionen sind durch periodische Schwankungen in der peripheren Parasitämie gekennzeichnet, die vermutlich auf einer Antigenvariation von PfEMP1 beruhen, welche jedoch bei Infektionen im Menschen bisher nie bestätigt werden konnte. Die Hauptziele dieser Arbeit sind daher die Analyse a) der longitudinalen Infektionsdynamik asymptomatische infizierter Individuen mit verschiedenen Graden von Semi-Immunität, b) der longitudinalen Expression des Antigen Repertoires von *P. falciparum* Parasiten und c) das Auftreten von PfEMP1-spezifischer Immunität mit der *var*-Gen-Expression zu korrelieren.

Zu diesem Zweck analysierten wir Proben aus einer longitudinalen Studie mit 56 lebenslang exponierten Erwachsenen aus Gabun die freiwillig kontrollierten experimentellen Malaria-Infektionen am Menschen (CHMI) unterzogen wurden. Wir korrelierten einen verzögerten Beginn der Infektion im Blutstadium mit einem weniger vielfältigen *var*-Gen-Expressionsmuster, einer geringeren Spitzenparasitämie, einer kürzeren Infektionsdauer und einer stärkeren und breiten Erkennung von PfEMP1-spezifischen Antikörper im Serum einer Gruppe von Freiwilligen, die wir als "Controller" bezeichneten. Mit Ausnahme der ersten Welle der Parasitämie zu Beginn der Infektion bei Probanden mit begrenzter Immunität, bei der die Parasiten ein sehr vielfältiges *var*-Gen-Expressionsmuster aufweisen, das aus subtelomerisch lokalisierten Genen der Gruppe B und der mit dem Schweregrad assoziierten Gruppe A besteht, haben wir den Nachweis erbracht, dass die aufeinanderfolgenden Parasitämiewellen durch Parasiten verursacht werden, die unterschiedliche *var*-Gen Varianten exprimieren. Mit zunehmender Dauer der Infektion und Immunität zeigen die Parasiten aller Probanden eine Verschiebung der Expression hin zu einer homogenen Expression einzelner Varianten, wobei dieses Muster von *var*-Genen der Gruppe B/C und C dominiert wird die in zentralen Regionen der Chromosomen zu finden sind. Vorläufige Daten bringen das Fehlen der Expression bestimmter *var*-Gene mit einer erhöhten Erkennung des kodierten PfEMP1 durch Antikörper in Verbindung, die entweder bereits vorhanden waren oder während der Infektion erworben wurden. Die Sequenzierung von Proben die eine dominante C-Typ Expression aufweisen, zeigte einen höheren Anteil an zirkulierenden Schizonten, möglicherweise als Folge einer schwächeren Zytoadhäsion der Parasiten im späteren Infektionsverlauf. Gleichzeitig zeigte sich, dass die Expression von *rif*-Genen, einer weiteren Familie von variablen Oberflächenantigenen (VSA), die an der Antigenvariation und der Immunevasion beteiligt sind, bei Parasiten, die den C-Typ exprimieren, geringer ist, was auf einen möglichen Verlust an Virulenz der Parasiten im Laufe der Zeit schließen lässt.

Mit dieser *in-vivo* Studie beschreiben wir zum ersten Mal wie die longitudinale Immunevasion bei chronisch infizierten Malaria Fällen abläuft. Wir zeigen, dass es eine allmähliche Erschöpfung des *var*-Gen-Repertoires über verschiedene Parasitenwellen hinweg stattfindet die gleichzeitig durch eine Zunahme von anti-PfEMP1 Antikörpern begleitet wird. Mit zunehmender Dauer der Infektion und Immunität exprimieren die Parasiten weniger *rif* und mehr C-Typ *Var*-Gene und verlieren graduell ihre Fähigkeit zu Adhärenzen was darauf hindeutet, dass chronischer Malaria durch Parasiten- und wirtsspezifische Faktoren gesteuert wird, die sich im Laufe der Zeit gegenseitig beeinflussen.

Figures:

Figure 1.: Incidence of malaria in 2021 and life cycle of <i>P. falciparum</i> parasites.....	11
Figure 2.: Age distribution of <i>P. falciparum</i> cases.....	15
Figure 3 Longitudinal infection dynamics and hypothesized antigenic variation in individuals infected with <i>P. falciparum</i> parasites.	18
Figure 4.: Features of the <i>var</i> multicopy gene family and their encoded PfEMP1 proteins.	19
Figure 5.: Sequestration of <i>P. falciparum</i> iRBCs impacts pathogenesis.	22
Figure 6.: Immune evasion of iRBCs via RIFINs and STEVORs.....	24
Figure 7.: Regulation of (mutually exclusive) <i>var</i> gene expression.	27
Figure 8.: <i>Var</i> gene expression by NF54 and 7G8 parasites in vitro and in vivo.....	29
Figure 9.: LaCHMI-002 (L2) study scheme and sampling strategy.	66
Figure 10.: Infectivity and <i>var</i> gene expression analysis of 7G8 parasites.	68
Figure 11.: Establishment of infections with <i>P. falciparum</i> parasites in naïve and life-long malaria exposed individuals.....	71
Figure 12.: The degree of PfEMP1 specific semi-immunity at baseline anti-correlates with the parasite's <i>var</i> expression.	73
Figure 13.: Characterization of the first parasitemia peak of <i>P. falciparum</i> infections.....	75
Figure 14.: Longitudinal tracking of infections in volunteers classified as non-controllers and controllers.....	77
Figure 15.: Longitudinal expressed <i>var</i> gene pattern and entropy is counteracted by acquired PfEMP1-specific immunity for non-controller and controller.....	79
Figure 16.: Antigenic variation is counteracted by the immune system.	81
Figure 17.: Increase of C-type expression is linked to infection length.....	84
Figure 18.: Transcriptomic-based staging of samples from early and late infection stages.	86
Figure 19.: GO-term analysis for significantly upregulated genes in late infection stages.....	88
Figure 20.: GO-term analysis for significantly upregulated genes in late infection stages.....	89
Figure 21.: Expression of <i>rif</i> genes depending on the phase of infection and <i>var</i> gene expression.....	91
Figure 22.: Samples overview of the 'natural infection study' within L2 study.....	93
Figure 23.: Naturally occurring mosquito bite infections are subordinated to seasonal precipitation.	94
Figure 24.: Longitudinal <i>var</i> gene expression pattern in parasites isolated from volunteers infected with local parasite strains.....	95

Supplementary Figures:

Supplementary Figure 1.: Control variables and extended data for the CHMI studies, the Luminex, and RT-qPCR assays.	128
Supplementary Figure 2.: <i>Var</i> gene specific RT-qPCR results for infections with NF54 parasites and naturally occurring infections.	129
Supplementary Figure 3.: Longitudinal <i>var</i> gene expression in regards to the parasitemia for controllers.....	134
Supplementary Figure 4.: Longitudinal <i>var</i> gene expression in regards to the parasitemia for non-controllers.....	139
Supplementary Figure 5.: Overlap of <i>var</i> gene variants expressed >1% by parasites from malaria-naïves, non-controllers and controllers at the 1 st parasitemia peak.	140
Supplementary Figure 6.: Validation of RNA-seq and RT-qPCR expression data.	141
Supplementary Figure 7.: Tapestation electropherograms for RNA samples.	147
Supplementary Figure 8.: R-scripted pipeline for the analysis of in vivo <i>P.falciparum</i> transcriptomics data (Tonkin-Hill et al. 2018).	162
Supplementary Figure 9.: Longitudinal <i>var</i> gene expression pattern of parasites isolated from volunteer infections with locally circulating parasite strains.	163

Tables:

Table 1.: qPCR pipetting scheme gDNA check.	41
Table 2.: (RT-)qPCR cycling for gDNA check and var gene RT-qPCR.	41
Table 3.: RNA template input for cDNA synthesis based on parasitemia of the RBC samples as a proxy for <i>P. falciparum</i> RNA content.	43
Table 4.: cDNA synthesis: Annealing, cDNA synthesis and enzyme inactivation program.	43
Table 5.: RT-qPCR pipetting scheme.	44
Table 6.: NF54 var gene RT-qPCR primer set.	44
Table 7.: 7G8 var gene RT-qPCR Primer Set.	46
Table 8.: Additional RT-qPCR primer sets (ring stage controls, housekeeping genes).	48
Table 9.: MSP1 genotyping: Pipetting scheme for the outer PCR to amplify the <i>msh1</i> gene locus.	49
Table 10.: MSP1 genotyping: PCR cycling of the outer PCR.	50
Table 11.: Genotyping; (nested)-inner PCRs for amplification of MSP1 alleles K1, RO33 and Mad20.	50
Table 12.: Genotyping;(nested)-inner PCR protocol.	50
Table 13.: MSP1 genotyping results of the 37 gDNA samples from LaCHMI-2 trial.	51
Table 14.: Overview of PfEMP1 domains and control proteins tested with plex10 and plex11 in the Luminex assays.	54
Table 15.: Quality measurements for samples analyzed by RNA-seq.	57
Table 16.: DBL α -tag PCR mix.	60
Table 17.: DBL α -tag PCR protocol.	60
Table 18.: Sample overview for RNA-seq.	85
Table 19.: List of upregulated genes in NF54 parasites from late infection stages ('C-type waves').	87
Table 20.: List of downregulated genes by NF54 parasites from late infection stages ('C-type waves').	89

Supplementary tables:

Supplementary Table 1.: Volunteers overview for the previously performed trials and Tübingen and Gabon (TüCHMI and LaCHMI-001) as well as for L2.	127
--	-----

Formulars:

Formular 1.: Calculation formular to determine the RELTEXP as the $\Delta\Delta C_t$ values*10,000 according to Pfaffl 2004.	48
Formular 2.: Calculation of the Shannon-index.	63

Abbreviations

3D7	3 rd dilution, 7 th clone
7G8	7 th dilution, 8 th clone
°C	celcius
μL/μg/μM	microliter/microgram/micromolar
ACT	artemisinin combined therapy
AL	artemether-lumefantrine
AMA1	apical membrane antigen 1
AQ	amodiaquine
AS	artesunate
arinyl-tRNA	arginyl-tRNA-synthetase
ASC	antibody secreting cells
AT	adenosine-thymine
ATS	acidic terminal sequence
BBB	blood brain barrier
BLAST	basic local alignment search tool
BNITM	Bernhard-Nocht Institute for Tropical Medicine
bp	base-pair
BSA	control bovine serum albumin
C1q	complement component 1q
C _t	cycle treshold
CD36	cluster of differentiation 36
CD236	glycophorin B
CD235a	glycophorin A
CDC	center for disease control and prevention
cDNA	complementary desoxyribonucleic acid
CERMEL	Centre de Recherches Médicales de Lambaréné
CHMI	controlled human malaria infection
CIDR	cysteine-rich interdomain region
CLAG	cytoadherence linked asexual protein
CLK	cell division control like kinase 1
cRPMI	complete Roswell Park Memorial Institute
CRW-WPC	cysteine-proline-XX-tryptophan/ tryptophanproline-cysteine conserved motif
CSA	chondroitin sulfate
CSP	sporozoite antigen via the circumsporozoite protein
DAMP	damage associated molecular pattern
DBL	duffy-binding-like
DC5	domain cassette 5
DC8	domain cassette 8
DC13	domain cassette 13
DEG	differential expressed genes
DHA	dihydroartemisinin
dNTP	deoxynucleotide triphosphates
EBA-175	erythrocyte binding antigen 175
EPCR	endothelial cell protein C receptor
EST	expressed sequence tag
fbs/aldolase	fructose 1,6-bisphosphate aldolase
Fc	fragment crystallizable
FCR3	<i>falciparum</i> Colombia resistant clone 3
FC	fold change
g	gram
GalNAc	N-acetyl-D-galactosamine
GC	guanine-cytosine

Abbreviations

gC1qR	globular C1q-binding protein receptor
gDNA	genomic desoxyribonucleic acid
GlcA or GlcUA	D-glucuronic acid
GLURP	glutamate-rich protein
H2A/B	histone 2A/B
H2K4me3	trimethylation of histone 2 lysine 4
H3K9ac	acetylation of histone 3 lysine 9
H3K9me3	trimethylation of histone 3 lysine 9
H3K27ac	acetylation of histone 3 lysine 27
H3K36me3	trimethylation of histone 3 lysine 36
HB3	Honduras clone 3
HBV	<i>Hepatitis B</i> virus
HCV	<i>Hepatitis C</i> virus
HH	head-to-head
HIS	polyhistidine
HIV	human immunodeficiency virus
HLA	human leucocyte antigen
HP1	heterochromatin protein 1
hpi	hours post infection/invasion
HPLC	high-performance liquid chromatography
hr(s)	hour(s)
HRP2	histidine-rich protein 2
HT/TH	head-to-tail/tail-to-head
ICAM-1	intercellular adhesion molecule
IgG	immune globulin G
IL-6	interleukin 6
IL-10	interleukin 10
IQR	inter-quartile range
(i)RBC	(infected) red-blood cell
IRS	indoor residual spraying
IT4	Indochina-Thailand clone 4
ITM	Institute for Tropical Medicine Tübingen
K1	allele of K1 strain (Thailand)
KAPA	Kapa Biosystems high-fidelity DNA polymerase
KAHRP	knob-associated histidine-rich protein
kb	kilobase
kDa	kilo Dalton
KEGG	Kyoto Encyclopedia of Genes and Genomes
L1	LaCHMI-001
L2	LaCHMI-002
L	liter
LAIR1	leucocyte-associated immunoglobulin-like receptor 1
LILRB1	leucocyte immunoglobulin-like receptor B1
LLINs	long-lasting insecticidal nets
lnc	long non-coding
MAHRP	membrane-associated histidine-rich protein 1
Mad20	allele of Mad20 (Madagascar)
MAVACHE	malaria vaccine with high efficiency
MFI	mean fluorescence intensity
MFS	malaria freezing solution
mL	milliliter
mmol	millimol
MQ	mefloquine

Abbreviations

mRNA	RNA messenger ribonucleic acid
MSP1	merozoite surface protein 1
MTS	malaria thawing solution
NK	natural killer
NTS	N-terminal segment
NF54	Nijmegen falciparum 54
NCBI	national center for biotechnology information
NIMA	never in mitosis
NEK	NIMA-related protein kinases
NEB	new England biolabs
ng	nanogram
OD	optical density
PAM	partitioning around medoids
PAR-1	protease-activated receptor 1
PC	protein C
PE	paired-end
PECAM-1	platelet endothelial cell adhesion molecule-1
PEXEL	<i>Plasmodium</i> export element
pf	<i>Plasmodium falciparum</i> parasites
PfEMP1	<i>P. falciparum</i> erythrocyte membrane protein 1
<i>P. falciparum</i>	<i>Plasmodium falciparum</i>
<i>pfmc-2tm</i>	<i>P. falciparum</i> Maurer's clefts 2 transmembrane (gene)
PfMC-2TM	<i>P. falciparum</i> Maurer's clefts 2 transmembrane (protein)
Pfs25, 230, 48/45	<i>Plasmodium falciparum</i> sexual-stage surface proteins
PfSPZ	<i>Plasmodium falciparum</i> sporozoite challenge
PHIST	<i>Plasmodium</i> helical interspersed subtelomeric
<i>P. knowlesi</i>	<i>Plasmodium knowlesi</i>
PlasmoDB	<i>plasmodium</i> database
<i>P. malariae</i>	<i>Plasmodium malariae</i>
<i>P. ovale</i>	<i>Plasmodium ovale</i>
PPQ	piperaquine
<i>P. reichenowi</i>	<i>Plasmodium reichenowi</i>
PTEX	<i>Plasmodium</i> translocon of exported protein
<i>P. vivax</i>	<i>Plasmodium vivax</i>
PVM	parasitophorous vacuolar membrane
PY	pyronaridine
RELTEXP	relative transcript expression
<i>Rif</i>	repetitive interspersed family (gene)
RIFIN	repetitive interspersed family (protein)
RIN	RNA integrity number
RNA	ribonucleic acid
RNA-seq	ribonucleic acid sequencing
RO33	allele from RO-33 (Ghana)
RPM	reads per million mapped reads
RPKM	reads Per Kilobase per Million mapped reads
RT	room temperature
(RT-q)PCR	real-time quantitative polymerase chain reaction
RTS,S	repeat region-T-cell epitope (CSP), hepatitis B surface antigen (2x)
<i>sbp1</i>	<i>skeleton binding protein 1</i> (gene)
SBP1	<i>skeleton binding protein 1</i> (protein)
scRNA-seq	single cell ribonucleic acid sequencing
sec	second
SERA5	serine repeat antigen 5
SF9	spodoptera frugiperda 9 cell line

Abbreviations

<i>sirA</i>	<i>sir2a</i> histone deacetylase (gene)
<i>sirB</i>	<i>sir2b</i> histone deacetylase (gene)
SMS	single-many-single
STD	standard deviation
<i>Stevor</i>	<i>subtelomeric variable open reading frame</i> (gene)
STEVOR	subtelomeric variable open reading frame protein (protein)
<i>Surfin</i>	<i>surface-associated interspersed gene family</i> (gene)
SURFIN	surface-associated interspersed gene family protein (protein)
TBS	tick blood smear
T _m	melting temperature
TM	transmembrane
TM	thrombospondin
TNF- α	tumor necrosis factor α
TOPO	topoisomerase
TT	tail-to-tail
ubiE/COQ5	2-methoxy-6-polyprenyl-1,4-benzoquinol methylase, mitochondrial, putative
UKE	University hospital/clinic Eppendorf
ULG	upregulated in late gametocytes
uORF	untranslated short open reading frame
V	volt
<i>Var</i>	variable
VAR2CSA	variable protein 2 binding to chondroitin sulfate
VarDB	<i>var</i> database
VFR	visiting family and relatives
VSA	variant surface antigen
WBC	white blood cell
WD	tryptophan-asparagine (repeat containing domain)
WHO	World Health Organization

1. Introduction

1.1 Malaria

1.1.1 Epidemiology and life cycle

With about 249 million cases and more than 608,000 deaths in 2022, malaria ranks as one of the most infectious and deadliest diseases worldwide. From 2000–2019 incidence and mortality rates enduringly declined but stalled in the previous years (WHO, 2023). About 95 % of registered cases occur in malaria-endemic countries located in the tropical and subtropical areas of the world with warm and humid climate (Figure 1 A) (Poespoprodjo et al. 2023; WHO 2023). Malaria is transmitted by female *Anopheles* mosquitoes breeding in water resources in areas in close human proximity with the highest transmission rate found in rural areas (WHO 2023). Furthermore, malaria is considered a poverty-related disease since higher incidence and mortality rates are reported in countries of with low social-economic standards, political and social instability or countries highly affected by natural disasters and climate change (Rossati et al., 2016). Malaria in humans is caused by five *Plasmodium* (*P.*) species namely *P. falciparum*, *P. vivax*, *P. malariae*, *P. ovale* and *P. knowlesi*, with *P. falciparum* representing the deadliest and most virulent form (Garnham, 1981; Jeyaprakasam et al., 2020). *P. falciparum* infections are responsible for 99 % of malaria cases in the African region while in e.g., South America, the Middle East or South-East Asia, *P. falciparum* and *P. vivax* coexist (Poespoprodjo et al., 2023; WHO, 2023). All *Plasmodium* species belong to the phylum of Apicomplexa, the order of Haemosporidia and are closely related to other ape-infecting *Plasmodium* species of the Laveranian subgenus, e.g., *P. reichenowi* (Krief et al., 2010).

P. falciparum parasites have a complex life cycle, altering between mosquito and human hosts. After an infective mosquito bite, within the first five to six days of infection, sporozoites reach and mature in the liver before up to ten thousands hepatic merozoites per infective sporozoite eventually egress to the circulation (Prudêncio et al., 2006; Shears et al., 2020). These merozoites invade yet uninfected red blood cells (RBCs) and replicate asexually through ring, trophozoite and schizont stages, which ultimately give rise to up to 8–36 daughter merozoites capable to repeat the cycle (Figure 1 B, Cowman and Crabb 2006; Singh and Chitnis 2012). A small proportion of the parasites can leave this 48-hour-long asexual replication cycle and develop into gametocytes. In total, five different gametocyte stages are described, with stages 1–4 being sequestered in the bone marrow and only stage V being found in circulation (Hawking et al., 1971; Joice et al., 2014; Smalley et al., 1981). Female and male stage V gametocytes are eventually taken up by a mosquito during a blood meal and fertilize to form a zygote in the mosquito's midgut. Motile zygotes (ookinetes) can cross the midgut epithelium and transform into oocysts at the midgut basal lamina. Within oocysts sporozoites are formed asexually by multiple mitotic nuclear

divisions, which transit, after the rupture of the oocyst, to the salivary glands, and can be transmitted to the next human host in a subsequent blood meal (Figure 1 B, Boddey and Cowman 2013).

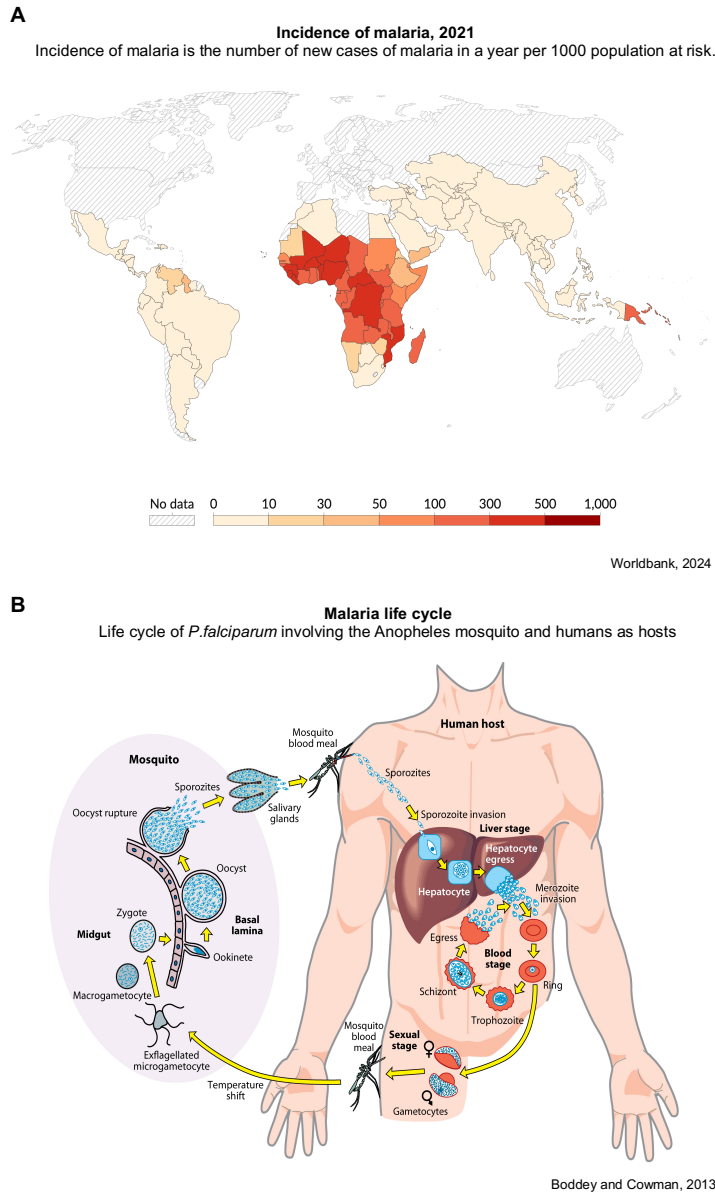


Figure 1.: Incidence of malaria in 2021 and life cycle of *P. falciparum* parasites.

A) World incidence map showing the number of new cases of human malaria (*P. falciparum*, *P. vivax*, *P. malariae*, *P. ovale* and *P. knowlesi*) in 2021 per 1,000 people at risk. Tropical and subtropical areas are strongly affected by malaria with 10–50 % of the population becoming newly infected each year with a strong focus on the African region. In South America, the Middle East and Asia a large proportion of cases is linked to infections with *P. vivax*, while infections in Africa are mainly caused by the deadliest agent causing malaria, *P. falciparum*. Color coding from light yellow to red indicate different levels of incidence. B) The life cycle of *P. falciparum* parasites: Female Anopheles mosquitoes transmit infective sporozoites from their salivary glands during blood meals to the human host. Within 5–6 days of infection, the sporozoites infect hepatocytes, multiply and egress from the liver by releasing thousands of hepatic merozoites from merosomes to the host's circulation. These merozoites can invade RBCs and mature within the RBC from ring, to trophozoite, and schizont stage. During the schizont stage the parasites undergo mitosis and form up to 36 daughter merozoites, which, after egress, invade yet uninfected RBCs and repeat the asexual replication cycle. A small proportion of parasites escape this cycle and mature to male and female gametocytes in the bone marrow. The last stage (stage V) is again released to the blood stream in order to be sucked up by another female Anopheles mosquito. In the mosquito's midgut the gametocytes are finally fertilized and form a motile zygote which penetrates the midgut wall and subsequently develops into an ookinete. The ookinete further matures into an oocyst which, after rupture, releases newly formed merozoites heading to the salivary glands to close the cycle.

1.1.2 Pathology of malaria

Epidemiological, geographic and biological factors highly correlate with the occurrence of incidence and mortality. In high transmission settings like Africa, malaria-related mortality is linked to severe malaria manifestations like cerebral malaria, severe anemia, acidosis or hyperlactemia (manifesting as deep breathing) mainly affecting children under the age of five with no or little previous exposure (Figure 2 A; Cunningham, A. J; Walther, M.; Riley 2013). In regions with lower transmission like South America or South East Asia, individuals remain susceptible to more severe disease outcomes until their adulthood presumably as they lose protective immunity acquired from earlier infections or remain close to an immunologically naïve state (Hidalgo et al., 2020). Moreover, various countries in which malaria

is non-endemic report symptomatic and even severe cases in malaria-naïve travelers or individuals visiting friends and relatives (VFRs) after their return from an endemic area (Kwak et al., 2021; Wichers et al., 2021). For example, Germany reported more than 800 symptomatic cases of imported *P. falciparum* cases in 2019, of which two cases had a fatal outcome despite a timely diagnosis and available treatment options (Falkenhorst et al., 2020).

Hallmarks of severe malaria manifestations like cerebral malaria, severe anemia and acidosis include impaired consciousness or coma, a low platelet count, thrombocytopenia and decreased plasma bicarbonate concentration, respectively (Brewster, Kwiatkowski, and White 1996; Cunnington, Riley, and Walther 2013; Idro, Jenkins, and Newton 2005). Clinical symptoms of malaria are related to the asexual blood replication cycle during which the parasite develops extensive amounts of biomass (Wiser, 2023). The occurrence of symptoms is linked to the direct interaction of infected RBCs (iRBCs) with endothelial cells and the lysis of the infected as well as not infected RBCs releasing or presenting parasite-specific metabolites or pathogen/damage-associated molecular pattern (PAMPs/DAMPs).

To interact with the endothelium, infected RBCs (iRBCs) sequester in the microvasculature in the lung, kidney, placenta and the brain, where they can cause congestion of RBCs perturbing tissue supply and induce an excessive pro-inflammatory cytokine production including e.g., tumor necrosis factor- α (TNF- α), interleukin-6 (IL-6) or IL-10. In the case of cerebral malaria, the induced cytokine storm can cause a interferon (IFN)- γ and perforin-mediated disruption of the blood brain barrier (BBB) (Avril et al., 2013; Coban et al., 2018; F. Duffy et al., 2019; Howland et al., 2013; Idro et al., 2005; Lennartz et al., 2015; Turner et al., 2013). Subsequently, disruption of the BBB can enhance the occurrence of microhemorrhages and brain swelling with both inducing immediate (e.g., coma) but also long-lasting neurological (e.g., neurological impairment) effects (Coughlan et al., 2024; Idro et al., 2005).

Despite possible episodes of previous exposures and acquired protection, pregnant women are another vulnerable group to severe disease since parasites are able to effectively occupy the placenta as a niche for proliferation (Sharma & Shukla, 2017). Pregnancy-associated malaria (PAM) is linked to parasites binding to chondroitin sulfate (CSA), which is highly enriched at the placenta during pregnancy (Fried et al., 2006). Thus, a large proportion of the parasite's biomass is relocated from the circulation to the placenta. CSA is a glycosaminoglycan composed of repeating disaccharide units of D-glucuronic acid (GlcA or GlcUA) linked to N-acetyl-D-galactosamine (GalNAc), which can, upon binding to iRBCs induce excessive immunopathologies involving the recruitment of e.g., macrophages, monocytes and cytotoxic T-cells to the intervillous space of the placenta, endanger both, the mother and the unborn child (Davison et al., 2006; Fried et al., 2006; Reeder et al., 1999; Sharma & Shukla, 2017). Consequently, PAM is linked to poor obstetrical outcomes including higher susceptibility for anemia and other infections in mothers, while higher rates of stillbirths, growth retardation, premature delivery and low birth weight is observed in fetuses (Menendez et al., 2000; Sharma & Shukla, 2017; Zakama et al., 2020).

During the asexual replication cycle, parasites continuously lyse a substantial amount of RBCs either directly when schizonts burst and release daughter merozoites or indirectly by presumably releasing

components that affect other, non-parasitized RBCs, leading to their phagocytosis and subsequent hemolysis (Kyeremeh et al., 2020). Excessive hemolysis of RBCs can contribute to severe anemia including very low levels of hemoglobin, fatigue and dizziness. In addition, hemolysis also enhances the likelihood of intermitted fever episodes of up to 41 °C (Gazzinelli et al., 2014). Respiratory distress and acidosis, another hallmarks of severe malaria, often coexists in individuals with (severe) anemia presumably as a consequence of perturbations in nutrient and gas exchange from and to the tissues (Cunnington, Bretscher, et al., 2013; Warimwe et al., 2012).

1.1.3 Vaccine and treatment strategies

Protection of individuals from infection and disease mostly relies on malaria prevention measures like long-lasting insecticidal nets (LLINs), indoor residual spraying (IRS) or vector control, e.g., via breeding site management to thereby reduce the number of infective mosquito bites (Nalinya et al., 2022; Unwin et al., 2023). Next to these preventive measures, the RTS,S subunit vaccine, which is based on the central repeat region (R) and a T-cell epitope (T) of the circumsporozoite protein (CSP) coupled to a viral surface protein (S), is currently rolled out in several African countries and is recommended by the WHO as a four-dose regimen for young infants aged 2–17 months (Laurens, 2019). Despite the limited efficacy of 17–36% against clinical or severe malaria, RTS,S represents the first WHO recommended antimalarial vaccine with the potential to protect in particular young children, who are mainly affected by severe disease courses. In addition, the low-dose CSP protein-based vaccine R21 with an estimated efficacy of about 75 % in children 5–17 months of age is currently tested in phase III clinical trials (Dattoo et al., 2021, 2022). Subunits of other proteins including AMA1, MSP1, EBA-175, VAR2CSA, targeting blood stages, and Pfs25, Pfs230, Pfs48/45, targeting transmission stages, have also been identified as potential vaccine candidates and are currently tested in clinical trials (Duffy and Patrick Gorres 2020). In addition to this, immunization regimens with either chemo-attenuated, irradiated or genetically modified whole sporozoite vaccines have been shown to allow a more complete immune-priming with more antigens being presented to the human host (Duffy and Patrick Gorres 2020; Minkah and Kappe 2021). Chemo-attenuated immunization, arrests parasites in their development at a certain life cycle stage (mostly during asymptomatic liver phase), were shown to protect from disease and to induce long-lasting sterile immunity *in vivo*, therefore representing potential future vaccine regimens (Favuzza et al., 2020; Mordmüller et al., 2017).

Several treatment strategies have been developed for already infected individuals. The currently used front-line drugs is a artemisinin combination therapy (ACT), combining anti-plasmodial features of short and long-lasting effects of artemisinin derivatives and other drugs, which interfere with different life cycle stages and metabolic pathways of the parasite (Arya et al., 2021; WHO, 2023). Commonly used combination therapies are artemether + lumefantrine (AL), artesunate + amodiaquine (AS + AQ), artesunate + sulfadoxine-pyrimethamine (AS + SP), artesunate + mefloquine (AS + MQ), artesunate + pyronaridine (AS + PY) or dihydroartemisinin + piperaquine (DHA + PPQ), which have replaced previous treatment regimens with chloroquine as they have shown to be less susceptible to induce

resistance (Arya et al., 2021; Ashley et al., 2018). Resistance, defined as a delay in clearance time after the drug administration, however, affects all antimalarials and is emerging in nearly all malaria endemic areas (Cui et al., 2015). The mechanism of action of most drugs are not yet fully understood and due to resistance, alternative drug targets have to be identified to reach the elimination and eradication aims of the WHO (WHO, 2023).

1.2 Asymptomatic malaria

1.2.1 The role of asymptomatic malaria in transmission

In high transmission settings such as Africa, especially children under the age of five with little or no pre-exposure are vulnerable to severe malaria (Figure 2; Cunnington, A. J; Walther, M.; Riley 2013). Previously acquired immunity was shown to allow protection from disease, but not necessarily from infection (Langhorne et al., 2008). Therefore, the recorded number for clinical and symptomatic cases are only the ‘tip of the iceberg’, since asymptomatic cases account for the majority of infections (Salgado et al., 2021). Individuals without severe malaria symptoms are frequently classified as asymptomatic or mild cases, although they may suffer, especially when long-term infected, from continuously low-grade hemolysis, intermitted symptomatic reoccurrences and can accumulate a large amount of parasite biomass in the spleen causing enlargement of the spleen, which can lead to hyper-reactive malarial splenomegaly syndrome (Chen et al., 2016; Elmakki, 2012). In such cases, symptomatic episodes are frequently short, non-fatal, or unspecific so that infections remain unnoticed and therefore untreated (Chen et al., 2016). Hence, long-term infections with temporal changes in symptoms refer to a chronic infection state in which the parasites can persist for a long period of several months to years (Ashley & White, 2014; Miller, 1994).

In malaria-endemic regions, chronic infections have been shown to span periods of up to 1.5 years, with 5–15-year-old, male schoolchildren representing the group with the longest duration of infection (Briggs et al., 2020). Similar infection durations were also reported in studies from non-endemic regions into which the malaria cases were imported (Ashley & White, 2014), or in historical studies with malaria-infected prisoners (Eyles, Young, 1951) or with individuals who underwent neurosyphilis treatment with a so-called ‘Malariotherapy’ (Bruce-Chwatt, 1963). Parasites from these chronically infected individuals represent the largest reservoir for the re-initiation of transmission (Figure 2; Langhorne et al. 2008). The ability to resume transmission is especially important, after periods of low vector abundance in the dry seasons (Andrade et al., 2020; Babiker et al., 1998; Langhorne et al., 2008; Miller, 1994; Tadesse et al., 2018). In dry seasons, nearly all infections are asymptomatic, leading to the hypothesis that *P. falciparum* might be able may sense and adopt to changes in its environment, with in turn has a direct impact on pathogenesis (Andrade et al., 2020; Portugal et al., 2017).

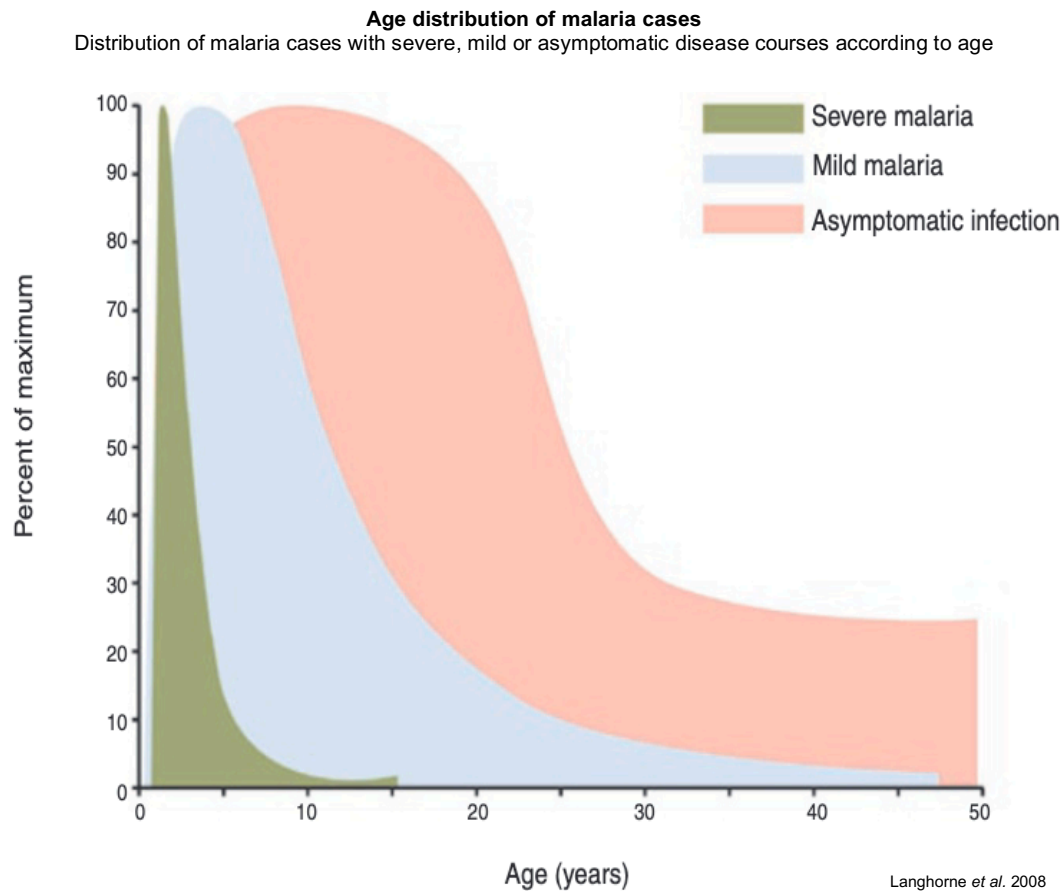


Figure 2.: Age distribution of *P. falciparum* cases.

A) Schematic illustrating the distribution of severe, mild and asymptomatic malaria infections according to age in endemic settings. Severe cases, presenting with cerebral malaria (CM), severe anemia (SA) or acidosis/hyperlactemia, are found in young age cohorts (under five years) and are fatal in 10 % of the cases. With increasing age and repeated exposure, the proportion of severe cases decreases due to the accumulation of cross-protective antibodies. Despite this, protection is incomplete meaning a large proportion of the population is chronically infected. In chronic infections, parasites persist unnoticed in the host for several months to years and can maintain transmission, which is especially important after periods of low vector abundance during the dry seasons. Even in older age cohorts, a large proportion of individuals remain constantly susceptible, most likely due to waning immunity, indicating that sterile immunity is rarely achieved.

1.2.2 Protection from disease via cross-reactive semi-immunity

Clinically silent or mildly symptomatic individuals acquired immunity from earlier infections and thus show an improved infection control by controlling parasitemia levels (Bachmann et al. 2019; Kapulu et al. 2022; Osier et al. 2008; Wichers et al. 2021). Blood stage immunity mainly relies on antibodies targeting variant surface antigens (VSAs) and invasion-related proteins like the apical membrane antigen 1 (AMA1) or the merozoite surface proteins (MSPs) (Chan et al. 2012; Kimingi et al. 2022; Rosenkranz et al. 2024).

VSAs are highly polymorphic protein families exhibiting diverse sequences and structures compared to other members of the same VSA family within the same or between strains (Babiker et al. 1998; Bouyou-Akotet, M'Bondoukwé, and Mawili-Mboumba 2015; Dzikowski and Deitsch 2009; Otto et al. 2019; Robert et al. 1996). *P. falciparum* possesses several VSA families including the major virulence

factor, the erythrocyte membrane protein 1 (PfEMP1) family, the repetitive interspersed (RIFIN) family, the subtelomeric variable open reading frame (STEVAR) family, the *P. falciparum* Maurer's clefts 2 transmembrane (PfMC-2TM) protein family and surface associated interspersed protein (SURFINs). Of these, the surface expressed erythrocyte membrane protein 1 (PfEMP1) was identified as the major target of host immunity (Chan et al. 2012). Higher levels of acquired immunity to PfEMP1, RIFIN and STEVAR have been associated with protection against severe disease since, and immunity to PfEMP1 variants linked to severity develops after relatively few infections (Turner et al., 2011, 2013, 2015). To protect the host, anti-VSA antibodies cause opsonization and agglutination of iRBC, preventing sequestration and rosetting and allowing more effective clearance of parasitized cells via monocytes, NK-cells or neutrophils (Aitken et al., 2020). Due to the polymorphic nature of PfEMP1s, the anti-PfEMP1 directed antibody response is thought to be mainly variant and strain-specific, but also provides some cross-protection in infections with heterologous parasite strains due to the recognition of common epitopes by IgG and IgM (Krause et al., 2007; Moll et al., 2007; Quintana et al., 2019).

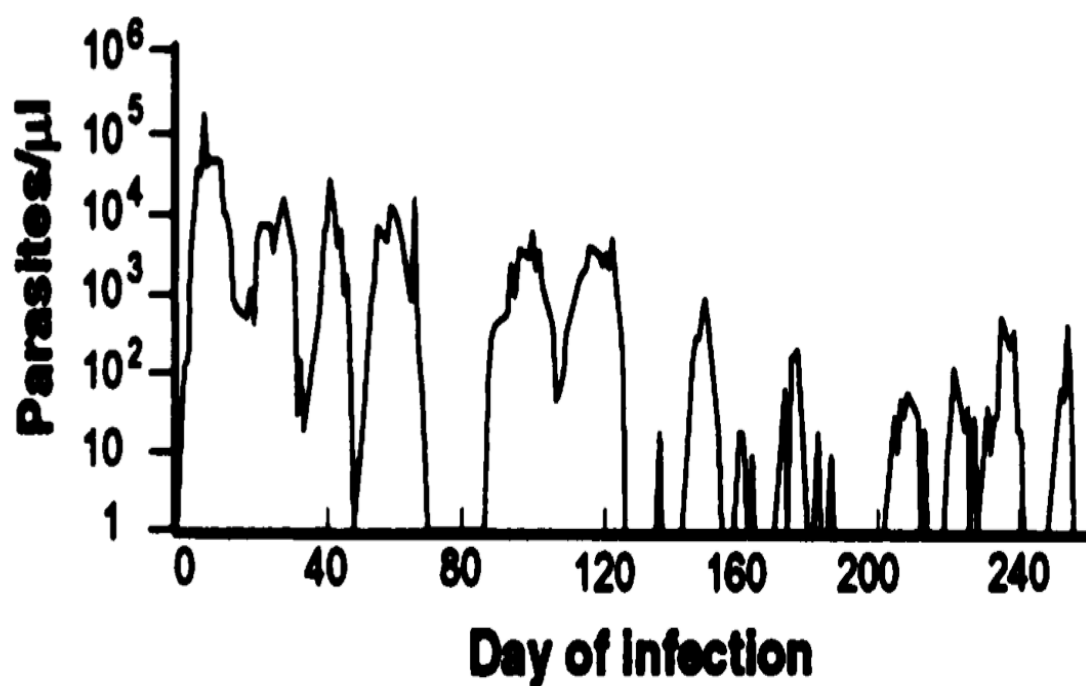
Strain-specific immunity is commonly long-lasting since immune-priming via germinal centers give rise to antibodies with high affinity (Achtman et al., 2005). These antibodies are commonly found in circulation for longer than 100 days or up to 1.5 years after infection clearance and accumulate across various infection gradually increasing the overall anti-plasmodial immunity and (cross-)protection from severe disease (Aitken et al., 2020; Hviid et al., 2022; Krause et al., 2007; Moll et al., 2007). Cross-protective antibodies are quickly activated, however, presumably die within the first hours or days of the infection due to reduced affinity binding to strain-transcended epitopes (Achtman et al., 2005; Bengtsson et al., 2013; Chène et al., 2018; Gamain et al., 2001; Kimingi et al., 2022; Lennartz et al., 2015; Osier et al., 2008). Similar to PfEMP1, immunity to invasion-related proteins like AMA1 and MSP is rather short-lived as the half-life of the antibodies is short and the AMA1- and MSP-specific antibody-secreting cells (ASCs) tend to wane quickly (Crompton et al., 2010; Fruh et al., 1991; Hui & Hashimoto, 2007; Yanik et al., 2023; Yman et al., 2019). Antibodies recognizing the surface proteins of merozoites (Richard et al., 2010) induce Fc-mediated effector functions including a reduced invasion efficiency, enhanced phagocytosis by monocytes and neutrophils, respiratory burst of neutrophils, NK-cell degranulation and complement fixation, respectively (Aitken, Mahanty, and Rogerson 2020; Gonzales et al. 2020; Rosenkranz et al. 2024). Despite the short-lived character of the immune response, the breadth of these Fc-mediated effector functions is strongly linked to the protection of severe or symptomatic malaria highlighting the importance of continuous and recent episodes of exposure to control the infection (Kapelinski et al., 2014; Kapulu et al., 2022; Osier et al., 2008; Wichers et al., 2021). Consequently, individuals with a wide breadth of antibodies that recognize VSA and merozoite antigens acquired during previous infections with various parasite isolates appear to be best protected against severe disease or even infection.

The innate immune system also contributes to resistance of the infection by limiting the number hepatic merozoites in the liver or asexually replicating parasites in circulation (Franklin et al., 2009). For this, phagocytic immune cells like macrophages are recruited in response to a pro-inflammatory signal

induced after the recognition of damage associated molecular pattern (DAMPs). These DAMPs include factors like Heme which is released after the burst of schizonts, free nucleic acids or glycosylphosphatidylinositol (GPI) on the surface of iRBCs (Gazzinelli et al., 2014). However, the innate response is inefficient and cannot keep up with the extensive proliferation rates neither in the liver nor in the asexual replication stage (Gazzinelli et al., 2014). Furthermore, there is evidence that the induction of a pro-inflammatory immune responses exacerbates the pathogenesis of malaria by enhancing the expression of endothelial receptors and promote parasites sequestration (Schofield & Grau, 2005). Further it may facilitate the occurrence of a cytokine storm at the site of sequestration which contributes to the development of e.g., cerebral malaria (Avril et al., 2013; Coban et al., 2018; Howland et al., 2013; Idro et al., 2005).

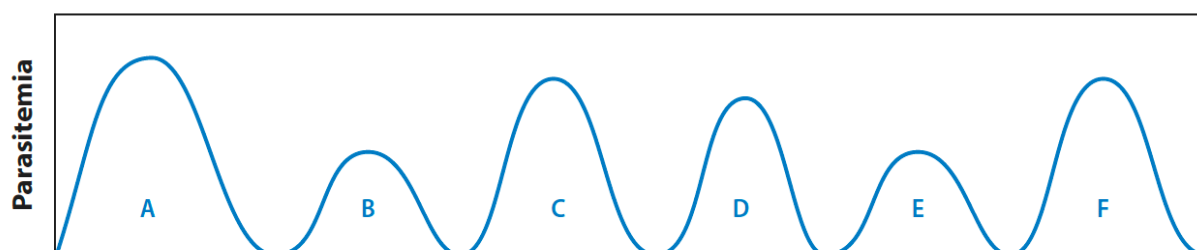
A

Longitudinal parasitemia in neurosyphilis patients undergoing Malariotherapy



Miller et al. 1994

B

Hypothesized antigenic variation in *P.falciparum* infections

Deitsch and Dzikowski. 2017

Figure 3 Longitudinal infection dynamics and hypothesized antigenic variation in individuals infected with *P. falciparum* parasites.

A) Longitudinal parasitemia tracking of a neurosyphilis patient who underwent Malariotherapy and displayed subsequent rise and fall of parasitemia over a period of 250 days with a trend towards lower parasitemia at the end of the infection. Gradually accumulating immunity to malaria does not clear the infection and but possibly reduces the level of peak parasitemia over time. B) Schematic illustrating antigenic variation of *P. falciparum* parasites over time with subsequent parasitemia waves being dominated by distinct variants of an antigen repertoire (labelled as A–F). Longitudinal immune evasion is anticipated by a gradual alternation through the antigen repertoire similar to other organisms like *P. knowlesi* or *T. brucei* (Galinski et al. 2018; Horn 2014; MacGregor et al. 2012; McCulloch et al. 2017).

1.3 Immune evasion

Parasites in chronically infected individuals can persist for a long period of time indicating that the parasites have developed several immune evasion strategies in order to avoid clearance by the host. Longitudinal parasitemia data from neurosyphilis patients undergoing Malariotherapy (Figure 2 B; Miller 1994), suggest that *P. falciparum* infections are characterized by a successive rise and fall of parasitemia with well-defined parasitemia waves (Figure 3 A). Other organism like *P. knowlesi* and *Trypanosoma brucei* display a highly similar longitudinal parasitemia course and were shown to gradually evade the immune system by exhausting an antigenic repertoire over time (Galinski et al., 2018; Horn, 2014; MacGregor et al., 2012; McCulloch et al., 2017). Thus, for a long time, it has been hypothesized that *P. falciparum* parasites follow a similar strategy relying on antigenic variation of their major virulence factor PfEMP1 (Figure 3 B), which however has not yet been proven for *P. falciparum* in the context of human infections. Crucial factors allowing immune evasion are related to distinct characteristics of PfEMP1s which are a) encoded by a multicopy gene family of *var* genes enabling antigenic variation, b) extensive sequence polymorphism of these genes to other strains and isolates and c) cytoadhesive abilities of PfEMP1s to bypass antigen presentation and clearance in the spleen.

1.3.1 *Var* multicopy gene family

Each parasite genome is equipped with a unique set of 45–90 highly polymorphic *var* genes coding for an equal amount of different PfEMP1 variants (Chan, Fowkes, and Beeson 2014; Otto et al. 2019; Walker and Rogerson 2023). The members of the *var* gene family can be segregated into four major groups based on their 5′-region (ups), their chromosomal localization, their transcriptional orientation, and their encoded protein domain composition responsible for binding to endothelial receptors (Figure 4; Gardner et al. 2002; Lavstsen et al. 2003; Kraemer and Smith 2003; Rask et al. 2010). African originating NF54 parasites (and its clonal line 3D7) exhibit 61 *var* genes in their antigen repertoire with ten different variants belonging to Group A (Otto et al. 2019; Rask et al. 2010; Salanti et al. 2003). Group A *var* genes are located at the subtelomere, are adjacent to B-type *var* genes and transcribed towards the end of the telomere (Figure 4 A). Group B-type *var* genes represent the largest *var* gene group consisting of 38 different variants (Otto et al. 2019; Salanti et al. 2003). B-type *var* genes are located most telomeric on the 14 *P. falciparum* chromosomes and are transcribed towards the center of the chromosomes (Figure 4 A; Rubio, Thompson, and Cowman 1996; Gardner et al. 2002; Lavstsen et al. 2003). 9 of these 38 B-type genes belong to the intermediate group B/C since they are located together with 13 genes of group C at central chromosomal regions, but possess a B-type 5′ upstream sequence. B, B/C and C-type *var* genes

encode PfEMP1s with duffy-binding-like (DBL) α 0 and cysteine-rich interdomain region (CIDR) α 2-6 domains in the N-terminal head structure, of which the latter mediates binding to the cluster of differentiation (CD36) receptor on the microvasculature. The expression of this CD36-binding phenotype has been associated with the occurrence of mild malaria (Figure 4 B; Jespersen et al. 2016; Robinson, Welch, and Smith 2003; Smith et al. 2013; Wichers et al. 2021).

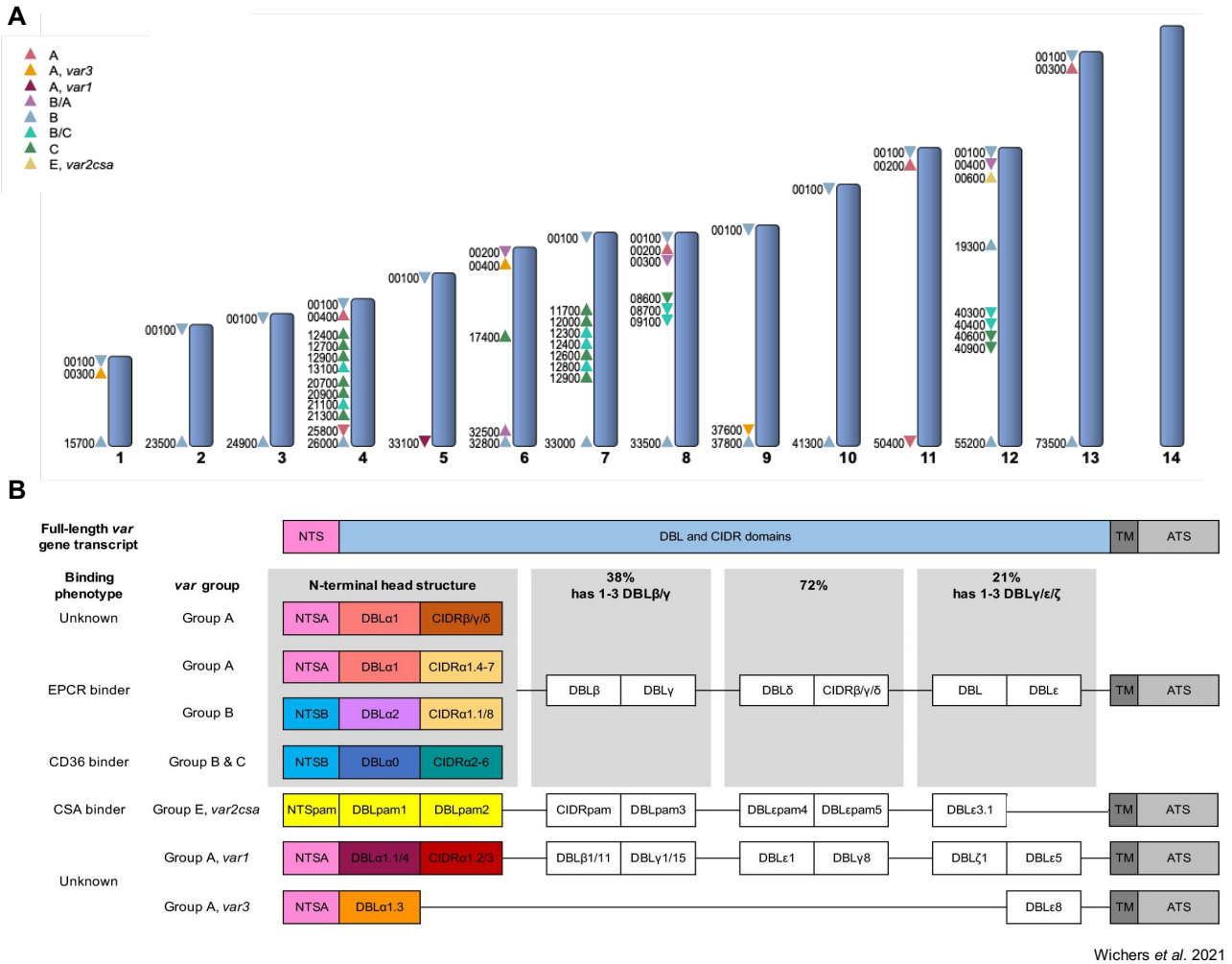


Figure 4.: Features of the var multicopy gene family and their encoded PfEMP1 proteins.

A) Distribution of var genes across the chromosomes of *P. falciparum*. B-type var genes are located at the telomeric end and transcribed towards the center of the chromosomes (blue). Some B-type var genes cluster together with centrally located C-type var genes (B/C-type genes, turquoise). A-type var genes are adjoined to B-type var genes but transcribed in opposite transcriptional directionality. Only a few B/A-types (purple) genes follow the same transcriptional orientation as B-type var genes. More conserved A-type var genes like var1 (dark red) and var3 (orange) as well as the inter-strain conserved type E var gene, var2csa are located at the subtelomere and are transcribed towards the telomeric end of the chromosome. IDs, abbreviated to the last 5 digits, complete ID names can be found in Table 6. B) Domain composition of var gene encoded PfEMP1s. B and C-type encoded PfEMP1s display a NTSB-DBL α 0-CIDR α 2-6 N-terminal head structure mediating the binding to CD36 associated with mild malaria. A-type encoded PfEMP1s display either a NTSA-DBL α 1-CIDR β /γ/δ or NTSA-DBL α 1-CIDR α 1.4-7 N-terminal head structure maintaining binding properties to a yet unknown receptor or EPCR, with both binding phenotypes associated with severe malaria. Some B-type PfEMP1 code for NTSB-DBL α 2-CIDR α 1.1/8 (B/A-type) with expression of these variants also linked to severe malaria. In combination with more C-terminal domains dual binding with other receptor like ICAM-1 or gC1qR is mediated. VAR2CSA has an alternative N-terminal head structure mediating the binding to CSA inside the placenta, while for more conserved variants VAR1 and VAR3 no potential binding partner has been discovered so far. TM: transmembrane domain, ATS: acidic terminal sequence, DBL: Duffy-binding-like, CIDR: Cysteine-rich interdomain region, NTS: N-terminal segment; PfEMP1: *P. falciparum* erythrocyte membrane protein 1, gC1qR: C1q-binding protein receptor

Contrary, expression of group A as well as four other B-type variants classified as B/A *var* genes has been linked to severe malaria episodes (Avril et al., 2013; Bengtsson et al., 2013; Ortolan et al., 2022; Turner et al., 2013). The A and B/A-type encoded PfEMP1 proteins are longer, display a more complex domain composition and differ from other PfEMP1s especially in their N-terminal head structure (Figure 4 B). A-type PfEMP1s code for a DBL α 1 domain followed by a specific CIDR domain (Figure 4 A, Rubio, Thompson, and Cowman 1996). The CIDR α 1 domain of the N-terminal head structure mediates binding to the endothelial cell protein C receptor (EPCR), while some A-types possess an alternative CIDR $\beta/\gamma/\delta$ domain whose actual binding phenotype is still unknown ('unknown A'), but the expression of both has been associated with severe malaria in young children (Jespersen et al. 2016; Rottmann et al. 2006; Turner et al. 2013; Walker and Rogerson 2023). Interestingly, two B/A PfEMP1s code for a DBL α 0 domain, commonly found in B and C-type PfEMP1s, and two others for a chimeric DBL α 2, sharing sequence identify with both DBL α 0 and DBL α 1 (Figure 4 A, Rubio, Thompson, and Cowman 1996). The DBL α 2 domain is part of a so-called domain cassette 8 (DC) which can mediate binding to various endothelial receptors simultaneously. For example, the DC8 (DBL α 2-CIDR α 1.1-DBL β 12-DBL γ 4/6) can mediate binding to the EPCR and the complement-specific globular C1q-binding protein receptor (gC1qR) which are linked to severe malaria episodes (Avril et al., 2013; Berger et al., 2013; Ghebrehiwet & Peerschke, 1998; Magallón-Tejada et al., 2016; Ortolan et al., 2022; Treutiger et al., 1997). Next to DC8, other domain cassettes were identified and linked to severity especially mediating binding to the EPCR receptor and other receptors via more C-terminally located domains (Avril et al., 2013; Berger et al., 2013). This, apart from binding to gC1qR both EPCR and CD36 binding parasites can bind to the intercellular adhesion molecule 1 (ICAM-1) via the more C-terminal located DBL β domain (Bengtsson et al., 2013; Ortolan et al., 2022).

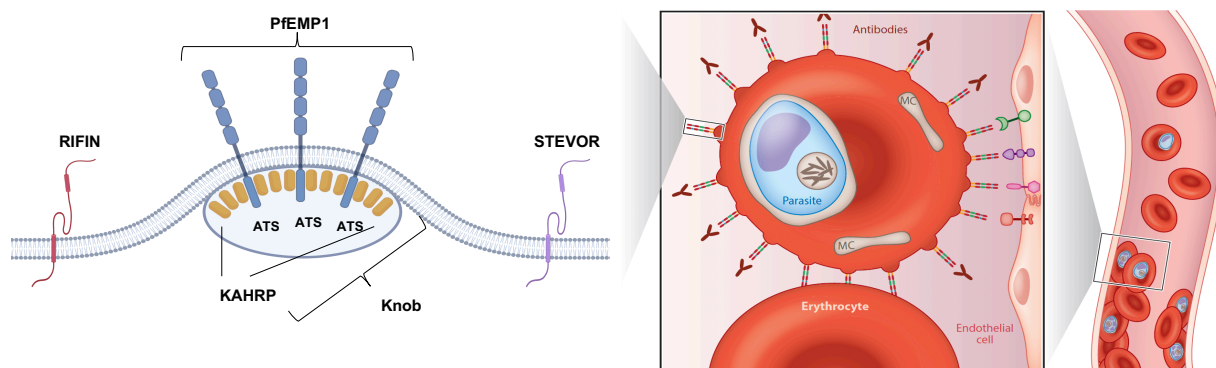
Additionally, a single *var1* and three *var3* genes exist within the A-type group, which show a high degree of conservation to similar variants from other *P. falciparum* isolates (Otto et al. 2019; Rask et al. 2010). Compared to other *var* genes, which are expressed early during the ring stage, *var1* seems to be continuously expressed during the cell cycle and is not reaching the surface of the RBC (Kyes et al., 2003). *Var3* coding for the shortest PfEMP1s with only three extracellularly exposed domains although neither a biological function nor a potential binding phenotype has been described for them (Otto et al. 2019; Wang et al. 2012). Furthermore, the inter-strain conserved E-type *var* gene variant, *var2csa*, has diverged from other *var* gene sequences and the expression of the encoded VAR2CSA protein has been associated with placental malaria, since it binds to chondroitin sulfate (CSA) expressed on placental tissues in pregnant women (Ayres Pereira et al., 2016; Salanti et al., 2003).

1.3.2 Sequestration

A key feature of the highly polymorphic PfEMP1 family is its ability to bind to various endothelial receptors on the surface of the microvasculature in order to bypass antigen presentation and clearance in the spleen. The human spleen fulfills crucial filtration functions e.g., by removing abnormal, malformed or old RBCs and recognize potentially harmful substances derived from infections or intoxications (Mebius & Kraal, 2005). Healthy, highly flexible RBCs can easily squeeze through the red pulp interendothelial slits in the spleen, while more rigid and larger cells stuck there, are phagocytized or forced into apoptosis (Henry et al., 2020). The maturation of parasites from the ring to the schizont stage is accompanied by a strong increase in iRBC membrane rigidity, making more mature parasites susceptible to splenic clearance (Henry et al., 2020). Hence, ring stage parasites which do not yet express PfEMP1 on the surface are found in the blood circulation of infected individuals, while trophozoites and schizonts sequester via PfEMP1 in various tissues of the host and thus bypass the splenic passage (CDC 2022; Musasia et al. 2022, Bachmann et al. 2022; Idro, Jenkins, and Newton 2005; Wiser 2023, Figure 5 A).

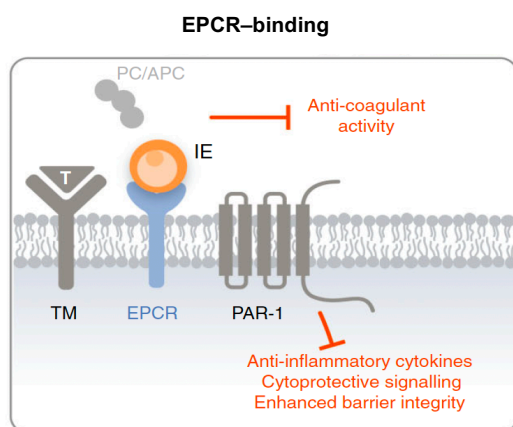
To mediate sequestration, PfEMP1s are exported to the surface of iRBCs and anchored in knob-like structures via the C-terminal acidic-terminal segment (ATS) and thereby displaying the highly polymorphic region extracellularly (Figure 5 A). Knobs protrusions dense with knob-associated

A



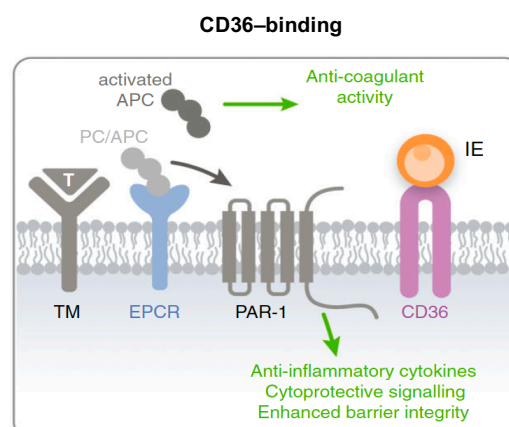
Deitsch and Dzikowski, 2017

B



Smith et al. 2013

C



Smith et al. 2013

Figure 5.: Sequestration of *P. falciparum* iRBCs impacts pathogenesis.

A) Schematic overview and three level zoom of parasites sequestration via PfEMP1. iRBC sequester at endothelial membranes of various tissues via interaction with surface molecules like EPCR, CD36, ICAM-1 or CSA to surpass splenic clearance (right and middle). Highly polymorphic PfEMP1s are exported to the surface of iRBC and anchored via their ATS domain at knob structures (left). Knobs are KAHRP dense structures maximizing the surface of the iRBC to facilitate binding. Other VSAs expressed on the surface of iRBCs include members of the RIFIN and STEVOR family. B) Predicted activation of pro-inflammatory responses subsequently to the binding of A and B/A-type encoded PfEMP1s to the EPCR receptor. Upon binding of the iRBC, competitive inhibition of protein C occurs causing anti-coagulant and suppress PAR-1 mediated cytoprotective signaling and barrier integrity. C) Contrary, PfEMP1s binding to CD36 do not interfere with protein C activated signaling, which presumably leads to a lower level of pro-inflammatory immune responses and less severe pathogenesis. RIFIN: repetitive interspersed family, PfEMP1; *Plasmodium falciparum* erythrocyte membrane protein 1, STEVOR subtelomeric variable open reading frame; ATS: Acidic-terminal segment; KAHRP: Knob associated histidine-rich protein; NTS.: N-terminal segment; DBL: Duffy-binding-like; CIDR: Cysteine-rich interdomain region; TM: thrombospondin; PAR-1: proteinase-activated receptor 1; IE; infected erythrocyte.

histidine-rich protein (KAHRP) that enlarge the surface of iRBCs to optimize sequestration (Figure 5 B; Chotivanich et al. 2002; Knuepfer et al. 2005). During the asexual replication cycle, the parasites mature inside the parasitophorous vacuole (PV) but establishes membranous structures like Maurer's clefts in the RBC cytosol for protein sorting and trafficking (Sam-Yellowe, 2009). Thus, after transitioning through *Plasmodium* translocon of exported proteins (PTEX) located at the parasitophorous vacuole membrane (PVM), PfEMP1 is trafficked through Maurer's clefts before being anchored at the RBC membrane (Batinovic et al., 2017; Boddey et al., 2016; De Koning-Ward et al., 2009; Hiller et al., 2007; Marti et al., 2004; Wickham et al., 2001).

Until now, more than 24 different endothelial cell surface moieties were shown to serve as receptors for cytoadhesion of *P. falciparum* (Bachmann et al. 2022). However, only for a subset of these receptors binding ligands were identified. These include the EPCR, CD36, ICAM-1, CSA, platelet endothelial cell adhesion molecule-1 (PECAM-1) and globular C1q-binding protein receptor (gC1qR) (Bachmann et al., 2022; Lee et al., 2019). However, although sequestration is crucial for parasite survival in the human host, it can lead to severe pathogenesis for example when parasites bind to EPCR, which is predominantly found on brain endothelial cells (Jespersen et al. 2016; Sahu et al. 2021; Turner et al. 2013; Walker and Rogerson 2023). The mechanism is not yet fully understood but it is described that PfEMP1 can competitively inhibit the binding of protein C (PC) to the EPCR receptor, thereby promoting a pro-inflammatory immune response at the site of sequestration, which is a hallmark of severe malaria (Figure 5 B; Avril et al. 2013; Esmon 2004; Jespersen et al. 2016a; Smith et al. 2013; Turner et al. 2015).

Contrary, the class B scavenger receptor CD36, which is expressed on various endothelial membranes primarily but is absent in the brain, is the target of the most B and C-type PfEMP1s mediating binding via the CIDRa2-6 domains (Febbraio et al., 2001; Silverstein & Febbraio, 2009). Simultaneously, it is assumed that the binding of the parasites to CD36 is less stationary than the binding of PfEMP1 to EPCR and that the iRBCs are rather rolling along endothelial membranes, which presumably leads to a lower level of pro-inflammatory signaling and thus overall less severe pathogenesis (Figure 5 C; Bachmann et al. 2022; Febbraio, Hajjar, and Silverstein 2001; Smith et al. 2013).

1.3.3 Immune evasion via other VSAs (STEVORs and RIFINs)

In addition to the most studied PfEMP1 family, so-called small VSAs were also shown to contribute to immune evasion. These gene families encompass the RIFIN (150–200 members) and the STEVOR family (30–33 members) (Cheng et al., 1998; Lavazec et al., 2006; Wahlgren et al., 2017). Next to these, other VSA families exist like PfMC-2TM proteins with 13 members and 10 hypervariable SURFINs, however, their involvement in immune evasion is poorly understood (Bachmann et al., 2009; Lavazec et al., 2006; Winter et al., 2005).

Similar to *var* genes, *rif* and *stevor* genes are located widespread across the parasite's chromosomes and display different transcriptional directionalities. Most *rifs* are located at the subtelomeric regions of the chromosomes, with approximately 25 % of, in particular A-type *rifs*, in direct chromosomal proximity to a B or A-type *var* gene with A-type *var* genes being co-regulated with neighboring *rif* genes due to a promotor sharing mechanism of gene pairs with diametral transcriptional directionality (Claessens et al., 2012; Lavstsen et al., 2003). RIFINs and STEVORs are expressed during multiple life-cycle stages, including human and mosquito stages, suggesting the proteins might be involved in highly diverse functions (Bachmann et al., 2012; Gonzales et al., 2020; McRobert et al., 2004; Petter et al., 2008). During the asexual replication cycle in the blood, the *rif* and *stevor* genes are mainly expressed in the early

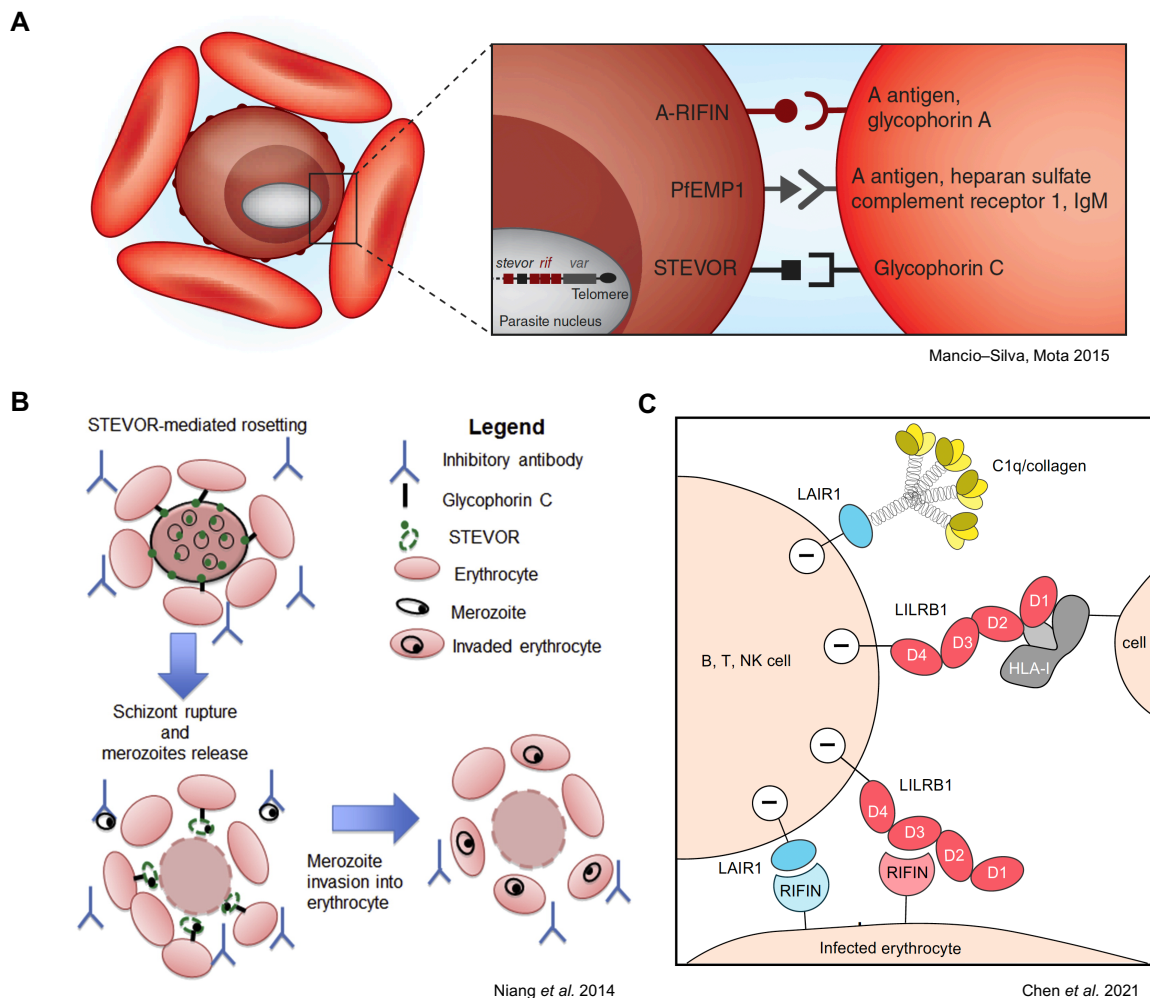


Figure 6.: Immune evasion of iRBCs via RIFINs and STEVORs.

A) Next to PfEMP1s, RIFIN and STEVOR can bind to surface receptors on uninfected RBCs like glycophorin A, C or blood group trisaccharides to form large rosettes. Presumably, this is advantageous for the parasite because a) exposure of PfEMP1 to the immune system is avoided and b) invasion of merozoites after the burst of schizonts is facilitated because new host cells are already in the immediate vicinity. B) Illustration of rosetting by STEVORs as an example. Expression of STEVORs is high during late trophozoite and schizont stages so that STEVORs can mediate binding to glycophorin C on the surface of yet uninfected RBCs. After rupture, merozoites can easily infect new RBCs which were bound in the rosette. C) RIFINs, which structurally mimic MHC molecules expressed by healthy human cells, interact with leucocyte immunoglobulin-like receptor B1 and B2 (LILRB1) and leucocyte-associated immunoglobulin-like receptor 1 (LAIR1) expressed on the surface of B, T and NK-cells telling our immune cells to leave iRBCs unscathed. This immunosuppressive function contributes to immune evasion of iRBCs during the human blood phase.

trophozoite stage, after *var* gene expression is terminated (Yam et al., 2017). Proteins of both families, RIFIN and STEVOR, are located in close proximity to surface exposed PfEMP1s and anchored to the RBC membrane via a single transmembrane domain and expose semi-conserved and hypervariable regions extracellularly (Figure 5 A) (Bachmann et al., 2012; Goel et al., 2015; Lavazec et al., 2006). However, only a subgroup of A-type RIFINs is surface exported, while B-type RIFINs presumably reside intracellularly (Petters et al., 2007, 2008). STEVORs and RIFINs support the formation of rosettes to shed surface antigens from being exposed via the binding of either glycophorin C (CD236), glycophorin A (CD235a) or the blood group A trisaccharide antigen of yet uninfected RBCs, respectively (Figure 6 A; Goel et al. 2015; Niang et al. 2014; H. Singh et al. 2017). Recent studies suggest that RIFINs can also directly promote immunosuppression via the binding to the leucocyte immunoglobulin-like receptor B1 (LILRB1) or leucocyte-associated immunoglobulin-like receptor 1 (LAIR1) on NK, B and T-cells e.g., (Harrison et al., 2020; Saito et al., 2017; Yokoyama et al., 2018) highlighting the potential of immune evasion of various VSA families on multiple levels (Figure 6 B). STEVORs have been additionally localized at the plasma membrane or the rhoptries in merozoites and have been convincingly shown to be involved in invasion (Bachmann et al., 2015; Goel et al., 2015; Niang et al., 2014; Wichers et al., 2019). Moreover, RIFINs and STEVORs are expressed during gametocyte stages, presumably contributing to their sequestration in the bone marrow (McRobert et al., 2004; Petters et al., 2008; Tibúrcio et al., 2012). Taken together, PfEMP1s, STEVORs and RIFINs are thought to collectively contribute to microvascular obstruction accelerating more severe pathologies of malaria involving tissue damage, inflammation, cerebral or placental malaria (Kaul et al., 1991; Sharma & Shukla, 2017; Warimwe et al., 2012).

1.4 Regulation of *var* gene expression

Var genes expression occurs in a mutually exclusive manner meaning that only single *var* gene variant is expressed at a given time in an individual ring-stage parasite. However, recent evidence from single cell data indicate that the parasite is more flexible in its *var* gene expression by expressing a single or multiple variants or even display little to no *var* gene expression, challenging the established dogma of mutually exclusive expression (Florini et al., 2024). Several factors were shown to influence *var* gene expression including a) the *var* gene as well as the intro promotor sequence b) the position inside the nucleus, chromatin structure and epigenetic marks and c) specific *var* gene sequence elements.

It is believed that the upstream promotor from which *var* gene expression is initiated together with a bi-directional promotor within the relatively conserved intron sequence can induce silencing of remaining *var* genes possibly by chromatin looping (Avraham et al., 2012; Epp et al., 2009). For this, intro originating, exon 1, long non-coding antisense transcripts intercalate with chromatin marks from other *var* genes to induce silencing (Figure 7; Amit-Avraham et al. 2015; Epp et al. 2009). A crucial role of the intro in *var* gene regulation seems likely since several regulatory marks including histone acetylations and alternative histone variants are enriched at the intro sequences and deletion of the intron strongly affects chromatin structure (Hollin & Le Roch, 2020). However, the upstream *var* promotor of a C-type *var* gene was shown to be sufficient to maintain mono-allelic expression of this gene while simultaneously silencing other *var* genes (Voss et al., 2006).

A large proportion of the *var* genes is epigenetically silenced presumably by a highly condensed heterochromatin structure in repressive nuclear clusters (Dzikowski & Deitsch, 2009). This structure is characterized by trimethylation of histone 3 lysine 9 (H3K9me3) and trimethylation of histone 3 lysine 36 (H3K36me3) which is bound by heterochromatin protein 1 (HP1) (Figure 7 A; Hollin and Le Roch 2020; Petter et al. 2011). To maintain a silenced state histone deacetylases like PfSir2A, PfSir2B and PfHDA2 keep regulatory *var* genes sequences in a deacetylate state (Figure 7 B). In this regard, PfSir2A was reported to influence expression and silencing of A, C and E-type *var* genes while PfSir2B contributes to the regulation of B-type *var* genes (Duraisingh et al., 2005; Freitas et al., 2005; Tonkin et al., 2009). To activate *var* gene expression heterochromatic regions transits into an active, euchromatic transcriptional state more closer at the center of the nucleus by replacing canonical histones H2A and H2B with alternative histone variants H2A.Z and H2B.Z at the *var* gene promotor sequence (Figure 7 B; M. F. Duffy et al. 2017; Flueck et al. 2009; Lopez-Rubio et al. 2007; Lopez-Rubio, Mancio-Silva, and Scherf 2009; Petter et al. 2011, 2013).

Moreover, the location of the *var* genes on the chromosomes impacts their regulation. The *var* gene promotor regions at the telomere are commonly less packed with heterochromatic marks and are continuously remodeled by histone deacetylases allowing a more dynamic expression of (sub)telomeric located B and A-type *var* genes (M. F. Duffy et al., 2017; Freitas et al., 2005; Hollin & Le Roch, 2020; Michel-Todó et al., 2023; Petter et al., 2011). Thus, these genes are characterized by higher “off-rates” and therefore more heterogenous switching pattern are observed e.g., in *in vitro* cultures (Andradi-Brown et al., 2024; Frank et al., 2007). For parasites expressing more centrally located, mainly C-type *var* genes, lower “off-rates” were reported indicating that these genes are less likely to be switched off quickly so that parasites are more determined and less likely to switch their expression to another variant (Frank et al., 2007).

To exploit its highly polymorphic repertoire of *var* genes in a time-dependent manner *var* gene switching is believed to be highly important for malaria chronicity (Kyes et al., 2007; Milne et al., 2021). For this, it was hypothesized that the parasites induces switches of the *var* gene expression over time to only gradually exhaust the repertoire (Dzikowski and Deitsch 2009; Dzikowski, Frank, and Deitsch

Figure 7.: Regulation of (mutually exclusive) var gene expression.

A) Schematic illustrating var gene expression is silenced by tightly packed heterochromatic structures involving H3K9me3 or H3K36me3 bound to HP1 (left). Acetylation of histones allows transcription normally indicated by active, euchromatic histone modifications like H3K9ac or H3K27ac (right). B) Elements regulating var gene expression. Silencing of var gene expression is maintained by specific histone deacetylases like PfSir2A, PfSir2B or PfHda2 which repress expression of different var gene groups. Simultaneously, promoter pairing of the var ups promoter together with a bi-directional promoter sequence inside conserved regions of the intron is believed to contribute to expression, silencing and especially mutually exclusive expression of var genes e.g., via an antisense lncRNA originating from the intron. Activation of var genes from a repressive cluster in the nucleus is characterized by euchromatic marks at the var gene sequences as demonstrated in A) allowing the transcription of the gene.

1.5 CHMI studies as a tool for in-depth analysis of var gene expression

In field isolates, the genomic sequences for var and other VSAs genes are unknown, which limits established methods to capture var gene expression. Moreover, examining antigenic variation of parasites *in vivo* requires a) a long-term study over several months and b) a short sampling interval to capture changes in var gene expression subsequent parasitemia peaks and troughs (Figure 3 A). Until now, a single study investigating the expression of var genes in 11 children from Papua New Guinea over a period of four months has described a very dynamic and variable picture, but also reoccurrence of certain var gene variants up to ten weeks. In addition, an association was found between higher multiplicity of infection and a more diverse expression of var genes as well as a longer duration of infection (Kaestli et al., 2004).

Another study suggests that in response to a changing antigenic phenotype of monoclonal *P. falciparum* infections individuals acquire and maintain phenotype-specific anti-VSA (Staalsoe et al. 2002). Kaestli et al. 2004 used multiple var-specific RT-PCRs and TOPO cloning coupled to Sanger sequencing (Kaestli et al. 2004), to amplify and sequence transcripts from field samples. However, the degenerated var primers targeting only selected upstream regions and N-terminal DBL α , CIDR α and DBL β domains and exhibit primer biases so that presumably only a small subset of the full var gene repertoire was amplified. In addition, most samples were collected bimonthly and not connected to the parasitemia so that a concise detection of changes in var expression was not possible. To overcome technical difficulties for the detection of var genes from field isolates more modern sequencing approaches including expressed-sequence tag (EST) coupled to next generation sequencing (NGS) or a *de novo* assembly of var transcripts from RNA-seq reads are currently state-of-the art methodologies (Andradi-Brown et al., 2024; Mackenzie et al., 2022; Wichers et al., 2021).

However, also these techniques have limitations and can only incompletely depict var gene expression *in vivo*: For the EST-approach, a highly variable 350–500 bp long fragment of the DBL α sequence within the N-terminal NTS-DBL α -CIDR head structure (DBL α -tag) is PCR-amplified in a highly similar manner than for the study from Kaestli et al. 2004. For this, the primers bind to relatively conserved flanking regions of the tag sequence and can amplify almost all var gene sequences. The only exception are inter-strain conserved variants, such as var2csa, which has no a DBL α domain in the N-terminal head structure, or var1 and var3, whose DBL α domains are not well covered by the primers (Mackenzie et al. 2022, Wichers 2021). In contrast to the study from Kaestli et al. 2004, reference sequences for more strains, clones and isolates including full-length var sequences are now available for *in silico*

comparisons of the sequenced DBL α -tags with these reference sequences. Thus, DBL α -tag sequences can be now annotated by best blast hit and subsequently their connected PfEMP1 domains based on

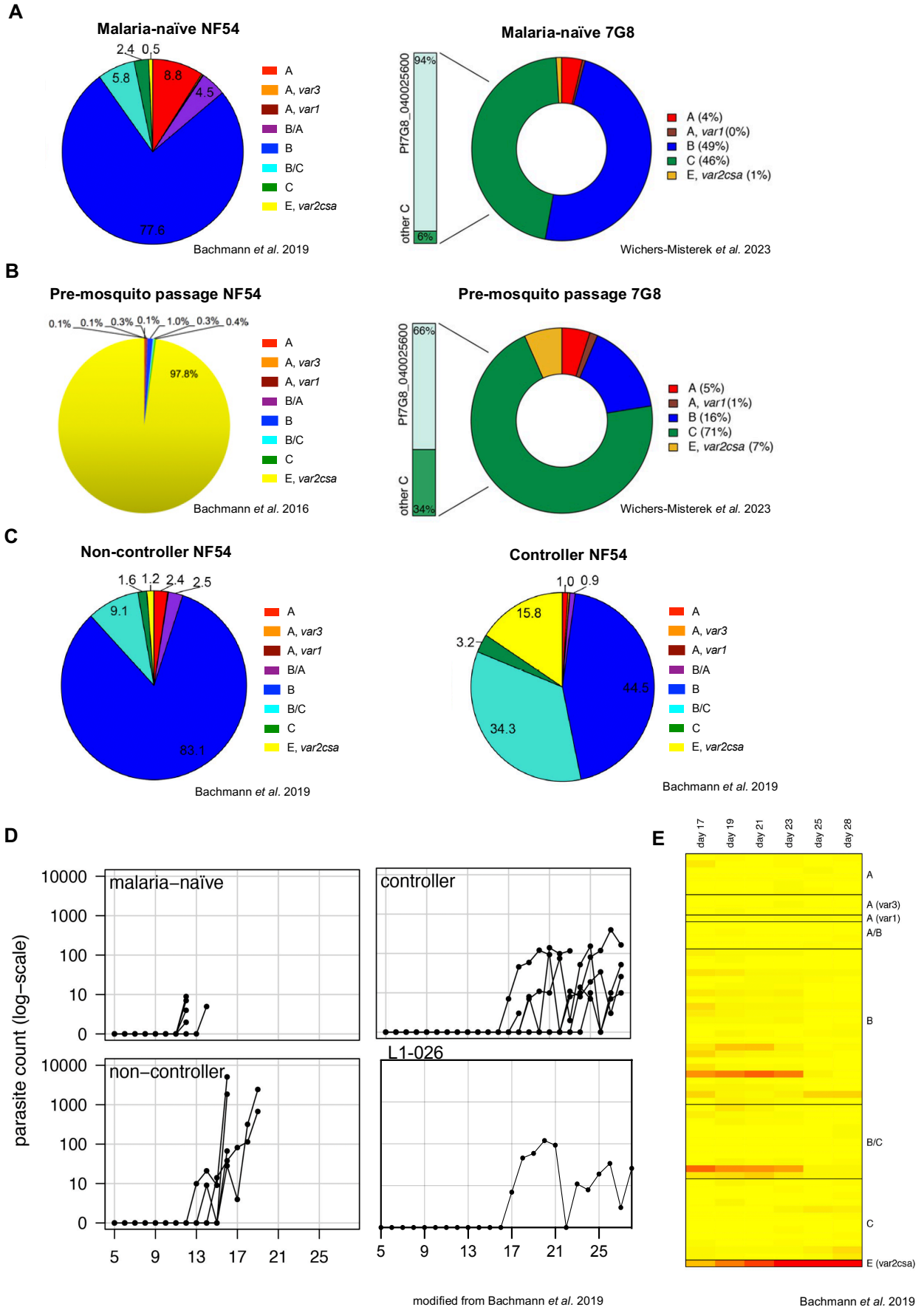


Figure 8.: Var gene expression by NF54 and 7G8 parasites *in vitro* and *in vivo*.

A) Left: NF54 *var* gene expression at the infection onset by parasites from malaria-naïve volunteers display a highly diverse pattern of especially B and severity-linked A-type *var* genes, while 7G8 parasites (right) retained expression of the single C-type *var* gene but also express a highly diverse B-type parasite population. B) Left: NF54 parasites dominantly express *var2csa* before they are passaged through the mosquito and administered to humans in CHMIs. Right: *in vitro* cultivated 7G8 parasites prior to mosquito passage display a more heterogenous expression pattern dominated by a single C-type *var* gene. C) Parasites from volunteers displaying a lower level of anti-malarial semi-immunity ('non-controllers') show a comparable expression pattern to parasites from malaria-naïve volunteers (left), while parasites isolated from more immune 'controllers' express a higher proportion of B/C-type *var* genes. D) The immune status of the volunteers, which correlates to differences in the expressed *var* gene profiles, has direct implication on the infection dynamics of the volunteers. Malaria-naïve volunteers are quickly treated after the onset of the blood stage infection (top, left). 'Non-controllers' can delay the infection onset for some days compared to malaria-naïve volunteers, develop a high parasitemia but also quickly developed malaria-related symptoms after the onset of the blood stage infection (bottom, left). More immune controllers do not necessarily require treatment, can further delay the infection onset and control the parasitemia to a lower level (top, right). Parasitemia curve from a single 'controller' (L1-026), which was closely monitored for 28 days display two clearly delineated parasitemia waves with peaks at day 20 and day 26 (bottom, right). E) Var gene expression pattern from parasites isolated from L1-026 display different *var* gene expression pattern across the two parasitic waves, the first being dominated by B and B/C genes while the 2nd is dominated by *var2csa*. Color-coding for *var* gene groups as indicated: A (red), *var1* (dark red), *var3* (orange), B/A (purple), B (blue), B/C (turquoise), C (green), E (*var2csa*, yellow).

sequence similarity to other DBL α domains from full-length *var* gene transcripts already deposited on *varDB*. However, also this methods has disadvantages so that for a certain proportion of DBL α -tags no highly similar sequence is found (novel sequences) and therefore the domain composition cannot be predicted (Mackenzie et al., 2022; Wichers-Misterek et al., 2023). Contrary, *de novo* assembly of *var* gene transcripts from RNA-seq reads can reflect *var* gene expression more accurately, as recently illustrated by a study by Andradi-Brown et al. 2024. However, sequencing methods and analysis pipelines are constantly improved and require advanced bioinformatic knowledge. Furthermore, a major disadvantage of both the EST and *de novo* RNA-seq approach is that they cannot properly distinguish between B and C-type *var* genes, which have highly similar sequences and protein domain compositions. To overcome this problem, recent evidence suggests that an *in silico* comparison of DBL α -tag and previously assembled sequences is possible to subsequently assign a most probable *ups* type (*ups* A, B or C), but requires further validation (Tan et al., 2023).

Thus, in recent years, controlled human malaria infection (CHMI) studies have become increasingly important for the investigation of *var* gene expression *in vivo*. For the parasite strains used for CHMIs, the genomes including *var* and other VSA genes is known. Therefore, gene expression on the genome-wide scale can be easily analyzed e.g., via RT-qPCR using primer-pairs for each *var* gene variant and during RNA-seq analysis reads can be easily mapped to the existing reference genome. In recent years, the Sanaria Inc. has developed a broad range of aseptic, purified and cryopreserved PfSPZ challenge products for CHMIs, which were shown to be safe and effective, enabling the generation of reproducible data in volunteers with different degrees of semi-immunity and parasites strains from different geographic origins (Epstein et al., 2017; Friedman-Klabanoff et al., 2019; Kibwana et al., 2022; Sauerwein et al., 2011; Spring et al., 2014; Stanisic et al., 2018). For more than 30 clinical trials at multiple sites in Africa, Europe, the US and Australia including more than 1200 volunteers CHMIs were performed with Sanaria PfSPZ challenge products including the African-originating strain NF54 and its clone 3D7, South-American originating 7G8 and South East-Asian originating NF135 parasites. For all three strains reference genomes were assembled, which show differences in their structure and sequence of immunological important regions and predicted T cell epitopes (Moser et al., 2020). Furthermore, they

display morphological differences across the VSA protein family and code for a different number of *var* genes.

Usually, CHMI are used to assess for example the safety or efficiency of immunization, vaccine or chemoprophylaxis regimens or anti-malarial drug efficacies (Kibwana, Kapulu, and Bejon 2022; Lell et al. 2018; Mordmüller et al. 2017, 2022; Sulyok et al. 2021). The effects of tested interventions on infection are usually observed over a period of one to four weeks after sporozoite inoculation (Kibwana et al., 2022). Depending on the degree of semi-immunity, treatment is also applied earlier for example, infected malaria-naïve volunteers are treated at the latest when the TBS is positive, when a certain parasitemia threshold (between 500 and 1000 pf/μL) is reached or when malaria-related symptoms appear.

Samples from some CHMI trials were used to analyze *var* gene expression either directly *ex vivo* or after short cultivation of the re-isolated parasites (Bachmann et al. 2019; Bhardwaj et al. 2024; Wichers-Misterek et al. 2023). Until now, *var* gene pattern from *ex vivo* samples were studied for both NF54 and 7G8 parasites. It was shown, that parasites isolated shortly after the infection onset from malaria-naïve volunteers show a highly diverse expression pattern of various *var* gene variants. For NF54 parasites, the expression pattern is dominated by B and A-type *var* genes, while 7G8 parasites express a diverse set of B-types to a lower level in combination with a distinct C-type variant (Figure 8 A; Bachmann et al. 2016; Wichers-Misterek et al. 2023). Interestingly, when these patterns were compared to the *var* gene expression prior to the mosquito passage, only NF54 parasites appear to fully reset the expression pattern from an exclusive expression of the conserved *var2csa* variant *in vitro*. Instead, 7G8 parasites from the pre-mosquito passage express a more heterogenous pattern which is dominated by the same C-type variant also expressed by in malaria-naïve individuals (Figure 8 B) (Bachmann et al., 2016; Wichers-Misterek et al., 2023). In this context, it was hypothesized that NF54 parasites presumably reset their entire expression profile to express at least one variants which is able to mediate sequestration and to adopt to a yet unknown host environment (Bachmann et al., 2016). Simultaneously, for 7G8 parasites the partial reset of the *var* gene pattern might be related to an epigenetically regulated imprinting mechanism, for which the parasites retains expression of *var* gene variants which were shown to be successful across multiple generations and infection cycles (Wichers-Misterek et al., 2023).

CHMIs in endemic regions have revealed an association between the expressed *var* gene profiles and preestablished immunity (Bachmann et al. 2019; Bhardwaj et al. 2024). The first study with life-long exposed adult Gabonese volunteers showed that, compared to parasites from malaria-naïve individuals, parasites from life-long exposed individuals showed a very similar *var* gene expression pattern if they exhibited a relatively low degree of semi-immunity, while parasites from more immune volunteers expressed a more restricted pattern dominated by B and B/C-type *var* genes (Figure 8 C; Bachmann et al. 2019; Bhardwaj et al. 2024). Since the low-immune volunteers showed a very early parasitemia onset, developed higher parasitemia and required treatment early on during the infection they were labelled as ‘non-controllers’ (Figure 8 D). The other volunteer group, so called ‘controller’,

showed significantly lower parasitemia, a delayed infection onset, and partly never reached the treatment threshold criteria, illustrating a direct link between *var* gene expression pattern and the individual's level of anti-malarial immunity (Figure 8 D). The data were recently confirmed by a study with 19 volunteers from the Gambia, which were previously classified into low ("sero-low") and high immunity individuals ("sero-high"), with "sero-low" individuals being less able to control parasite kinetics while the *var* gene expression profile showed a highly diverse expression pattern of mainly group B *var* genes (Bhardwaj et al., 2024)

1.6 Aim of the thesis

In the study from Bachmann et al. 2016, parasites from a single volunteer monitored for the maximum of 28 days displayed a strongly different *var* gene expression pattern across two discrete parasitemia waves indicating significant changes of the *var* gene expression over time. As indicated earlier such changes of the *var* gene expression pattern were anticipated based on data from other organisms (Figure 8 D, E; Figure 3 A; Galinski et al. 2018; MacGregor et al. 2012). However, after day 28 the study was terminated and it was not possible to assess whether the changes in the antigenic phenotypes were linked to *var* gene switching or antibody selection. Thus, studies including more volunteers and longer study frames are needed to verify these findings and illustrate a more complete picture of antigenic variation of *P. falciparum* parasites during the course of human infections. Thus, we here present for the first time data from a unique longitudinal CHMI study, which was conducted from 2019–2021 by the clinical trial team in Lambaréné (Gabon) together with researchers from ITM (Tübingen, Germany) and RadboudUMC (Nijmegen, The Netherlands). During the trial, 56 individuals underwent six subsequent infections with either African-originating NF54 parasites or 7G8 parasites from South America in order to assess the cross-protective potential of different *P. falciparum* strains on a life-long malaria exposed cohort of volunteers. In contrast to other CHMI studies, treatment of the volunteers was only initiated upon detection of parasitemia in combination with malaria-related symptoms, so that volunteers were allowed to remain infected over a maximal time frame of about 1.5 years while being closely monitored. From these volunteers, we received and analyzed 584 longitudinal samples to:

- a) accurately characterize the longitudinal infection dynamics of asymptomatic individuals with varying degrees of pre-acquired semi-immunity,
- b) evaluate the expression of the *P. falciparum* antigen repertoire during the course of human infections, and
- c) to correlate the occurrence of PfEMP1-specific antibodies with the change in *var* gene expression.

2. Material and Methods

2.1 Material

2.1.1 Chemicals and reagents

Chemical/reagent	Manufacturer (Location (city/country))
Roswell Park Memorial Institute (RPMI) 1640 medium	AppliChem (Darmstadt, Germany)
Disodium hydrogen phosphate (Na₂HPO₄)	Carl Roth GmbH & Co. KG (Karsruhe, Germany)
Sodium hydrogen carbonate (NaHCO₃)	Sigma-Aldrich (St.Louis, Montana, USA)
Hypoxanthine	Sigma-Aldrich (St.Louis, Montana, USA)
Gentamycin	Ratiopharm (Ulm, Germany)
Albumax II	Thermo Fisher Scientific™ (Waltham, Massachusetts, USA)
Percoll	Cytiva (Uppsala, Sweden)
D-Sorbitol	Sigma-Aldrich (St.Louis, Montana, USA)
D-glucose	Merck KGaA (Darmstadt, Germany)
Sodium hydroxide (NaOH)	Merck KGaA (Darmstadt, Germany)
Sodium chloride (NaCl)	Merck KGaA (Darmstadt, Germany)
Potassium dihydrogen phosphate (KH₂PO₄)	Merck KGaA (Darmstadt, Germany)
Potassium chloride (KCl)	Merck KGaA (Darmstadt, Germany)
Glycerol	Carl Roth GmbH & Co. KG (Karsruhe, Germany)
Giemsa azur eosin methylene blue solution	Sigma-Aldrich (St.Louis, Montana, USA)
UltraPure™ Agarose	Invitrogen (Carlsbad, California, USA)
Acetic acid	
EMSURE® ACS,ISO,Reag. Ph Eur Ethanol, absolute for analysis	Merck KGaA (Darmstadt, Germany)
Ethidium bromide (EtBr)	Carl Roth GmbH & Co. KG (Karsruhe, Germany)
Ethylenediaminetetraacetic acid (EDTA)	Carl Roth GmbH & Co. KG (Karsruhe, Germany)
QuantiTect SYBR Green PCR	Qiagen
Tris	Carl Roth GmbH & Co. KG (Karsruhe, Germany)
TRIzol®	Invitrogen (Carlsbad, California, USA)
High performance liquid chromatography (HPLC) H₂O	J.T. Baker (Phillipsburg, New Jersey, USA)
1-bromo-3-chloropropane (I-BCP)	Merck KGaA (Darmstadt, Germany)
EMSURE® ACS,ISO,Reag. Ph Eur Chloroform, for analysis	Merck KGaA (Darmstadt, Germany)
Nuclease-Free-Water (RNase-Free-H₂O)	Qiagen (Hilden, Germany)
Methanol per analysis (p.A.), absolute	neoFroxx GmbH (Einhausen, Germany)
2-Propanol (Isopropanol)	Carl Roth GmbH & Co. KG (Karsruhe, Germany)
Mineral Oil	Merck KGaA (Darmstadt, Germany), Sigma Life Science
Random Primers 300 µg (3 µg/µL)	Invitrogen (Carlsbad, California, USA)
5X First Strand Buffer	Invitrogen (Carlsbad, California, USA)
0.1 M DTT	Invitrogen (Carlsbad, California, USA)
10 mM dNTP Mix	Invitrogen (Carlsbad, California, USA)
MgCl₂	Thermo Fisher Scientific™ (Waltham, Massachusetts, USA)
BD buffer	Solis BioDyne (Taru, Estonia)
GeneScan™ 500 LIZ™ Dye size standard	Thermo Fisher Scientific™ (Waltham, Massachusetts, USA)

Hi-Di™ buffer	Thermo Fisher Scientific™ (Waltham, Massachusetts, USA)
Crystal Gas (1% O₂, 5% CO₂, and 94% N₂)	AirLiquide (Düsseldorf, Germany)

2.1.2 Human blood and serum

Characteristics	Source
Human blood (0+)	Blood bank UKE
Human serum	Interstate Blood Bank (Memphis, Tennessee, USA)

2.1.3 Media

Medium	Composition
RMPI complete Medium (cRPMI) in ddH₂O, sterile-filtered adjusted to pH 7.2 with NaOH Storage at +4°C	1.587 % (w/v) RPMI 1640 12 mM NaHCO ₃ 0.2 mM Hypoxanthine 20 mg/L Gentamycin 0.5 % Albumax II 2.5 % human serum (HS)

2.1.4 Buffers and Solutions

Buffer/Solution	Composition/Company
60 % Percoll Storage at +4 °C	67 % (v/v) Percoll stock solution 33 % (v/v) cRPMI 0.08 g/mL D-Sorbitol
90 % Percoll stock solution sterile filtered Storage at	90 % (v/v) Percoll 10 % (v/v) 10X PBS
PBS (10X) in ddH₂O Storage at +4 °C	14.4 g/L Na ₂ HPO ₄ 80 g/L NaCl 2.4 g/L KH ₂ PO ₄ 2 g/L KCl
Malaria Freezing Solution (MFS) in ddH₂O, sterile filtered Storage at +4° C	208 mM D-Sorbitol 139 mM NaCl 35 % (v/v) Glycerol
Malaria Thawing Solution (MTS) in ddH₂O, sterile filtered Storage at +4 °C	3.5 % (w/v) NaCl
Sorbitol solution in ddH₂O, sterile filtered Storage at +4° C	5 % (w/v) D-Sorbitol
Giemsa staining solution in H₂O (tap water) Storage at RT	10 % (v/v) Giemsa solution
TAE (50X) buffer in ddH₂O Storage at RT	5 mM NaCH ₃ COOH 40 mM Tris
TAE (1X) buffer in ddH₂O Storage at RT	2 mM EDTA
Orange G (6X) dye in ddH₂O Storage at +4 °C	4 g/L Orange G 15 % (v/v) Glycerol
LowCross-Buffer® Storage at -20 °C	Candor Bioscience GmbH (Wangen, Germany)
70 % Ethanol	70% (v/v) Ethanol, absolute

In HPLC H₂O, sterile filtered
Storage at RT

DNase I Stock solution 2.7 U/μL

DNase I in RNase-free H₂O

Storage at -20 °C

DNase I solution (digest) 0.4 U/μL

Prepared upon usage

RT-qPCR Primer Mix; 2 μM forward Primer (fwd)

1:50 dilutions from 100 μM Primer Stock solutions in HPLC H₂O 2 μM reverse Primer (rev)

2.1.5 Enzymes and antibodies

Enzyme	Manufacturer (Location (city/country))
--------	--

DNase I (RNase-Free) lyophilized	Qiagen (Hilden, Germany)
----------------------------------	--------------------------

RNaseOUT™ recombinant ribonuclease inhibitor (5000 U, 40 U/μL)	Invitrogen (Carlsbad, California, USA)
--	--

SuperScript™ III Reverse Transcriptase (10000 U, 200 U/μL)	Invitrogen (Carlsbad, California, USA)
--	--

FirePol Taq	Solis BioDyne (Taru, Estonia)
-------------	-------------------------------

2.1.6 DNA standards

Standard	Manufacturer (Location (city/country))
----------	--

GeneRuler 100 bp Plus DNA Ladder	Thermo Fisher Scientific, USA
----------------------------------	-------------------------------

2.1.7 Kits

Kit	Manufacturer (Location (city/country))
-----	--

RNeasy MinElute® Cleanup Kit	Qiagen (Hilden, Germany)
------------------------------	--------------------------

Storage at +4 °C

RNase-Free DNase Set	Qiagen (Hilden, Germany)
----------------------	--------------------------

Storage at RT

QIAamp® DNA Mini Kit	Qiagen (Hilden, Germany)
----------------------	--------------------------

Storage at RT

RNA Pico Chips (for Agilent 2100 Bioanalyzer System)	Agilent Technologies
--	----------------------

NucleoSpin® Gel and PCR Clean-up	Macherey-Nagel (Düren, Germany)
----------------------------------	---------------------------------

KAPA HiFi HotStart PCR Kit	Roche, Basel (Schweiz)
----------------------------	------------------------

2.1.8 Cell lines

Cell-line	Manufacturer (Location (city/country))
-----------	--

NF54: Sanaria's master cell bank (lot: RKV01-092505) Aliquot A	Sanaria Inc. (Rockville, Maryland, USA)
--	---

NF54: Sanaria's master cell bank (lot: RKV01-092505) Aliquot B	Sanaria Inc. (Rockville, Maryland, USA)
--	---

7G8: Sanaria's working cell bank (lot: SAN03-021214) Aliquot 1	Sanaria Inc. (Rockville, Maryland, USA)
--	---

7G8: Sanaria's working cell bank (lot: SAN03-021214) Aliquot 2	Sanaria Inc. (Rockville, Maryland, USA)
--	---

2.1.9 Oligonucleotides for PCRs

Primer	Sequence (5' → 3')	Publication
--------	--------------------	-------------

MSP1_fwd.	TTCGGCACATTCTTCCATAA	Robert et al. 1996
MSP1_rev.	ATTCATTAATTTCTTCATATCCATC	Robert et al. 1996
K1_fwd.	GAAATTACTACAAAAGGTGCAAGTG-ATTO550-label	Robert et al. 1996
K1_rev.	AGATGAAGTATTTGAACGAGGTAAAGTG	Robert et al. 1996
RO33_rwd.	GCAAATACTCAAGTTGTTGCAAAGC-HEX5-label	Robert et al. 1996
RO33_rev.	AGGATTTCAGCACCTGGAGATCT	Robert et al. 1996
Mad20_fwd.	GAACAAGTCGAACAGCTGTTA-FAM-label	Robert et al. 1996
Mad20_rev.	TGAATTATCTGAAGGATTTGTACGTCTTGA	Robert et al. 1996
331_varF_dg 2	tcgtcggcagcgtcagatgtgtataagagacagGCAMGMAGTTTYGCN GATATWGG	Wichers et al. 2021
312_brlong3	gtctcgtgggctcggagatgtgtataagagacagTCTTCDSYCCATTCVT CRAACCA	Wichers et al. 2021
P5-PCR index primer	AATGATACGGCGACCACCGAGATCTACAC[i5]TCGTCG GCAGCGTC	Nag et al. 2017, Wichers et al. 2021
P7-PCR index primer	CAAGCAGAAGACGGCATAACGAGAT[i7]GTCTCGTGGGC TCGG	Nag et al. 2017, Wichers et al. 2021

2.1.10 Technical equipment and devices

Equipment/devices	Manufacturer (Location (city/country))
Heraeus, Megafuge 1.0R (Centrifuge culture lab)	Thermo electron corporation (Osterode, Germany)
Heratherm IGS100 Incubator	Thermo Fisher Scientific, Massachusetts, USA
Waterbath (37 °C) 1083 (GFL)	Lauda (Lauda-Königshofen, Germany)
CRYSTAL-Gemisch (1 % O₂, 5 % CO₂, 94 % N₂)	Air Liquide (Paris, France)
BVC control Fluid aspiration system	Vacuumbrand GmbH & Co. KG (Wertheim, Germany)
Eppendorf Centrifuge 5810 R (Falcon tubes 15- and 50 mL)	Eppendorf (Hamburg, Germany)
LightCycler® 480	Roche (Basel, Switzerland)
Eppendorf Centrifuge 5804 R (96 and 384 well plates)	Eppendorf (Hamburg, Germany)
Pipet-Lite™ XLS LTS™ 0.1-2 µL	Mettler Toledo (Columbus, Ohio, USA), Rainin
Pipet-Lite™ XLS LTS™ 0.5-10 µL	Mettler Toledo (Columbus, Ohio, USA), Rainin
Pipet-Lite™ XLS LTS™ 2-20 µL	Mettler Toledo (Columbus, Ohio, USA), Rainin
Pipet-Lite™ XLS LTS™ 20-200 µL	Mettler Toledo (Columbus, Ohio, USA), Rainin
Pipet-Lite XLS LTS 100-1000 µL	Mettler Toledo (Columbus, Ohio, USA), Rainin
AutoRep E	Mettler Toledo (Columbus, Ohio, USA), Rainin
Pipet-Lite™ XLS+™	Mettler Toledo (Columbus, Ohio, USA), Rainin
Peqlab Primus 25 Thermocycler	VWR International (Radnor, Pennsylvania, USA)
2100 Bioanalyzer instrument	Agilent Technologies
Eppendorf Thermomixer F1.5	Eppendorf (Hamburg, Germany)
C1000 Touch Thermal Cycler	Bio-Rad Laboratories, Inc. (Hercules, California, USA)
Microwave	Micromaxx™
P1000, P200, P20, P10 Pipetman Pipettes	Gilson Inc. (Middleton, Wisconsin, USA)
ChmiDoc XRS+ System	Bio-Rad Laboratories, Inc. (Hercules, California, USA)
VWR® VV3, Vortex Schüttler	VWR International (Radnor, Pennsylvania, USA)
Applied Biosystem™ 3130/3130x DNA Analyzer	Thermo Fisher Scientific, Massachusetts, USA
Zeiss Axio light microscope	Carl Zeiss AG (Oberkochen, Germany)

2.1.11 Labware and disposables

Labware/disposables	Manufacturer (Location (city/country))
FALCON®, 50 mL Polypropylene Canonical Tube, nuclease-free	Corning Inc. (Corning, New York, USA)
FALCON®, 15 mL Polypropylene Canonical Tube, nuclease-free	Corning Inc. (Corning, New York, USA)
Costar®, Stripette® 5 mL, sterile	Corning Inc. (Corning, New York, USA)
Costar®, Stripette® 10 mL, sterile	Corning Inc. (Corning, New York, USA)
Costar®, Stripette® 25 mL, sterile	Corning Inc. (Corning, New York, USA)
Filter tip 20 µL	SARSTEDT AG & Co. KG (Nümbrecht, Germany)
Biosphere® Filter Tips (2-20 µL)	SARSTEDT AG & Co. KG (Nümbrecht, Germany)
Filter tip 200 µL	SARSTEDT AG & Co. KG (Nümbrecht, Germany)
Filter tip 1000 µL	SARSTEDT AG & Co. KG (Nümbrecht, Germany)
Filtropur S 0.2 (sterile filtration of solutions)	SARSTEDT AG & Co. KG (Nümbrecht, Germany)
Stericup Quick Release-GP Sterile Vacuum Filtration system, 0.22 µm pore size	Merck KGaA (Darmstadt, Germany), Millipore
Safe-Lock Tubes 1.5 mL	Eppendorf (Hamburg, Germany)
Objektträger (76x62 mm), glass slides	Engelbrecht (Edermünde, Germany)
Petri dishes for cell culture (145 x 20 mm)–30 mL	Greiner Bio (Kremsmünster, Austria)
Petri dishes for cell culture (92x16 mm)–10 mL	SARSTEDT AG & Co. KG (Nümbrecht, Germany)
Petri dishes for cell culture (60x16 mm)–5 mL	SARSTEDT AG & Co. KG (Nümbrecht, Germany)
Nalgene™ Cryo 1 °C Freezing Container	Thermo Fisher Scientific (Waltham, Massachusetts, USA)
Lock&Lock-plastic boxes (cell culture)	iSi Deutschland GmbH (Solingen, Germany)
Mikro-Schraubrohre 2 mL (cryotube)	SARSTEDT AG & Co. KG (Nümbrecht, Germany)
Tube 15 mL, sterile (15 mL falcon tube, cell culture)	SARSTEDT AG & Co. KG (Nümbrecht, Germany)
Adhesive qPCR Seal (nuclease-free)	SARSTEDT AG & Co. KG (Newton, North Carolina, USA)
Encode Tip, sterile, 0.5 mL	Mettler Toledo (Columbus, Ohio, USA), Rainin
384 Well Lightcycler plate PP	SARSTEDT AG & Co. KG (Nümbrecht, Germany)
Pipet tips GP-L LTS 1000 µL 768/8	Mettler Toledo (Columbus, Ohio, USA), Rainin
Pipet tips GP-S LTS 20 µL 960A/10	Mettler Toledo (Columbus, Ohio, USA), Rainin
Pipet tips GP-S LTS 250 µL 960A/10	Mettler Toledo (Columbus, Ohio, USA), Rainin
Multiply®-µStrip Pro 8-strip	SARSTEDT AG & Co. KG (Nümbrecht, Germany)
the X-TRACTA Generation II	Biozym (Hamburg, Germany)
Multiply®-µStrip Pro 8-strip	SARSTEDT AG & Co. KG (Nümbrecht, Germany)
96 well plates (GeneScan)	Thermo Fisher Scientific, Massachusetts, USA
MultiScreen HTS BV Filter Plate 1.2 µM (MSBVS 1210)	Merck Millipore (Bellerica, Massachusetts, USA)

2.1.12 Software, input files and databases

Software/Database (version/year)	Source/developer
-------------------------------------	------------------

REDCap® (12.0.19)	Vanderbilt University
VarDB	
PlasmoDB	https://plasmodb.org
STAR (version: 2.7.10a)	Alexander Dobin (https://github.com/alexdobin/STAR)
Featurecounts (version 2.0.6)	Liao, Smyth, and Shi 2013, 2019
PlasmoDB-59_Pfalciparim_3D7_genome.fasta	https://plasmodb.org/plasmo/app/downloads
PlasmoDB-62_Pfalciparum3D7.gff	https://plasmodb.org/plasmo/app/downloads
Plasmodium falciparum transcriptome manuscript	Tonkin-Hill et al. 2018, https://github.com/gtonkinhill/falciparum_transcriptome_manuscript
R	Version 4.3.1
Varia tool	Mackenzie et al. 2022 https://github.com/GCJMackenzie/Varia
MS Office (2019)	
Galaxy Webtool	https://usegalaxy.org/
GraphPad Prism (version: 10.2.1 (339))	GraphPad Software, Boston (USA)
cd-hit (version: 4.8.1)	Weizhong Li (https://github.com/weizhongli/cdhit/release)
Seqtk (version 1.3-r106)	Heng Li (https://github.com/lh3/seqtk/releases)
cUps (2023)	Qian Feng (https://github.com/qianfeng2)
Biorender	https://www.biorender.com/
RAWGraphs 2.0	Mauri et al. 2017 (https://app.rawgraphs.io/)
LightCycler software	LightCycler® 480 software 1.5.1.62 SP3 (Roche)

2.2 Methods

2.2.1 Routine cell culture for NF54/7G8: Sanaria's master cell bank parasites

Thawing: RPMI complete Medium (cRPMI) media was pre-warmed and samples were thawed at 37 °C (water bath). Thawed samples were transferred to a sterile 15 mL falcon tube and supplemented for in total three times with 1x equal volume of Malaria Thawing Solution (MTS). For this, each supernatant was discarded following centrifugation at 755 g for 3 min at RT. The remaining pellet was resuspended in 5 mL of cRPMI and transferred to a 5 mL peri dish and hematocrit level was adjusted to 5 % with 0+ RBCs obtained from the blood bank at the University Hospital Eppendorf (UKE). Petri dishes were incubated at 37 °C in gas mix (1% O₂, 5% CO₂, and 94% N₂) filled and sealed plastic boxes. The following day, media was removed using autoclaved, sterile glass pipettes applied to a vacuum pump leaving only settled RBCs left in petri dishes. Fresh, pre-warmed cRPMI media was added to reach 5% hematocrit utilizing sterile Stripettes®.

Cell culture maintenance: Culture dishes were checked bidaily by Giemsa smears. For this, 1-2 µL RBCs from culture dishes were pipetted on and smeared across a glass slide. The cells on the slides were fixed by briefly immersing the slide in a staining through filled with absolute methanol (1 min) and afterwards stained in 10 % Giemsa solution for 10–15 min. Stained blood smears were analyzed by light microscopy (100X, oil immersion) to calculate parasitemia (ratio count (infected-) vs. count (uninfected RBCs)) and to quantify the parasite stages (ring, early trophozoite, late trophozoite, schizont, gametocyte) based on the distinct morphological differences between the blood stages of *P. falciparum*.

(ratio count (specific stage) vs. count (total infected cells). Culture dishes were kept at parasitemia < 2% and supplemented with fresh, prewarmed cRPMI at least every second day. Petri dishes were placed in a sealed plastic box in gas mix (1% O₂, 5% CO₂, and 94% N₂) atmosphere and incubated at 37 °C.

Freezing: Infected RBC cultures (~2–3 % ring stage parasitemia) from 10 mL petri dishes (5 % hematocrit) were transferred to a sterile 15 mL falcon tube and spun down at 755 g for 3 min at RT. The media phase was discharged and the remaining 500 µL pellet was pipetted into a cryotube and gradually supplemented with 1 mL Malaria Freezing Solution (MFS). The cryotube was stored in an Isopropanol-filled freezing container -80 °C. After one week the cryotubes were transferred to a liquid nitrogen tank (-195.8 °C).

2.2.2 Synchronization of NF54/7G8: Sanaria's master cell bank parasites with D-Sorbitol

For the analysis of highly synchronized ring stage parasite RNA, per culture dish a Giemsa staining was performed (section 2.2.1) and cultures containing mostly (>50 %) ring stage parasites at > 2% parasitemia underwent a synchronization protocol. For this, RBCs were resuspended and transferred to a sterile 15 mL falcon tube, centrifuged at 755 g for 3 min at RT and the supernatant was discarded. Next, the RBC pellet was resuspended in 5x volume units 5 % D-Sorbitol solution and incubated for ~10 min at 37 °C (water bath) to allow osmotic lysis of trophozoite and schizont stages which are sensitive to D-Sorbitol due to their new permeation pathways (Ginsburg et al., 1983). After centrifugation (755 g, 3min, RT), the light red supernatant was discarded and the pellet washed once in 5 mL cRPMI medium. The remaining RBC pellet was resuspended in fresh cRPMI and supplemented with 0+ RBCs to a final hematocrit level of 5 %. Petri dishes were placed in sealed plastic boxes, filled with gas mix (1% O₂, 5% CO₂, and 94% N₂) for 20 sec and incubated at 37 °C. Synchronization results in cultures containing parasites aged 0–12 hrs post invasion. For tighter synchronization, the protocol was repeated after 6 hrs to obtain parasites aged 6–12 hrs post invasion.

2.2.3 Controlled invasion of NF54/7G8: Sanaria's master cell bank parasites with Percoll

Following the same parasite cycle after synchronization, ring stage parasites which developed to schizonts underwent controlled invasion to enhance the synchronicity of the culture. Giemsa staining was performed to ensure the presence of late stage schizonts. These stages are separated from other stages by density gradient using 60 % Percoll solution (Rivadeneira et al., 1983). For this purpose, iRBCs are resuspended in culture medium, transferred to a sterile 15 mL falcon tube, centrifuged (755 g for 3 min at RT) and most of the supernatant discarded. The RBCs were resuspended in ~5–6 mL of remaining cRPMI media and carefully superimposed to a new sterile 15 mL falcon tube, which was prefilled with ~5–6 mL of 60 % Percoll solution. After gentle centrifugation (Eppendorf centrifuge; 180 g, 5 min, RT; acceleration 7, deceleration 1), an iRBC layer of schizonts is visible on top of the Percoll solution. The supernatant above the layer was discarded and schizonts were collected with a P1000 pipette into a new 15 mL falcon tube. After addition of 10 mL of cRPMI media, the iRBCs were pelleted at (755 g for 3 min, at RT) and the supernatant removed. The remaining schizont pellet was resuspended

in 10 mL of culture medium, supplemented with RBCs to 5 % hematocrit, culture boxes filled with gas mix (1% O₂, 5% CO₂, and 94% N₂) for 20 sec and incubated for 4 hrs at 37 °C to allow bursting of the schizonts and reinvasion of new RBCs. Parasites aged 0–4 hrs post invasion. After another 4 hrs, the cultures were again synchronized to remove remaining schizonts according to the synchronization protocol (section 2.2.2). To avoid potential impacts of Sorbitol and Percoll treatments on the transcriptomic profile of *P. falciparum* parasites, tightly synchronous 0–4 hpi old ring stage parasites were allowed to progress another cycle before harvest similar as elsewhere described (Bachmann et al., 2012; Wichers et al., 2019).

For harvesting, tightly synchronized ~4–8 hrs old ring stage parasites at 2–3 % parasitemia, were resuspended in culture medium, transferred to a nuclease-free 15 mL falcon tube, spun down (755 g for 3 min at RT) and the supernatant was removed. The remaining RBC pellet was lysed using 5x volume units of pre-warmed TRIzol®, shaken vigorously and incubated for 3 min at 37 °C (water bath) before storing at -80 °C.

2.2.4 Inclusion criteria, samples processing and parasitemia quantification of *ex vivo* blood samples

The longitudinal L2 study (Pan African Clinical Trials Registry number: PACTR201901672024347) was approved by the Gabonese national ethics committee (Comité National d’Ethique de la Recherche) on 12/15/2018. Furthermore, sample analysis in trial partner sites in Tübingen (trial supervision) and in Hamburg was approved by local ethical committees, respectively. Healthy volunteers (aged 18–45) living close to the trial conducting site, the Centre de Recherches Médicales de Lambaréné (CERMEL) in Lambaréné, Gabon, were recruited for the LaCHMI-002 study. Individuals who were tested positive for sickle-cell trait, HIV, HBV, HCV, cardiovascular diseases and pregnancy or showed abnormal total blood counts or biochemistry were informed and excluded from the recruitment process. The included volunteers were checked for absence of parasites at baseline via thick blood smear (TBS). The volunteers underwent six consecutive CHMI infections at 8-week intervals with either Sanaria® PfSPZ Challenge (7G8) or (NF54) sporozoites by direct venous inoculation. From day five post infection, volunteers were screened for malaria parasites by routine blood drawings (Figure 9, Supplementary Table 1) three times per week until day 28 post-infection (4 weeks) and twice per week thereafter until the next challenge infection is applied (8 weeks interval) or the end of the trial. During each visit, blood was drawn for subsequent analyses, however not exceeding 500 mL of blood per single volunteer in total during the entire trial. Subsequently a thick-blood smear (TBS) was taken to determine the asexual parasitemia which was confirmed by a second slide lecturer and upon strong deviations a third lecture was conducted. Per visit, the average TBS parasitemia (mean of 2–3 lectures), date, time, blood volume and adverse events were registered. Blood was drawn into Heparin and EDTA-tubes according to the trial’s guidelines (Lell and McCall 2018). All event data were registered on paper first and later in a REDCap® database.

EDTA blood processing (samples < 1000 pf/μL): Blood tubes were placed in 15 mL falcon tubes and centrifuged for 5 min at 2000 g at RT. The top phase (plasma) was transferred to an Eppendorf tube and

stored at -20 °C for selected time points (at baseline, and prior to each CHMI in eight-week intervals). The remaining RBC pellet was resuspended in 5x volume of PBS. In another 15 mL falcon tube 7 mL of Ficoll was prepared and superimposed with the diluted RBC sample. If no plasma was collected, Ficoll gradient was performed with whole blood. After 20 min of centrifugation (2000 x g, RT, deceleration off) the pellet was washed with PBS, lysed in 5x volume of prewarmed TRIzol® and stored at -80 °C.

EDTA blood processing (samples > 1000 pf/μL): After the Ficoll gradient, the RBC pellet was resuspended in 10 mL of sterile PBS. The sample was then again pelleted (2000 g, 5 min, RT) and resuspended in 3x volume of PBS. Next, the suspension was filtered through PBS calibrated Plasmodipur-filter to remove white blood cells (WBCs). After pelleting, the RBCs were rapidly lysed in 5x volume of prewarmed TRIzol® and stored at -80 °C.

gDNA samples: For the analysis of gDNA, the PBS wash fractions from the EDT sample processing were kept and collected, centrifuged at 755 g for 3 min at RT and the remaining pellet was resuspended in 300 μL PBS and stored at -80 °C.

2.2.5 Isolation of *P. falciparum* RNA

Total RNA was extracted from TRIzol®-lysed RBCs either from volunteers or *in vitro* culture (section 2.2.1, 2.2.3 and 2.2.4). The TRIzol sample was thawed at 37°C and split into 1 mL aliquots. Per 1 mL of TRIzol®, either 200 μL of cold Chloroform or 100 μL of 1-bromo-3-chloropropane (BCP) was added to individual safe-locked Eppendorf tubes (1.5 mL). Individual Eppendorf tubes were shaken vigorously for 15 sec to allow proper mixing and incubated for 3 min at RT. After centrifugation (30 min, 25000 g, +4 °C), the samples were placed on ice and the aqueous phases were collected in RNase-free 15 mL falcon tubes. After addition of equal amounts of 70 % Ethanol, the samples were briefly vortexed. Subsequently, the manual of the RNeasy MinElute® Cleanup Kit (Qiagen) was followed for RNA purification. Briefly, the entire RNA from each sample was fixed on RNeasy MinElute® column membranes by repeated loading of 700 μL sample volumes and centrifuging (30 sec, 8000 g, RT) steps. The column was then washed with 350 μL RW1 (Qiagen, RNeasy MinElute® Kit) wash buffer. DNase I stock solution was diluted 1:7 in RDD buffer (Qiagen RNase-Free DNase Set®), each sample column was loaded with 80 μL of DNase I solution and incubated for 30 min to allow digestion of remaining DNA. After several washing (350 μL RW1 buffer and 2x 500 μL RPE (both Qiagen, RNeasy MinElute® Kit)) and centrifugation steps (30 sec, 8000 g, RT, last wash step with RPE for 2 min), a dry spin (5 min, 1000 g, RT), the samples were eluted two times in either 2x 14 μL (NF54 culture samples), 2x 27 μL (patient sample parasitemia < 1000 pf/μL) or 2x 51 μL (patient sample parasitemia > 1000 pf/μL). For all samples 1 μL of eluted RNA was utilized for nanodrop measurements and another 1 μL was used to check for remaining DNA content by qPCR (section 2.2.6).

2.2.6 Control qPCR for residual genomic DNA in *P. falciparum* RNA samples

Remaining gDNA in RNA samples interferes with transcriptomic analyses, therefore removal with DNase I is crucial. To estimate the amount of possibly remaining *P. falciparum* gDNA content, qPCR using primers for the ring stage-expressed core gene *sbp1* (*skeleton binding protein 1*) was performed. For this, 1 μ L of RNA solution was utilized and diluted with nuclease-free H₂O to a final concentration of 50 ng/ μ L. A primer-mix consisting of forward and reverse *sbp1* primers were prediluted in HPLC H₂O (1:50) from 100 μ M (stock solution) to 2 μ M (working solution) into a single Eppendorf tube. *P. falciparum* NF54 gDNA isolated from culture samples served as a positive control and nuclease free H₂O as a negative control. The following pipetting scheme and qPCR protocol was followed:

Table 1.: qPCR pipetting scheme gDNA check.

Reagent	Concentration	Per reaction (μ L)	Final concentration/amount
Nuclease-free H ₂ O		1.5	
2x SYBR Green PCR Master mix	2x	5	1x
Primer-Mix <i>sbp1</i>	2 μ M each	2.5	0.5 μ M each
Template RNA/gDNA	\leq 50 ng/ μ L	1	\leq 50 ng
Total volume		10	

qPCR reactions were prepared in a 384 well plate afterwards sealed with a PCR foil using a scratcher. Plates were briefly centrifuged (short spin) to remove potential bubbles and to collect all reagents at the conical tip of the well plates. Plates were placed in the LightCycler® 480 and RT-qPCR was initiated with the LightCycler® 480 software 1.5.1.62 SP3 according to (Table 2).

Table 2.: (RT-)qPCR cycling for gDNA check and *var* gene RT-qPCR.

Time	Temperature (°C)	Cycles (x)	Description
15 min	95	1	Activation step for HotStart DNA polymerase
15 sec; 1 min	95; 60	40	Denaturation; Annealing and Elongation
	60-95	2.5 °C/sec.	Melting
1 min	40	1	Cooling

After the cycling, fit point analysis was applied to each sample using the same software to determine the threshold and C_t values (in duplicates). Samples with both replicates showing C_t values <35 in combination with a specific T_m values (Table 7) underwent an additional gDNA digestion (section 2.2.7) and control qPCR to check absence of gDNA. Samples showing deviating T_m values (e.g., due to primer dimers or unspecific PCR products) were considered to be clean for *P. falciparum* gDNA.

2.2.7 DNA digestion in solution

RNA samples with remaining gDNA content (section 1.2.5) underwent an additional DNA digestion in solution. For this, the eluted RNA was filled to 87.5 μ L with RNase-free H₂O and supplemented with 10 μ L RDD buffer (Qiagen, RNeasy MinElute® Kit) and 2.5 μ L DNase I stock solution. After 30 min, another 2.5 μ L of DNase I stock solution was added to the solution and again incubated for 30 min. Afterwards, per sample, 350 μ L of RLT (Qiagen, RNeasy MinElute® Kit) and 250 μ L Ethanol (absolute) was added to each Eppendorf tube. RNeasy MinElute® columns were loaded and centrifuged (30 sec, 8000 g, RT). Column washing was performed in two steps utilizing 500 μ L RPE (Qiagen, RNeasy MinElute® Kit). Following a dry spin step (5 min, 1000 g, RT), the RNA was eluted in 2x 27 μ L of RNase-free H₂O. 1 μ L of eluted RNA was utilized for nanodrop measurements and another 1 μ L was used to check for remaining DNA content (section 2.2.5).

2.2.8 Determination of the specificity, efficiency and dynamic range of the *var*-qPCR

Primer efficiencies and specificity were determined earlier by colleagues on the LightCycler® 480 PCR machine following the standard protocol for qPCR (section 2.2.5, Table 2). For this, various inputs of NF54 gDNA (10 ng, 1 ng, 0.1 ng, 0.01 ng, 0.001 ng and 0.0001 ng) were amplified in 0.5 μ M (each) pre-diluted primer-mixes. C_t-value derived from reactions with different log concentrations were plotted and the primer efficiencies were determined calculated using the slope: $E = -1 + 10^{(-1/\text{slope})}$. Generated amplicons were melted by increasing the temperature in steps of 2.5 °C/sec at the end of the protocol to assess the melting temperature of the specific amplicons as a reference for following qPCR reactions.

Primer check prior to RT-qPCR reactions: For facilitation, pre-dilutions of primer-mixes (2 μ M, each) were prepared in deep well plates. These ready-to-use primer-mixes were added to a final concentration of 0.5 μ M to the qPCR reactions (Table 1) using multichannel pipettes. A qPCR test was performed with new primer dilutions to check for correct amplicons using gDNA as a template. Each amplicon was reassessed for correct melting temperature, similar C_t value compared to previous primer checks and absence of primer dimers to ensure that all 52 or 68 primer dilutions were suitable for subsequent RT-qPCR analysis of all 7G8 or NF54 *var* genes, respectively (Table 7, 8).

2.2.9 cDNA synthesis

cDNA was synthesized from RNA serving as a double stranded template for RT-qPCR reactions. Total RNA isolated from (i)RBCs contains a mixture of *P. falciparum* specific RNAs and human derived RNAs in varying proportions. Thus, instead of using the RNA concentration measured by nanodrop, we estimated the amount of *P. falciparum* RNA per sample based on the parasitemia of the sample (section 2.2.4). We estimated that RNA from 10,000 parasites per cDNA reaction is sufficient for our analysis. Therefore, RNA from high parasitemia samples (>910 pf/ μ L (910 pf/ μ L x 11 μ L template volume = 10010 pf)) was diluted accordingly with nuclease-free H₂O to reach a maximum of 10,000 parasites per reaction (Table 3). For samples which require more than 11 μ L input volume to reach 10,000, the input

volume was not further increased to avoid overloading of the RT reaction (total volume of 20 μ L per reaction). Afterwards, the cups were placed on ice and 1 μ L of random primers (2 μ g/ μ L) and 1 μ L of deoxynucleotide triphosphate (dNTPs) (10 mM each) were added. RNA denaturation and random primer annealing was conducted for 5 min at 65 °C on a Primus 25 advanced Thermocycler. Subsequently, per cup 4 μ L of 5x First-strand buffer, 1 μ L of Dithiothreitol (100 mM DTT), 1 μ L of Superscript III reverse transcriptase (20U/ μ L) and 1 μ L (RNase OUT, 40U/ μ L) were added to a final volume of 20 μ L. The cDNA synthesis was carried out on a Peqlab Primus 25 Thermocycler (Table 4).

Table 3.: RNA template input for cDNA synthesis based on parasitemia of the RBC samples as a proxy for *P. falciparum* RNA content.

Sample parasitemia (pf/ μ L)	Intake cDNA synthesis-PCR for 10,000 parasites per reaction
>910 pf/ μ L	1-11 μ L depending on the parasitemia, add nuclease-free H ₂ O to a total volume of 11 μ L
<910 pf/ μ L	11 μ L

Table 4.: cDNA synthesis: Annealing, cDNA synthesis and enzyme inactivation program.

Time (min.)	Temperature (°C)	Cycles (x)	Description
5	25	1	Primer annealing
60	50	1	cDNA synthesis
15	70	1	Inactivation of the SS III transcriptase
∞	8		End/Storage

If more than one cDNA reaction was performed per samples, these were combined in a safe-lock Eppendorf tube. All cDNA reactions were diluted 1:4 with nuclease-free water to a final volume of 80 μ L and stored at -20 °C.

2.2.10 *var* gene RT-qPCR for samples with an NF54 and 7G8 genotype

For samples from NF54 CHMI infections, 61 primer pairs amplifying each individual NF54 *var* gene variant were used. Additionally, primer pairs for two situins (*sir2A*, *sir2B*), coding for histone deacetylases involved in the epigenetic control of *var* gene expression, the ring-stage expressed genes *sbp1*, *mahrp* (membrane-associated histidine-rich protein 1) and *kahrp* (knob-associated histidine-rich protein) (Looker et al., 2019; Rug et al., 2006; Spycher et al., 2003, 2008) were included. The *fructose 1,6-bisphosphate aldolase* and *arginyl-tRNA-synthetase* were used as housekeeping genes (Table 8). The RT-qPCR protocol (Table 5) was optimized to 10 μ L PCR reaction volumes in 384 well plates using 2 μ L of 1:4 diluted cDNA template. To generate sufficient amounts of cDNA template for 68 RT-qPCR reactions in duplicates (68 x 2 x 2 μ L = 272 μ L), we prepared 80 μ L cDNA template by four 20 μ L cDNA reactions and diluted it 1:4 with nuclease-free H₂O to a final volume of 320 μ L. Dilution of cDNA is necessary

Material and Methods

avoid PCR inhibition by cDNA synthesis reagents. The significantly smaller *var* gene repertoire of 7G8 required only three cDNA reactions for 53 primer pairs tested in total (45 *var* genes + *sirA*, *sirB*, *sbp1*, *mahrp*, *kahrp*, *fructose 1,6-bisphosphate aldolase*, *arginyl-tRNA-synthetase*) (Table 7,8).

The following pipetting scheme was used to test primer pairs in duplicates in the LightCycler 480®:

Table 5.: RT-qPCR pipetting scheme.

Reagent	Concentration	Per reaction (μ L)	Final concentration/amount
Nuclease-free H ₂ O		0.5	
2x SYBR Green PCR Master mix	2x	5	1x
Primer-Mix (68 primer pairs)*	2 μ M each (fwd. and rev.)	2.5	0.5 μ M each (fwd. and rev.)
Template cDNA/gDNA		2	
Total volume		10	

*Sequences of the tested primer pairs can be found in Table 6 and 7

Table 6.: NF54 *var* gene RT-qPCR primer set.

A single primer pair targets two B-type variants simultaneously (PF3D7_0324900, PF3D7_0300100) due to high sequence similarity. All primers are HPLC purified, their primer efficiencies and T_m values determined according to section 2.2.7.

Primer ID	Designer/Reference	<i>P. falciparum</i> gene ID	Description	Forward (5'→3') Sequence	Reverse (5'→3') Sequence	Mean C _t with 2.5 ng gDNA	Efficiency	T _m value (°C)
001+002	Ali Salanti; (Salanti et al., 2003)	PF3D7_0100100	<i>var</i> , B-type	TGCGCTGATAACTCACAACA	TGCGCTGATAACTCACAACA	16.71	2.026	79.22
005+006	Ali Salanti; (Salanti et al., 2003)	PF3D7_0421104	<i>var</i> , B-type	GACGAGGAGTCGGAAAAGAC	TGGACAGGCTTGTGAGAG	15.89	1.983	81.45
009+010	Ali Salanti; (Salanti et al., 2003)	PF3D7_1100100	<i>var</i> , B-type	GAGGCTTATGGGAAACCAGA	AGGCAGTCCTTGGCATCTTT	20.10	1.975	78.78
011+012	Ali Salanti; (Salanti et al., 2003)	PF3D7_1100200	<i>var</i> , A-type	GACGGCTACCACAGAGACAA	CGTCATCATCGTCTTCGTTT	15.93	1.949	85.32
021+022	Anna Bachmann; (Bachmann et al. 2019)	PF3D7_1240300	<i>var</i> , B/C-type	ACGCAGAAGTACAAGAGATGC	ATCCGGTGATGTCGTTCCCT	15.62	1.948	75.25
027+028	Matthias Frank; (Frank et al., 2007)	PF3D7_1255200	<i>var</i> , B-type	GCGAGGTCTCTCGTCTCTG	ATGACGAAGAAGCAGCAGGT	15.90	1.951	78.79
029+030	Ali Salanti; (Salanti et al., 2003)	PF3D7_1200100	<i>var</i> , B-type	CGGAGGAGGAAAAACAAGAG	TGCCGTATTGAGACCACAT	18.98	1.947	78.69
033+034	Ali Salanti; (Salanti et al., 2003)	PF3D7_1300300	<i>var</i> , A-type	CACAGGTATGGGAAGCAATG	CCATACAGCCGTGACTGTTC	16.45	2.040	79.26
039+040	Ali Salanti; (Salanti et al., 2003)	PF3D7_0324900, PF3D7_0300100	<i>var</i> , B-type	CAATCTGCGCAATAGAGAC	CCACTGTGAGGGGTTTCT	15.72	1.937	80.37
043+044	Ali Salanti; (Salanti et al., 2003)	PF3D7_0412400	<i>var</i> , C-type	ACCGCCCCATCTAGTGATAG	CACCTGGTGATGTGGTGTA	15.57	2.016	81.37
045+046	Ali Salanti; (Salanti et al., 2003)	PF3D7_0412700	<i>var</i> , C-type	TAAAAGACGCCAACAGATGC	TCATCGTCTCTGCTCTCGTC	15.9	2.018	83.04
049+050	Ali Salanti; (Salanti et al., 2003)	PF3D7_0400100	<i>var</i> , B-type	GACGACGATGAAGACGAAGA	AGATCTCCGCAATTCGAATC	15.98	2.007	77.29
053+054	Ali Salanti; (Salanti et al., 2003)	PF3D7_0421300	<i>var</i> , B-type	TGCAACGAAACATTAGCACA	AGCAGGGGATGATGCTTAC	14.70	1.901	78.14
055+056	Ali Salanti; (Salanti et al., 2003)	PF3D7_0425800	<i>var</i> , A-type	AAACACGTGATGCGGATA	GACGCCGAGGAGGTAAATAG	15.8	1.905	76.26
057+058	Ali Salanti; (Salanti et al., 2003)	PF3D7_0426000	<i>var</i> , B-type	TGACGACTCTCAGACGAAG	CTCCACTGACGGATCTGTG	16.46	1.863	83.15
059+060	Ali Salanti; (Salanti et al., 2003)	PF3D7_0533100	<i>var1csa</i> , A-type, pseudogene	AAGAAAGTGCCACAACATGC	GTTCGTACGCCTGTGCTTTA	15.83	1.975	78.83
061+062	Anna Bachmann; (Bachmann et al. 2019)	PF3D7_0500100	<i>var</i> , B-type	GAGTGGTGGTAACACGGAGA	ATCTTGAGCGCAGTTGGG	16.67	1.958	80.12
065+066	Matthias Frank; (Frank et al., 2007)	PF3D7_0800300	<i>var</i> , B/A-type	GGAGGAGGAAGAGGAAAACG	CCACCTCTCTGTGTGTTG	15.46	1.961	82.24
069+070	Ali Salanti; (Salanti et al., 2003)	PF3D7_0800100	<i>var</i> , B-type	GTCGTGGAAAACGAAAGGT	TATCTATCCAGGGCCCAAAG	17.59	1.889	76.55

Material and Methods

071+072	Ali Salanti; (Salanti et al., 2003)	PF3D7_0632500	<i>var</i> , B/A-type	ATGIGTGCAGAGAAGGTGAAG	TGCCTTCTAGGTGGCATAACA	18.50	1.911	78.10
073+074	Ali Salanti; (Salanti et al., 2003)	PF3D7_0711700	<i>var</i> , C-type	CAATTTTCCGACGCTTGTA	CACATATAGCGCCGTCTTA	19.49	1.886	81.24
077+078	Matthias Frank; (Frank et al., 2007)	PF3D7_0712300	<i>var</i> , B/C-type	GGTGGAGGTAGTCCACAGGA	CAGCTATTTCCCCACCAGAA	17.46	1.957	78.86
079+080	Anna Bachmann; (Bachmann et al. 2019)	PF3D7_0712000	<i>var</i> , C-type	ATGAATTGGGCAAAAAGTGTAC G	TCATTCCAAATTGGTGCTAGTGA	15.54	1.921	75.00
081+082	Ali Salanti; (Salanti et al., 2003)	PF3D7_0712900	<i>var</i> , C-type	CACACATGTCCACCACAAGA	ACCCTTCGTGGTGTCTTCC	15.51	1.933	82.97
083+084	Ali Salanti; (Salanti et al., 2003)	PF3D7_0712800	<i>var</i> , B/C-type	ACGTGGTGGAGACGTAAACA	CCTTGTGTGTGCCACTTTG	15.84	1.901	76.16
085+086	Anna Bachmann; (Bachmann et al. 2019)	PF3D7_0712600	<i>var</i> , C-type	TGCACGACCAAATGAAAAAGGA	ATCGGTGGCACCTGTTTCTC	15.63	1.902	77.95
091+092	Ali Salanti; (Salanti et al., 2003)	PF3D7_0808700	<i>var</i> , B/C-type	TTTGTCGGAAAGACGATACA	ATCTGGGGCAGAATTACCAC	20.21	1.835	76.49
093+094	Ali Salanti; (Salanti et al. 2003)	PF3D7_0900100	<i>var</i> , B-type	TGCAAACCACCAGAAGAAAG	GTTCTCCGIGTGTCTCTCT	15.68	1.977	82.21
099+100	Ali Salanti; (Salanti et al., 2003)	PF3D7_1300100	<i>var</i> , B-type	ACAAAGGAACGTCCATCTCC	GCCAAATCTCCACATGATCG	15.74	1.916	79.34
101+102	Ali Salanti; (Salanti et al. 2003)	PF3D7_0809100	<i>var</i> , B/C-type	TGCAAGGGTGCTAATGGTAA	CCTGCATTTTGACATTCGTC	20.34	1.841	76.07
103+104	Ali Salanti; (Salanti et al., 2003)	PF3D7_0632800	<i>var</i> , B-type	GACAAATACGGCGACTACGA	TGTTTCACCCATTCTTCAA	18.48	1.975	80.51
107+108	Ali Salanti; (Salanti et al., 2003)	PF3D7_0420700	<i>var</i> , C-type	TCACAACCTGACCCCTACT	TCTTCGTCGTGTGTCATCCTC	15.57	2.000	79.97
109+110	Ali Salanti; (Salanti et al., 2003)	PF3D7_0937600	<i>var</i> 3, A-type	TGACCAAGACGAAGTATGGAA	TTGATCTCTGTCGCTGTC	15.88	1.991	75.40
119+120	Thomas Lavstsen; (Lavstsen et al., 2005)	PF3D7_0937800	<i>var</i> , B-type	ACAACAATTCGCAAGCAAG	TTCCCTCGCTCCTCTTCAT	16.60	2.084	77.41
121+122	Wai-Hong Tham; (Tham et al., 2007)	PF3D7_0600400	<i>var</i> 3, A-type	GCACATTATCAAACGCCC	AACCAGCTGCCTTGTGCAA	17.01	1.994	76.38
123+124	Ron Dzikowski; (Dzikowski et al., 2006)	PF3D7_0808600	<i>var</i> , C-type	CCTAAAAAGGACGCAGAAGG	CCAGCAACACTACCACCAGT	15.56	2.001	77.77
125+126	Madelaine Dahlbäck; (Dahlbäck et al. 2007)	PF3D7_0700100	<i>var</i> , B-type	GTCCTCTATGTGGAGTAAAAAG AA	AGTACCGTTATCTGGGTTTATAGGC	15.66	2.011	74.25
127+128	Madelaine Dahlbäck; (Dahlbäck et al., 2007)	PF3D7_0833500	<i>var</i> , B-type	AATCAGAAAAGTGTAATTCAG GAG	TTTACTATCATCACTGACACGCATT	15.89	1.972	74.89
139+140	Anna Bachmann; (Bachmann et al. 2019)	PF3D7_1240600	<i>var</i> , C-type	ACAAATAGTGATCCTGTAAATGAA CC	TGTTTGTATCCCACCTTTTCGC	15.59	2.069	73.75
141+142	Anna Bachmann; (Bachmann et al. 2019) Plos Pathogens	PF3D7_1373500	<i>var</i> , B-type	CAAGGAGGTAGCGGTGATCC	TAGCCTCACCATGCACCTCG	16.13	1.999	78.86
143+144	Anna Bachmann; (Bachmann et al. 2019)	PF3D7_0223500	<i>var</i> , B-type	GTGGAAGGGCGGTGATCC	AGTTTCACITTTCACTTGCTCGT	15.83	2.067	77.15
153+154	Anna Bachmann; (Bachmann et al. 2019)	PF3D7_1219300	<i>var</i> , B-type	TAATGTCGCCAAACCTGCAC	TCCACTTTATIGTTTGTATCCCACT	15.80	1.984	76.74
155+156	Anna Bachmann; (Bachmann et al. 2019)	PF3D7_0421100	<i>var</i> , B/C-type	GTGGTAAAGACGGAGCCACT	CCTTCACGTTGTCTGCTCACT	16.02	2.025	78.62
157+158	Anna Bachmann; (Bachmann et al. 2019)	PF3D7_0600200	<i>var</i> , B/A-type	GGAAGGAAATTTGGCAAGCTCA	TATTTCCGCACGGATGCCTT	15.73	1.944	79.38
159+160	Anna Bachmann; (Bachmann et al. 2019)	PF3D7_1240400	<i>var</i> , B/C-type	TGATGGCACAATCCCACCAG	AACGTGTCAATCATCGTGGT	15.45	1.944	74.92
161+162	Anna Bachmann; (Bachmann et al. 2019)	PF3D7_1240900	<i>var</i> , B/C-type	ACAGAAATGGTGGAAGAGGTGA	GCCGGAAGTGTAGTAGGATCG	15.78	1.936	78.34
163+164	Anna Bachmann; (Bachmann et al. 2019)	PF3D7_0412900	<i>var</i> , B/C-type	AGGGTGTGGATGACCGAAAC	TCCCATTTCCTTCGCCGTTC	16.24	2.016	76.90
165+166	Anna Bachmann; (Bachmann et al. 2019)	PF3D7_0413100	<i>var</i> , B/C-type	GGGTGTGGATGACCGAAACT	TCCTTTTCAGACGTATTGCACC	15.76	1.985	76.06
169+170	Anna Bachmann; (Bachmann et al. 2019)	PF3D7_0420900	<i>var</i> , C-type	TGGTGATAAGGACGGTGCCA	CGTCCITCACGTGTCTGCTCC	14.98	1.936	79.25
171+172	Anna Bachmann; (Bachmann et al. 2019)	PF3D7_0200100	<i>var</i> , B-type	TCCACCACTAGTGACATACCT	GAAACATCAGTATCAACGTTTGT	16.58	1.930	74.20
173+174	Anna Bachmann; (Bachmann et al. 2019)	PF3D7_0400400	<i>var</i> , A-type	ACAAGTCAATTGAGAGGCGA	TCGCATGAATTTGCAGGACC	15.82	1.940	80.22
175+176	Anna Bachmann; (Bachmann et al. 2019)	PF3D7_0733000	<i>var</i> , B-type	TGGTAAACAAGTGTGAATACGG A	TCATCCACTTGGTGGGGIT	16.41	1.990	74.00
177+178	Anna Bachmann; (Bachmann et al. 2019)	PF3D7_1041300	<i>var</i> , B-type	GGATACAACTGCCAAACATGC	TCTGACAAACGTCCATGCAA	17.50	1.987	73.49
235+236	Anna Bachmann; (Bachmann et al. 2019)	PF3D7_0115700	<i>var</i> , B-type	TGGTGACTGGTAGTGGTGT	TTTCGTGCACGTCCTTCCCA	16.94	1.920	76.62

Material and Methods

239+240	Anna Bachmann; (Bachmann et al. 2019)	PF3D7_1150400	<i>var</i> , A-type	AGCGACTCCGGATCCAATT	ACATCTTTTGTGCTTCGCT	16.01	1.912	75.07
241+242	Anna Bachmann; (Bachmann et al. 2019)	PF3D7_1200400	<i>var</i> , B/A-type	ACGCGTGCCTCIGACTATAA	CCTACCACGCGTAGAGCTT	19.97	1.896	77.73
243+244	Anna Bachmann; (Bachmann et al. 2019)	PF3D7_1200600	<i>var2csa</i> , E-type	TGGAAGTGGAGGTGATGGAT	GGAGGTGGTATTCTATCACAAGGA	15.84	2.056	74.11
245+246	Anna Bachmann; (Bachmann et al. 2019)	PF3D7_0617400	<i>var</i> , C-type	CTGACGAACCCGATGAGGAG	TCCICTGTGTTTGGTGGTGCT	15.66	1.965	77.09
247+248	Anna Bachmann; (Bachmann et al. 2019)	PF3D7_0800200	<i>var</i> , A-type	ACCTGTGGATACAAGCGATGT	TCTGCATCTCTTTCCTCGGT	16.07	1.947	74.68
251+252	Anna Bachmann; (Bachmann et al. 2019)	PF3D7_0712400	<i>var</i> , B/C-type	TGGGAAGCAAAATTGTGGTGT	TGGGTCATCTTTTCCGTGCT	16.01	2.000	76.32
255+256	Anna Bachmann; (Bachmann et al. 2019)	PF3D7_0100300	<i>var3</i> , A-type	ACCCCTACACGTCACCTAAA	ACCATCACCCTTACTTGGTGT	16.39	2.061	75.17

Table 7.: 7G8 *var* gene RT-qPCR Primer Set.

All primers are HPLC purified, their efficiencies and T_m values were determined according to section 2.2.7.

Primer ID	Designer/Reference	<i>P. falciparum</i> gene ID	Description	Forward (5'→3') Sequence	Reverse (5'→3') Sequence	Mean C_t with 2.5 ng gDNA	Efficiency	T_m value (°C)
257+258	Anna Bachmann; (Wichers-Misterek et al., 2023)	Pf7G8_020005600	<i>var</i> , B-type	GTGGATAAAACAAAAAGGGACG A	TACGTCCAGCACCATTGCTT	17.68	2,014	73.81
259+260	Anna Bachmann; (Wichers-Misterek et al., 2023)	Pf7G8_020026900	<i>var1csa</i> -A-type	TCAAAAGGTCATGGTGAGGGA	TCTGTCCACCAATCTTGGCG	17.52	2,057	75.50
261+262	Anna Bachmann; (Wichers-Misterek et al., 2023)	Pf7G8_060022500	<i>var</i> , B-type	AACCTGCTACCATTGCCACT	ACCCACGTTTGGTAGITCC	17.81	2,032	81.17
263+264	Anna Bachmann; (Wichers-Misterek et al., 2023)	Pf7G8_010005600	<i>var</i> , A-type	AGTGCAAACAGCATGTGAA	TATCGACTCGTGCATGTCGT	17.54	2,047	73.35
265+266	Anna Bachmann; Wichers-Misterek et al. 2023	Pf7G8_120024200	<i>var</i> , C-type	GGTGAGTGGATTGTTTCCA	GTTGTGATAGATTCCCCGGA	17.34	1,975	75.02
267+268	Anna Bachmann; (Wichers-Misterek et al., 2023)	Pf7G8_120024100	<i>var</i> , B-type	TGGGCAACAAGGTACAATGA	TTCCCGCAAAGTGTGCAC	17.43	2,014	75.76
269+270	Anna Bachmann; (Wichers-Misterek et al., 2023)	Pf7G8_120005700	<i>var2csa</i> , E-type	CGCTGGTTTACCGAATGGGC	GCAAACATTGTGTGGGCAAC	17.61	1,996	74.99
271+272	Anna Bachmann; Wichers-Misterek et al. 2023	Pf7G8_040030800	<i>var</i> , B-type	GTGCAGAGGAGGCAAAAGGAA	TTTTTACCGTCGGGGGCAG	18.62	2,065	78.84
273+274	Anna Bachmann; (Wichers-Misterek et al., 2023)	Pf7G8_040025600	<i>var</i> , C-type	GGCAAGCGCAACAAATCGTA	GCAGCACCACCACCATTAAC	17.44	2,064	77.07
281+282	Anna Bachmann; (Wichers-Misterek et al., 2023)	Pf7G8_050005500	<i>var</i> , A-type	CCAGATCTAGAGACGTTTCGCC	CCTTCTTCTCCTTTCCCGACA	17.46	2,038	77.87
285+286	Anna Bachmann; (Wichers-Misterek et al., 2023)	Pf7G8_070018200	<i>var</i> , B-type	TGAAGGATGACGACGAAGAAGG	TGGTTGGCAATATCCGATGAG A	17.19	2,082	75.01
287+288	Anna Bachmann; (Wichers-Misterek et al., 2023)	Pf7G8_070018000	<i>var</i> , B-type	GGGCCGAAGACTTTTGTAGG	TGGTTCGCGCGCAATTATG	17.25	1,976	76.34
289+290	Anna Bachmann; (Wichers-Misterek et al., 2023)	Pf7G8_070017600	<i>var</i> , C-type	CCCCTGTGATCAAACCCGAA	ATGACAGCGGGGTGTGTGAA	17.50	1,985	79.60
291+292	Anna Bachmann; (Wichers-Misterek et al., 2023)	Pf7G8_070017300	<i>var</i> , C-type	GGATGCAGGTGGTACAACACT	AACCATCAACGGTTCCATAGTCA	17.56	2,057	73.37
295+296	Anna Bachmann; (Wichers-Misterek et al., 2023)	Pf7G8_120045700	<i>var</i> , B-type	AAAAACGAGCTGCACGTAGTA	TGCATCAACGGTTTGATATCCAT T	17.22	1,985	72.70
297+298	Anna Bachmann; (Wichers-Misterek et al., 2023)	Pf7G8_120045800	<i>var</i> , B-type	ACCTCCACGACGTCAACACA	AATGAGTGGCTAGCATCACCA	17.61	1,942	76.32
299+300	Anna Bachmann; (Wichers-Misterek et al., 2023)	Pf7G8_120046200	<i>var</i> , C-type	TGGAAAAGACGTGTACGAAACA	GCTGCTAACAGTTTCCCAAC	17.28	2,001	76.15
303+304	Anna Bachmann; (Wichers-Misterek et al., 2023)	Pf7G8_120046600	<i>var</i> , C-type	AATGGTCGTCGTGGTGAAC	TCCGCACAACCTGACCTTC	17.19	1,992	77.08
307+308	Anna Bachmann; (Wichers-Misterek et al., 2023)	Pf7G8_080038300	<i>var</i> , B-type	GGTGGTGGTAGAAGAAGTGGTA	GTACTGTTTCCACCGTTTGCAT	17.25	2,016	75.76
309+310	Anna Bachmann; (Wichers-Misterek et al., 2023)	Pf7G8_090042800	<i>var</i> , B-type	GCCCAAGATGTGATTGAAGACG	TCATTGTTTGTGTATGCTGTCG	17.32	1,962	73.96
311+312	Anna Bachmann; (Wichers-Misterek et al., 2023)	Pf7G8_120005400	<i>var</i> , B-type	GACGTCGGAAGCACCAGTAA	TGCTTGAATCCTCTATACTACTG T	17.36	2,028	75.63
313+314	Anna Bachmann; (Wichers-Misterek et al., 2023)	Pf7G8_080005400	<i>var</i> , B-type	CAGCCGCAGGTACATACAT	ACGCATACTTCTCACCAGCC	17.62	2,032	78.46

Material and Methods

315+316	Anna Bachmann; (Wichers-Misterek et al., 2023)	Pf7G8_030030400	var, B-type	AGTTTCAATGGGTATGATTGCGA	ACGACACCAAAACAGAACAGT	17.20	1,986	73.34
317+318	Anna Bachmann; (Wichers-Misterek et al., 2023)	Pf7G8_030005900	var, A-type	GTCCGACAAAACTTGAGTCCA	TTGGGCGAATCTTCGAGGG	17.82	2,008	76.92
319+320	Anna Bachmann; (Wichers-Misterek et al., 2023)	Pf7G8_060005400	var, B-type	GAAGGAATGGATCCTGGCGAT	TACTTTTGGATCTCCCTGAGCTTC	17.74	1,973	72.84
321+322	Anna Bachmann; (Wichers-Misterek et al., 2023)	Pf7G8_000005200	var, B-type	AAAGGAACAATCTGAATGTAATC GT	TTCGAACGATAAAATGTTCTCTC A	17.30	2,130	72.95
323+324	Anna Bachmann; (Wichers-Misterek et al., 2023)	Pf7G8_010005400	var, B-type	TCGTGGAGAAGATGGAAGCG	TCACCAAATTTCTGTCTCTCCGC	17.49	2,063	75.61
325+326	Anna Bachmann; (Wichers-Misterek et al., 2023)	Pf7G8_040005600	var, B-type	CAAAACCCGCTGGTGTCAATG	AACCGCTTCGTCTCTCTCG	17.43	1,964	79.19
329+330	Anna Bachmann; (Wichers-Misterek et al., 2023)	Pf7G8_050037900	var1csa-A- type	TTGTTGAAGATGAAACACACAAA AA	TCTCCATGGGGTGTAAGAAAT	17.89	1,969	74.07
331+332	Anna Bachmann; (Wichers-Misterek et al., 2023)	Pf7G8_050005300	var, B-type	AGATGAAACGCTTCCGCCA	GAAGTAGGTGGGGCGTTTGA	18.42	1,978	83.18
333+334	Anna Bachmann; (Wichers-Misterek et al., 2023)	Pf7G8_070005200	var, B-type	CTGGTAGTGACGCCACCAAA	TCTGTGACACCGTGGACTC	17.50	2,024	78.58
335+336	Anna Bachmann; (Wichers-Misterek et al., 2023)	Pf7G8_120060000	var, B-type	GAGACAAGACGTCGGAAGCA	GCAAGCCTCTTTATACCTGGTG	17.22	1,974	75.75
337+338	Anna Bachmann; (Wichers-Misterek et al., 2023)	Pf7G8_080014200	var, C-type	GGTAGTGCTGGTGGTAGTAGG	TCATCAACGTTCCATAGCCAC	17.16	1,955	73.91
339+340	Anna Bachmann; (Wichers-Misterek et al., 2023)	Pf7G8_080013900	var, B-type	TGTAGTGGTGATGGTGAGGA	ATGTATGCCACATTTTGGACATT G	17.62	1,994	74.00
341+342	Anna Bachmann; (Wichers-Misterek et al., 2023)	Pf7G8_080013800	var, C-type	AACCTTGGGACGAAAGCACC	GGGGTCGTCGTGGTTTCT	17.67	2,001	77.46
343+344	Anna Bachmann; (Wichers-Misterek et al., 2023)	Pf7G8_090005600	var, B-type	AGTGGTAAGGAACGATATTGTGA	AGGTTTACATGCAACAGAACAGT C	17.32	2	75.11
349+350	Anna Bachmann; (Wichers-Misterek et al., 2023)	Pf7G8_040017900	var, B-type	TTTGGAACAATCGCACTCACC	GGCGAGAGGCCCATAGTAT	17.46	1,919	74.00
351+352	Anna Bachmann; (Wichers-Misterek et al., 2023)	Pf7G8_040017600	var, C-type	TGGTTCGAGGAATGGGCAGA	TCACCACITTGATCTTCTCCCT	17.48	2,019	74.92
353+354	Anna Bachmann; (Wichers-Misterek et al., 2023)	Pf7G8_050038400	var, B-type	TGGATTGTCGGAGGAAGCAAA	GTGATGGCTTCCACACGG	17.67	1,956	78.26
355+356	Anna Bachmann; (Wichers-Misterek et al., 2023)	Pf7G8_070018300	var, C-type	AACATGCAACGCACCAATGA	ACTAGCGCATGTGCATTTTCA	17.61	2,012	77.35
361+362	Anna Bachmann; (Wichers-Misterek et al., 2023)	Pf7G8_070017100	var, B-type	AGGAGATTGGAACACAGCAAATG G	CGCGAGCATCACCACCTTCA	17.65	1,991	77.57
363+364	Anna Bachmann; (Wichers-Misterek et al., 2023)	Pf7G8_120046400	var, B-type	CCCCCTTACTTCCGATACCTTG	ACAATGCTCGTGACCTGGTAG	17.26	1,998	77.08
365+366	Anna Bachmann; (Wichers-Misterek et al., 2023)	Pf7G8_120046700	var, B-type	GTGGTACTAGACCCGTGGGA	CTACCACCAGCACGAATAGC	17.77	1,942	80.49
371+372	Anna Bachmann; (Wichers-Misterek et al., 2023)	Pf7G8_050038200	var, A-type	ACGGGAAAGTGGGAATGACG	TTTGTGGTGGTGGTGTGT	17.47	2,004	84.43
377+378	Anna Bachmann; (Wichers-Misterek et al., 2023)	Pf7G8_140084600	var, B-type	TGGTGGTAACGGTGCTATGT	TGGTGGTAACGGTGCTATGT	17.28	2,021	76.93

For amplification, the RT-qPCR cycling protocol in Table 5 was utilized and the amplicons were checked for correct melting points. Calculated C_t values for amplicons with T_m curves showing double peaks (containing primer-dimer) or completely aberrant T_m values were excluded from further analysis. For a maximum of five primer-pairs, RT-qPCR reaction could be repeated with remaining cDNA, if necessary, e.g., if only one of the two amplicons showed a correct T_m value or in case C_t values between both duplicates differed in $C_t > 3$. Amplicons with lower C_t values were prioritized for repetition. For analysis, fit point analysis (LightCycler® Software 1.5.1.62 SP3) was applied to each sample to determine the threshold and C_t values (in duplicates). Software-obtained C_t values were averaged and $\Delta\Delta C_t$ values were calculated according to Pfaffl et al. 2004 shown in Formular 1, based on the primer efficiencies from each primer pair and the relative ΔC_t value (calculated as the C_t value difference of the

target gene expression and its amplification level with 2.5 ng gDNA) to the housekeeping gene *arginyl-tRNA-synthetase* (Pfaffl 2004, Table 6, 7, 8).

Formular 1.: Calculation formular to determine the RELTEXP as the $\Delta\Delta C_t$ values*10,000 according to Pfaffl 2004. With E representing primer efficiencies of the target and housekeeping genes, and ΔC_t representing the difference of the mean C_t value for target or housekeeping genes on 2.5 ng gDNA and the mean C_t value of the observed gene expression.

$$\text{RELTEXP } (\Delta\Delta C_t * 10,000) = \frac{E^{\Delta C_t} (\text{AVG } C_t (\text{gDNA-target gene}) - \text{AVG } C_t (\text{RT-qPCR-target gene}))}{E^{\Delta C_t} (\text{AVG } C_t (\text{gDNA-arginyl-tRNA-synthetase}) - \text{AVG } C_t (\text{RT-qPCRarginyl-tRNA-synthetase}))}$$

Table 8.: Additional RT-qPCR primer sets (ring stage controls, housekeeping genes).

All primers are HPLC purified, their primer efficiencies and T_m values determined according to section 2.2.7.

Primer ID	Designer/Reference	<i>P. falciparum</i> gene ID	Description	Forward (5' → 3') Sequence	Reverse (5' → 3') Sequence	Mean C_t with 2.5 ng gDNA	Efficiency	T_m value (°C)
135+136, Sir2a	Anna Bachmann; (Bachmann et al. 2019)	PF3D7_0421101	<i>sir2a</i> histone deacetylase	TCCCAAGTTTCGAGGGTCA	CAGGATACTTCCAAAACCCCA	16.09	2.039	75.12
133+134, Sir2b	Anna Bachmann; (Bachmann et al. 2019)	PF3D7_0421102	<i>sir2b</i> histone deacetylase	ACAATCGTTAGGTGCCCAAT	TGTTGTCATGCTCTTATGCT	16.07	2.046	71.88
115+116, Aldolase	Ali Salanti; (Salanti et al., 2003)	PF3D7_1444800	fructose-bisphosphat aldolase	TGTACCACCAGCCTTACCAG	TTCCTTGCCATGTTTCAAT	16.98	1.974	78.21
131+132, SBP1	Michael F. Duffy; (Petter et al., 2011)	PF3D7_0501300	<i>sbp1</i> ring stage control	TTAGCCGACGAACCAACACA	TTCGGTTGTCCTCTGGTACTGCA	17.21	1.951	75.43
215+216, Arginyl-tRNA	Anna Bachmann; (Bachmann et al. 2019)	PF3D7_1218600	arginyl-tRNA synthetase	TTCAAAACACGAAGTGAACAAC	AATTCTCTGCAGCAAGTCGC	17.09	1.964	74.54
393+394, kahrp	Anna Bachmann (unpublished)	PF3D7_0202000	knob-associated histidine-rich protein	AAGCACCACAGGTTACCAA	CAACTGTTCCCTGGGGTTGT	15.84	2.059	79.64
453+454, mahrp-1	Anna Bachmann (unpublished)	PF3D7_1370300	membrane-associated histidine-rich protein 1	CCATGCACCTCATTCTACCC	TCATGAGCGTGTGCAGGTTT	16.02	2.097	77.10

2.2.11 Sample inclusion criteria for *var* gene analysis following RT-qPCR

To rule out that *var* gene transcripts are e.g., not amplified due to a detection problem (e.g., due to low parasitemia) or the existence of yet unidentified submicroscopic infections with natural strains within the NF54 and 7G8 samples, for which the RT-qPCR primers are not working (Supplementary Figure 2), we have defined additional quality criteria for samples to be included in the analysis: Only RT-qPCR samples which (i) showed an average C_t value for the *arginyl-tRNA-synthetase* housekeeping gene of < 31 and (ii) with > 2/3 of all NF54 or 7G8 *var* gene variants correctly amplified (Supplementary Figure 1 C) were included.

2.2.12 Genomic DNA isolation from *P. falciparum*

gDNA was isolated for genotyping *P. falciparum* in blood samples from patients. For this, gDNA was isolated from in total of 37 blood samples following a standardized protocol (QIAamp® DNA Mini Kit). In brief, 200 μ L RBC pellet was diluted 1:1 in PBS. An Eppendorf tube was prepared with 40 μ L protein kinase K and the diluted RBC pellet was added to the solution and vigorously mixed. Next, the samples were lysed by adding an of equal amounts of QIAamp® DNA Mini Kit AL lysis buffer, vortexed and

incubated for 10 min at 56 °C. The samples were loaded on a QIAamp® DNA Mini Kit QIASpin column, washed and eluted in 2x 25 µL nuclease-free H₂O according to the manufacturers protocol. DNA concentration and OD quality (260/230, 260/280) was determined using 1 µL eluted DNA with a nanodrop. The DNA was stored at -80 °C.

2.2.13 Genotyping

Due to the polymorphic character of *var* genes, these can also be used for genotyping (Day et al., 2017). Only *var* transcripts from the NF54 strain can be detected by our RT-qPCR using primers for all 61 NF54 *var* genes. In endemic settings and especially in longitudinal trials, there is a potential risk for mosquito transmitted malaria infections with locally circulating parasite strains. Transcripts derived from these local parasite strains can maximally only be partly amplified by *var* gene primers specific for another genomic background like NF54 (Supplementary Figure 2), thus alternative analysis assays (e.g., EST-approach) are required to analyze *var* gene expression in field strains. A complete genotyping involving the measurement of MSP1, MSP2 and GLURP polymorphisms is ongoing for LaCHMI-002 and is performed as elsewhere described by colleagues in Tübingen (Falk et al., 2006) according to WHO and MMV guidelines (Informal consultation organized by the Medicines for Malaria Venture and cosponsored by the World Health Organization, 2006). Meanwhile, we followed a MSP1 genotyping approach for a subset of only 37 samples from 25 volunteers for whom gDNA samples were collected. For this, a series of PCRs to 1st amplify a larger MSP1 locus (outer PCR; Table 9, 10) and subsequently distinct alleles loci of K1, RO33 and FCR3 (nested)-inner PCR was performed (Table 11, 12). To avoid spillover contamination from other tubes, the outer and (nested)-inner PCR reactions were superimposed with 50 µL mineral oil. To ensure better primer annealing during the PCRs, touch-down PCRs with stepwise 0.5 °C annealing temperature drops starting at either 60 °C (outer MSP1-PCR), 65 °C (Mad20), 67 °C (RO33) or 70 °C (K1) for eight cycles followed by 30 cycles at final annealing temperatures (Table 10, 12) were performed. Outer PCR products were diluted 1:500 in RNase-free H₂O and used as templates in the three (nested)-inner PCRs. gDNA previously isolated from NF54 and 7G8: Sanaria's master cell bank and the FCR3 isolate were used as positive controls for the K1, RO33 and Mad20 alleles, respectively.

Table 9.: MSP1 genotyping: Pipetting scheme for the outer PCR to amplify the *msp1* gene locus.

Reagent	Concentration	Per reaction (µL)	Final concentration/amount
Buffer BD	10X	4	1X
MgCl ₂	25 mM	4	2.5 mM
MSP1_fwd.	10 µM	1.6	0.4 µM
MSP1_rev.	10 µM	1.6	0.4 µM
dNTPs	2.5 mM	0.8	0.05 mM
gDNA		1	

Material and Methods

FirePol Taq	5 U/ μ L	0.32	0.04 U/rct.
Nuclease-free H₂O		26.68	
Total volume		40	

Table 10.: MSP1 genotyping: PCR cycling of the outer PCR.

Time	Temperature (°C)	Cycles (x)	Description
4 min	95	1	Heat activation
30 sec	94	8	Denaturation, Annealing, Elongation
40 sec	60-0.5 touch		
40 sec	72		
30 sec	94	30	Denaturation, Annealing, Elongation
40 sec	56		
40 sec	72		
∞	8		End/Storage

The outer PCR products were checked for correct amplicon size (~1 kb) on a 2.5 % agarose gel run in 1X TAE buffer for 30 min at 120 V. Per 50 mL of agarose gel one drop of Ethidium bromide was added. Gels were loaded with 12 μ L per sample (5 μ L PCR product, 2 μ L 6X Orange G containing loading buffer and 5 μ L of RNase-free H₂O) and 500 ng GeneRuler 100 bp Plus DNA Ladder in the 1st and last position.

Table 11.: Genotyping; (nested)-inner PCRs for amplification of MSP1 alleles K1, RO33 and Mad20.

Reagent	Concentration	Per reaction (μ L)	Final concentration/amount
Buffer BD	10X	4	1X
MgCl₂	25 mM	4	2.5 mM
K1/RO33/Mad20_fwd.	10 μ M	1.6	0.4 μ M
K1/RO33/Mad20_rev.	10 μ M	1.6	0.4 μ M
dNTPs	2.5 mM	0.8	0.05 mM
gDNA	Outer product: 1:500 in RNase-free H ₂ O	1	
FirePol Taq	5 U/ μ L	0.32	0.04 U/rxn.
Nuclease-free H₂O		26.68	
Total volume		40	

Table 12.: Genotyping;(nested)-inner PCR protocol.

Time	Temperature (°C)			Cycles (x)	Description
4 min	95			1	Heat Activation
	RO33	Mad20	K1		Allele

Material and Methods

30 sec	94	94	94	8	Denaturation, Annealing, Elongation
30 sec	67-0.5 touch	65-0.5 touch	70-0.5 touch		
25 sec	72	72	72		
30 sec	94	94	94	30	Denaturation, Annealing, Elongation
30 sec	63	61	66		
25 sec	72	72	72		
∞	8			End/Storage	

Forward primers for amplifying the K1, Mad20 and RO33 alleles were labelled at the 5'-end with different fluorophores to analyze the amplicon sizes by GeneScan. For this, per sample, 2 μ L of each (nested)-inner PCR product (RO33, Mad20 and K1) are diluted 1:100 with HPLC H₂O in a final volume of 200 μ L. Of this pre-dilution, 2 μ L were pipetted into a 96 well plate and mixed with 12.25 μ L GeneScan™ 50-500 (-250) LIZ™ color size standard pre-diluted in Hi-Di™ buffer (0.25 μ L in 12 μ L Hi-Di™ per reaction). The standard contains a repertoire of predefined, fluorescently-labeled DNA fragment lengths as a reference. Standard fragment lengths are compared to the fluorescently labeled fragments of interest to determine the allele family by color and the exact bp-length. If allele lengths deviated from the positive control allele lengths from Sanaria NF54 and 7G8 (K1-203 bp and RO33-132 bp, respectively), the samples were classified as samples from mosquito infections with local parasite strains, unrelated to the applied CHMIs. The GeneScan results can be found in Table 13.

Table 13.: MSP1 genotyping results of the 37 gDNA samples from LaCHMI-2 trial.

Sample ID (volunteer-ID challenge/day)	Expected genotype ⁺	Allele type	Allele length(s) (bp)	MSP1 genotype prediction	RT-qPCR result (CHMI or NI)	Comment
gDNA NF54	NF54	K1	203	N.A.	N.A.	Positive control
gDNA 7G8	7G8	RO33	132	N.A.	N.A.	Positive control
gDNA FCR3	FCR3	Mad20	186	N.A.	N.A.	Positive control
L2-32.22A-C+19	7G8	RO33	132	7G8	CHMI (7G8)	Ok
L2-33.55A-C+14	7G8	RO33	132	7G8	CHMI (7G8)	Ok
L2-32.71A-C+21	7G8	RO33	132	7G8	CHMI (7G8)	Ok
L2-32.01A-C2+62	NF54	K1	203	NF54	CHMI (NF54)	Ok
L2-32.12A-C2+17	NF54	K1	203	NF54	CHMI (NF54)	Ok
L2-32.11B-C5+7*	NF54	K1	203	NF54	CHMI (NF54)	Ok, carry over
L2-32.16B-C5+17*	7G8	K1	203	NF54	CHMI (NF54)	Ok, carry over
L2-32.22A-C2+19	NF54	K1	203	NF54	CHMI (NF54)	Ok
L2-32.42A-C2+28	NF54	K1	203	NF54	CHMI (NF54)	Ok
L2-32.44B-C2+28	NF54	K1	203	NF54	CHMI (NF54)	Ok
L2-32.52B-C5+17*	7G8	K1	203	NF54 (CHMI)	Not tested	No RNA sample
L2-32.58B-C5+5*	7G8	K1	203	NF54 (CHMI)	Not worked	Inconclusive
L2-32.67A-C2+37	NF54	K1	203	NF54	CHMI (NF54)	Ok
L2-32.71A-C2+21	NF54	K1	203	NF54	CHMI (NF54)	Ok

Material and Methods

L2-32.72B-C2+44	NF54	K1	203	NF54	CHMI (NF54)	Ok
L2-32.75B-C+14	NF54	K1	203	NF54	CHMI (NF54)	Ok
L2-32.81A-C5+42	NF54	K1	203	NF54	NI	Inconclusive
L2-32.08A-C+8	7G8	K1	230	NI	NI	Natural infection carried in
L2-32.45A-C+14	7G8	K1	212+207	NI	NI	Natural infection carried in
L2-32.46A-C+13	7G8	K1	177	NI	NI	Natural infection carried in
L2-32.85A-C+9	7G8	K1	129	NI	Not worked	Natural infection carried in
L2-32.94A-C66	7G8	Mad20	195	NI	NI	Natural infection carried in
L2-32.06B-C2+37	NF54	K1	221	NI	No tested	Natural infection carried in
L2-32.15A-C2+20	NF54	RO33 + K1	132#+168	NI	NI	Natural infection carried in
L2-32.16B-C+12	NF54	Mad20	195	NI	Not tested	Natural infection carried in
L2-32.44B-C6+98	NF54	RO33	132#	NI	NI	Natural infection (late infection stages)
L2-32.48B-C2+47	NF54	K1	149	NI	Not tested	Natural infection carried in
L2-32.52B-C+12	NF54	RO33	132#	NI	Not tested	Natural infection carried in
L2-32.53A-C2+7	NF54	/	/	/	NI	Natural infection carried in
L2-32.58B-C6+50	NF54	RO33+K1+Mad20	132#+149+213	NI	Not tested	Natural infection (late infection stages)
L2-32.58B-C6+54	NF54	K1+Mad20	149+213	NI	Not tested	Natural infection (late infection stages)
L2-32.67A-C5+44	NF54	K1	168	NI	NI	Natural infection (late infection stages)
L2-32.67A-C6+131	NF54	K1	177	NI	NI	Natural infection (late infection stages)
L2-32.74B-C+7	NF54	K1+Mad20	203+240	NI	Not tested	Natural infection carried in
L2-32.74B-C+12	NF54	K1+Mad20	212+240	NI	Not tested	Natural infection carried in
L2-32.74B-C+14	NF54	K1+Mad20	212+240	NI	Not tested	Natural infection carried in
L2-32.94A-C5+50	NF54	RO33	132#	NI	NI	Natural infection (late infection stages)

+Expected genotype (7G8/NF54): CHMI with Sanaria® PfSPZ Challenge (7G8) or (NF54) was performed beforehand.

*K1 allele length of 203 (resembling the NF54) genotypes were found in four early C5 samples in Sequence B, suggesting carry-over infections from previous NF54 challenges.

#-marked RO33 allele with length 132 most likely not linked to 7G8. No *var* amplicons found with 7G8 RT-qPCR and according to Bouyou-Akotet, M'Bondoukwé, and Mawili-Mboumba 2015, local stains with an RO33 and 130 sequence length occur in field isolates a study conducted in Libreville, Gabon.

Comment: "inconclusive": MSP1 genotyping was not confirmed by RT-qPCR results.

MSP1 and RT-qPCR results were used to split the samples of the LaCHMI-002 study into two cohorts: (i) the '*CHMI-study*' with volunteer samples infected with NF54 and 7G8 parasites, and (ii) a '*natural infection study*' with volunteer samples infected with local strains or mixed genotypes (NF54 and local *P. falciparum* genotype). Samples from the '*CHMI-study*' were analyzed with either the NF54- or 7G8-specific *var* gene RT-qPCR, '*natural infection study*' samples were processed via the EST approach (DBL α -tag approach; section 2.2.15). For samples from the remaining volunteers and time-points, which were not yet covered by the MSP1 genotyping approach, NF54 or 7G8 *var* gene RT-qPCR was performed either to detect the *var* gene expression pattern or to exclude a CHMI-related infection, e.g., if no/very few *var* transcripts were amplified due to the polymorphic nature of the genes (Supplementary Figure 2). Consequently, for almost all samples a very good genotype estimation could be made by a combination of these two assays, however genotyping involving MSP1, MSP2 and GLURP is required to confirm monoclonal NF54 and 7G8 infection throughout the longitudinal trial setting.

2.2.14 Luminex Assay

Antibody-detection assays were performed as described elsewhere in collaboration with Louise Turner and Thomas Lavstsen at the University of Copenhagen (Bachmann et al. 2019; Wichers et al. 2021). In total, 44 HIS-tagged CIDR and DBL domains as well as five control proteins (GLURP, SERA5, HRP2, CSP and BSA) were expressed in *Drosophila* SF9 cells and purified by nickel affinity chromatography (Lau et al., 2015; Turner et al., 2015). Apart from the negative control BSA, the measurement of (cross-protective) PfEMP1-specific antibodies glutamate-rich protein (GLURP) serine-repeat antigen (SERA5), histidine-rich protein 2 (HRP2), and circumsporozoite protein (CSP) indicate previous exposure acquired from previous episodes of exposure (Aoki et al., 2002; Plassmeyer et al., 2009; Poti et al., 2020; Turner et al., 2011). Antibody recognition of PfEMP1 and control proteins were measured with two different Luminex plexes: Plex 10 measures N-terminal CIDR domains from various *P. falciparum* isolates conferring binding to EPCR via CIDR α 1, CD36 via CIDR α 2–6, and the unknown A receptor via CIDR δ . Since plex10 is designed to capture antibodies against different subtypes of domains (e.g., CIDR α 1.1/4–8), which are derived from various field isolates (e.g., raj116, 1994) or laboratory-adapted strains (e.g., HB3, IT4), this plex measures previous exposure based on cross-reactivity of these antibodies. The PfEMP1 domains contained in plex11 are 3D7/NF54-specific, allowing measurement of cross-reactivity of previously acquired antibodies against 3D7/NF54 proteins at baseline and longitudinal acquisition of antibody after subsequent CHMIs during the trial.

Plasma samples (collected with heparin or EDTA-tubes) were diluted 1:40 in LowCross-Buffer® and vigorously mixed. LowCross-Buffer® showed comparable results for plasma from heparin and EDTA-blood samples, whereas the commonly used ABE buffer did not (Supplementary Figure 1 G). The filters of the 96 well microtiter plates were calibrated with 100 μ L LowCross-Buffer® for 2–30 min. 50 μ L of coated beads (pre-diluted stock in 5 mL LowCross-Buffer®) were added to the microtiter plate and washed three times with 100 μ L LowCross-Buffer® utilizing a vacuum system.

Material and Methods

Table 14.: Overview of PfEMP1 domains and control proteins tested with plex 10 and plex11 in the Luminex assays. The plex 10 captures PfEMP1-specific antibodies binding to EPCR, unknown A and CD36. However, most domains originated from strains like IT4 or HB3, which are genotypically different from the local circulating 3D7 strains as well as the inoculated strains NF54 and 7G8. Detected antibodies are therefore cross-reactive recognizing shared protein sequence and steric similarity among the proteins derived from different parasite strains. Contrary, the plex 11 captures antibodies which are directly targeting 3D7/NF54 antigens which were introduced through the CHMIs.

Plex	Parasite strain (var gene)	Domain	N-terminal binding phenotype	Cutoff for seropositivity (mean MFI + 2x STD from malaria-naïves plasma)
Plex 10	IT4 (IT4var06)	CIDRα1.1	EPCR	2966.00
	raj116_var8	CIDRα1.1	EPCR	1087.00
	Sanger (ERS010178_NODE_17177)	CIDRα1.8a	EPCR	1043.00
	Sanger (ERS010031_NODE_1881_4)	CIDRα1.6b	EPCR	714.00
	Field isolate (1994-2)	CIDRα1.4	EPCR	888.00
	HB3 (HB3var03)	CIDRα1.4	EPCR	766.00
	IT4 (IT4var22)	CIDRα1.4	EPCR	491.00
	Field isolate (2083-1)	CIDRα1.7	EPCR	382.00
	Field isolate (1965-2)	CIDRα1.5	EPCR	577.00
	HB3 (HB3var35)	CIDRδ1	Unknown A	751.00
	HB3 (HB3var05)	CIDRδ1	Unknown A	548.00
	IT4 (IT4var02)	CIDRδ1	Unknown A	523.00
	IT4 (IT4var24)	CIDRα2.2	CD36	1491.00
	IT4 (IT4var26)	CIDRα3.3	CD36	331.00
	IT4 (IT4var30)	CIDRα2.1	CD36	435.00
	IT4 (IT4var33)	CIDRα2.4	CD36	670.00
	IT4 (IT4var45)	CIDRα2.9	CD36	632.00
	IT4 (IT4var61)	CIDRα2.7	CD36	745.00
	GLURP	Control	Control	523.22
	SERA5	Control	Control	224.25
	HRP2	Control	Control	335.76
	CSP	Control	Control	569.97
	BSA	Control	Control	177.08
Plex 11 (3D7)	3D7 (PF3D7_0400400)	CIDRα1.1	EPCR	688.38
	3D7 (PF3D7_1150400)	CIDRα1.4	EPCR	484.25
	3D7 (PF3D7_0425800)	CIDRα1.6a	EPCR	734.88
	3D7 (PF3D7_0800300)	CIDRα1.6a	EPCR	371.28
	3D7 (PF3D7_0600200)	CIDRα1.8a	EPCR	731.56
	3D7 (PF3D7_1300300)	CIDRδ1	Unknown A	349.26
	3D7 (PF3D7_0533100)	CIDRα1.3	var1	1070.53
	3D7 (PF3D7_0937600)	var3	var3	1055.00
	3D7 (PF3D7_1300100)	CIDRα2.4	CD36	1069.88
	3D7 (PF3D7_0833500)	CIDRα3.1	CD36	470.88
	3D7 (PF3D7_0808600)	CIDRα3.2	CD36	413.53
	3D7 (PF3D7_0733000)	CIDRα3.4	CD36	248.16
	3D7 (PF3D7_0426000)	CIDRα4	CD36	554.92
	3D7 (PF3D7_0421100)	CIDRα4	CD36	536.80
	3D7 (PF3D7_1200600)	var2CSA	var2CSA	322.00
	3D7 (PF3D7_0400400)	DBLα1.2	N-terminal head structure (EPCR)	881.00
	3D7 (PF3D7_0400400)	DBLβ12	C-terminal domain (EPCR)	747.00
	3D7 (PF3D7_0400400)	DBLγ11	C-terminal domain (EPCR)	399.00
	3D7 (PF3D7_0400400)	DBLγ6	C-terminal domain (EPCR)	282.00
	3D7 (PF3D7_0412700)	DBLδ1	C-terminal domain (CD36)	332.00
	3D7 (PF3D7_0800200)	DBLε4	C-terminal domain (unknown A)	657.00
	3D7 (PF3D7_0400100)	DBLγ5	C-terminal domain (CD36)	370.00
	3D7 (PF3D7_1100200)	DBLγ12	C-terminal domain (unknown A)	421.00
	3D7 (PF3D7_1200400)	DBLz5	C-terminal domain (CD36)	319.00
	3D7 (PF3D7_0808600)	CIDRγ2	C-terminal domain (CD36)	799.00
	3D7 (PF3D7_0420700)	CIDRγ6	C-terminal domain (CD36)	793.00

Next, 50 µL of prediluted sample per well was added and resuspended for 30 sec at 600 rpm. The sample and beads were incubated in the dark for 30 min at 400 rpm and subsequently 50 µL phycoerythrin-conjugated goat anti-human IgG (secondary antibody; 1:3500 in LowCross-Buffer®) was added for 30 min at 400 rpm to the wells. Afterwards, the wells were washed for three times 100 µL LowCross-Buffer® with the vacuum system. Mean fluorescence intensities (MFI) against domains from Table 14 were measured via the BioPlex¹⁰⁰ system. Per volunteer a maximum of seven samples at approximately eight weeks intervals (1x baseline, 5x prior to each new CHM and one follow-up sample) were measured (Supplementary Table 1). Raw MFI data per antigen was compared for non-controller and controller. Seropositivity was reached when the MFI signal surpassed the cutoff, defined as the mean MFI signal (+2STD) obtained from 17 malaria-naïve Danish controls. Based on previous experience (ref: Bachmann 2019), samples with a BSA > MFI 1000 were excluded from the analysis due to overall high reactivity with all antigens tested (L2-32.55A, L2-32.75B and L2-32.76B; 2x non-controller and 1x controller).

Since the impact of the 7G8 infections in sequence A did not affect the total PfEMP1 IgG levels for the tested antigens of the volunteers (Figure 10 D), the data from plasma samples collected prior to the 1st CHMI in sequence A (7G8) and the 2nd CHMI (NF54) were merged. Therefore, 'baseline' – samples refer to samples collected prior to the 1st CHMI in sequence A (7G8) and the 2nd CHMI in sequence A (NF54). For sequence B only samples collected prior to the 1st CHMI were referred to as 'baseline' – samples.

Moreover, per volunteer, plasma samples were collected for the entire trial duration at eight-week intervals (6x CHMI x 8 weeks = 48 weeks). For the CHMI cohort, the plasma samples were longitudinally analyzed to a maximum of 40 weeks/per volunteer, since many volunteers acquired a natural infections in CHMI6 (Figure 9). If natural infections occurred before CHMI6 e.g., L2-032.67A, L2-032.79A, L2-032.90A, L2-032.77B and L2-032.91B (Figure 9) the respective plasma sample was excluded manually from the analysis of the CHMI sample cohort.

2.2.15 Processing of RNA-seq samples and bioinformatic analysis

In total 57 WBC-depleted samples from 22 volunteers with NF54 parasites and 46 WBC-depleted samples from 19 volunteers with local parasite strains were retrieved (Supplementary Table 1, Figure 9, section 2.2.12) and processed for bulk RNA-seq. Even though bulk RNA-seq was performed on samples from both the 'CHMI-study' and the 'natural infection-study', only samples of the 'CHMI-study' were analyzed within this thesis.

Two batches of three (batch1) and 54 (batch2) NF54-infected CHMI RNA samples were sent to the NGS Core Facility of the University Hospital Bonn for library preparation and sequencing. Apart from *P. falciparum* RNA, blood samples also contain a substantial amount of human RNA, which is mostly derived from reticulocytes as well as globin mRNA and should be removed prior to sequencing to enrich for *P. falciparum* mRNA (Mastrolakos et al., 2012; Melé et al., 2015). To ensure sufficient *P. falciparum* sequencing coverage in field isolate samples, we sequenced three samples (batch 1) at a high sequencing depth of 125 Mio. paired-end(PE)-reads (2x 150bp). Based on the correlation between the amount of mapped *P. falciparum* reads and TBS parasitemia in these samples, we estimated sequencing

depths according to the sample's TBS result. According to our estimations, samples with a parasitemia of below 1000 pf/μL were sequenced at 100 Mio. PE-reads, 1000-2000 pf/μL at 50 Mio. PE-reads, 2000–3500 pf/μL at 40 Mio. PE-reads, 3500-5000 pf/μL at 30 Mio. PE-reads and >5000 pf/μL at 20 Mio. PE-reads. With this strategy we aimed for a total of approx. 5–10 Mio. *P. falciparum* reads per sample, but at least 1 Mio *P. falciparum* reads were set as threshold for our transcriptomic analysis pipeline (Tonkin-Hill et al., 2018). For 47 of 57 samples (82 %) we obtained sequencing data and for 24/57 (42 %) we obtained more than 1 Mio. *P. falciparum* reads (Table 15) despite high RNA integrity in all samples (Supplementary Figure 7). Moreover, we included six *in vitro* cultivated, synchronized ring stage NF54 samples for comparison (Table 15, bottom). For this we used, two different aliquots from the NF54: Sanaria's master cell bank parasites (Aliquot A and B), which surpassed different cycles of *in vitro* cultivation: Aliquot A, 1x 14 and; 2x 17 generations and Aliquot B: 1x 21 and 2x 24 generations. Of these, one sample was excluded because due to extremely low *P. falciparum* mapped reads (< 10.000; 1x Aliquot B (24 generations)).

RNA-integrity-check via Bioanalyzer and TapeStation: RNA-integrity was checked before samples were sent for sequencing using the 2100 Bioanalyzer system as well as by the sequencing facility using a TapeStation (Supplementary Figure 7). For the Bioanalyzer analysis, 1 μL eluted RNA was transferred to an Eppendorf tube, diluted to a final concentration of 5 ng/μL with RNase-free H₂O and then heated to 70 °C for 2 min. Finally, the tubes were cooled on ice and the manufacturer's protocol provided in the Kit was followed (Agilent RNA 6000 Pico Kit). Even though RIN values have only limited significance to assess RNA quality with mixed species (human and parasite), high RNA quality was asserted by the high mean RIN value of 7.8 and that only a single sample showed a partly degraded electropherogram upon visual inspection (Table 15, Supplementary Figure 7). Since we observed a higher degree of agreement among both the Bioanalyzer and TapeStation assays, thus, for facilitation reasons only the TapeStation results are attached.

Library preparation and sequencing: Customized library preparation was performed using the NEB Next Poly(A) mRNA magnetic isolation module and NEBNext Ultra II Directional RNA Library Prep Kit. The NEB Kit has been established and optimized for the generation of libraries from *P. falciparum* field samples and their high transcriptome AT-richness (Andradi-Brown et al., 2024; Chappell et al., 2020; Oyola et al., 2012; Tonkin-Hill et al., 2018; Wichers et al., 2021). In contrast to the established protocols, globin mRNA depletion was infused to the library preparation protocol by the sequencing facility using the QIAseq FastSelect globin depletion Kit. 150 bp paired-end sequencing read libraries were constructed in accordance with the manufacturer's protocol with modifications involving a twelve cycle PCR amplification with KAPA polymerase resulting into final library sizes of 150–300 bps. Sequencing was finally performed on an Illumina NovaSeq 6000 sequencing device.

Material and Methods

Table 15.: Quality measurements for samples analyzed by RNA-seq.

Sample ID	Genotype	Parasitemia (pf/ μ L)	RNA conc. (ng/ μ L)	Eluted volume (μ L)	RIN- value/visual inspection* (Tapestation)	Batch N°	% <i>P.</i> <i>falciparum</i> of total reads	Sequencing dept (in Mio. paired- end reads)	QC (fastqc) % adaptor content	Mapped reads (STAR)	Included (yes/no) Staging/pipeline (>100k reads)
L2-32.01A C2+21	NF54	1065,5	37,4	101	8,5; ok	2	3,11	50	20	743,121	Yes/Yes
L2-32.01A C2+23	NF54	992	17,9	101	7,2; ok	2	N.A.	100	N.A.	N.A.	No/No
L2-32.01A C2+58	NF54	1510	33,6	101	8,4; ok	2	N.A.	50	N.A.	N.A.	No/No
L2-32.11B C4+21	NF54	895,7	8,9	66	7,1; ok	2	N.A.	100	N.A.	N.A.	No/No
L2-32.11B C4+26	NF54	5114,7	12,6	66	7,1; ok	2	9,22	20	20	1,632,812	Yes/Yes
L2-32.12A C2+16	NF54	1412,5	10,1	101	7,1; ok	2	25,43	50	25	5,231,901	Yes/Yes
L2-32.12A C3+21	NF54	4514,5	15,5	101	6,6; ok	2	11,22	30	75	2,357,691	Yes/Yes
L2-32.14A C2+21	NF54	5555	51,9	101	7,8; ok	2	5,82	20	30	924,805	Yes/Yes
L2-32.14A C2+23	NF54	1945	21,5	101	7,4; ok	2	8,97	50	40	2,941,480	Yes/Yes
L2-32.16B C2+19	NF54	3080	12,2	101	8,0; ok	2	N.A.	40	N.A.	N.A.	No/No
L2-32.16B C2+21	NF54	1351,5	21,8	101	8,2; ok	2	3,27	50	40	786,721	Yes/Yes
L2-32.22A C2+19	NF54	9801,5	263,5	101	7,7; ok	2	N.A.	20	N.A.	N.A.	No/No
L2-32.22A C3+19	NF54	6103	32,1	101	7,4; ok	2	7,15	20	30	563,058	Yes/Yes
L2-32.22A C3+37	NF54	1568	111,3	101	7,7; ok	2	0,92	50	55	259,974	Yes/No
L2-32.23A C2+19	NF54	2655	29,6	101	8,0; ok	2	6,25	40	30	1,533,337	Yes/Yes
L2-32.42A C2+23	NF54	8058	20	101	6,1; ok	2	11,29	20	60	1,238,040	Yes/Yes
L2-32.44B C+14	NF54	1413,5	55,4	101	8,5; ok	2	1,15	50	60	307,919	Yes/No
L2-32.44B C+19	NF54	1705,7	16,8	101	7,9; ok	2	38,52	50	30	3,498,031	Yes/Yes
L2-32.44B C+21	NF54	10348	38,5	101	8,5; ok	2	9,20	20	70	1,235,047	Yes/Yes
L2-32.44B C+23	NF54	533	35,6	101	8,7; ok	2	N.A.	100	N.A.	N.A.	No/No
L2-32.44B C+37	NF54	1700,5	11,4	101	7,2; ok	2	N.A.	50	N.A.	N.A.	No/No
L2-32.44B C+44	NF54	4746,5	19,3	101	8,1; ok	2	N.A.	30	N.A.	N.A.	No/No
L2-32.44B C2+28	NF54	11224,7	186,1	101	8,3; ok	2	0,24	20	60	52,337	No/No
L2-32.44B C2+44	NF54	2945,5	30,2	101	7,2; ok	2	4,79	40	50	900,625	Yes/Yes
L2-32.44B C3+19	NF54	1392	19,4	101	8,5; ok	2	5,73	50	30	2,046,835	Yes/Yes
L2-32.44B C3+21	NF54	1565,3	22,2	101	8,0; ok	2	2,74	50	35	800,739	Yes/Yes
L2-32.44B C3+51	NF54	11562	32,4	101	8,4; ok	2	16,82	20	60	1,639,270	Yes/Yes
L2-32.55A C2+19	NF54	8397,5	8,8	66	7,4; ok	1	51,40	125	0	70,975,929	Yes/Yes
L2-32.55A C2+21	NF54	1137	10,7	66	7,4; ok	1	19,27	125	0	26,903,153	Yes/Yes
L2-32.67A C2+16	NF54	1697,7	40,2	101	8,5; ok	2	2,24	50	35	506,509	Yes/Yes
L2-32.67A C2+19	NF54	1085,5	36,2	101	9,3; ok	2	1,66	50	40	383,458	Yes/No
L2-32.67A C2+51	NF54	4717	27,3	101	8,3; ok	2	0,05	30	60	8,002	No/No
L2-32.71A C2+21	NF54	3498	31,8	66	7,3; ok	1	64,34	125	0	73,255,087	Yes/Yes
L2-32.72B C+19	NF54	8375	13,2	54	6,5; ok	2	14,23	20	35	1,768,482	Yes/Yes
L2-32.72B C+23	NF54	3649	8,1	101	6,4; ok	2	12,49	30	30	2,183,832	Yes/Yes

Material and Methods

L2-32.72B C2+26	NF54	1911,5	17,4	101	7.7; ok	2	7,19	50	45	1,963,514	Yes/Yes
L2-32.72B C2+28	NF54	1694	12,4	101	7.8; ok	2	3,39	50	65	1,082,317	Yes/Yes
L2-32.75B C4+28	NF54	2224	26,2	101	7.8; ok	2	0,17	40	65	35,167	No/No
L2-32.76B C+19	NF54	14416	13,2	101	7.6; ok	2	11,31	20	55	1,402,662	Yes/Yes
L2-32.76B C+21	NF54	1728	18,2	101	--	2	N.A.	50	N.A.	N.A.	No/No
L2-32.77B C+19	NF54	3025,7	46,7	101	8.4; ok	2	2,85	40	60	565,343	Yes/Yes
L2-32.77B C+21	NF54	2275	81	101	8.6; ok	2	1,58	40	55	418,634	Yes/No
L2-32.77B C2+9	NF54	1041	56,4	101	8.8; ok	2	0,61	50	70	243,504	Yes/No
L2-32.79A C2+19	NF54	8971,5	44,4	101	7.2; ok	2	19,39	20	60	1,938,168	Yes/Yes
L2-32.79A C2+21	NF54	13824	12,9	101	5.5; partly degraded	2	17,81	20	30	1,556,467	Yes/Yes
L2-32.79A C2+26	NF54	2378	37,1	101	8.9; ok	2	5,07	40	25	1,209,271	Yes/Yes
L2-32.79A C2+30	NF54	1398	33,5	101	8.3; ok	2	1,34	50	30	399,614	Yes/No
L2-32.79A C3+21	NF54	1163	10,7	101	7.6; ok	2	N.A.	50	N.A.	N.A.	No/No
L2-32.79A C3+37	NF54	1341	18,8	101	8.0; ok	2	0,68	50	65	214,178	Yes/No
L2-32.88B C+19	NF54	1904	16,5	101	6.0; ok	2	N.A.	50	N.A.	N.A.	No/No
L2-32.88B C+21	NF54	1881	10,8	101	7.2; ok	2	5,64	50	40	1,179,031	Yes/Yes
L2-32.88B C4+47	NF54/NI	1136	8,9	101	7.4; ok	2	1,60	50	35	400,127	No/No
L2-32.90A C2+19	NF54	4717,5	32,9	101	7.6; ok	2	6,10	30	50	1,050,157	Yes/Yes
L2-32.90A C2+21	NF54	6923	42,9	101	8.3; ok	2	N.A.	20	N.A.	N.A.	No/No
L2-32.90A C2+30	NF54	1098	61,4	101	8.8; ok	2	1,20	50	40	325,110	Yes/No
L2-32.90A C3+21	NF54	2059	24,5	101	7.9; ok	2	1,35	40	45	291,510	Yes/No
L2-32.90A C3+23	NF54	3178	42,5	101	8.5; ok	2	0,54	40	60	100,933	Yes/No
L2-32.90A C3+37	NF54	1472	40,3	101	7.8; ok	2	0,85	50	75	224,026	Yes/No
L2-32.91B C+21	NF54	20047,5	24,8	101	8.8; ok	2	7,92	20	60	1,020,846	Yes/Yes
L2-32.91B C2+28	NF54	1325,5	49,3	101	8.6; ok	2	N.A.	50	N.A.	N.A.	No/No
NF54 1 (Aliquot A)	NF54	2 % rings	435,1	101	9.2; ok	2	30,15	5	80	1,028,975	Yes/No
NF54 2 (Aliquot A)	NF54	3 % rings	412,7	101	8.8; ok	2	33,58	5	75	1,356,799	Yes/No
NF54 3 (Aliquot A)	NF54	3.5 % rings	311,1	101	8.9; ok	2	59,31	5	40	6,344,257	Yes/No
NF54 4 (Aliquot B)	NF54	3.5 % rings	275,0	101	9.0; ok	2	61,04	5	40	6,252,133	Yes/No
NF54 5 (Aliquot B)	NF54	3.5 % rings	305,9	101	9.1; ok	2	11,96	5	85	109,536	Yes/No

*RIN values for field samples less suitable quality indicator as the samples contains rRNA from two species and human and *P. falciparum* 18 and 28S rRNAs have different sizes. Visual inspection “ok”: Presence of a 18S and 28S rRNA signals without degradation.

Quality check using *fastqc* and read mapping using *STAR* to the 3D7 reference genome: *fastqc*-files underwent quality check using ‘*fastqc*’ and poor-quality bases were trimmed off using ‘*sickle*’ with option -q20. Indexing of the reference was executed with *STAR* with *STAR --runMode genomeGenerate --genomeDir . --genomeFastaFiles PlasmoDB-59_Pfalciparim_3D7_genome.fasta*. Next, the mapping was performed *STAR --runThreadN 8 --genomeDir . --readFilesIn fwd.fastq.gz rev.fastq.gz --readFilesCommand gzcats --outSAMtype BAM SortedByCoordinate --outFileNamePrefix sample_name*.

Gene expression analysis: Counting mapped reads to *var* exon1 only has been shown to resemble the actual *var* expression pattern (Dimonte et al., 2016; Otto et al., 2019b; Wichers et al., 2021). Thus, .bam RNA-seq files were processed with 'featurecounts' in order to count features assigned to exons instead of entire genes. Looping of all included RNA-seq files was executed following `featureCounts -t exon -f -T 10 -p -Q 5 -g ID -a PlasmoDB-62_Pfalciparum3D7.gff --countReadPairs -o counts_all.txt *.bam` allowing options to count for exons only (-t), paired-end reads (-p) and setting a mapping quality of 5 (-Q) next to required arguments. Duplicates within the excel output file were removed and rpkm values were calculated by (1) counting the total reads per sample and divide it by 1.000.000 ("scaling factor"), then (2) divide the read counts of each exon by the "scaling factor" (RPM) and finally divide by the length of the gene in kb (rpkm). Exon1 expression in rpkm for all NF54 *var* genes were extracted and compared to the RT-qPCR $\Delta\Delta C_t \cdot 10.000$ of the respective sample. Similarly, *rif* expression pattern were analyzed by counting mapped features to *rif* exon2 (Cheng et al., 1998; Gardner et al., 1998; Joannin et al., 2008; Petter et al., 2008).

Transcriptomic-based stage quantification and group comparisons utilizing a preestablished pipeline: Differences in global *var* gene expression was performed between early (1st waves, B-type *var* genes rpkm sum is superior to all other *var* gene groups) and late (downstream waves, B/C and C-type *var* gene rpkm sum is superior to all other *var* gene groups) time points during infection by applying a pre-established transcriptomic pipeline by Gerry Tonkin-Hill (Tonkin-Hill et al., 2018). The pipeline uses R-based 'subread' and 'featurecounts', counts total reads and quantifies transcriptomic-based parasite stage profiles by comparison to a dataset describing distinct expression characteristics of asexual ring (8 hpi), early trophozoite (19 hpi), late trophozoite (30 hpi) and schizont (42 hpi) as well as sexual stage V gametocytes (López-Barragán et al., 2011). It corrects for ring stage transcriptomic profiles only via 'RUV.4' and removes unwanted variation commonly observed in *in vivo* samples via a comparison to a control set of genes from another publication (Vignali et al., 2011). Final differential expression was performed with limma/voom DEG comparison incorporated in the pipeline script (Supplementary Figure 8).

2.2.16 DBL α -tag PCR for samples with a natural infection genotype

The investigation of *var* gene expression in samples with a natural infection genotype via DBL α -tag was part of a Master thesis conducted by Lea Allerchen. Prior to the DBL α -tag PCR, similar to section 2.2.8, a single cDNA reaction involving a maximum of 11 μ L RNA per sample were used to generate a double stranded template for PCR reactions. The DBL α -tag PCR amplifies the 350–500 bp long fragment from the sequence coding for the DBL α domain of the PfEMP1 N-terminal head structure (NTS-DBL α -CIDR). Optimized polymerase (KAPA Hifi HotStart DNA polymerase) and degenerated forward and reverse (331_varF-dG2, 312_brlong2) primers were used to for PCR amplification (section 2.1.9). The forward and reverse primers are mixes containing alternative base pairs at selected positions

(‘wobbels’) to amplify polymorphic regions of a sequence more efficiently. Lower case bases represent annealing sites for a second indexing PCR (section 2.2.17).

Table 16.: DBL α -tag PCR mix.

Reagent	Concentration	Per reaction (μ L)	Final concentration/amount
Nuclease-free H ₂ O		14.25	
KAPA HiFi buffer	5x	5	1x
Primer-Mix (fwd. and rev.)	20 μ M each	2.5	2 μ M each
KAPA HiFi HotStart Polymerase	1 U/ μ L	0.5	0.5 U/rxn
dNTPs	10 mM	0.75	0.3 mM
Template cDNA/gDNA		2	
Total volume		25	

Table 17.: DBL α -tag PCR protocol.

Time (min.)	Temperature (°C)	Cycles (x)	Description
2	95	1	Activation step for hot-start enzyme KAPA HiFi HotStart DNA polymerase
20 sec.	98 (Ramp 3°C/sec)	5	Denaturation, Annealing and Elongation
1 sec.	65 (Ramp 3°C/sec)		
30 sec.	54 (Ramp 0,5 °C/sec)		
1,25	68 (Ramp 3°C/sec)		
20 sec.	98 (Ramp 3°C/sec)	30	Denaturation, Annealing and Elongation
30 sec.	54 (Ramp 3°C/sec)		
1,25	68 (Ramp 1°C/sec)		
2	72 (Ramp 3°C/sec)	1	
∞	4	∞	End/Storage

Lyophilized primers were diluted to 100 μ M in TE buffer and further diluted in a primer mix of each 20 μ M in HPLC H₂O. 5 μ L 5 X KAPA HiFi buffer with MgCl₂, 0.75 μ L dNTPs, 2.5 μ L DBL α -tag primer mix, 0.5 μ L KAPA HiFi HotStart Polymerase and 14.25 μ L RNase-free H₂O were added to 2 μ L cDNA template and the PCR protocol was initiated (Table 17). The PCR product was checked for correct amplicon size (350–500 bp) on a 2.5 % agarose gel in 1X TAE buffer for 30 min at 120 V. Per 50 mL of agarose gel one drop of ethidium bromide was added. Gels were loaded with 12 μ L per sample (5 μ L PCR product, 2 μ L 6X Orange G and 5 μ L of RNase-free H₂O) and 500 ng GeneRuler 100 bp Plus DNA Ladder in the 1st and last position.

2.2.17 Purification of DBL α -tag RT-PCR products

Agarose-gels showed a substantial number of primer dimers of 100–150 bp. To increase sequencing efficiency, we further purified the amplicons using the NucleoSpin® Gel and PCR Clean-up kit. For this, the remaining PCR product (~20 μ L per sample) was separated from the primer dimers by another 2.5 % agarose gel run for 30 min at 120V. Next, the PCR product bands of correct size were cut under trans UV (ChemiDoc XRS+) using the the X-TRACTA Generation II. The agarose piece was weighted and mixed with NTI (four times w/v) binding buffer and heated at 50 °C for 5–10 min to dissolve the agarose (see NucleoSpin® Gel and PCR clean-up protocol; Macherey-Nagel). Next, 700 μ L sample was loaded on a NucleoSpin® Gel and PCR Clean-up column and centrifuged for 30 s at 11.000 \times g. The flow-through was discarded and the membrane-bound PCR product was washed with 700 μ L NT3 buffer and centrifuged for 30 s at 11.000 \times g. After drying of the silica membrane for 1 min at 11.000 \times g, the PCR product was eluted from the column with 15 μ L NE elution buffer by centrifugation for 1 min at 11.000 \times g. The eluted PCR product was visualized on a 2.5 % agarose gel to ensure sufficient recovery of the DNA after the clean-up and visualize purity. Purified DBL α -tag PCR products were sent for sequencing to collaborators at the University of Copenhagen.

2.2.18 Sequencing of DBL α -tag products

Sequencing of the DBL α -tag DNA fragments was performed by collaborators at the University of Copenhagen (Rasmus Jensen, Thomas Lavstsen). Library preparation was conducted similar to previously published protocols (Nag et al., 2017; Wichers et al., 2021). In brief, the overhang DBL α -tag primer sequences (section 2.2.15) severed as annealing sites for sample-specific indexing primers (0.065 μ M primers and 2 μ l of the 1st PCR amplicon as a template in 20 μ l final reaction volume) in a second indexing PCR with following steps: Heat activation at 95 °C for 15 min, 20 cycles of 95 °C for 20 s, 60 °C for 1 min and 72 °C for 1 min, and one final elongation step at 72 °C for 10 min. Then, 4 μ L of each PCR product were pooled and purified utilizing AMPure XP beads according to the manufacturer's protocol. Finally, pooled PCR products were inspected on an agarose gel to ensure purity and analyzed via Nanodrop and Bioanalyzer to estimate the concentration. Sample pools were diluted to 4 nM and mixed with other PCR product pools e.g., from other projects and/or organisms preferably with higher GC content to compensate for the AT richness of *P. falciparum* and thus enabling base-balanced sequencing. Sequencing was performed on an Illumina MiSeq instrument (MiSeq v3 flow cell) obtaining paired-end 2 \times 300 bp reads.

2.2.19 Bioinformatic processing and prediction of DBL α -tag

Indexed fastq-files were processed through the Galaxy webtool. For this, zipped .fastq files were uploaded to the server and trimmed utilizing 'trimmomatic' applying a four-base sliding window and a Phred quality score of 20, excluding low quality sequences. Alignment of fwd. and rev. .fastq files was performed with 'fastq-join' with a 0% mismatch rate over 4 bps. Finally, .fastq files were converted to

.fasta files using 'fasta' and short reads (<200 bps) were filtered out with 'filter fasta'. Next, the non-*var* sequences with alternative index-primer sequences were filtered out with 'grep' (for *i* in *.fasta ; do inam=\${i/.fasta/}; grep -B 1 '^GCA' \${i}| grep -v -- '^--\$' > \${inam}_GCA.fasta"; done) and finally 23 base-pair long index-primer sequences were cut off using 'seqtk' (for file in *_GCA.fasta; do filename=\$(echo \${file} | sed 's/_GCA.fasta//'); seqtk trimfq -b 23 -e 23 \${filename}_GCA.fasta > \${filename}_GCA-primer.fasta; done). Subsequently, *var* sequences were analyzed using the 'Varia' tool to quantify and predict the domain composition of the encoded full-length PfEMP1 based on the amplified DBL α domain sequence (Mackenzie et al., 2022). For this, the *Varia* tool software utilizes a) the integrated the *Vsearch* program (version 2.27.0) to cluster DBL α sequences from each sample with 95 % sequence identity, b) blasts and compares representative cluster sequences to *varDB*, consisting of >200.000 previously sequenced and annotated *var* gene sequences, with 93 % identity over 200 nucleotides to identify the most similar blast hit and c) predicts the domain composition of the encoded PfEMP1 protein by similarity search in the *varDB*. Only samples with > 500 total reads after cleaning were included in the analysis. The *Varia* tool predicts *var* gene sequences for all *var* gene groups, including the more conserved variants of the *var* subfamilies *var1*, *var2csa* and *var3*. These variants either encode for an alternative DBL domain (*var2csa*, DBLpam1/2) or have strongly divergent sequences (*var1*, *var3*) which the DBL α -tag primers cannot properly amplify, and respective clusters were therefore manually removed from the analysis. Cluster sequences without DBL α blast hit (presumably contaminants or unspecific PCR products) and cluster accounting for less than 1% of the total reads were excluded from the analysis. Since the *Varia* tool only annotates DBL α 0/1/2 domains, a discrimination between B- and C-type *var* genes, which both contain DBL α 0 domain is not possible (Wichers et al., 2021). Thus, we complemented the *Varia*-tool pipeline with a recently established *ups* prediction tool ('*cUps*', (Tan et al., 2023), classifying cluster sequences into *var* A, B and C-types based on similarity to previously assembled DBL α sequences with a defined *ups* classification. Not predictable sequences with a DBL α 0 domain were classified as B-or-C-type, while DBL α 1 and 2 containing sequences were classified as A and DC8-types, respectively.

To cluster identical DBL α -tag sequences in samples obtained from a single volunteer over time, we merged all cluster sequences from the volunteer in a separate .fasta file and clustered them with 'cd-hit' using 97 % sequence identity (cd-hit -i \${filename} -c 0.97 -o \${filename}).

2.2.20 Visualization and statistical analysis of various datasets

Visualization and statistical analyses were performed with great support from the in-house Biostatistician Ralf Krumkamp utilizing either GraphPad Prism (version: 10.2.1 (339)), R (version 4.3.1), RAWGraphs (version: 2.0) and MS PowerPoint. Boxplots showing median and interquartile ranges were used for continues variables. Heatmaps show either the absolute expression (Figure 21) or RELTEXP with a 40 % cutoff to resolve *var* gene pattern of lowly expressed genes (Figure 10, Figure 11, Supplementary Figure 5). Pie charts display the *var* gene pattern as RELTEXP either for volunteer groups at the onset of infection (Figure 10, Figure 11), the mean expression during the 1st parasitic wave from non-controller and controller (Figure 13) or absolute expression throughout the infection peaks

for individual volunteers (Figure 16, Figure 24, Supplementary Figure 3, Supplementary Figure 4). Kaplan-Meier plot indicate a proportion of volunteers gradually turning TBS+ with 7G8 parasites (Figure 10), or TBS- after an infection with NF54 parasites (Figure 14). For super plots, the individual datapoints obtained from one single sample (Figure 10, Figure 12, Figure 18, Supplementary Figure 6) or as a merge from various volunteers at the same time point (Figure 18) we combined with mean or median, displayed as boxplots with interquartile ranges, values. Significance testing was performed on mean and median values only. Mean RELTEXP is shown as superimposed bar charts per individual group (*var* group, chromosomal localization, binding phenotype) (Figure 12, Figure 16). Paired Wilcoxon tests and non-paired Mann-Whitney-U tests were performed for comparisons with a cut-off of $\alpha < 0.05$ for significance, multiple comparisons were corrected by the Bonferroni-Dunn method. For correlations, non-parametric Spearman R including confidence intervals were calculated. For the calculation of the Shannon-index the following formula was used:

Formular 2.: Calculation of the Shannon-index.

P_i represents the proportion of a particular var gene expression in relation to the total var gene repertoire.

$$\text{Shannon} - \text{index} = - \sum_{i=0}^R p_i \ln p_i$$

For which p_i represents the proportion of a particular *var* gene in relation to the total *var* genes (maximum 61 NF54 *var* genes in the repertoire). Moving averages were calculated across ten neighboring data points with 95 % confidence intervals. Area-plot smoothing was performed with R utilizing the loess function which polynomial regression fitting. To fit the curve through actually measured parasitemia values a polynomial degree of 2 with a span factor of $\alpha = 0.05$ for smoothing were applied for volunteer L2-032.44B (Figure 16). Other volunteers encountered TBS negative results more frequently during their infection than e.g., L2-032.44B which makes polynomial curve fitting through the actual measured data points more challenging. For accuracy reasons we therefore did not fit and smooth longitudinal infection dynamics of other volunteers (Supplementary Figure 3, Supplementary Figure 4). To combine clinical trial and experimental data, a RedCap® database was developed. For this, clinical trial data, which was made available through the trial staff, was uploaded to the database system and subsequently supplemented with experimental data from various assays e.g., RNA isolation, RT-qPCR, MSP1 genotyping, Luminex and RNA-seq. Data was retrieved from the database as MS excel files for more downstream analysis of the measured parameters from the trial and the experiments.

For the longitudinal expression analysis, the initial CHMI with 7G8 parasites in sequence A was removed from subsequent analyses and the trial scheme of sequence A and B time axis aligned. For this, NF54 infections occurring in the 2nd CHMI of sequence A were aligned to the 1st CHMI of sequence B.

3. Results

3.1 Objective and sampling of the LaCHMI-002 longitudinal clinical trial

The randomized open-label controlled human malaria infection (CHMI) study LaCHMI-002 (L2) took place in Gabon from 2019–2022 and was the second study in a series of clinical trials starting with LaCHMI-001 (L1) at the Centre de Recherches Médicales de Lambaréné (CERMEL) (Lell et al., 2018). The overall aim of the trial was to longitudinally assess the cross-protectivity of individuals with various degrees of semi-immunity upon consecutive infections with two geographically distinct *P. falciparum* isolates. Based on the results from previously conducted CHMI studies at the CERMEL, the local population displays a range of semi-immunity to malaria which is most likely based on gradually acquired immunity following previous episodes of exposure (Lell et al. 2018; Lell and McCall 2018). According to these studies, about 40 % of the volunteers were expected to be unable to control the infections, develop a patent parasitemia of > 1000 pf/ μ L and malaria related symptoms which require immediate treatment (symptomatic malaria; parasitemia and malaria-related symptoms). Another 40 % of individuals was expected to control the infection despite the detection of microscopic and submicroscopic parasitemia (asymptomatic malaria; parasitemia without malaria-related symptoms) and the remaining 20 % are fully protected from infection ('clearer'). These observations are in line with previous observations which suggest that despite previous malaria episodes, accumulating immunity allows protection from disease instead of protection from infection (Langhorne et al., 2008). Depending on the degree of semi-immunity and infection control, more immune individuals can for example delay the infection onset, develop less symptoms and limit the asexual parasitemia compared to less immune or first-time infected individuals (Bachmann et al. 2019).

Therefore, for this study, 56 healthy volunteers (aged 18–45), with an expected wide range of preestablished semi-immunity to malaria, living close to the trial conducting site in Lambaréné, Gabon, were recruited. The included volunteers were checked for absence of parasites at baseline via thick blood smear (TBS) and randomly allocated into two infection regimens of 28 individuals each (Sequence A and B), without applying presumptive parasite treatment (Figure 9). Within these different infection regimens, the volunteers were repeatedly inoculated intravenously at eight-week intervals with 3,200 aseptic, purified sporozoites of *P. falciparum* of either the clone 7G8 (Brazilian origin) or strain NF54 (Netherlands/ African origin) (Figure 9). In previously conducted dose-escalation studies with malaria-naïve volunteers, 3,200 *P. falciparum* intravenously injected sporozoites were found to reliably induce infections with Sanaria® PfSPZ Challenge (7G8) or (NF54) sporozoites (Laurens et al. 2019; Mordmüller et al. 2015; Sulyok et al. 2021). The infection regimen for volunteers in sequence A included one dose of 7G8, followed by five consecutive doses of NF54, and in sequence B four consecutive doses of NF54, followed by one dose of 7G8, followed by one final dose NF54 (Figure 9).

Results

Each volunteer's blood was screened at least three times per week until day 28 after inoculation and twice per week thereafter until day 56 and before a new CHMI was applied. Single-dose treatment with artemether-lumefantrine (AL) was performed only upon microscopic evidence of parasites in combination with malaria-related symptoms, allowing the tracking of asymptomatic infections. Final treatment with AL was performed at the trial's end point after the completion of six CHMIs as well as upon microscopic evidence of parasites during the follow-up period. To minimize the risk of transmission of an isolate with a geographically distinct origin (7G8, Brazilian origin) to the local

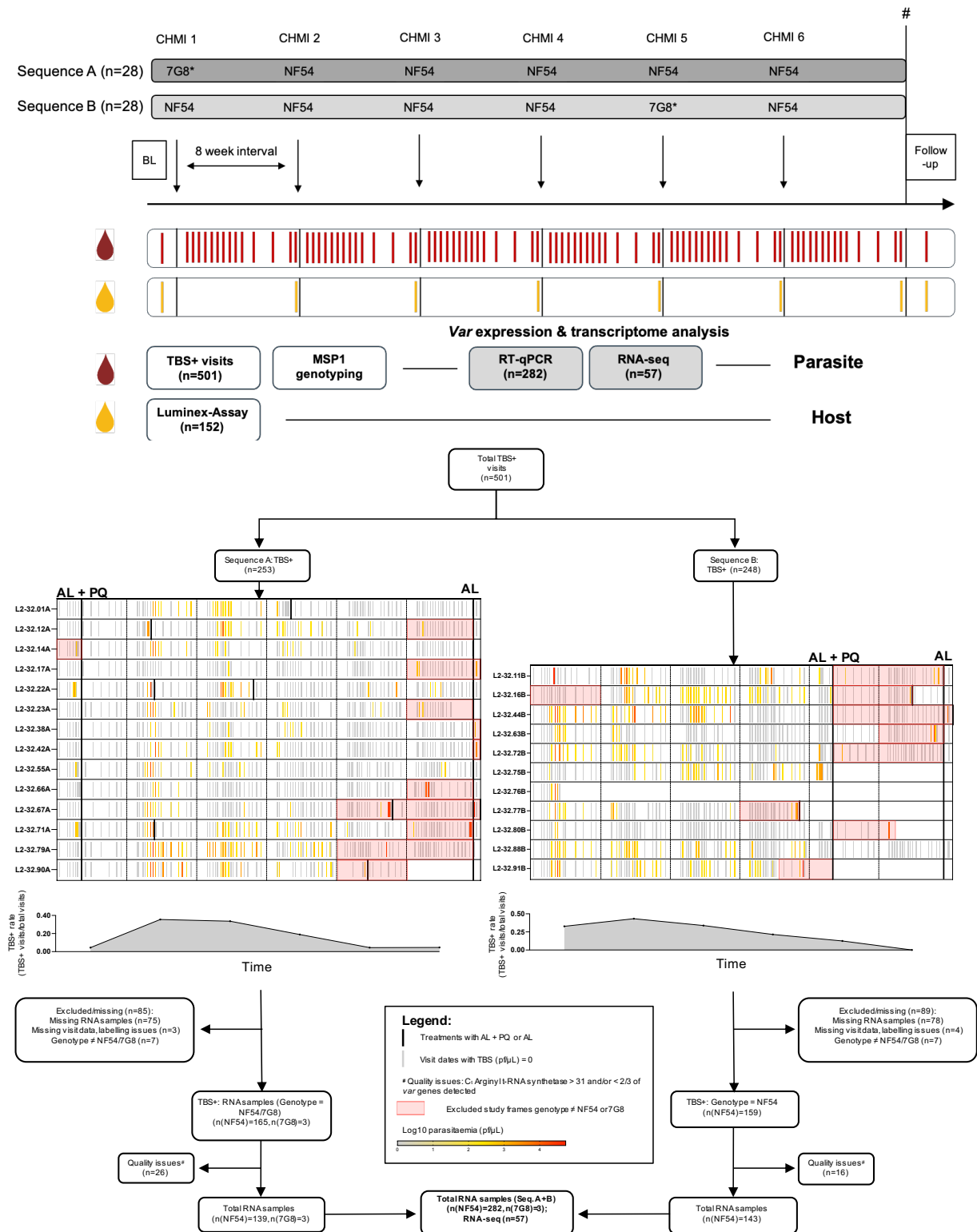


Figure 9.: LaCHMI-002 (L2) study scheme and sampling strategy.

56 volunteers were recruited and randomly allocated into two sequences of each 28 individuals. Upper panel: Sequence A: One dose of 7G8, followed by five consecutive doses of NF54. Sequence B: Four consecutive doses of NF54, followed by one dose of 7G8, followed by one final dose of NF54. CHMI challenges were applied in eight weeks' intervals. Blood sampling (red lines) was conducted at least three times per week up until day 28 post infections and twice per week thereafter. RNA samples were taken whenever the thick blood smear was positive for parasites. Treatment with Artemether/lumefantrine (AL) was applied upon detectable parasitemia in combination with malaria-related symptoms and at the trial end-point (#). Treatment with Artemether/lumefantrine + Primaquine (AL+PQ) was applied latest at day 17 post infection following 7G8(*). Plasma samples were collected prior to each CHMI (yellow lines). Only a subpopulation of 25/52, corresponding to $n=282$ parasitic blood samples, volunteers showed an NF54 or 7G8 genotype at least at one-time point following our preliminary MSP1- and RT-qPCR-based genotyping approach. Of these, $n=57$ parasitic blood samples were WBC-depleted and additionally analyzed via RNA-seq. Lower panel, left (sequence A): 253/501 TBS+ visits from 14 volunteers infected at least at one time point NF54 or 7G8 parasites. Of these, 85 visit time points were excluded due to a lack of sample availability ($n=75$), missing/incomplete visit date information ($n=3$) and a deviating genotype (\neq NF54/7G8) ($n=7$). The remaining NF54 ($n=165$) and 7G8 ($n=3$) samples were analysed via var gene specific RT-qPCR. Following the application of strict quality measures (C_i (arginyl-tRNA-synthase) < 31 and detection of correct amplicons for 2/3 of the var gene repertoire,) $n=26$ samples were excluded from the analysis. Upper panel and lower panel right (sequence B): 248/501 TBS+ visits were registered from 11 volunteers infected with either NF54 at least at one time point during the trial. Of these, $n=89$ visits were excluded due to a lack of sample availability ($n=78$), missing/incomplete visit date information ($n=4$) and deviating genotypes (\neq NF54/7G8) ($n=7$). The remaining NF54 ($n=159$) were analysed via var gene specific RT-qPCR. No volunteer sample with 7G8 parasites was detected and collected in sequence B. Following the application of strict quality measures (C_i (arginyl-tRNA-synthase) < 31 and detection of correct amplicons for 2/3 of the var gene repertoire,) $n=16$ samples were excluded from the analysis. TBS- visits are displayed in light grey while TBS+ results are colored according to a log10 parasitemia scale. To calculate the TBS positivity rate (plots below the sample schemes of each sequence), the amount of TBS+ samples per CHMI was divided by the total amount of NF54/7G8 genotype-linked visits registered for this CHMI. Light red marked study periods: Excluded study frames due to natural infection (genotypes \neq NF54/7G8). Treatments are indicated by black lines. BL=baseline, TBS= thick blood smear.

population, volunteers undergoing 7G8 challenge were routinely treated with Artemether/lumefantrine and Primaquine (0.25 mg/kg) latest at day 17 post infection to kill sexual and asexual parasite stages (Djimé & Lefèvre, 2009; Sutanto et al., 2013; White, 1998). Parasitemia was assessed by thick blood smear (TBS) and is currently analyzed by RT-qPCR by colleagues in Tübingen. Instead of the expected 20 %, only 4/56 (7 %) of the volunteers were classified as 'clearer' as they tested TBS negative according to the initial TBS slide readings during the entire study. The lower percentage might be explained by the total period of the study of 1.5 years with a total of 6 challenge infections.

Following our preliminary MSP1 and RT-qPCR genotyping approach, 25/52 volunteers (48 %) showed a monoclonal infection with either 7G8 or NF54 for at least at one time point, corresponding to a total of 501 TBS positive (TBS+) samples from these volunteers (monoclonal CHMI samples) during the entire trial period (Figure 9). The remaining volunteers were either infected by mosquito bites with locally circulating parasite isolates (natural infections) or acquired a natural infection on top of a challenge infection from a CHMI (mixed infections). A total of 232 samples were collected from mixed and natural infections (Figure 22). Therefore, the sample cohort was split into a subset of samples with monoclonal NF54 or 7G8 parasites only (in the following called the 'CHMI-study') and a subset of samples with parasites with a genotype deviating from NF54 or 7G8 (in the following called the 'natural-infection (NI)-study'). For the volunteers of the 'CHMI-study', RNA samples were taken for only 348 of 501 (69.5 %) possible TBS+ visits to not exceed the maximum volume for blood donations of 500 mL per volunteer in the trial's time frame (Lell & McCall, 2018). TBS+ blood samples were processed via Ficoll gradient centrifugation and, in case of a TBS results of > 1000 pf/ μ L, additionally filtered through a Plasmodipur filter to deplete WBCs. The additional filtering step reduced the amount of human cells and subsequently human-derived RNAs making RNA sequencing of the *Plasmodium* species in the sample more likely to be successful (Andradi-Brown et al., 2024; Auburn et al., 2011; Wichers et al., 2021).

In both study arms, for 174/501 (34.7 %) TBS+ visits no blood sample was available (Figure 9; missing RNA samples), for 7/327 (2.1 %) of the remaining blood samples were excluded due to missing/incomplete trial visit data or inconclusive tube labelling (Figure 9; missing visit data, labelling issues). Using our MSP1 and RT-qPCR genotyping approach we identified 13 volunteers who either displayed genotypes from the CHMI and NI infections simultaneously (mixed infections) or in a temporally separated manner. Thus, in total 14/327 (4.3 %) of the samples were excluded from the 'CHMI-study', added to the sample cohort of the 'NI-study' and subsequently analyzed via DBL α -tag (Figure 9; Genotype \neq NF54/7G8; Figure 22). The natural and mixed infections were either carried sub-microscopically into the trial since no presumptive treatment was performed or occurred with increasing duration of the clinical trial, mostly following CHMI 5 and CHMI 6 (Figure 9, lower panel: light red colored time frames). This observation is also supported by the decreasing rate of NF54 positive TBS results over time (Figure 9; grey area-plots below each schematic) for both sequences, indicating a correlation of reduced NF54 TBS positive samples and infection duration. Whilst strain-specific immunity for NF54 is increasing the likelihood of infection with a local parasite strain for which the volunteers might not have developed sufficient protection seems to increase.

The remaining 324 (165x sequence A and 159x sequence B) NF54 genotype and three (sequence A only) 7G8 genotype RNA samples were processed and analyzed via RT-qPCR using specific primers for the entire *var* gene repertoire from NF54 or 7G8, respectively (Table 6, Table 7). Finally, NF54 (n=282) and 7G8 (n=3) samples were included in the analysis fulfilling strict quality requirements of C_t values below 31 for the housekeeping gene *arginyl-tRNA synthetase* (normalizer) and successful amplification of at least 2/3 of the entire *var* gene repertoire. Of these, n=57 samples were WBC depleted and underwent RNA sequencing. From the included 25 volunteers in both study arms, in total 152 plasma samples were collected prior to each CHMI and analyzed for PfEMP1 recognition via Luminex assay (Figure 9, upper panel).

3.2 Analysis of *var* gene profiles of 7G8 parasites from lifelong-exposed individuals

The infectivity of Sanaria® PfSPZ Challenge (7G8) in lifelong-exposed volunteer cohorts seem to be reduced compared to Sanaria® PfSPZ Challenge (NF54) as we observed that only 3/13 (23 %) of the volunteers infected with 7G8 were indeed TBS+ with 7G8 parasites by day 17 (sequence A), while 6/10 (60 %) of volunteers were TBS+ with NF54 parasites within the same period (sequence B) (Figure 10 A). 100% of volunteers infected with NF54 sporozoites were TBS+ until day 19. It is possible that more volunteers infected with 7G8 would have been tested positive after day 17, however treatment was latest initiated at that day for volunteers of sequence A to avoid the formation of gametocytes and transmission of a geographically distinct strain to local communities.

In total, three samples from CHMIs with 7G8 were obtained from three different volunteers (L2-32.22A, L2-32.55A and L2-32.71A) and analyzed by RT-qPCR. Similar to the *var* expression pattern in parasites isolated from malaria-naïve volunteers in previously performed CHMI studies (Mordmüller et al. 2022;

Results

Sulyok et al. 2021), high expression of a distinct C-type variant (PF7G8_040025600) was detected in all three parasite samples, but broad expression of B-type *var* genes was also seen at a lower level (Wichers-Mistere et al. 2023, Figure 10 B, C).

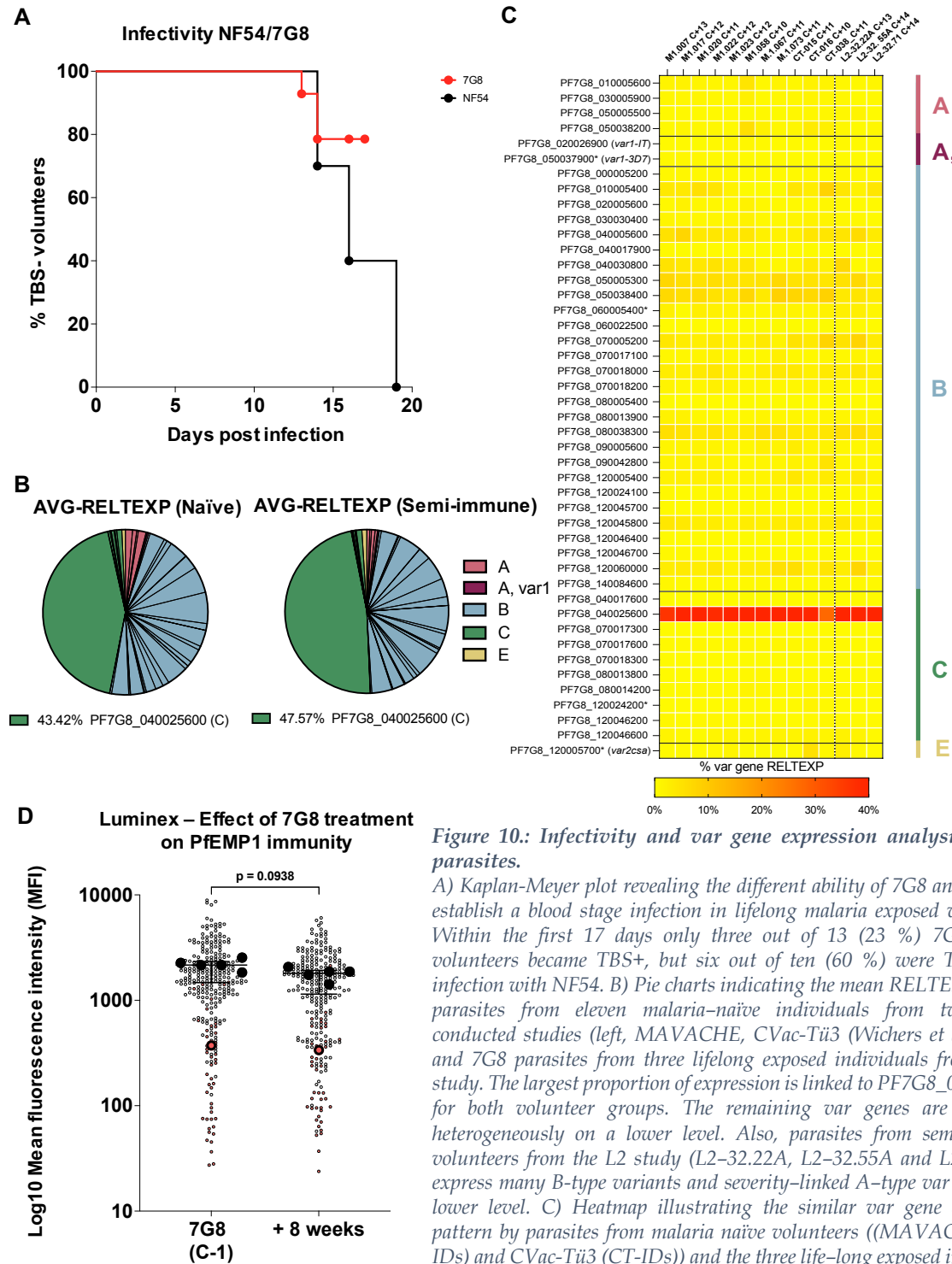


Figure 10.: Infectivity and var gene expression analysis of 7G8 parasites.

A) Kaplan-Meier plot revealing the different ability of 7G8 and NF54 to establish a blood stage infection in lifelong malaria exposed volunteers. Within the first 17 days only three out of 13 (23 %) 7G8-infected volunteers became TBS+, but six out of ten (60 %) were TBS+ after infection with NF54. B) Pie charts indicating the mean RELTEXP of 7G8 parasites from eleven malaria-naïve individuals from two earlier conducted studies (left, MAVACHE, CVac-Tü3 (Wichers et al., 2023)) and 7G8 parasites from three lifelong exposed individuals from the L2 study. The largest proportion of expression is linked to PF7G8_040025600 for both volunteer groups. The remaining var genes are expressed heterogeneously on a lower level. Also, parasites from semi-immune volunteers from the L2 study (L2-32.22A, L2-32.55A and L2-32.71A) express many B-type variants and severity-linked A-type var genes at a lower level. C) Heatmap illustrating the similar var gene expression pattern by parasites from malaria naïve volunteers ((MAVACHE; M1-IDs) and CVac-Tü3 (CT-IDs)) and the three life-long exposed individuals (L2-32.22A, L2-32.55A and L2-32.71A) on a single volunteer level. D) Super plot showing PfEMP1-specific antibody levels measured as mean fluorescence intensity (MFI) for the 44 tested PfEMP1 domains (both plexes) in the Luminex assay for six volunteers from sequence A at baseline (7G8, C-1) and 8 weeks after the initial challenge with 7G8. Challenge with 7G8 parasites and treatment of volunteers latest at day 17 post infection did not cause a measurable elevation of PfEMP1 immunity levels. AVG: average, var gene color code as indicated.

For 6/14 (43 %) of analysed volunteers in sequence A (Figure 9) we obtained paired plasma samples at baseline (7G8, C-1) and 8 weeks afterwards. The overall antibody response to all 44

tested PfEMP1 domains remained unaltered in plasma of volunteers from sequence A comparing baseline and eight weeks post induction (Figure 10 D). This indicates that either the parasite load was not sufficient to build up additional PfEMP1-specific immunity, or that the antibodies produced were not cross-reactive with the antigens tested. From these volunteers, a single 7G8-infectable volunteer (Figure 10 D, L2-32.22A; red labels) with the lowest average baseline immunity was the only volunteer who developed an infection with 7G8 parasites (red circles) hinting towards a low immunity level. Unfortunately, this effect could not be further explored due to the unavailability of further samples since for the other two volunteers which were infected with 7G8 parasites. In the case of L2-32.71A no paired (baseline (C-1) and + 8 weeks) samples were collected and the plasma from L2-32.55A was excluded due to an overall high reactivity with the negative control BSA. For the remaining volunteers which stayed TBS negative during sequence A (n=5, Figure 10 D, black dots) the total PfEMP1-specific IgG levels were overall higher but also remained unaltered at both time points.

These findings indicate that the *var* gene expression pattern of 7G8 parasites isolated from malaria-naïve and individuals with possibly low immunity levels despite being life-long malaria exposed is highly similar, and that volunteers with higher baseline PfEMP1 antibody level might a) have a higher degree of protection against 7G8 infection and b) are accumulating no further (cross-)protectivity for the tested antigens following the infection with 7G8 parasites and the obligatory treatment with AL+PQ.

3.3 Classification of volunteers according to their degree of semi-immunity into non-controllers and controllers

In endemic settings, volunteers recruited for CHMIs have varying degrees of semi-immunity impacting their ability to control the infection (Figure 11 A, Langhorne et al., 2008; Lell et al., 2018; Lell & McCall, 2018). Until now, there is no gold standard to measure the degree of semi-immunity to *P. falciparum* infections in pre-exposed individuals. Thus, we first aimed to classify the volunteers into non-controller and controllers similar to Bachmann et al. 2019 and Bhardwaj et al. 2024. For this, we integrated volunteers' data from Bachmann et al. 2019 which were infected similarly to the L2 study with 3,200 PfSPZ to our dataset. Bachmann et al. 2019 identified six non-controllers and six controllers, however for one volunteer no blood sample for *var* gene analysis was collected and another one was excluded since the RT-qPCR displayed expression of only very few different *var* genes. To illustrate a more complete picture of different states of semi-immunity we also infused data from twelve malaria-naïve volunteers from earlier studies who were either inoculated with 3,200 or 800 PfSPZ (Bachmann et al., 2016). From 25 volunteers from the L2 'CHMI-study' we identified a total of 13 non-controllers (52 %) and 11 controllers (44 %), which roughly resembles the expected distribution of volunteers and their ability to control the infection in Lambaréné, Gabon (section 3.1). For one volunteer (L2.32.11B) no baseline sample was collected and therefore excluded from the analysis. From malaria-naïve volunteers to controller, the expressed *var* gene entropy (measured as Shannon index) is decreasing while the time of blood stage infection onset (determined as day post infection with first positive TBS) is increasing resulting in separated volunteer groups using a Partitioning Around Medoids (PAM) clustering

Results

algorithm (Figure 11 B). Of note, volunteers of L2 who received treatment following detectable TBS parasitemia and malaria-related symptoms in one CHMI but decided to continue for later CHMIs (L2-32.12A, L2-32.22A and L2-32.71A, all 'non-controllers') were seemingly not able to switch to the volunteer group in a subsequent infection eight week later. Thus, we suggest that neither the initial

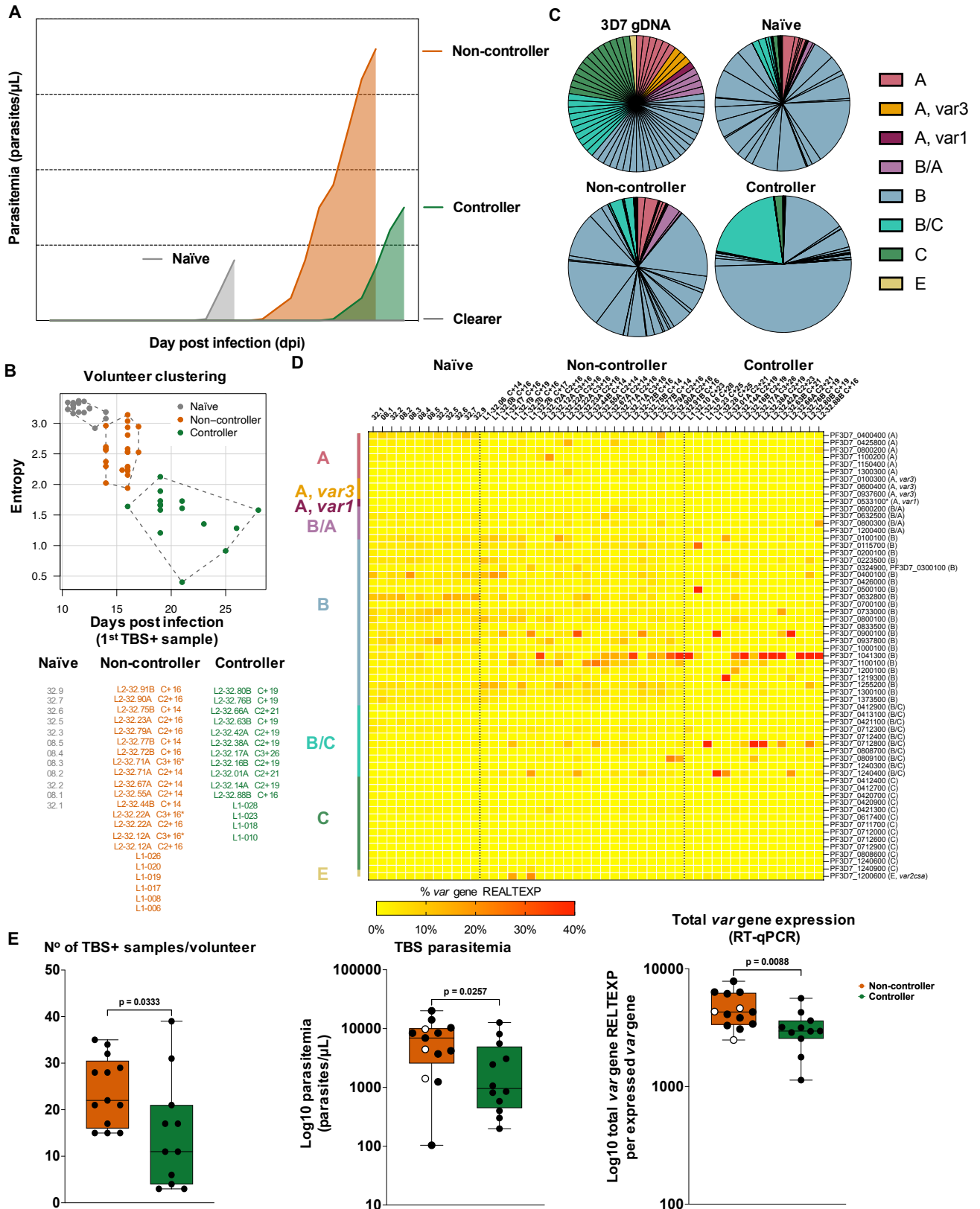


Figure 11.: Establishment of infections with *P. falciparum* parasites in naïve and life-long malaria exposed individuals

A) Schematic overview of naïve and semi-immune (non-controllers, controllers, clearers) volunteer infection onset dynamics. Naïve volunteers are treated quickly after inoculation at low parasitemia levels while non-controller show a delayed onset of microscopic visible parasites in the blood and develop higher levels of parasitemia compared to controllers. Additionally, controller can further delay the infection onset compared to non-controllers while clearer do not show microscopic evidence of parasites despite inoculation with sporozoites. B) Partitioning Around Medoids (PAM) clustering of volunteers recruited in three CHMI trials (TüCHMI, L1 and L2) allows unbiased categorization and differentiation of naïves (received 800 or 3200 Sanaria® PfSPZ Challenge (NF54) sporozoites, high *var* gene entropy and early infection onset, $n=11$, 08 or 32-IDs), non-controllers (high *var* gene entropy and slightly delayed infection onset, $n=6$ (L1; Bachmann et al. 2019) and $n=13$ for L2) and controllers (low *var* gene entropy and strongly delayed infection onset, $n=4$ (L1; Bachmann et al. 2019 and 11 for L2) according to their *var* gene profile and the onset of TBS positivity. Sample IDs like L2-032.12A C2+16 included the volunteer ID (L2-032.12A) with the respective sequence (A or B), the challenge, the sample is originated from (C2 = 2nd challenge from volunteer L2-032.12A) and the days post infection (C2+16) the sample was collected. C) Representative examples of *var* gene expression pattern displayed by parasites isolated from malaria-naïves (top, right), non-controllers (bottom, left) and controllers (bottom, right) at infection onset compared to gDNA distribution (top, left) showing a broad activation of (sub-)telomeric B-type and also A-type *var* genes for parasites from malaria naïves and non-controllers, and a more restricted *var* pattern for parasites from controller with more centromeric B/C type *var* genes expressed. D) Heatmap sorted according to PAM clustering, showing individual *var* gene expression pattern in % of total *var* expression from all individual volunteers recruited in three CHMI trials (TüCHMI, L1 and L2). E) Boxplots showing higher numbers of longitudinally sampled TBS+ blood smears (left) and higher TBS parasitemia (middle) for non-controllers during the 1st infection peak. Total parasite's *var* gene expression from the individual's 1st parasitemia peak sample is higher for parasites from non-controllers than for controllers (right panel). Peak parasitemia and total *var* gene expression could not be determined for three threatened volunteers L2-032.22A, L2-032.55A and L2-032.71A due the onset of symptoms and the application of a treatment. For them, the highest parasitemia before treatment and the respective total *var* expression are displayed (open circles). *Var* gene group coloring as indicated: A-types in light red, *var3* genes in orange, *var1* gene in dark red, B/C-type genes in purple, B-type genes in light blue, B/C-type genes in turquoise, C-type genes in dark green, E-type gene in yellow. Non-controllers and controllers as indicated in dark orange dark green, respectively. Significance levels were assessed with Mann-Whitney U-tests.

infection with NF54 parasites not the treatment application induced a significant increase in infection control for these volunteers. In line with the observation from Bachmann et al. 2019 and Bhardwaj et al. 2024, we observed a heterogeneous *var* gene expression pattern by parasites from malaria-naïve and non-controller individuals involving in particular severity-associated B and A-type *var* genes. Contrary, for parasites from controller the expression pattern is dominated by a single or few variants only (Figure 11 C, D). These variants include PF3D7_1041300 (B), PF3D7_0712800 (B/C) or PF3D7_1240400 (B/C) which strongly dominate the *var* gene pattern in parasites from 9/11 L2 controllers as well as in 3/4 L1 controllers and with both B/C variants being associated to mild-malaria outcomes. Simultaneously, a higher parasitemia and number of longitudinally collected TBS+ samples for non-controllers was observed, indicating a better and faster control of infection by controllers (Figure 11 E; (Bachmann et al. 2019)). Additionally, we compared RT-qPCR results of the total *var* gene expression, measured by summing up the expression of each *var* gene of the repertoire, revealing higher total *var* expression by parasites from non-controllers while still having an equal amount of *var* genes amplified in samples from non-controllers and controllers (Figure 11 E, Supplementary Figure 1). These observed effects for non-controllers and controllers were not caused by differences in biological sex ratio or age distribution (Supplementary Figure 1 A, B), nor by differences in the gene expression levels of the control genes fructose-bisphosphate aldolase (*fba*) or skeleton-binding protein1 (*sbp1*) (Supplementary Figure 1 D).

In conclusion, the unbiased clustering of individuals according to the day of infection onset and the expressed *var* entropy of the parasites allowed a clear separation of individuals with different levels of

Results

exposure and infection control indicated by the reduced asexual parasitemia, the number of longitudinally collected TBS+ samples and the lower total *var* gene expression.

3.4 Degree of semi-immunity affects the *var* gene expression pattern

To verify the classification of individuals into non-controllers and controllers on the host immunity level we performed a Luminex assay similar to Bachmann et al. 2019 and measured the antibody reactivity to a predefined selection of 44 PfEMP1 domains as well as control proteins including GLURP, SERA5, HRP2 and CSP. Luminex data can be either analyzed by comparison of absolute mean fluorescence intensity (MFI) for each antigen or by calculating the seroprevalence of an antigen in comparison to MFI signal from yet unexposed malaria-naïve volunteers. Thus, for a seroprevalence assessments, we included all available baseline plasma samples from volunteers in sequence A and B ((85 % of non-controllers (n=11/13), 91 % of controllers (n=10/11,) (Supplementary Table 1)) and calculated the seroprevalence for each of the 44 PfEMP1 domains based on the measured MFI signal in relation to the MFI + 2STD signal from malaria-naïve volunteers. Since the initial infection with 7G8 parasites in sequence A did not alter the plasma's reactivity to both plexes (Figure 10 D), the data from baseline samples collected prior to the 1st challenge and 8 weeks later were pooled as a new 'baseline'

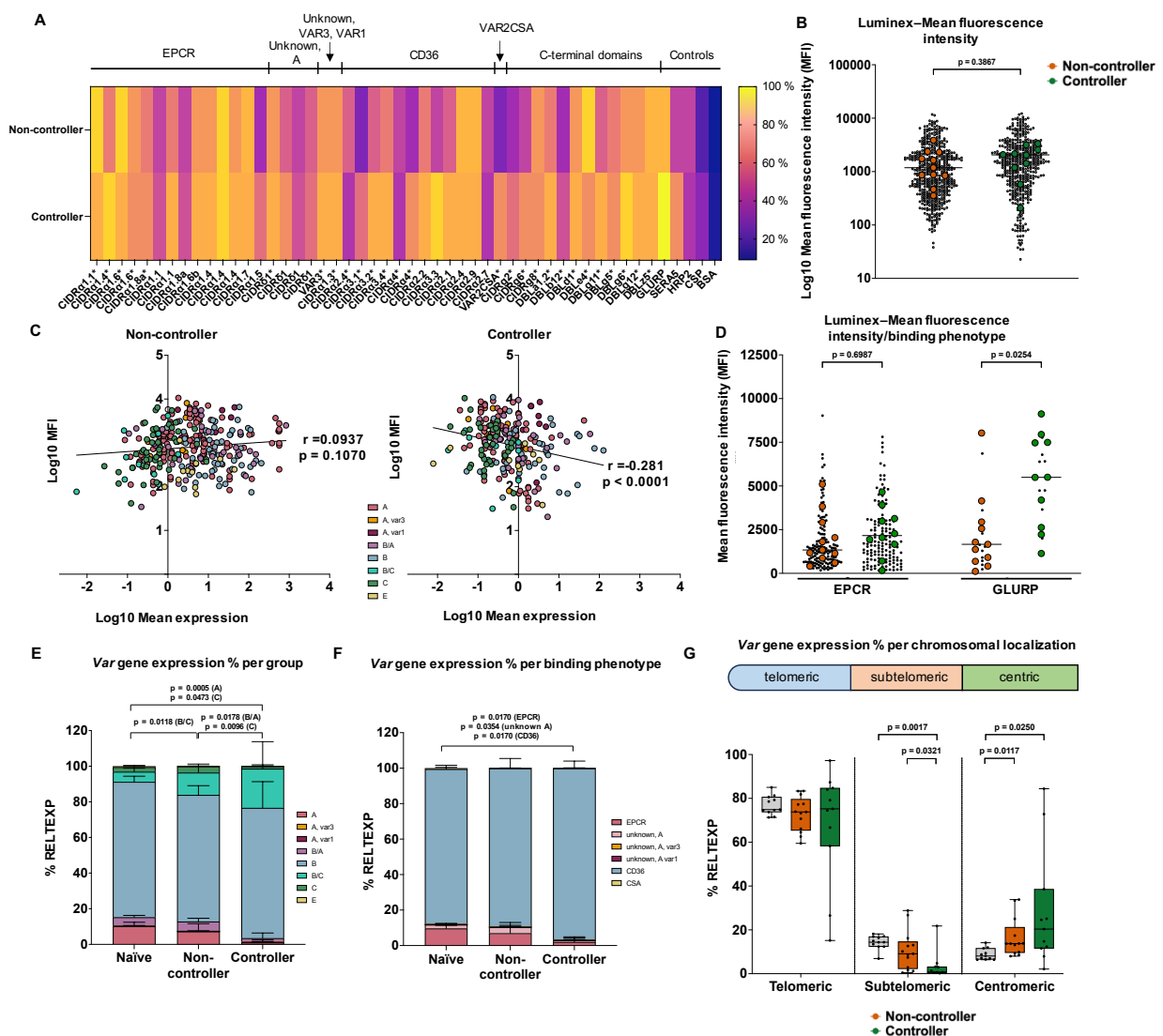


Figure 12.: The degree of PfEMP1 specific semi-immunity at baseline anti-correlates with the parasite's var expression.

A) Heatmap showing the mean seroprevalence from all volunteers per group for 44 PfEMP1 antigens from two different custom-made PfEMP1-specific Luminex plex, calculated by taking the mean MFI + 2x STD from malaria naïve Danish individuals as cutoff for seroprevalence. In total, 27 different domains from NF54/3D7 (plex11, labelled with *) and 17 other PfEMP1 domains derived from different strains (plex 10) as well as five control antigens are displayed. B) Quantification of mean PfEMP1 and control antigen MFI in plasma merged from controllers (n=10) versus non-controllers (n=11) showing a trend towards higher sero-recognition in controllers plasma compared to non-controllers. C) Non-parametric spearman correlation of log10 MFI signals from a subset of 27/44 3D7/NF54-specific domains (plex 11) with log10 mean var gene expression illustrating that only more immune controllers can significantly suppress expression of NF54 var gene variants upon higher PfEMP1-specific antibody levels. D) Overall, controllers show higher levels of absolute MFI signals across all PfEMP1 domains with most discriminating levels to non-controllers being antibody levels to EPCR-binding PfEMP1s (14x different EPCR-binding PfEMP1 domains per n=11 non-controllers and n=10 controllers from two independent Luminex plex not significant) and GLURP (1x domain per volunteer). Similar trends are observed for the immunity levels of the other tested domains from PfEMP1 with the N-terminal binding phenotypes unknown A, var3, var1, CD36 and CSA, although these trends are not significant (Supplementary Figure 1 E). E) Quantification of relative expression of var gene groups shows differences with a significantly decreased expression of severity-linked A and B/A type var genes and increased expression of B/C var genes in parasites from controllers (n=11) compared to parasites from malaria-naïves and non-controllers (n=13). F) Quantification of expressed var genes according the binding receptors of their encoding PfEMP1s at the onset of infection for parasites from malaria-naïves, non-controllers and controllers. G) Boxplots showing relative var gene expressed stratified according to their chromosomal localization for parasites from malaria-naïves, non-controllers and controllers at infection onset. With increasing baseline PfEMP1 semi-immunity, parasites express a higher proportion of B/C- and less A-type var genes and the encoding binding phenotype. Simultaneously, we observed a reduced proportion of subtelomeric- and a higher proportion of central-located var genes. Non-controller and controller as indicated in dark orange and dark green, respectively. Var gene group coloring as indicated: A-types in light red, var3 genes in orange, var1 gene in dark red, B/C-type genes in purple, B-type genes in light blue, B/C-type genes in turquoise, C-type genes in dark green, E-type gene in yellow. Non-controllers and controllers as indicated in dark orange dark green, respectively. MFI: mean fluorescence intensity, STD: standard deviation. Significance levels assessed with Mann-Whitney U-tests corrected for multiple tested with the Bonferroni method.

sample data. Overall, the plasma for controllers showed a trend towards higher seropositivity compared to non-controllers on a single antigen level (Figure 12 A) as well as on absolute MFI levels quantified across all tested antigens (Figure 12 A, B). However, a clearer separation between non-controllers and controllers was observed when we correlated the absolute MFI signal from the subset of 27/44 3D7/NF54-specific PfEMP1 domains (plex 11) to the expressed var genes at the infection onset (Figure 12 C). We observed a direct link between higher antibody levels and the absence of NF54 var gene variants which are specifically targeted by these antibodies in plasma from controllers (Figure 12 C, right). Contrary, within the scope of our assay, low-immune controllers were unable to suppress the expression of distinct NF54 var genes (Figure 12 C, right) an antibody-dependent manner. In addition, the plasma reactivity measured as MFI, targeting PfEMP1 antigens with binding phenotypes EPCR, CD36, and CSA or yet unknown binding phenotypes show a trend towards higher baseline total IgG levels in plasma samples from controller compared to non-controllers with antibody levels targeting GLURP being most discriminating between non-controllers and controllers (Figure 12 D, Supplementary Figure 1 E). Interestingly, the trend towards higher levels of IgG targeting EPCR-binding PfEMP1s in controllers was linked to lower expression of severity-linked A and B/A var genes (Figure 12 E) highlighting the suppressive role of PfEMP1-specific antibodies on var gene expression. Instead, parasites from life-long exposed controller express a higher level of mild malaria linked B/C type var genes compared to parasites from malaria-naïve volunteers (Figure 12 E). We further characterized this effect by stratification of the relative var gene expression according to the expected binding phenotype of the encoding PfEMP1s as well as their chromosomal localization (Figure 12 E, F). It appears that with increasing levels of PfEMP1 semi-immunity from malaria-naïves to controller individuals, the proportion of expressed var genes coding for PfEMP1s with EPCR and unknown A

receptor binding phenotypes is lower and *var* gene variants coding for CD36 binding PfEMP1 are almost exclusively expressed (Figure 12 E). In addition, and compared to malaria-naïve volunteers, the parasites from non-controllers already express a higher proportion of *var* genes which are located more closely to the centromere (Figure 12 G). This trend is even stronger for parasites from controllers indicating that a higher plex reactivity correlates with a tendency to express genes which are located in closer proximity to the centromere while higher antibodies levels targeting especially EPCR-binding PfEMP1s suppress parasites expressing subtelomeric-located A and B/A-type *var* genes.

Based on our results we hypothesize that a *P. falciparum* parasite population aims for establishing a blood stage infection with a relatively broad *var* gene expression pattern with mostly B-type *var* genes located at the telomeric ends of the chromosomes, but also severity-linked subtelomerically located A and B/A-type *var* genes can be found at lower proportions. With increasing immunity, there is an overall reduction in parasitemia, a delay in the onset of infection and a restriction of the *var* gene expression pattern to a single or very few variants of mild malaria linked B/C-type *var* genes located closer to the centromere.

3.5 Characterization of the 1st parasitic wave

Both expression pattern from less immune non-controllers and more immune controllers are dominated by a more or less heterogenous pattern of B-type *var* genes, respectively. To evaluate the determinants for the expression of distinct *var* gene variants during the infection onset, we compared the average *var* gene expression pattern from non-controllers and controllers during the first parasitemia peak (day 0) including incline (up to -5 days) and decline (up to +7 days) (Figure 13 A). Even though the entropy of the expressed *var* genes in parasites from non-controllers and controllers differed for the first TBS+ sample (Figure 11 B, D; Figure 12 D, E) as well as for the entire first peak (Figure 13 A, left and right graphs), the parasites expressed similar *var* variants from their genomic repertoire at a higher level (Figure 13 B). Additionally, when we compared the expression of higher expressed variants (>1 % of total RELTEXP) from non-controller parasites to the variants highly expressed by parasites from malaria-naïves and controllers (Figure 13 B, Supplementary Figure 5), we observed that all three volunteer groups despite their different degree of semi-immunity and ability to control the infection share eleven B-type and one B/A-type *var* gene(s).

In total, parasites from malaria-naïve volunteers and non-controllers express a higher number of *var* genes (25, 26 variants, respectively) than parasites from controller (16 variants) highlighting the less diverse character of the expression pattern by parasites from controller (Figure 13 B). From these variants a substantial amount of genes are shared between all three groups (12/25 (48%, malaria-naïves), 12/26 (46 %, non-controllers) 12/16 (75%, controllers) but parasites from malaria-naïve volunteers and non-controllers express additional variants mostly referring to severity linked A and B/A-type *var* genes (Figure 13 B, Supplementary Figure 5). Some variants were also just expressed by parasites from non-controllers (n=5), malaria-naïve (n=7) and controllers (n=1) individuals or were

Results

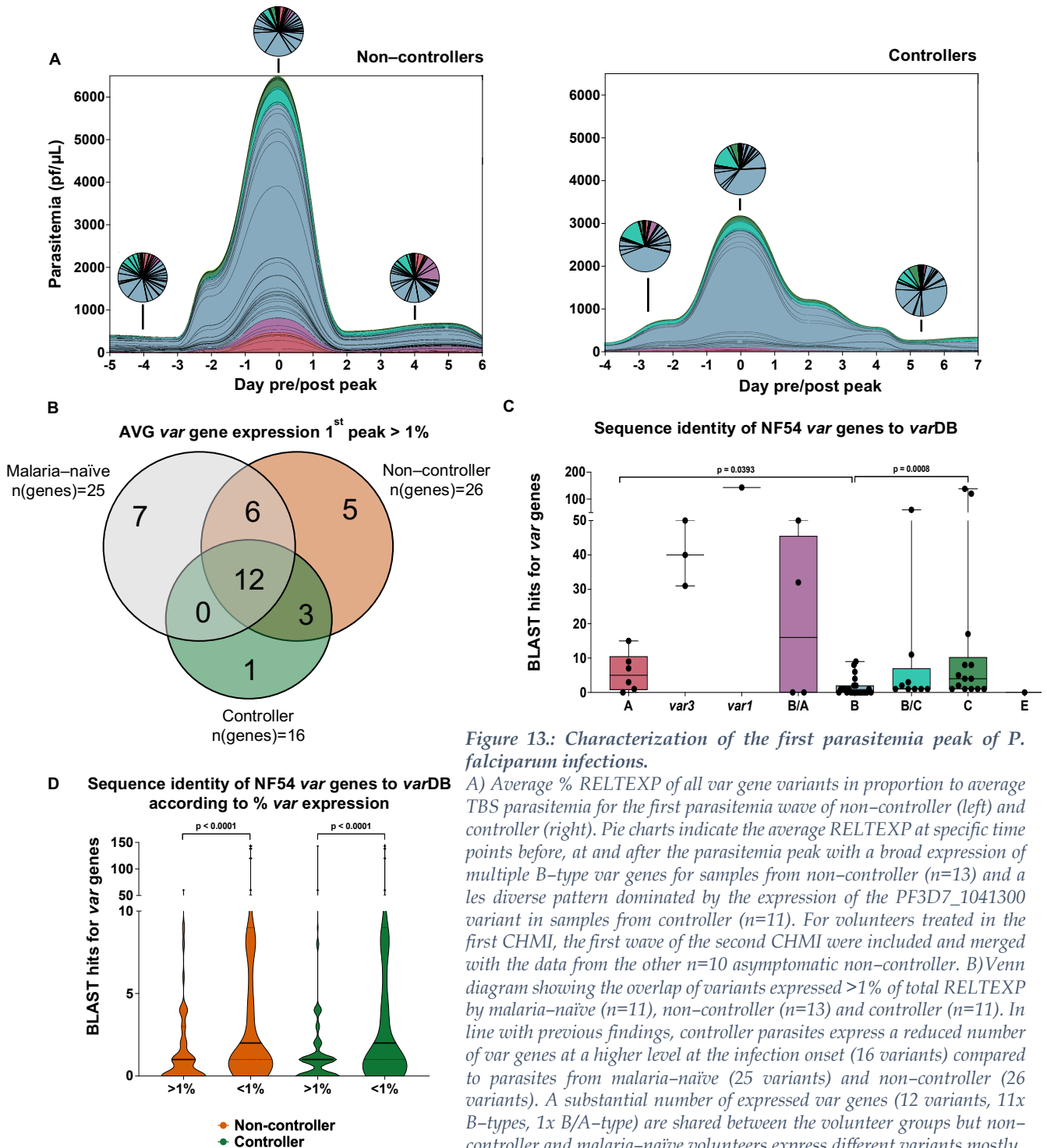


Figure 13: Characterization of the first parasitemia peak of *P. falciparum* infections.

A) Average % RELTEXP of all var gene variants in proportion to average TBS parasitemia for the first parasitemia wave of non-controller (left) and controller (right). Pie charts indicate the average RELTEXP at specific time points before, at and after the parasitemia peak with a broad expression of multiple B-type var genes for samples from non-controller (n=13) and a less diverse pattern dominated by the expression of the PF3D7_1041300 variant in samples from controller (n=11). For volunteers treated in the first CHMI, the first wave of the second CHMI were included and merged with the data from the other n=10 asymptomatic non-controller. B) Venn diagram showing the overlap of variants expressed >1% of total RELTEXP by malaria-naïve (n=11), non-controller (n=13) and controller (n=11). In line with previous findings, controller parasites express a reduced number of var genes at a higher level at the infection onset (16 variants) compared to parasites from malaria-naïve (25 variants) and non-controller (26 variants). A substantial number of expressed var genes (12 variants, 11x B-types, 1x B/A-type) are shared between the volunteer groups but non-controller and malaria-naïve volunteers express different variants mostly

referring to severity linked B/A and A-type variants. Contrary, controller parasites express less severity-linked A and B/A-types (Supplementary Figure 5). C) Boxplots showing the number of BLAST hits for NF54 var gene sequences (>500 bp sequence similarity) when compared to over 200,000 published var sequences retrieved from varDB (Mackenzie et al. 2022). Each dot represents a single var gene variant of the NF54 repertoire allocated to the respective var group. D) Assignment of the var gene BLAST hit results to highly (>1% of total RELTEXP of each sample collected at the 1st parasitemia peak) and lowly (<1% of total RELTEXP of each sample collected at the 1st parasitemia peak) expressed var genes for parasites from non-controller (n=13) and controller (n=11). Violin plots indicate that variants expressed at a threshold of at least 1% have significantly lower BLAST hits than the variants expressed below 1%. Var gene group coloring as indicated: A-types in light red, var3 genes in orange, var1 gene in dark red, B/C-type genes in purple, B-type genes in light blue, B/C-type genes in turquoise, C-type genes in dark green, E-type gene in yellow. Non-controller and controller as indicated in dark orange dark green, respectively. Significance levels were assessed with Mann-Whitney U-tests corrected for multiple testing using the Bonferroni method.

shared across two volunteer groups only (Figure 13 B). In malaria-naïve volunteers parasites exclusively express highly immunogenic and severity-linked Pf3D7_0400400 (A), Pf3D7_110200 (A)

and Pf3D7_0833500 (B/A) as well as Pf3D7_0200100 (B), Pf3D7_042600 (B), Pf3D7_041100 (B/C) and Pf3D7_0712300 (B/C).

Apart from Pf3D7_1240300 (B/C), which is exclusively expressed to a higher degree by parasites from controller, the expression pattern from parasites in non-controllers and controllers highly overlap however a variety of A, B/A and B variant being expressed to a significantly lower degree by parasites from controller (Pf3D7_0425800 (A), Pf3D7_0800200 (A), Pf3D7_0600200 (B/A), Pf3D7_0800200 (B/A), Pf3D7_0115700 (B), Pf3D7_0300100 (B), Pf3D7_0324900 (B), Pf3D7_0632800 (B), Pf3D7_0937800 (B), Pf3D7_1373500 (B) (Supplementary Figure 5)) as previously observed for both groups (Figure 12 D) while expression for other B-types still remains high. Among the twelve genes which are highly expressed by parasites from the three volunteer groups Pf3D7_1041300 (B), Pf3D7_0900100 (B), Pf3D7_1255200 (B), Pf3D7_1100100 (B) were particularly highly expressed and Pf3D7_0412400 (C), Pf3D7_0808700 (B/C) and Pf3D7_1219300 (B) exclusively expressed by parasites from semi-immune volunteers (non-controller and controller).

Since most highly expressed variants are shared between parasites from the different volunteer groups, the expression pattern in life-long malaria exposed individuals is likely still determined by the intrinsic expression 'program' the parasites have to establish the blood phase. Previously acquired immunity can therefore restrict the level of *var* gene expression heterogeneity by negative selection (Figure 11 B), but seems to be unable to recognize a particular set of B and B/C-type *var* genes. When we performed a BLAST search of the NF54 *var* gene sequences of the highly expressed *var* genes against the *var* gene database (VarDB), containing more than 200.000 previously published full-length *var* gene sequences from various isolates using a threshold of 99% sequence similarity over at least 500 bp, we observed that B-type *var* gene sequences are less conserved within the worldwide parasite population compared to A and C-type sequences (Figure 13 C). Furthermore, when assigning the number of BLAST hits to the individual *var* gene sequences expressed during the initial parasitic wave, we observed that *var* genes being expressed on average > 1 % show significantly lower blast hits and therefore a lower degree of sequence conservation than variants expressed < 1 % (Figure 13 D). Therefore, we hypothesize that the parasite population entering the blood phase expresses a highly diverse *var* expression pattern of preferably less conserved B-type *var* genes. Since PfEMP1s normally show a high level of epitope sharing to other strains and isolates, cross-protective antibodies from earlier episodes of infection might therefore effectively target more conserved PfEMP1s reducing the overall *var* gene diversity while less conserved variants remain unrecognized.

3.6 Longitudinal assessment of parasitemia and infection duration

Interestingly, when we counted the number of longitudinally recorded TBS+ samples per volunteer, we observed that controllers are significantly less frequently TBS positive throughout the trial than non-controllers (Figure 11 E). Thus, we hypothesized that the different degree of semi-immunity we observed between non-controllers and controllers might also impact on the longitudinal infection

Results

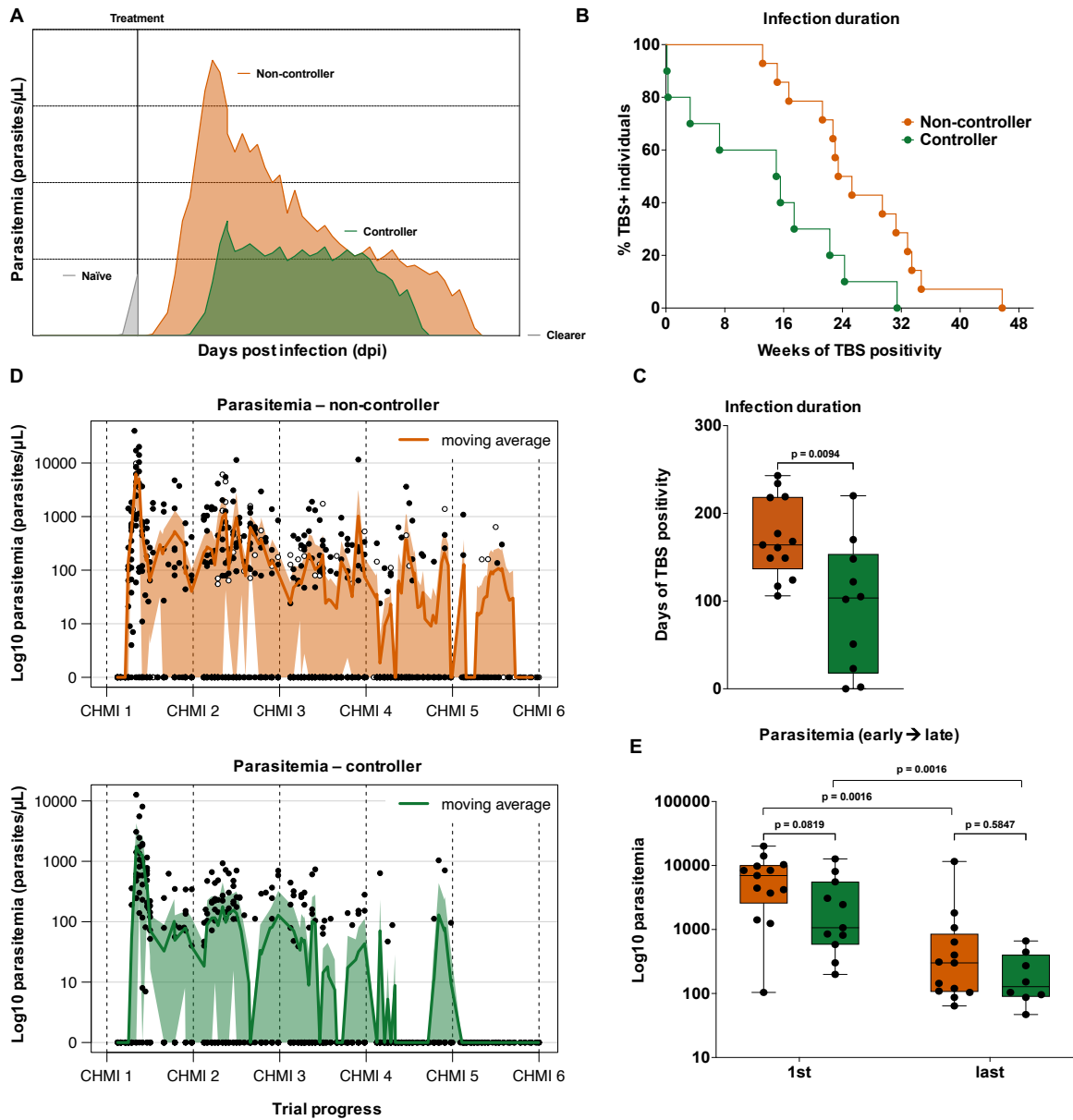


Figure 14: Longitudinal tracking of infections in volunteers classified as non-controllers and controllers. A) Schematic showing the course of CHMI infections in malaria-naïve, non-controller and controller volunteers. B) Kaplan-Meier plot suggest reduced days of TBS positivity for controllers ($n=10$, 1x individual withdrew) compared to non-controllers ($n=13$). C) Quantification of the duration of TBS positivity for non-controllers ($n=13$) and controllers ($n=10$, 1 individual withdrew) shows that parasites persist for a median of 60 days longer in non-controllers than controllers. D) Individual time-axis aligned parasitemia values for non-controllers (upper panel) and controllers (lower panel). Moving average was calculated for ten neighboring samples and show a gradual drop of TBS parasite densities until the end of 4th or the 5th CHMI for controllers ($n=11$) and non-controllers ($n=13$), respectively. E) Quantification of first peak parasitemia (1st) compared to the last collected TBS+ sample (last) showing higher parasitemia values for non-controllers ($n=13$) at infection onset than controllers ($n=11$ at onset and $n=8$ at last time point (1x withdrew, 2x TBS+ only once during the trial). Non-controllers and controllers as indicated in dark orange and dark green, respectively. Significance levels were assessed with Mann-Whitney U-tests corrected for multiple tested using the Bonferroni method.

dynamics of the respective volunteer groups (Figure 11, Figure 12, Figure 14 A). Therefore, we first counted the days of longitudinal TBS positivity for all volunteers and found controllers to be able to clear microscopic infections at a median of approx. 60 days more quickly than non-controllers (Figure 14 B, C). For the three symptomatic volunteers (L2-32.22A, L2-32.55A and L2-32.71A) the accurate infection duration could not be calculated due to the treatment application following the 1st NF54 infection. For these individuals the total days of TBS+ was calculated from the subsequent NF54

infection onwards for which these volunteers stayed asymptomatic until the end of the trial. In addition to this, the merge of the longitudinal parasitemia data from all non-controllers and controllers showed a) that non-controllers develop up to a 10 fold higher median TBS parasitemia compared to controllers at the infection onset similar to Figure 11 E) and b) a stronger reduction of parasitemia reduction over time by non-controller (median: 18 fold reduction) compared to controllers (median: 5 fold reduction). However, both volunteer groups were not distinguishable when comparing the last sample in which the parasitemia oscillated around a median of 100–300 pf/μL in both groups indicating that non-controllers catch-up to controllers during the course of infection (Figure 14 D, E). Therefore, the observed higher strain-specific PfEMP1 immunity levels at baseline (Figure 12) seems to have a direct impact on the parasitemia at the onset and course of infection as well as the infection length.

3.7 Longitudinal *var* gene expression pattern

3.7.1 Tracking of *var* gene entropy and anti-PfEMP1 immunity over time

Since the ability to control the infection better has been linked to the expression of a more restricted *var* gene pattern (Bachmann et al. 2019, Figure 11 B, C, D), we investigated the *var* gene entropy over time in parasites from non-controllers and controllers. Continuing the analysis of the baseline samples (Figure 11, Figure 12), we also performed NF54 *var* gene-specific RT-qPCR for all longitudinally collected volunteer samples from the CHMI cohort (Supplementary Table 1). For this, we calculated and plotted the expressed *var* gene entropy (measured as the Shannon index) per volunteer group in chronological order. Parasites from controllers remain relatively stable in their expressed *var* entropy, whereas parasites from non-controllers display higher *var* entropy at the beginning of each challenge infection, which is declining within a single CHMI, but also over the course of the entire trial (Figure 15 A). The high entropy *var* expression pattern of parasites from non-controllers at the beginning of the infection decreased sharply in the first eight weeks of infection and shifted to a lower entropy expression pattern, but increased again after the administration of new NF54 sporozoites in the second CHMI. The same trend was also observed after the third inoculation with NF54 sporozoites ((Figure 15A), upper panel), although the effect was less pronounced. Interestingly, the three volunteers (L2-032.22A, L2-032.55A and L2-032.71A) who received a treatment due to malaria-related symptoms in the first CHMI with NF54 (Figure 15 A, open circles) displayed highest *var* entropy values in the second CHMI on a comparable level to the first CHMI. Moreover, all three volunteers were still classified as non-controllers in an expanded PAM clustering algorithm using the samples from the second CHMI (Figure 11 B). By contrast, the expressed *var* gene entropy of parasites from controllers started at lower levels (Figure 11 C, Figure 15 B) and did not significantly increase after CHMI 2 and 3 as in parasites from non-controllers (Figure 16 A, lower panel). A quantification of the *var* gene entropy score revealed that only parasites from non-controllers significantly reduce the *var* entropy score over time aligning to similar levels to parasites from controllers (Figure 15 B).

Results

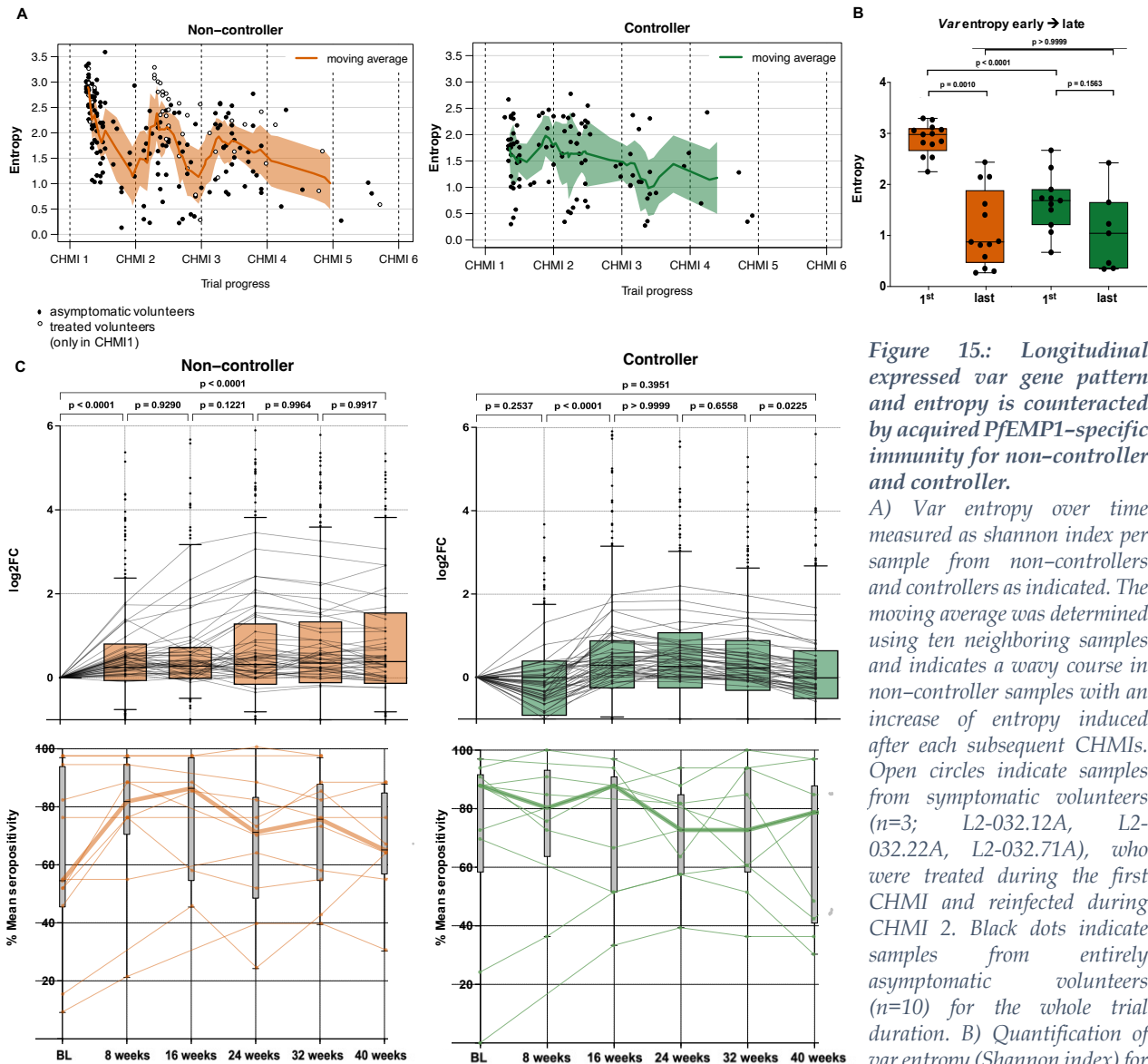


Figure 15.: Longitudinal expressed var gene pattern and entropy is counteracted by acquired PfEMP1-specific immunity for non-controller and controller.

A) Var entropy over time measured as shannon index per sample from non-controllers and controllers as indicated. The moving average was determined using ten neighboring samples and indicates a wavy course in non-controller samples with an increase of entropy induced after each subsequent CHMIs. Open circles indicate samples from symptomatic volunteers ($n=3$; L2-032.12A, L2-032.22A, L2-032.71A), who were treated during the first CHMI and reinfected during CHMI 2. Black dots indicate samples from entirely asymptomatic volunteers ($n=10$) for the whole trial duration. B) Quantification of var entropy (Shannon index) for

first (1st) and last samples (last) from non-controllers ($n=13$; 1st and last samples) and controllers ($n=11$; 1st sample, $n=7$ last sample (1x withdrew, 2x TBS+ only once during the trial and 1x did not pass the quality requirement of our RT-qPCR) show a strong decrease over time in parasites from non-controllers, but only a minor reduction in parasites from controllers. At onset, non-controllers parasites express a significantly higher var entropy (Figure 11), while at the end of TBS positivity, parasites from both volunteer groups show a low, not significantly different var entropy. C) Boxplots with IQR and 95 % confidence interval showing \log_2FC of the mean fluorescence intensity (MFI) data from merged from non-controllers ($n=11$) showing significantly higher PfEMP1-specific antibodies for 44 tested antigens (Table 14) which remained higher than baseline levels even after 40 weeks of infection (top, left). Mean seroprevalence in % (ratio of antigens showing higher MFI signal compared to the mean MFI of malaria-naïve individuals + 2 STD) indicate lower seropositivity at baseline for non-controllers similar to Figure 12 B. For non-controllers the seroprevalence quickly increases from 55 % to about 80 % within eight weeks of infection and reaches saturation (bottom, left). \log_2FC (calculated as indicated before) of the mean fluorescence intensity (MFI) data from merged from controllers ($n=10$) showing significantly higher reactivity of the plasma with the tested antigens after 16 weeks, however no significant increase was observed during the 40 weeks of monitoring (top, right) % mean seroprevalence (calculated as indicated before) showing unaltered levels of seroprevalence throughout the infection until week 40. Non-controllers and controllers as indicated in dark orange and dark green, respectively (bottom, right). Significance levels assessed with Mann-Whitney U-tests corrected for multiple tested with the Bonferroni method.

Non-controllers show an overall trend of lower baseline PfEMP1-specific immunity levels for all PfEMP1 binding phenotypes (Figure 12 A, B, C, Supplementary Figure 1 E), but seem to align to controller over time for parasitemia and the parasite's var entropy levels (Figure 14 E, Figure 15 B).

Thus, we wondered whether non-controllers can acquire further PfEMP1 immunity or even catch up to the levels of the controllers. Measuring the longitudinal acquisition for all 44 tested antigens, as the fold change compared to the baseline level showed significantly higher PfEMP1-specific antibody levels in plasma samples from non-controllers after the first 8 weeks of infection and which stayed higher throughout the infection until week 40 (Figure 15 C, upper panel, Supplementary Figure 1 G). Simultaneously, the seropositivity which was observed to be lower for non-controllers at baseline (Figure 12 A) increased from about 55 % to about 80 % of all antigens tested within 8 weeks (Figure 15 C, lower panel), although the variation across the volunteers was too high to observe significant effects. Interestingly, a significant increase of PfEMP1-specific antibodies was detected for controllers after 16 weeks, however overall PfEMP1-specific antibody levels remained at a constant level during the 40 weeks (Figure 15 D, upper panel). In line with this finding, the seroprevalence of plasma samples from controllers which showed a higher baseline level (Figure 15 D) stayed relatively high throughout the infection (Figure 15 D, lower panel) suggesting that only non-controllers are able to significantly increase their PfEMP1-specific antibody responses for the tested antigens. This observation is in line with Figure 15 A illustrating that parasites are able to boost the *var* gene entropy subsequently to homologous CHMI only in low immune non-controllers. With increasing time and PfEMP1 immunity, also parasites of non-controllers can no longer boost the entropy comparably to parasites from controller suggesting an important role for accumulating PfEMP1 immunity to restrict the expression of the *var* gene repertoire.

3.7.2 Antigenic variation of the malaria parasite *P. falciparum*

Simultaneously with the observed decrease of *var* gene entropy over time, the expression pattern of *var* groups was changing. The longitudinal quantification of the relative *var* gene expression showed that parasites from non-controllers expressed higher levels of A and B/A type *var* genes (Figure 12 D and Figure 16 A) compared to parasites from controllers at infection onset, while parasites from non-controllers at later infection stages expressed a *var* gene pattern comparable to parasites from controllers at the infection onset which is dominated by mostly B, B/C and also C type *var* genes (Figure 16 A). When allocating the *var* genes to their chromosomal localization instead of the *var* group, we noticed, that for parasites from non-controllers, genes located at the subtelomere are significantly higher expressed at the infection onset than at later infection stages or when compared to parasites from controllers (Figure 16 B). Moreover, with increasing time, the proportion of expressed genes located in central regions is increasing. The higher proportion of expressed *var* genes encoding EPCR-binding PfEMP1s (Figure 12 E, Figure 16 C) by non-controllers parasites strongly decreased over time while parasites from controllers almost exclusively expressed *var* gene which encode for PfEMP1s binding to CD36 at both the infection onset and later during the infection (Figure 16 C).

Since the overall expression pattern on the *var* group level is altered with increasing infection time, we next investigated the longitudinal *var* gene expression pattern of parasites from each volunteer individually. For this, *var* gene expression was tracked for each gene variant of NF54 and plotted in relation to the measured TBS parasitemia (Figure 16 D, Supplementary Figure 3, Supplementary Figure

Results

4). Figure 16 D shows a representative analysis from one non-controller, which displays great changes in the *var* gene expression over time. In the first parasitemia wave, parasites express almost all *var* genes from the NF54 repertoire, but preferentially of group B similarly observed in Figure 11 and Figure 12. However, for subsequent waves of parasitemia, dominant expression of a single or few variants is detected (39 % – 77 %). Variants dominantly expressed once during a parasitemia wave were not found

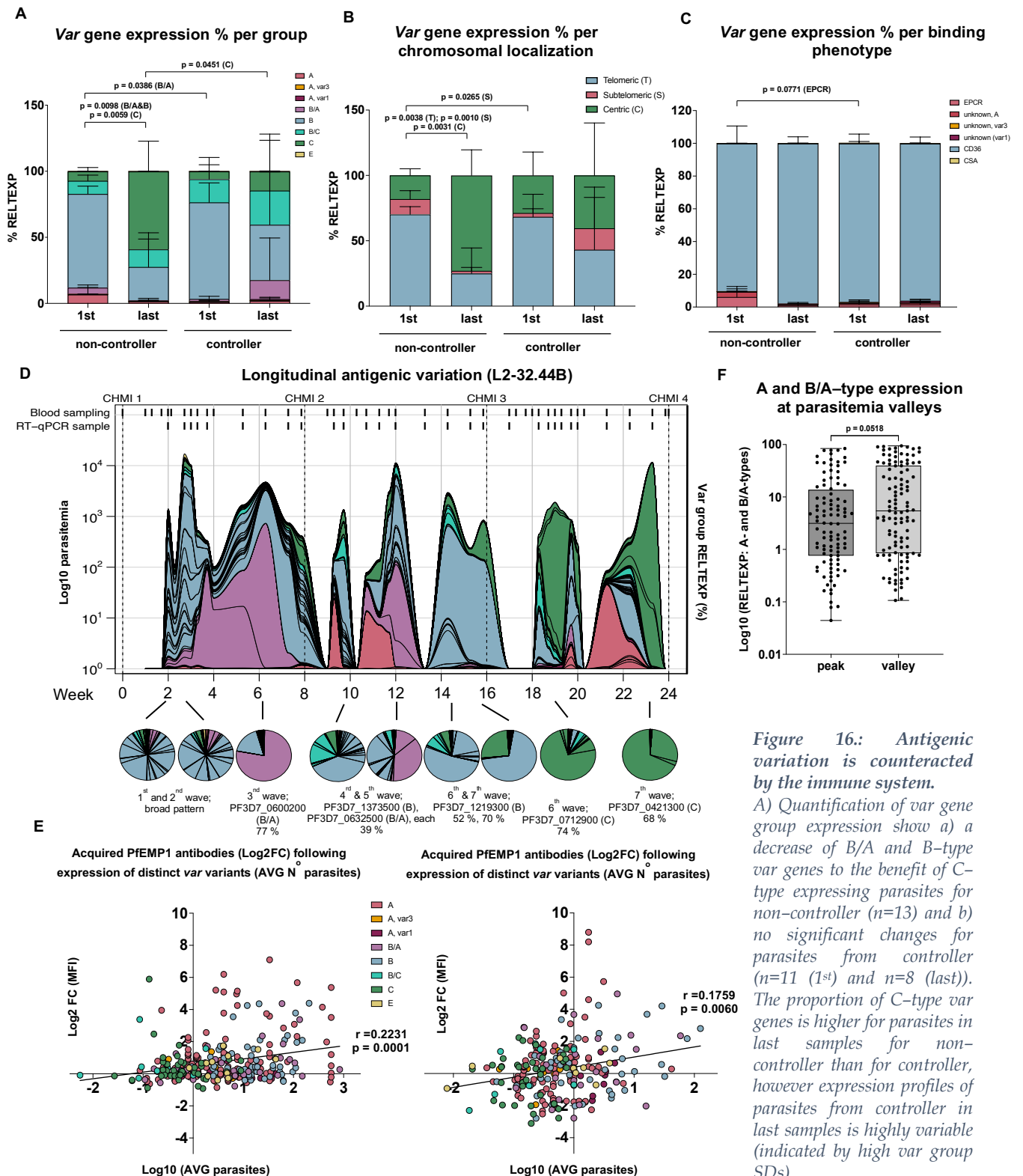


Figure 16.: Antigenic variation is counteracted by the immune system.

A) Quantification of *var* gene group expression show a) a decrease of B/A and B-type *var* genes to the benefit of C-type expressing parasites for non-controller ($n=13$) and b) no significant changes for parasites from controller ($n=11$ (1st) and $n=8$ (last)). The proportion of C-type *var* genes is higher for parasites in last samples for non-controller than for controller, however expression profiles of parasites from controller in last samples is highly variable (indicated by high *var* group SDs).

B) RELTEXP *var* gene expression according to their chromosomal localization: Early to late decrease of telomeric and subtelomeric variants to the benefit of central located *var* genes in parasites from non-controllers. No significant change of *var* gene expression according to their chromosomal localization in parasites from controllers over time. C) RELTEXP *var* gene expression according to the encoding PfEMP1 binding phenotype. Parasites from non-controllers and controllers display no differences in the expressed N-terminal binding phenotypes apart from a tendency of less EPCR-binder expressed in controllers. D) Representative example of antigenic variation by NF54 parasites during the course of infection in a non-controller individual. Parasitemia is shown on a logarithmic scale (left Y-axis), with *var* gene expression as the % of parasites expressing a specific variant (*var* expression/parasitemia) at a given time filling the area under the curve (right Y-axis, % RELTEXP). At first, the parasites express a broad *var* gene pattern that includes nearly all *var* genes from the NF54 repertoire, especially B-types. Subsequent waves of parasitemia are dominated by a few or a single variant only. Over time the proportion of C-type *var* genes is increasing and severity-linked A-types are found mostly at the start or end point of parasitemia waves. E) Non-parametric spearman's rank correlation of acquired recognition of particular PfEMP1 domains (measured by Luminex as log2FC MFI of baseline plasma to eight weeks post initial infection) and relative gene expression of the encoding *var* variant (in % of total *var* expression) normalized to peak parasitemia for non-controllers (n=13; left panel) and controllers (n=11; right panel). The data indicates that there is a fair correlation between acquired antibody responses against dominantly expressed variants at the parasitemia peaks within the analyzed eight-week interval for both volunteer groups. Correlation seems to be the best for A-type PfEMP1s, which are overrepresented on the plex (section 2.2.13, Table 14). F) RELTEXP of A and B/A-type *var* gene expression at parasitemia peaks and valley (defined as all samples except peak samples) from all non-controller (n=13) and controller (n=7; for n=3 only a single peak was registered and therefore not part of the analysis). The 1st parasitemia peak was excluded since A) showed that A-types are more commonly observed when a broad pattern is expressed. In line with D) A and B/A-type *var* genes are higher expressed in samples from parasitemia valleys (n=113) than peaks (n=100). Non-controllers and controllers are indicated in dark orange and dark green, respectively. *Var* gene group coloring as indicated: A-types in light red, *var3* genes in orange, *var1* gene in dark red, B/C-type genes in purple, B-type genes in light blue, B/C-type genes in turquoise, C-type genes in dark green, E-type gene in yellow. AVG: average, MFI: mean fluorescence intensity. Significance levels were assessed with Mann-Whitney U-tests corrected for multiple tested with the Bonferroni method.

highly expressed in subsequent waves of parasitemia in the same volunteer, suggesting that the individuals are able to build up a variant-specific protection against these variants.

To investigate whether the volunteers built up an PfEMP1 variant-specific antibody response for highly expressed variants, we calculated the mean *var* gene expression of samples at peak parasitemia during the first challenge infection from non-controllers and controllers and correlated the expression data with antibody data targeting 27 domains of the 3D7/NF54-specific Luminex plex (Table 14). We observed a positive correlation between highly expressed variants and increasing antibody levels against corresponding PfEMP1s for both non-controllers (Figure 16 E, left) and controllers (Figure 16 E, right). The higher correlation coefficient for non-controller is most likely due to the antibody acquisition for EPCR binding A-type PfEMP1s, which are, despite being lowly expressed, recognized by the 3D7-plex and almost entirely absent in controller parasites (Figure 16 E, left; red-colored dots).

For some parasitemia waves of volunteer L2-44.32B (Figure 16 D, wave 3, 4, 5, 6 and 7) the expressed variants during the incline or the decline of the wave seem to be different to the variant being expressed at the peak and mostly belong to the severity-linked A and B/A *var* gene groups. We also observed this effect occasionally in waves from multiple volunteers (L2-32.01A, L2-32.11B, L2-32.12A, L2-32.14A, L2-32.16B, L2-32.22A, L2-32.38A, L2-32.42A, L2-32.77B, L2-32.88B), and it was not restricted to samples from non-controllers or controllers (Supplementary Figure 3, Supplementary Figure 4). Quantification of the relative A and B/A-type expression from parasitemia peak compared to all other time points indicate that indeed a higher proportion of these genes is expressed during the in- and decline phase of a parasitemia wave (Figure 16 F). The effect was not significant, but might be

Results

potentially higher in real parasitemia valleys with submicroscopic parasitemia for which no samples were collected during the trial.

As indicated for L2-032.44B in Figure 16 D, the proportion of C-type *var* gene expression increases over time and dominates the expression at the last two parasitemia peaks. Since we already observed a significant increase of mild-malaria linked B/C and C type *var* genes for more immune controllers at baseline (Figure 12 D) and for less immune non-controllers over time (Figure 16 A), we wondered whether this C-type shift is a conserved feature of NF54 *P. falciparum* infections. Indeed, the analysis of longitudinal expression changes by parasites from 13 analyzed non-controllers and eleven controllers revealed a significant increase of central located B/C and C-type *var* genes (Figure 16 D, Figure 17, Supplementary Figure 3, Supplementary Figure 4). We quantified this shift across all volunteers and observed that C-type expression was more common in samples collected close to the time when volunteers were able to clear a microscopic infection (Figure 17 A). To measure this, the most dominantly expressed *var* group was determined per parasitemia peak and whenever the parasite population shifted in its most dominantly expression of the *var* group, this shift was included in the analysis (heterologous shifts) (e.g., B-type → A-type → C-type). Homologous *var* gene shifts of the same group (e.g., B-type to another B-type *var* gene) were factored out to synchronize the time axis of the volunteers who had a different number of peaks over time, most likely depending on their individual degree of semi-immunity. In addition, parasites from non-controllers required more time to

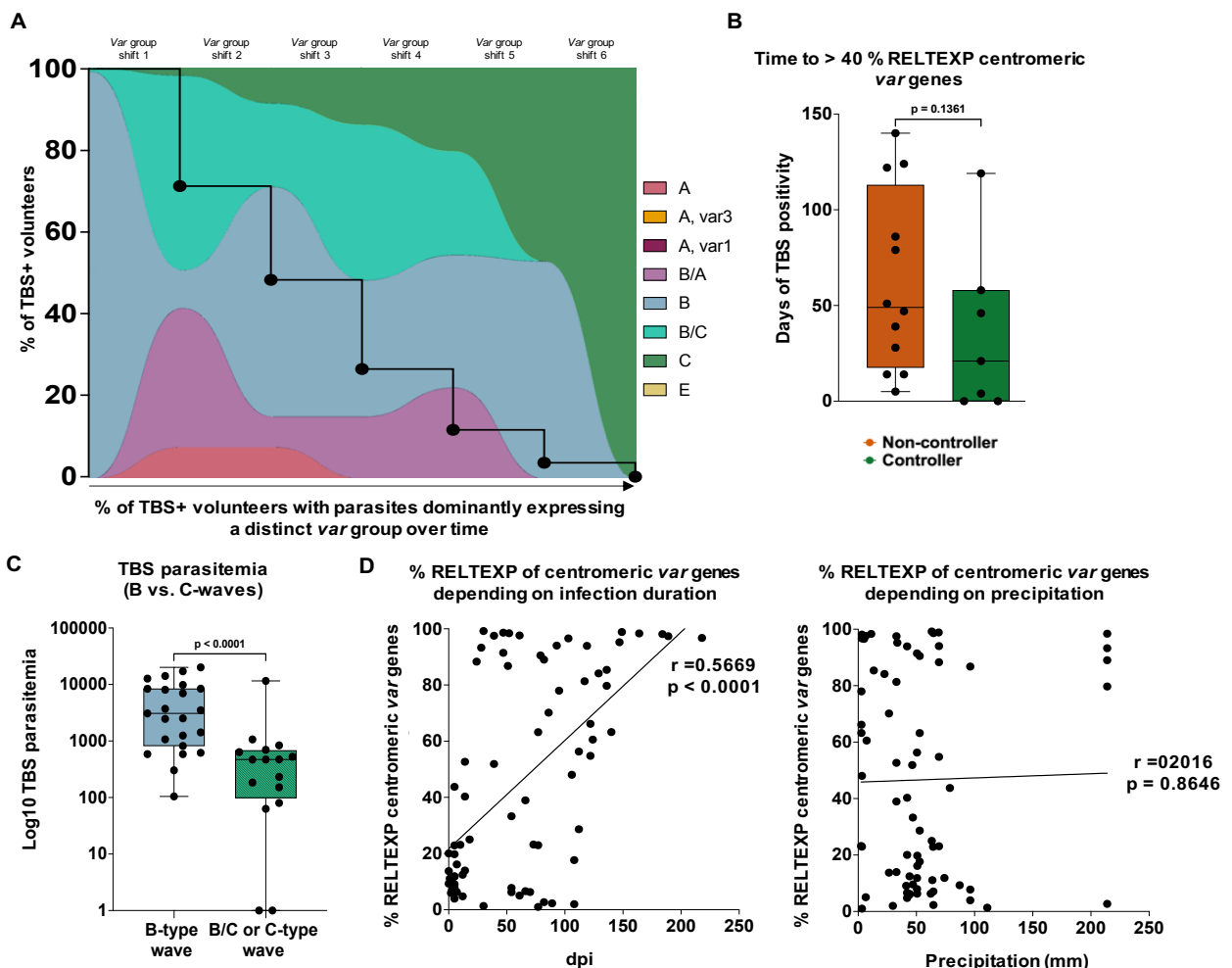


Figure 17.: Increase of C-type expression is linked to infection length.

A) Percent of TBS+ volunteers (Y-axis) with parasites dominantly expressing a distinct *var* group over time (area plot). Merged data from all volunteers indicate that parasites from non-controllers and controllers start expressing B-type variants early during the infection and shift to a dominant expression of C-types in subsequent waves of parasitemia. The time axis is aligned for all volunteers (n=13 (non-controllers), n=11 (controllers)) according to their *var* gene group shifts, meaning that only heterologous *var* group shifts are considered. The closer the volunteers are to clear a microscopic infection, the more frequently the parasites dominantly express C-type *var* genes. B) Quantification of days post infection after parasites show a dominant expression (> 40 %) of centrally located *var* genes (mean of all groups B/C and C genes) shows that parasites from controllers (n=7) express central-located *var* genes more quickly than parasites from non-controllers (n=12). Dominant expression of central genes (> 40 %) detected for n=12/13 of non-controllers (92 %) and n=7/11 (63 %) of controllers, with n=3 of controllers, which were TBS+ only at a single time during the infection and did not display a C-type dominated pattern. C) TBS parasitemia at infection onset (n=23 individuals; non-controllers (n=13) and controllers (n=10), one controller was excluded for this analysis since the parasites displayed a B/C dominated pattern at the onset already) was found higher at B-type waves at the infection onset compared to late infection stage C-type waves. D) Correlation of RELTEXP of central located *var* genes to either days post infection (left panel) or precipitation (right panel) at parasitemia peaks indicating that the expression of central located *var* genes is rather linked to the infection duration than seasonality effects (parametric Pearson correlation). Since longitudinal infections profiles were less frequently obtained from controllers, only data from non-controllers (n=13) peaks were included. The precipitation data was retrieved for individual days, however displayed mm values were calculated as the average of the week in which the sample was taken. *Var* gene group coloring as indicated: A-types in light red, *var3* genes in orange, *var1* gene in dark red, B/C-type genes in purple, B-type genes in light blue, B/C-type genes in turquoise, C-type genes in dark green, E-type gene in yellow. Non-controller and controller as indicated in dark orange dark green, respectively. Significance levels were assessed with Mann-Whitney U-tests.

display a dominant B/C and C-type expression (dominant expression defined as ≥ 40 % of the total *var* RELTEXP) than parasites from controller (median difference 28 days) (Figure 17 B). This shorter time suggests that volunteers with a higher baseline PfEMP1 immunity not only undergo the shift from B-type to C-type *var* genes faster, but also have a more rapid exhaustion of the parasite's antigenic repertoire, which could explain, e.g., the shorter infection time we observed in controllers (Figure 14 B, C ; Figure 17 C). Interestingly, compared to A, B/A and B-type *var* genes, B/C and C-type *var* genes are located closer to the centromere so that we assume that the C-type shift at the end of an infection more might be related to an overall activation of central located genes.

For infections during the wet and dry season in malaria-endemic regions, striking differences in the occurrence of symptomatic and asymptomatic cases as well as in the transcriptional profiles of the parasites have been described (Almelli et al., 2014; Andrade et al., 2020). Thus, it has been hypothesized that the parasites can adopt to environmental changes e.g., to cause more asymptomatic infections with a reduced likelihood to endanger the host at times when precipitation and vector abundance is low, to eventually resume transmission in the subsequent wet seasons. The samples from the 'CHMI-study' are not subordinated to seasonal effects and thus samples from this cohort represent an adequate control group for seasonal effects occurring in relation to host-parasite interactions. We observed, that parasite's adaptation to express C-type *var* genes was more likely depended on the infection duration itself (Figure 17 D, left) instead of seasonality effects like local precipitation (Figure 17 D, right). Thus, we suggest that the observed C-shift might be a conserved feature of NF54 *P.falciparum* infections and is not dependent on external factors like the transition from dry to wet season.

3.8 Characterization of parasites expressing C-type *var* genes

B and C-type PfEMP1s bind to the same endothelial receptor CD36 via their N-terminal CIDRa2-6 domain allowing sequestration of trophozoites and schizonts to endothelial membranes. In section 3.5, Figure 13 C, we hypothesize that a preference for B-type expression at the infection onset might be

Results

linked to the degree of sequence conservation which is lower for B-types than for example for A and C-types. To further characterize especially late infection stages, in which the PfEMP1 immunity is higher and the parasites express preferably C-type *var* genes we performed a genome-wide transcriptomic analysis of samples from early and late infection time points. For this, we compared the transcriptomic profile of 25 samples with a B-type dominated expression pattern (B-type expression represent the highest % of total RELTEXP from RT-qPCR) from 16 volunteers at early infection time points (1st wave, 'B-type waves') with eight samples with a C-type dominated expression pattern (C-type expression represent the highest % of total RELTEXP from RT-qPCR) from late infection stages (last wave(s), 'C-type waves') (Table 18).

Table 18.: Sample overview for RNA-seq.

33 samples with a dominate B-type expression from 16 volunteers were compared with eight samples with dominate C-type expression from four volunteers. Expression data for total relative B and C-type expression strongly overlap from RT-qPCR and RNA-seq. Samples were sequenced at a median of 20.6 Mio reads with in median 1.2 Mio *P.falciparum* mapped reads pr sample. For this analysis, samples with mapped *P.falciparum* reads > 100.000 reads were included. RNA quality for these samples can be found in Table 15.*-marked sample from a volunteer (L2.32.11B) not routinely included in previous analysis since we only obtained samples from CHM14 onwards; representing only late infection stages.

Sample ID	Wave type	B-type expression (%) RT-qPCR	C-type expression (%) RT-qPCR	B-type expression (%) RNA-seq	C-type expression (%) RNA-seq	Total reads	Total Pf reads	Schizont expression profile (%)
L2.32.11B C4+26*	C	42.72	48.43	37.76	52.42	17,709,087	1,632,812	0.00
L2.32.44B C3+19	C	10.39	80.32	8.47	85.69	35,710,210	2,046,835	0.00
L2.32.44B C3+21	C	4.33	88.69	3.45	91.68	29,261,007	800,739	3.56
L2.32.44B C3+51	C	1.03	98.71	3.10	94.95	9,744,482	1,639,270	0.00
L2.32.77B C2+9	C	5.49	84.27	4.13	72.93	39,692,178	243,504	1.40
L2.32.90A C2+30	C	1.96	85.52	2.03	95.14	27,042,338	325,110	0.23
L2.32.90A C3+21	C	1.34	89.65	1.54	92.57	21,553,532	291,510	0.00
L2.32.90A C3+23	C	0.81	95.13	1.30	94.68	18,791,283	100,933	0.16
L2-32.01A C2+21	B	77.03	21.74	90.67	0.74	23,884,128	743,121	0.00
L2-32.12A C2+16	B	73.37	4.53	78.09	2.19	20,573,583	5,231,901	0.00
L2-32.12A C3+21	B	78.54	5.22	89.40	2.33	21,010,652	2,357,691	0.00
L2-32.14A C2+21	B	82.59	5.59	88.61	1.91	15,881,562	924,805	0.00
L2-32.14A C2+23	B	83.16	8.11	85.44	2.56	32,790,607	2,941,480	0.00
L2-32.16B C2+21	B	73.76	8.88	76.47	2.05	24,057,503	786,721	0.00
L2-32.23A C2+19	B	71.14	22.28	79.23	3.71	24,536,873	1,533,337	0.00
L2-32.42A C2+23	B	97.13	0.25	96.20	0.39	10,965,450	1,238,040	0.00
L2-32.44B C+14	B	83.42	4.36	83.35	2.59	26,760,381	307,919	0.16
L2-32.44B C+19	B	81.17	4.42	86.06	0.75	9,081,210	3,498,031	0.00
L2-32.44B C+21	B	84.24	3.20	87.90	0.65	13,429,975	1,235,047	0.00
L2-32.55A C2+19	B	78.19	0.41	67.97	0.41	138,093,126	7,0975,929	0.00
L2-32.55A C2+21	B	57.64	1.38	62.78	0.48	139,621,600	2,6903,153	0.00
L2-32.67A C2+16	B	85.17	2.09	85.80	2.45	22,646,515	506,509	0.00
L2-32.67A C2+19	B	79.91	1.41	81.30	1.98	23,081,194	383,458	0.00
L2-32.72B C+19	B	80.35	62.41	80.95	0.96	12,425,877	1,768,482	0.00
L2-32.72B C+23	B	1.69	6.35	75.47	3.46	17,481,153	2,183,832	0.00
L2-32.77B C+19	B	87.38	3.59	87.82	1.93	19,866,553	565,343	0.00
L2-32.77B C+21	B	85.69	5.38	87.07	1.37	26,559,384	418,634	0.00
L2-32.76B C+19	B	87.06	2.10	80.67	4.77	12,397,390	1,402,662	0.00
L2-32.79A C2+19	B	64.72	1.90	59.37	0.77	9,994,869	1,938,168	0.00
L2-32.79A C2+21	B	42.08	6.01	37.43	0.97	8,738,998	1,556,467	0.00

Results

L2-32.88B C+21	B	71.32	10.06	71.75	0.88	15,564,670	1,179,031	0.00
L2-32.90A C3+19	B	93.50	3.06	92.78	1.82	17,204,352	1,050,157	0.00
L2-32.91B C+21	B	86.89	0.95	91.70	0.85	12,883,776	1,020,846	0.00

For verification purposes, we compared *var* gene expression patterns obtained by RT-qPCR and RNA-seq from identical samples and found very high agreement between the relative B and C-type expression (Table 18) as well as generally for all genes (mean difference: -0.05 (+3.42/-3.52) %) (Supplementary Figure 6 A). Apart from the 33 samples displayed in Table 18 we included nine additional samples from other time points with during the infection (\neq early or late infection stages) as well as five samples from *in vitro* cultivation for which we tested the expression with both methods RT-qPCR and RNA-seq (Table 15, Table 18, Supplementary Figure 6 A). Electropherograms for RNA samples undergoing RNA-seq can be found in Supplementary Figure 7. The agreement between both

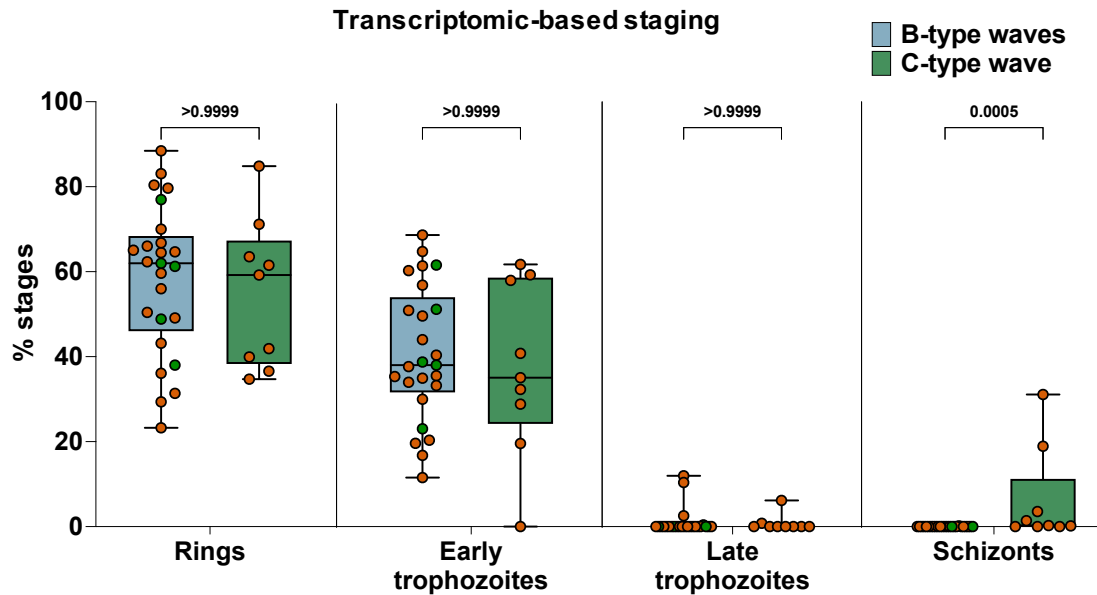


Figure 18.: Transcriptomic-based staging of samples from early and late infection stages.

In total, the transcriptomic profile of 25 samples from 16 volunteers at early (1st peak) infection stages were compared with eight samples from four volunteers at late infection stages (last wave(s)) showing similar stage distributions for ring, early trophozoite and late trophozoite stages (samples showing at least > 100,000 *P.falciparum* mapped reads were included). The median % of schizonts was (0.23 %) low in late, C-type (green) expressing parasites but significantly higher than for B-type (blue) expressing parasites. Samples from non-controllers and controllers are indicated as orange and dark green respectively.

methods was very high except for two genes (PF3D7_0300100, PF3D7_0324900) which have a high sequence similarity and, thus, design of individual RT-qPCR primers was not possible. The used primer pair amplifies transcripts from both genes simultaneously and cannot discriminate between the individual gene variants. The total expression measured for both genes with one primer-pair via RT-qPCR was significantly lower than the total expression of each gene measured via RNA-seq (Supplementary Figure 6 A).

To compare the expression pattern from early and late infection stages we infused the sequencing data into a preestablished analysis pipeline from Tonkin-Hill et al. 2018. The pipeline was designed to analyze expression differences from *ex vivo* samples from volunteers which were infected with

Results

P.falciparum parasites. The pipeline can be split roughly into two parts, one assessing the stage distribution of parasites from the sample based on the overall expression profile and the other performing differential expression of samples from two predefined groups (limma/voom DEG).

Applying the stage comparison from the 1st pipeline step to early and late infection stages revealed a similar distribution of ring, early trophozoite and late trophozoite stages in both B and C-type

Table 19.: List of upregulated genes in NF54 parasites from late infection stages ('C-type waves').

List of significantly upregulated genes by parasites expressing C-type var genes compared to parasite populations expressing B-type var genes ('B-type waves') identified by a preestablished analysis pipeline for RNA-seq (Tonkin-Hill et al. 2018, Supplementary Figure 8) using samples from Table 18. Of the 39 upregulated genes, seven C-type var genes (red, antigenic variation) are significantly upregulated as well as some genes which have been shown to be upregulated in schizont stages and transmission stages (blue). Furthermore, some of the genes encode for proteins which are linked to (epigenetic) gene regulation (yellow), cytoadhesion (green), various metabolism pathways (grey) and are thought to be interactors with PfEMP1 or involved in protein trafficking to the red blood cell membrane (red). Genes with an adjusted p-values <0.05 were considered significant and included in the list.

GeneID	logFC	P-value	Adjusted P-value	Description	Function
PF3D7_0420900	6,22	6,24E-08	6,94E-05	erythrocyte membrane protein 1, PfEMP1 (C)	Antigenic variation
PF3D7_0420700	6,27	3,89E-07	3,46E-04	erythrocyte membrane protein 1, PfEMP1 (C)	Antigenic variation
PF3D7_0421100	4,84	8,52E-07	6,31E-04	erythrocyte membrane protein 1, PfEMP1 (B/C)	Antigenic variation
PF3D7_0421300	3,81	1,84E-06	1,17E-03	erythrocyte membrane protein 1, PfEMP1 (C)	Antigenic variation
PF3D7_0311700	2,72	3,34E-06	1,65E-03	plasmepsin VI	Transmission stage plasmepsin (Nasamu et al. 2020)
PF3D7_0204900	2,53	7,44E-06	2,93E-03	ubiE/COQ5 methyltransferase, putative	Ubiquinone biosynthesis, Metabolimics (KEGG)
PF3D7_0711700	2,30	1,00E-05	3,43E-03	erythrocyte membrane protein 1, PfEMP1 (C)	Antigenic variation
PF3D7_1445400	0,77	1,93E-05	6,12E-03	protein serine/threonine kinase-1	CLK1, kinase involved in replication and splicing (Agarwal et al. 2011, Colwill et al. 1996)
PF3D7_1316600	1,32	2,45E-05	7,27E-03	choline-phosphate cytidylyltransferase	Glycerophospholipid metabolism (KEGG)
PF3D7_0702200	1,23	3,43E-05	8,96E-03	lysophospholipase, putative	LPL20, phosphatidylcholine synthesis (Sheokland et al. 2021)
PF3D7_0728700	2,21	4,05E-05	9,37E-03	alpha/beta hydrolase, putative	?
PF3D7_0810800	1,26	4,21E-05	9,37E-03	hydroxymethylidihydropterin pyrophosphokinase-dihydropteroate synthase	Intermetabolite enzyme (Shiota et al. 1964)
PF3D7_0532400	1,07	5,57E-05	1,18E-02	lysine-rich membrane-associated PHISTb protein	PfEMP1 interactor (Jensen et al. 2019)
PF3D7_1240600	3,30	6,44E-05	1,30E-02	erythrocyte membrane protein 1, PfEMP1 (C)	Antigenic variation
PF3D7_1105100	1,45	7,72E-05	1,49E-02	histone H2B	Epigenetic regulation (Hoeijmakers et al. 2013, Bennet et al. 1995)
PF3D7_0511800	0,85	9,71E-05	1,80E-02	inositol-3-phosphate synthase	Inositol phosphate metabolism (KEGG)
PF3D7_0316200	2,24	1,23E-04	2,19E-02	conserved Plasmodium protein, unknown function	?
PF3D7_1234700	1,65	1,38E-04	2,21E-02	CPW-WPC family protein	ULG8 upregulated in late gametocytes (PlasmoDB)
PF3D7_0717700	0,76	1,39E-04	2,21E-02	serine--tRNA ligase, putative	Aminoacyl-tRNA biosynthesis (KEGG)
PF3D7_0712600	4,52	1,54E-04	2,36E-02	erythrocyte membrane protein 1, PfEMP1 (C)	Antigenic variation
PF3D7_0532300	1,10	1,62E-04	2,41E-02	Plasmodium exported protein (PHISTb), unknown function	PfEMP1 interactor (Jensen et al. 2019)
PF3D7_0301300	1,09	1,83E-04	2,62E-02	alpha/beta hydrolase, putative	Vascular adhesion and membrane integrity (Spillman et al. 2011)
PF3D7_1035800	1,21	1,90E-04	2,64E-02	probable protein, unknown function	?
PF3D7_0108100	1,99	1,98E-04	2,66E-02	conserved Plasmodium protein, unknown function	?
PF3D7_0509700	2,06	2,25E-04	2,86E-02	conserved Plasmodium protein, unknown function	?
PF3D7_0829800	2,63	2,39E-04	2,90E-02	unspecified product	?
PF3D7_0933300	1,89	2,41E-04	2,90E-02	conserved Plasmodium protein, unknown function	?
PF3D7_0718100	1,55	2,73E-04	2,96E-02	exported serine/threonine protein kinase	Exported protein, virulence and cytoadhesion (Maier et al. 2008)
PF3D7_0416000	0,96	2,71E-04	2,96E-02	RNA-binding protein, putative	RNA-binding (PlasmoDB)
PF3D7_0917900	0,57	2,62E-04	2,96E-02	heat shock protein 70	Stress induced protein (Kumar et al. 1991)
PF3D7_0219700	1,22	2,85E-04	3,02E-02	Plasmodium exported protein (PHISTc), unknown function	PfEMP1 interactor (Jensen et al. 2019)
PF3D7_0216500	2,26	3,12E-04	3,23E-02	conserved Plasmodium protein, unknown function	?
PF3D7_1201600	2,26	3,55E-04	3,32E-02	NIMA related kinase 3	NEK3, kinase involved in cell cycle regulation, sexual stages (O'Connell et al. 2003, Tibaric et al. 2021)
PF3D7_0935800	2,26	3,33E-04	3,32E-02	cytoadherence linked asexual protein 9	CLAG9, involved in PfEMP1 trafficking and cytoadhesion (Goel et al. 2010)
PF3D7_0404600	1,80	3,43E-04	3,32E-02	conserved Plasmodium membrane protein, unknown function	?
PF3D7_0911900	0,56	3,58E-04	3,32E-02	fastatin	Expressed in schizonts, facilitates invasion (Kailash et al. 2006)
PF3D7_0316600	1,15	4,74E-04	4,30E-02	formate-nitrite transporter	Formate and lactate transporter, metabolism (Marchetti et al. 2013)
PF3D7_1004200	1,25	4,85E-04	4,31E-02	WD repeat-containing protein, putative	Cell-cycle control, chromatin dynamics and transcription regulation (Xu et al. 2011)
PF3D7_0412400	1,96	5,09E-04	4,44E-02	erythrocyte membrane protein 1, PfEMP1 (C)	Antigenic variation

Results

expressing parasites. However, some parasites in late infection stages, display a schizonts-like transcriptomic profile which was not observed for B-type expressing parasites at early infection stages (Figure 18). The proportion of parasites was small (median: 0.23%) but significantly higher than for the early infection stages (median: 0.00%). This is surprising as trophozoites and schizonts are barely detected in blood drawings from infected individuals, because they are rapidly removed from circulation when passing the spleen. Interestingly, parasites from C-type waves showed a higher total *var* gene expression (measured as the ratio of total RELTEXP/*var* gene) among all samples from early and late infections stages with the RT-qPCR (Supplementary Figure 6 B, left). This effect seems to be depended on the parasitemia of the sample since no difference in total *var* gene expression was observed for the RNA-seq sample subset (33 samples) which were collected only upon a parasitemia > 1000 pf/μL for both the RT-qPCR (Supplementary Figure 6 B, right) and RNA-seq (Supplementary Figure 6 C). Since the parasitemia is overall decreasing over time when C-type expression is emerging (Figure 14 E), it seems that a higher amount of total *var* gene expression is emerging from a lower amount of parasites at late infection stages correlating to a potential weaker sequestration ability of these parasites (Cooke et al., 2001; Nash et al., 1989).

Before differential expression analysis, the samples from early and late infection stage undergo several correction steps (removal of unwanted variation, comparison to a reference *in vivo* sample dataset, stage correction). After correction, a partial separation of early and late infection time points ('B-type' vs. 'C-type-waves') was achieved (Supplementary Figure 8, Tonkin-Hill et al. 2018; Vignali et al. 2011). Differential expression analysis of samples from early and late time points ('B-type' - vs. 'C-type-waves') revealed 39 upregulated genes and twelve significantly downregulated in late 'C-type waves' (Table 19 and 20). From a total of 13 C-type *var* genes in the NF54 *var* gene repertoire, seven variants were significantly upregulated in 'C-type waves'. The remaining upregulated genes are encoding for proteins involved in a) protein export and interaction with PfEMP1 (PHISTb,c, exported serine/threonine kinase; (Jensen et al., 2020; Maier et al., 2008)), b) cytoadhesion (CLAG9, α/β-hydrolase (Goel et al., 2010; Spillman et al., 2016)), c) change in parasites metabolomics and lipidomics (e.g., ubiE/COQ5, CLK1; LPL20 (Agarwal et al., 2011; Colwill et al., 1996; Sheokand et al., 2021) or d) epigenetic regulation (H2B, WD repeat containing protein (Bennett et al., 1995; Hoeijmakers et al., 2013; Xu et al., 2011)). Some upregulated genes have also been shown to be upregulated in schizont, gametocyte and transmission stages (falstatin, plasmepsin VI, NEK3; (Nasamu et al., 2020; O'Connell et al., 2003; Pandey et al., 2006;

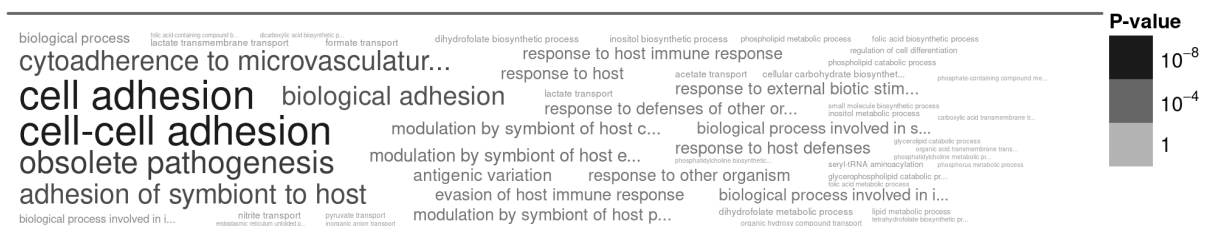


Figure 19.: GO-term analysis for significantly upregulated genes in late infection stages.

Go-terms retrieved from the PlasmoDB illustrated in a word cloud indicate that upregulated genes at late infection stages are involved in multiple biological processes including cell adhesion, antigenic variation as well as other metabolic processes. Font size indicate the proportional distribution of GO-terms.

Results

Tibúrcio et al., 2021)). This set of upregulated genes not only confirms the differences in *var* gene expression (from B to C-type expression) observed by RT-qPCR but also pinpoint to other genes possibly involved in alteration of parasites cytoadhesive ability in later infection stages (Figure 18). Functionality of proteins encoded by the gene list was assessed via a literature research and databases (KEGG: Search in Kyoto Encyclopedia of Genes and Genomes to indicate protein functions and pathways and PlasmoDB). To illustrate and summarize the findings from Table 19, we performed a GO-term analysis for the significantly altered genes via PlasmoDB. Genes upregulated in late infection stages seem to be involved in multiple biological processes, however most dominantly in cell adhesion or cell-cell adhesion, antigenic variation (Figure 19). In addition, also metabolic processes seem to be altered at a lower level which is in line with Table 19.

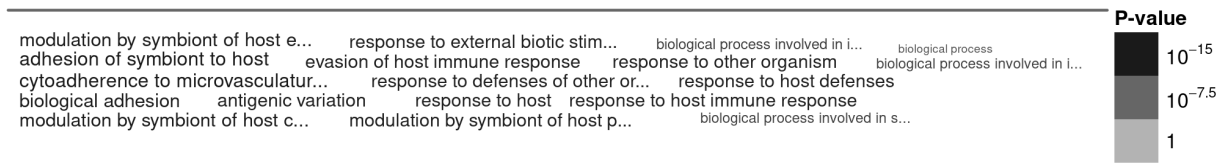


Figure 20.: GO-term analysis for significantly upregulated genes in late infection stages.

Go-terms retrieved from the PlasmoDB illustrated in a word cloud indicate that downregulated genes at late infection stages are involved in multiple biological processes but no dominate GO term was found. Font size indicate the proportional distribution of GO-terms.

The significantly downregulated genes by parasites expressing C-type *var* genes (upregulated in B-type expressing parasitic waves) all belong to the *rif* multi-gene family which are involved in immune evasion e.g., by silencing NK, T or B-cell effector functions (Table 20; (Harrison et al., 2020; Xie et al., 2021; Yokoyama et al., 2018). Apart from lacking data points for PF3D7_0324800 and PF3D7_0617500, the downregulated *rifs* code for Mauer's clefts exported A-type *rifs* and the majority of the genes is characterized by a A2 5'-upstream regions indicating a transcription directionally to the telomere (Petter, Bonow and Klinkert, 2008, Table 20). GO-term analysis of these genes revealed that as expected a potential role of these *rifs* in antigenic variation, cell adhesion, immune evasion or host defenses

Table 20.: List of downregulated genes by NF54 parasites from late infection stages ('C-type waves').

List of significantly downregulated genes by parasite populations expressing C-type *var* genes compared to those expressing B-type *var* genes ('B-type waves'). Downregulated genes all belong to the *rif* family and are located in close chromosomal proximity to A, B/A and B-type *var* genes. *Rifs* are located either directly (1st *rif*) next to the *var* gene or have one other *rif* in between (2nd *rif*). T=telomeric, S=subtelomeric, C= central located *rif* gene.

GeneID	logFC	P-value	Adjusted P-value	Description (group/rups)	Chromosomal localization (T, S, C)
PF3D7_1300200	-4,03	6,06E-10	2,69E-06	rifin (A/rupsA2)	T; Tail to tail to B-type <i>var</i> gene and head to tail to A-type <i>var</i> gene (1st <i>rif</i>)
PF3D7_0800400	-3,76	1,73E-08	3,46E-05	rifin (A/rupsA2)	T; Tail to tail to B/A-type <i>var</i> gene (1st <i>rif</i>)
PF3D7_0800500	-4,31	2,34E-08	3,46E-05	rifin (A/rupsA/B)	T; Tail to tail to B/A type <i>var</i> gene (2nd <i>rif</i>)
PF3D7_0400300	-2,62	3,32E-06	1,65E-03	rifin (A/rupsA2)	T; Tail to tail to B-type <i>var</i> gene and head to tail to A-type <i>var</i> gene (1st <i>rif</i>)
PF3D7_0324800	-2,75	5,17E-06	2,30E-03	rifin (?/?)	T; Tail to tail to B-type <i>var</i> gene (1st <i>rif</i>)
PF3D7_1000200	-2,76	7,90E-06	2,93E-03	rifin (A/?)	T; Tail to tail to B-type <i>var</i> gene (1st <i>rif</i>)
PF3D7_0632400	-3,04	3,20E-05	8,90E-03	rifin (A/rupsA2)	T; Tail to tail to B-type <i>var</i> gene (1st <i>rif</i>)
PF3D7_0300200	-2,61	3,92E-05	9,37E-03	rifin (A/rupsA2)	T; Tail to tail to B-type <i>var</i> gene (1st <i>rif</i>)
PF3D7_0901500	-2,62	1,39E-04	2,21E-02	rifin (A/rupsA1)	C; unrelated to <i>var</i> genes
PF3D7_0617500	-2,88	2,21E-04	2,86E-02	rifin, pseudogene	C; Head to head to C-type <i>var</i> gene (1st <i>rif</i>)
PF3D7_0100200	-2,93	2,71E-04	2,96E-02	rifin (A/rupsA2)	T; Tail to tail to B-type <i>var</i> gene (1st <i>rif</i>)
PF3D7_0732900	-2,52	3,41E-04	3,32E-02	rifin (A/rupsA2)	T; Tail to tail to B-type <i>var</i> gene (1st <i>rif</i>)

adhesion but less pronounced than for the upregulated genes in late infection stages (Figure 19, Figure 20).

To further explore the role of *rifs* which seemed to be upregulated during the ‘B-type waves’, we analyzed the raw rpkms of all *rifs* on an individual level. We observed that the most *rifs*, which are higher expressed during the ‘B-type waves’ are either located in direct chromosomal proximity (1st *rif*) or have one other *rif* in between (2nd *rif*) to a B or B/A-type *var* genes oriented ‘tail-to-tail’ towards the *var* gene (Table 19, Figure 21 A, (Petter et al., 2008)). Thus, we performed a global expression analysis of 158 annotated *rifs* in PlasmoDB in relation to their chromosomal orientation to the *var* genes and found that the majority of the *rif* expression is indeed linked to *rif* in close chromosomal proximity (1st or 2nd *rif*) to a B-type *var* gene and that these *rifs* are typically for Maurer’s clefts exported A-type RIFIN proteins with a rupsA1 or rupsA2 promotor (Figure 21 B, C, D, Supplementary Figure 6 E, Table 20). In line with the data obtained from the differential expression analysis (Table 20) we could demonstrate that the expression of *rifs* was in general reduced for samples exhibiting a C-type expression profile (Figure 21 B, D) and that this effect was not related to a reduced parasitemia of samples with C-type expression (Figure 21 E). Of note, the parasitemia for C-type waves is overall reduced indicated by lower parasitemia levels at late infection stages (Figure 14 E) but did not differ for the sample subset undergoing RNA-seq since these samples were only collected with a parasitemia > 1000 pf/μL. Simultaneously, we verified that the effect is not due to for example an altered sequencing depth (Supplementary Figure 6 D).

In previous studies, it was reported that distinct *rif* variants are co-expressed with A-type *var* genes in close chromosomal proximity sharing the same promotor locus only in a specific ‘head-to-head’ orientation (Figure 12 A; Claessens et al. 2012; Lavstsen 2003). A correlation analysis of *var* and *rif* expression, revealed a co-regulation of *rifs* which are adjacent to A-type *var* genes in head-to-head orientation, similar to findings from Claessens et al. 2012 and Lavstsen et al., 2003, but no co-regulation of neighboring B-type *var* and *rif* genes in tail-to-tail orientation (Figure 21 F). In total we identified only five C-type *var* genes with a *rif* in direct chromosomal proximity which are either oriented in head-to-tail or head-to-head to the respective *var* gene. Interestingly for these gene pairs we also observed a positive correlation of *rif* and *var* gene expression like previously observed for *rifs* located close to A-type *var* genes (Figure 21 F, right). In this context also the *rif* (Pf3D7_1200500) seems to be co-regulated with type E *var* gene *var2sca* which is the dominantly expressed variants *in vitro* (Figure 21 B, Supplementary Figure 9 F; Bachmann et al. 2019).

Consequently, from our data we assume that during early ‘B-type-waves’ at the infection onset, *rifs* are overexpressed but expression is not linked with the neighboring *var* gene. Simultaneously, at late ‘C-type-waves’ the *rif* expression is downregulated but co-regulated to some C-type *var* genes similar to *rifs* in close chromosomal proximity as A-type *var* genes.

Next to a comparison of early and late infection stages, we initially also compared the transcriptome from onset samples from non-controller and controller and found deregulated *var* gene expression in

Results

both groups, however the variability among the samples was too high to find significant differences of highly or lowly expressed *var* gene variants in samples from non-controllers or controllers.

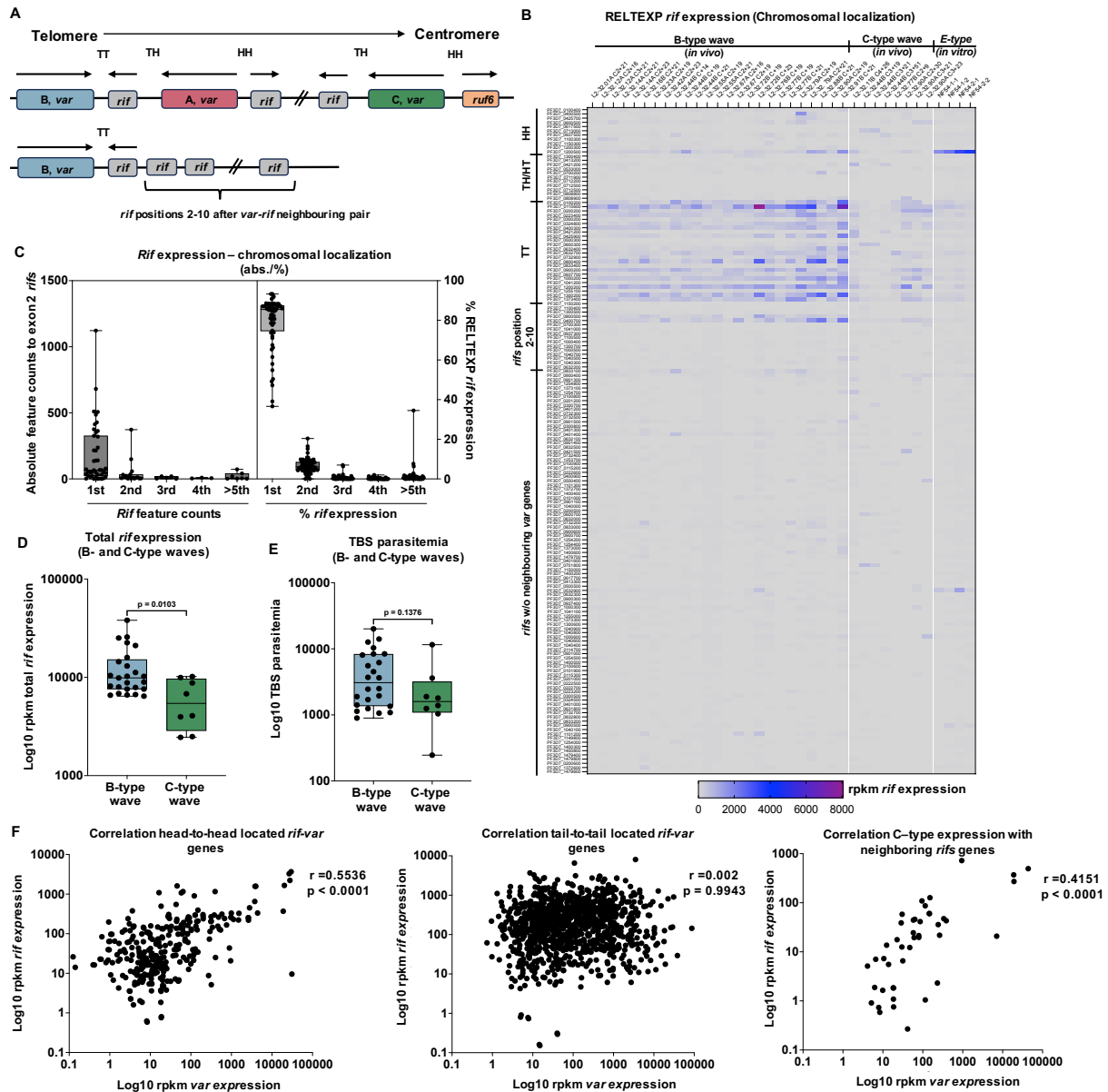


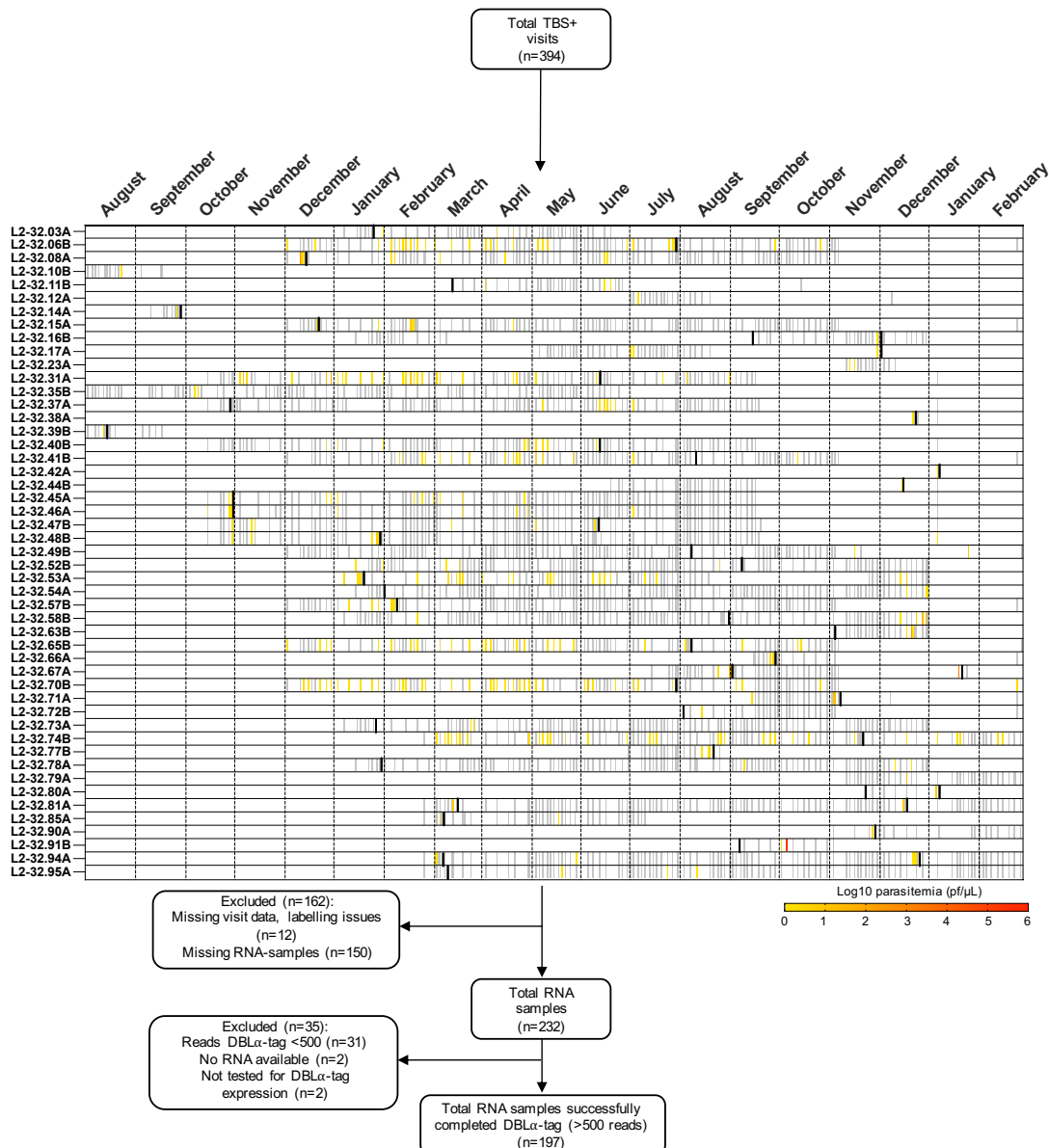
Figure 21.: Expression of *rif* genes depending on the phase of infection and *var* gene expression.

A) Schematic representing the chromosomal localization and transcriptional orientation of *var* genes and *rif* genes from the telomeric end to more central regions (PlasmoDB). Most B-type *var* genes are located at the telomere of the chromosome with either a single or up to ten *rif* genes located in direct proximity in tail-to-tail orientation (TT). A-type *var* genes are usually located adjacent to this *rif* cluster and are frequently surrounded by two *rifs*, one in tail-to-head (TH or HT) orientation (the same *rif* which is in TT orientation to the B-type *var* gene) and another one in head-to-head (HH) orientation. C-type *var* genes are located closer to the centromere and have either no or a single neighboring *rif* with varying orientations. B) Heatmap showing *rif* expression as rpkm *rif* expression across different infection waves of volunteer samples sorted by 'B-type' and 'C-type waves' as well as in vitro NF54 culture samples with high *var2csa* (E-type) expression. *Rifs* are sorted according to their chromosomal proximity to a *var* gene and are either directly neighboring a *var* gene in head-to-head (HH), tail-to-head/head-to-tail (TH/HT) or tail-to-tail (TT) orientation, or are one of up to ten *rifs* directly adjacent to a *var* gene (*rifs* position 2-10). The remaining *rifs* are located elsewhere on the chromosome (*rifs* w/o neighbouring *var* genes). Double entry of some *rifs* due to two different orientations to different *var* genes (e.g., *rif* in between telomeric and subtelomeric B and A-type *var* genes). The *rif* PF3D7_1200500 in HT orientation to *var2csa* (PF3D7_1200400) is coregulated in in vitro samples (Supplementary Figure 9 F). C) Quantification of raw rpkm feature counts (left) and % of total rpkm *rif* expression (right) according to their chromosomal distance to a *var* gene. D) Comparison of total *rif* expression in samples from early 'B-type' and late 'C-type waves' a significant reduction of total *rif* expression for 'C-type waves'. E) The same comparison shows no difference in parasitemia of these samples. F) Depending on their orientation *var*- and *rif* genes are co-regulated (HH orientation, left) or independently regulated (TT orientation, right), even though the later orientated *rifs* are most abundantly expressed (B). Correlation was performed on all sequenced samples ($n=42$, >100,000 mapped *P. falciparum* reads). Significance levels assessed with Mann-Whitney-U test.

3.9 Longitudinal analysis of naturally occurring *P. falciparum* infections (mosquito bite infections)

3.9.1 Sample cohort characterization

According to our genotyping results (section 2.2.12, Table 13), almost all volunteers (49/56, 88 %) were naturally infected with a locally circulating strain at least once during the trial leading to division of the samples into a CHMI and natural infection study (Figure 22). In total, n=394 parasite samples from n=49 volunteers were allocated to the natural infection sample cohort ('NI-study') following the genotyping approach (section 2.2.12, Figure 22). Similar to the 'CHMI-study', the volunteers were tracked with a neat sampling and visit interval from 2–7 days according to the trials procedure and encompassed the detection of visits with no detectable TBS parasitemia (in grey) and TBS+ visits (Figure 22, color-coded log10 scale). For n=150 of the TBS+ visits (38 %), no blood samples were collected for RNA analysis and n=12 samples were excluded due to mislabeling or a lack of reliable traceability to a specific volunteer or a date.



Results

Figure 22.: Samples overview of the ‘natural infection study’ within L2 study.

In total, 394 TBS+ visits were assigned to infections with non-NF54 or -7G8 genotypes according to genotyping approaches. Almost all recruited volunteers ((n=49/56, 88 %), L2-IDs labelling according to previous description in Figure 9)) were infected at least at a single time point with locally circulating parasite strains during the trial from August 2019 to February 2021. Heatmap depicts all registered TBS+ (log10 colored-scale bars) and TBS-visits (grey bars) for each volunteer tested positive with local parasite genotypes. Treatments with AL are indicated by black bars. TBS+ visits (n=162) were not included in the analysis because either no RNA-sample was collected (n=150, 38 %) or samples were collected for which no corresponding visit date was registered (e.g., tube labeling issues) (n=12, 3 %). Consequently, n=232 remaining samples were eligible for the DBL α -tag sequencing approach. For n=2 (1 %) samples, the RNA was not available and other n=2 (1%) samples were not tested for var expression with the DBL α -tag approach. After sequencing, n=35 (15 %) samples were excluded as they did not reach the minimum of 500 reads which was set as threshold for analysis (section 2.2.18). AL: artemether-lumefantrine, TBS: tick-blood smear.

To validate whether the natural infections are subordinated to the seasonal fluctuations of the *Anopheles* mosquito populations despite the repeated CHMIs during the L2 study, we retrieved satellite precipitation data for Lambaréné, Gabon from August 2019 until February 2021 and correlated monthly aggregated precipitation data to the ratio of TBS+ visits per corresponding month (Figure 23). The precipitation is strongly affecting the availability of mosquito breeding spaces and is therefore a crucial indicator for seasonality and transmission in endemic areas (Kar et al., 2014; Tompkins & Ermert, 2013; Yamba et al., 2023; Zayed et al., 2023). Thus, we correlated the rate of TBS+ visits for the separated sample cohort with the precipitation data. As expected, for the samples from the ‘NI-study’ the TBS positivity rate was the highest during extensive rainfall seasons (October 2019 - May 2020 and October 2020 - February 2021) and the lowest during the dry season (June 2020 - September 2020). However, the maximum TBS positivity rate is delayed by approximately 1–2 months to the monthly precipitation maximum (Figure 23). According to previously published literature, this effect is frequently observed in seasonal transmission settings in which shortly after a significant increase of precipitation, the

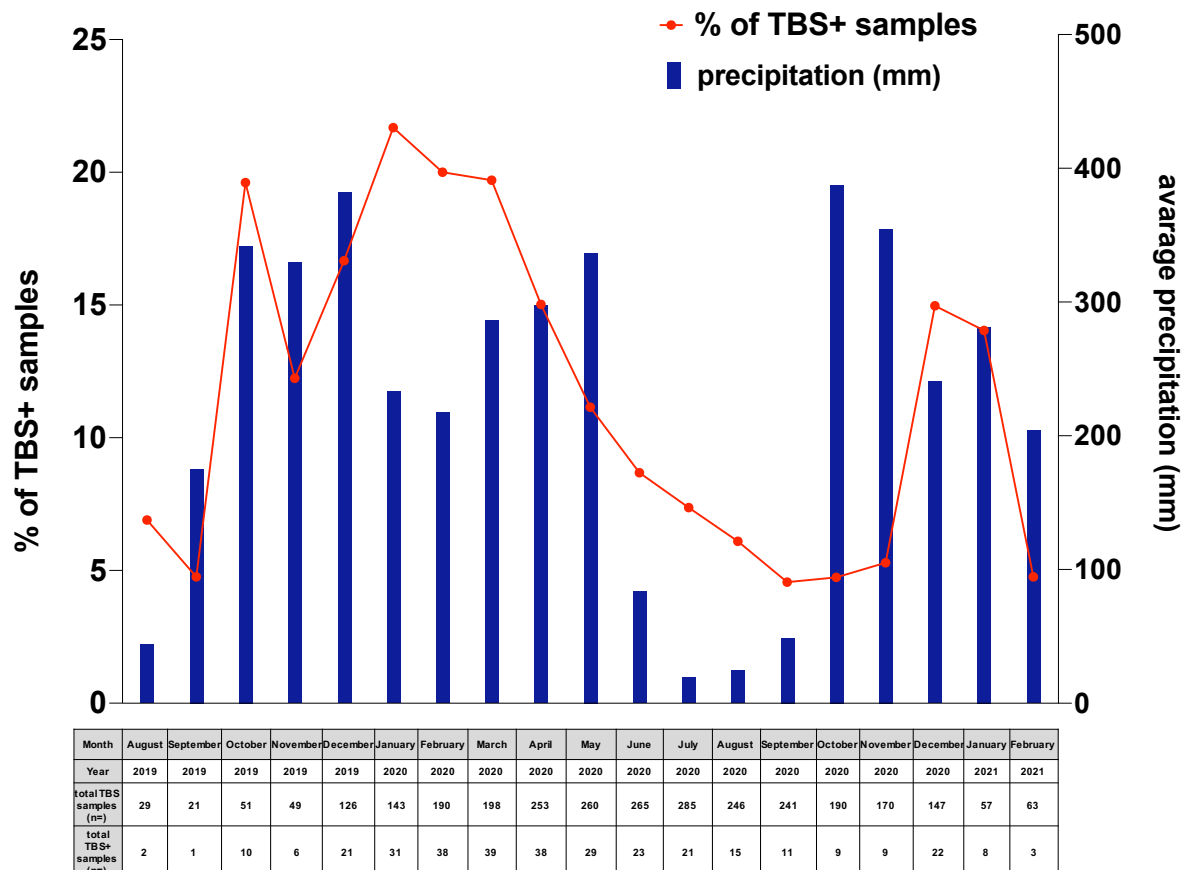


Figure 23.: Naturally occurring mosquito bite infections are subordinated to seasonal precipitation.

Monthly tracking of the TBS positivity rate (total monthly TBS+ visits/total monthly registered visits) (red line, left Y-axis) correlates with the satellite obtained precipitation data for Lambaréné, Gabon, from August 2019 – February 2021 (bars, right Y-axis). TBS positivity is delayed by about 1–2 months to the onset of the wet season because the mosquito population needs to expand before an increase of malaria incidence is observed.

(infective) mosquito populations firstly expand in size with increasing abundancy of breeding spaces before higher transmission rates and a higher malaria incidence rate is observed (Yamba et al., 2023).

3.9.2 Antigenic variation in naturally occurring *P. falciparum* infections

Since the genome sequences of the polymorphic *var* genes is not known for field isolates, alternative approaches are necessary to analyze their *var* gene expression. First, samples can be analyzed with an expressed-sequence tag (EST) approach involving the amplification and sequencing of a short, relatively conserved region, within the coding sequence of the DBL α domain in the PfEMP1 N-terminal head structure, with a subsequent blast of the sequence to determine the DBL α subtype. Subsequently, the fully-length PfEMP1 domain composition is predicted using the Varia tool based on a comparison with *var*DB (Mackenzie et al., 2022; Wichers et al., 2021). Second, bulk RNA-seq with *de novo* assembly of *var* gene transcripts is possible (Andradi-Brown et al., 2024; Tonkin-Hill et al., 2018; Wichers et al., 2021). RNA sequencing of samples was possible for a small sample subset (n=48/232 (21 %)), which showed a TBS of over 1000 pf/ μ L and which additionally underwent WBC depletion by Plasmodipur filtration to increase the proportion of parasite RNA for sequencing (section 2.2.4). All high parasitemia RNA samples have been sent to the sequencing facility, but we are still waiting for a large proportion to be sequenced. In the meantime, all low and high parasitemia samples were analyzed by the DBL α -tag approach. For this, from the remaining 232 eligible RNA samples 35 samples were excluded from experiment or analysis, because the RNA was utilized either for other experiments or less than 500 reads were obtained, which was defined as threshold (section 2.2.18, Figure 22).

To verify the observations from the ‘CHMI-study’ participants we planned to analyze the samples as similar as possible to the samples from the ‘CHMI-study’. However, for cross-sectional and longitudinal field studies an estimation of the infection onset date is challenging, especially when no baseline treatment is applied. Thus, a similar analysis segregating the volunteers of the ‘CHMI-study’ in non-controllers and controllers based on the day post infection of TBS positivity and the parasite’s *var* expression pattern (Figure 11 C) was not possible. Nevertheless, we hypothesized that, irrespectively from knowing a clear infection starting point, infections would progress similarity to infections from the ‘CHMI-study’ e.g., in terms of how parasites alternate through the antigen repertoire (Figure 16 D, Figure 17 A). Thus, we analyzed DBL α -tag data from four selected volunteers, for whom a relatively high number of TBS+ dates were registered and corresponding RNA samples were collected (L2-32.31B: 24 samples, L2-32.65B: 16 samples, L2-32.70B: 24 samples, L2-32.74B: 21 samples). The analysis of these samples revealed different numbers of unique DBL α -tag sequences ranging from 82 (for L2.32.31B) to 103 (for L2.32.65B). For L2-32.74B, which displayed 100 unique DBL α -tag sequences across the infection, genotyping revealed a polyclonal infection with at least two strains (section 2.2.12, Table 13)

Results

indicating that the polyclonicity of infection might be responsible for the different repertoire sizes as well as the larger repertoires compared to NF54 (61 *var* genes).

The longitudinal analysis of each individual infection showed that, irrespectively of the size of the DBL α -tag sequence repertoire, the parasites displayed a *var* gene pattern dominated by a single or few variants at the parasitemia peaks, similar to the *var* expression pattern in the successive parasitemia

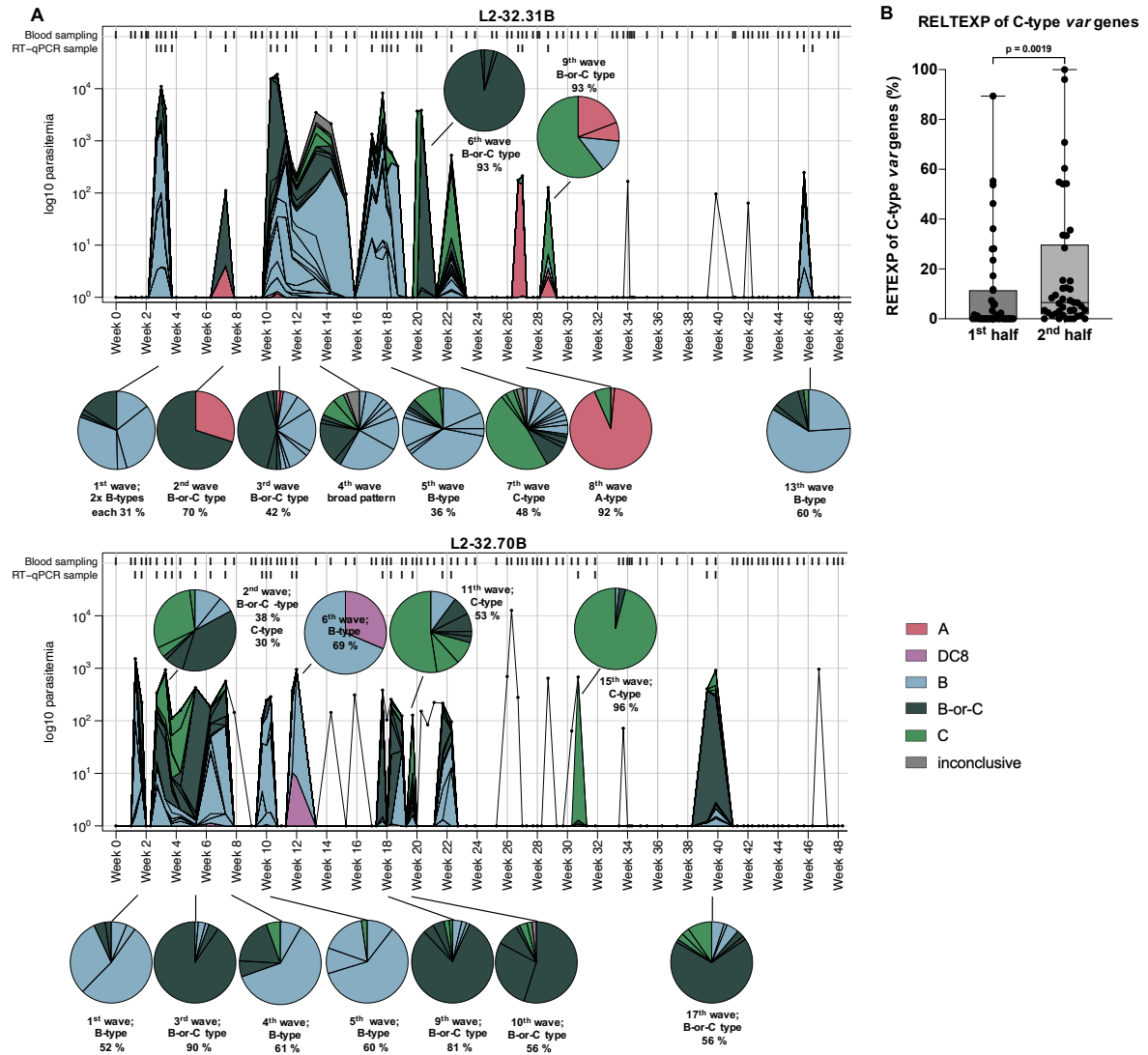


Figure 24.: Longitudinal *var* gene expression pattern in parasites isolated from volunteers infected with local parasite strains.

A) Representative examples of parasitemia and *var* gene expression in two longitudinally tracked volunteers across a study time frame of 48 weeks showing mostly single variant dominated *var* gene expression at parasitemia peaks similar to infections tracked within the 'CHMI-study'. B- or C-type *var* gene sequences could not be allocated to a particular *var* gene group, but are of type B or C due to their encoded DBL α domain. Sampling intervals are indicated above of the respective volunteer plot and if no samples were collected the time points were left blank. Similar to infections from volunteers in the 'CHMI-study', A-type *var* genes are only occasionally expressed, but dominated a distinct parasitemia wave in volunteer L2-32.21B (9th wave). B) Using the upsC tool by Tan et al. 2023, *var* groups were assigned to DBL α -tag sequences from samples of the four longitudinally tracked volunteers (L2-32.31B, L2-32.65B, L2-32.70B, L2-32.74B). Samples were split in half (1st and 2nd half of the infection) and quantification of total C-type *var* gene RELTEXP per sample from earlier and later infection time points was performed. The results indicate a gradual increase of C-type expression overtime also in less controlled infection settings. Significance levels were assessed with Mann-Whitney-U tests. A-type *var* genes (red), B/A-type *var* genes with DBL α 2 sequence contained within DC8 (purple), B-type *var* genes (blue), B- or C-type *var* genes (petrol), C-type *var* genes (green) and inconclusive predictions (grey), DC8: domain cassette 8.

peaks detected for volunteers of the 'CHMI study' (Figure 16 D, Figure 24 A). Therefore, the gradual exhaustion of the antigenic variation repertoire in NF54 parasites observed in the 'CHMI-study' under controlled conditions is therefore comparable to natural mosquito-bite infections with field parasite strains. Similar to the controlled NF54 infection, A-type *var* genes (red) are expressed, in particular, at lower parasitemia densities ("parasitemia valleys") rising further interest in the actual role of these genes in the maintenance of infections (Figure 16 D, Supplementary Figure 9). To investigate, whether parasites from natural infections also shift towards the expression of C-type *var* genes with increasing infection duration, we have integrated the recently developed 'upsC' prediction tool (Tan et al., 2023), which allows the discrimination of B and C-type *var* genes based on their *ups* promotor sequence, into the Varia tool pipeline (Mackenzie et al., 2022). Interestingly, the comparison of samples from these four volunteers collected earlier (1st half of the samples) or later (2nd half of the samples) during the infection, showed a significant increase of C-type annotated *var* genes, which we also observed to a greater extent for infections of the 'CHMI-study' (Figure 17 A, Figure 24 B). Thus, we conclude, that the observations and findings on the infection dynamics of *P. falciparum* made in the 'CHMI study' are transferable to less structured, natural environments with infections caused by mosquito bites.

4. Discussion

In this thesis, we analyzed longitudinal *var* gene expression data from a unique CHMI study including 56 life-long malaria-exposed African adults who underwent six consecutive CHMIs, once with the South-American originating 7G8 clone and five times with African-originating NF54 parasites. CHMI-studies are conceptualized to assess for example the safety or efficiency of immunizations, vaccines or chemoprophylaxis regimes as well as for the study of anti-malarial drug efficacy. Depending on the study aims and outcomes they generally run for a maximum of 28 days (Kibwana, Kapulu, and Bejon 2022; Lell et al. 2018; Mordmüller et al. 2017, 2022; Sulyok et al. 2021). For this study, treatment was only applied upon the detection of parasites by TBS in combination with malaria-related symptoms. Thus, the special aspect of the here presented study was, that volunteers were regularly sampled and allowed to stay parasite positive as long as they remained asymptomatic over a period of approximately 1.5 years. Since the *var* gene sequences of the applied strains (NF54/7G8) is known, this study represents a unique setup to study changes of the expression from the entire *var* gene repertoire at high resolution in ongoing *P. falciparum* infections using a highly sensitive RT-qPCR approach.

Var gene expression in life-long malaria-exposed individuals infected with 7G8 parasites

The African-originating strain NF54 has been extensively used for CHMIs with malaria-naïve and semi-immune individuals whereas the 7G8 clone derived from a South-American isolate has mainly been used for heterologous CHMIs with malaria-naïve volunteers (Kibwana et al., 2022; Moser et al., 2020; Silva et al., 2022). Until now, this clonal line has never been applied to African adults and a treatment on day 17 was mandatory during this trial to not introduce a South-American genotype to the African parasite population. In our volunteer cohort we identified only three volunteers positive for 7G8 parasites in sequence A of the trial presumably with very low baseline immunity (Figure 9, Figure 10 A, D). Since no presumptive treatment was applied to the volunteers prior to the 1st CHMI, many volunteers carried a submicroscopic infection into the trial. Based on our data, we hypothesize that infections are more difficult to establish when volunteers are already infected with another strain possibly explaining the low infectivity with 7G8 as well as with NF54 parasites. In general, however, the infectivity with NF54 parasites was higher than for 7G8 parasites until day 17 (Figure 10 A). Here, treatment was applied so that it is possible that more volunteers would have developed detectable parasitemia with 7G8 parasites after the treatment at day 17. However, CHMIs with 7G8 seem to be less successful in this life-long exposed Gabonese volunteer cohort compared to with NF54 parasites. We cannot exclude that batch effects affecting the quality within or across different strains or clones of the PfSPZ challenges might contribute to differences in the infectivity. However, there might also be a biological explanation for this: The South-American 7G8 parasites have a more restricted *var* gene repertoire of 45 *var* genes compared to 61 *var* genes in NF54 parasites. The reduced amount of variants could by default reduces the heterogeneity of the expressed pattern which is likely key for the establishment of infections with NF54 parasites (Bachmann et al. 2019; Bhardwaj et al. 2024). Even though the *var* gene repertoire 3D7/NF54 and 7G8 parasites are very different, it was shown that even

strains and clones from different geographical origins have a moderate degree of epitope sharing (Moser et al., 2020; Otto et al., 2019). Thus, the 7G8 clone exhibiting a smaller repertoire could be more susceptible to cross-protective immunity acquired from earlier infections and to evade the immune system causing a more efficient clearance.

Similar to NF54 parasites, 7G8 parasites also induce expression of a highly diverse *var* gene pattern of especially B-type *var* genes in malaria-naïve volunteers at the onset of infection but in parallel 7G8 parasites were also shown to dominantly express a single C-type *var* gene variant (PF7G8_040025600) (Wichers-Misterek et al., 2023). The expression of this C-type variant was shown to be incompletely reset during the mosquito passage, so that Wichers-Misterek et al. 2023 hypothesized that the parasites can rely on both, highly diverse PfEMP1 expression or the expression of a single PfEMP1 variant which was potentially successful in previous hosts to explore a yet unknown host environment. We suspect that these three volunteers were comparable susceptible to 7G8 as malaria-naïve volunteers despite their life-long malaria exposure, as 2/3 volunteers required treatment due to signs of malaria in subsequent challenges with NF54. Furthermore, the plasma sample tested from one the three volunteers revealed a significantly lower reactivity to our PfEMP1-specific Luminex assay indicating a rather low anti-PfEMP1 immunity (Figure 10 D). The three life-long exposed volunteers with 7G8 parasites showed a heterogenous expression pattern of many B-type *var* genes at lower levels and also a dominant expression of this C-type variant PF7G8_040025600 similar to parasites from malaria-naïve volunteers (Figure 10 B, C, (Wichers-Misterek et al., 2023)). Consequently, our data confirms the data from Wichers-Misterek et al. 2023 for low-immune individuals while further research is required to assess changes of the 7G8 *var* gene profile in more immune individuals.

Subgrouping of life-long malaria-exposed volunteers based on strain-specific immunity

In previous CHMI studies, the degree of semi-immunity was correlated to a higher degree of antibody-dependent Fc-mediated effector functions targeting e.g., VSAs, MSP1 and AMA1 which was linked to better infection control for example by limiting the parasitemia or delaying the onset of infection (Achan et al., 2020; Aitken et al., 2020; Gonzales et al., 2020; Osier et al., 2008; Rosenkranz et al., 2024; Yman et al., 2019). Both observations were additionally linked to differences in the parasite's *var* gene expression during the infection onset of a CHMI (Bachmann et al. 2019; Bhardwaj et al. 2024). In this context, Bachmann et al. 2019 identified six 'non-controllers' and six 'controllers' in a cohort of life-long exposed Gabonese adults with different levels of previously acquired anti-PfEMP1 immunity. Interestingly, parasites from less immune non-controllers displayed a highly diverse *var* gene pattern dominated by B and A-type *var* genes, while parasites from more immune controllers expressed only a limited number of genes mainly from group B or B/C. This observation was recently confirmed in a CHMI study with 19 volunteers from The Gambia, where low immunity individuals ("sero-low") were less able to control parasite kinetics and NF54 parasites displayed a higher entropy of *var* gene expression (Bhardwaj et al., 2024). Until now, no gold standard to assess individual's degree of semi-immunity to malaria has been established. Systems serology analyses with L2 samples are still ongoing, thus in agreement with

Bachmann et al. 2019, we correlated the day of TBS positivity of the volunteers with the corresponding entropy of *var* gene expression to distinguish between different degrees of previous exposure in our volunteer cohort. The clustering approach identified thirteen non-controllers and eleven controllers in our volunteer cohort (Figure 11 B). Volunteer groups displayed differences, with controllers delaying the day of infection onset, developing lower TBS parasitemia while the parasites from these individuals express a lower level of severity-linked A and B/A type *var* genes and an increase of central located B/C type *var* genes compared to less-immune malaria-naïve or life-long exposed non-controller like initially demonstrated by Bachmann et al. 2019 (Figure 11 E, Figure 12 D).

Next, we measured levels of anti-PfEMP1 immunity in all individuals using a similar custom-made PfEMP1-specific Luminex assay as Bachmann et al. 2019. Luminex assays are extensively used on plasma samples from field or CHMI studies to detect antibodies recognizing known antigens like MSP1 or AMA1, but are also used to detect cross-reactivity to selected PfEMP1 domains like EPCR-binding CIDR α domains linked with severity of malaria infections (Achan et al., 2020; Bachmann et al., 2019a; Cham et al., 2008; Collins et al., 2022; Reyes et al., 2024; Turner et al., 2011; Wichers et al., 2021). Overall, we measured the breadth of the anti-PfEMP1 immunity against 44 different PfEMP1 domains with known binding features including a large variety of 19 different A-type encoded PfEMP1s (CIDR α 1.1/1.4-1.8, CIDR δ 1: EPCR and unknown binding phenotype), twelve different B, B/C or C-type encoded PfEMP1 (CIDR α 2/3/4: CD36 binding phenotype), the conserved variants VAR1, VAR3 and VAR2CSA (CIDR α 1.3 (VAR1); full-length VAR3 or VAR2CSA: unknown or CSA binding phenotype, respectively) as well as ten more C-terminal domains from various PfEMP1s with two different Luminex plex. Comparable to Bachman et al. 2019, non-controllers showed a trend to lower anti-PfEMP1 antibody levels and a reduced seroprevalence to PfEMP1 antigens than controllers suggesting that the ability to control the infection and restrict the expressed *var* entropy is associated with a broader and higher anti-PfEMP1 immunity (Figure 12 A, B, D). Furthermore, detected immune responses of 27 NF54/3D7-specific PfEMP1 domains from plex 11 showed that only controllers, with a higher degree of anti-PfEMP1 immunity, can effectively suppress the expression of corresponding *var* gene variants suggesting a higher degree of protective strain-specific immunity (Figure 12 C). Of note, antibodies targeting GLURP were found to be most discriminating between the groups indicating that controllers might have a more recent history of exposure compared to non-controllers (Figure 12 C, Drakeley et al. 2005).

However, since the world-wide PfEMP1 domain repertoire is almost infinite, the Luminex assay can only measure anti-PfEMP1 antibodies for a small subset of PfEMP1 domains and thus might miss local predominant and important domains. To tailor our serological analyses more specifically to 3D7/NF54 PfEMP1 domains, we currently perform serological profiling via comprehensive libraries of a more concise parasite-specific epitope repertoire including 274 different PfEMP1 domains and 80 control proteins (AlphaScreen®) (Hassan et al. 2023; Kanoi et al. 2018, 2020; Stucke et al. 2019; Takashima et al. 2022). Furthermore, in collaboration with colleagues in Tübingen, the volunteer's plasma is currently screened for IgG antibodies against various merozoite surface antigens, MSPs and AMA1. As indicated

earlier, the breath of these IgG Fc-mediated effector functions, which include an enhanced phagocytosis of merozoites by monocytes or neutrophils, agglutination of merozoites, antibody dependent complement-mediated lysis or neutrophilic antibody-dependent respiratory burst (ADRB) activity, are associated with protection from severe or symptomatic malaria and different infection kinetics in CHMI studies (Achan et al., 2020; Kapelski et al., 2014; Kapulu et al., 2022; Osier et al., 2008; Wichers et al., 2021). Therefore, it will be extremely interesting to compare already established assays for assessing semi-immunity with our Luminex data and *var* entropy-based approach, which may be more strain-specific than the assays based on (3D7-derived) merozoite antigens.

We conclude that similar to other previously conducted studies, a higher degree of semi-immunity has immediate effects on how infections are established in individuals (Bachmann et al. 2019; Bhardwaj et al. 2024; Kapulu et al. 2022; Osier et al. 2008). According to our findings, we hypothesize that in more immune individuals, the expressed *var* gene pattern is less heterogenous because of a higher levels of a broad, cross-protective anti-PfEMP1 antibodies restricting the number of expressed variants from the antigenic repertoire. These cross-protective antibodies seem to less able to target less sequence conserved *var* genes from group B of NF54 parasites so that parasites expressing these variants dominate the expression pattern in both non-controllers and controllers (Figure 13 A, C). As a consequence, more immune individuals can a) delay their infection onset (Figure 11 B), b) limit the parasitemia (Figure 11 E), and c) restrict expression of severity-linked A and B/A types (Figure 12 D), which is in line with findings from other studies, showing that immunity against variants causing severe disease are developed relatively quickly after only a few infections (Bachmann et al. 2019; Cham et al. 2009). Of note, since the majority of volunteers exhibiting parasites expressing A and B/A-type *var* genes were asymptotically infected in this study, it is possible that during previous episodes of exposure, a sufficient cross-protective anti-PfEMP1 immunity was already developed to suppress the expression of severity-associated variants to a lower level.

Longitudinal infection dynamics

According to our data, the degree of semi-immunity also had implications for the longitudinal development of the infection. Non-controllers showed a longer infection duration (Figure 14 B, C) and tested parasite-positive by TBS more frequently than controller (Figure 11 E). During the course of the trial, parasitemia and the parasite's expressed *var* entropy strongly declined in non-controllers aligning to the values of controllers at the end of the infection (Figure 14 A, E; Figure 16 A, B). After each of the first three CHMIs, the parasites from non-controllers could regain a more diverse *var* expression pattern, although to a lower level than in the previous CHMI. This highlights the importance of the parasite's ability to epigenetically reset it's *var* gene expression by generating a diverse pattern, which is linked to prolonged infections and maybe also the success of reinfection (Figure 16 A, Bachmann et al. 2016; Wichers-Misterek et al. 2023). Since the non-controllers were the only individuals who further accumulated anti-PfEMP1 immunity, especially during the first eight weeks of infection (Figure 15 C), we hypothesize that non-controllers stay TBS positive for a longer period since they require more time

to develop a broad anti-plasmodial immune response thereby aligning to controllers and eventually clearing the infection. However, volunteers were infected with locally circulating strains even after NF54 clearance, suggesting the immunity to be parasite strain-specific (Figure 9, Figure 22). Consequently, our data suggests that the lack of broad anti-PfEMP1 antibody response in non-controllers at the infection onset might allow the parasite to reinfect the new host with high *var* entropy ultimately leading to a longer infection duration. Contrary, cross-protective immunity gained from earlier malaria episodes in controllers is restricting the number of *var* genes expressed at infection onset already and retains the entropy throughout the infection to a lower level allowing clearance faster than for non-controllers (Figure 16).

Antigenic variation over time

Longitudinal assessment of the *var* gene expression pattern by non-controller revealed that with increasing anti-PfEMP1 immunity, the highly diverse *var* gene pattern which is dominated by subtelomeric B and A-type *var* genes is gradually transitioning to a less diverse pattern with higher proportion of centrally located B/C and C-type *var* genes (Figure 16 C, D, E). Earlier studies hypothesized that NF54 parasites most likely favor a ‘bet-hedging’ strategy involving the expression of multiple different PfEMP1s to “explore” the human host environment so that at least one/a few parasites express variant(s) with optimal cytoadhesive abilities that are not recognized by the immune system can establish the infection (Abdi et al., 2016; Bachmann et al., 2016; Rovira-Graells et al., 2012). However, to avoid presentation of the entire PfEMP1 repertoire, it was speculated that the parasites retain a subset of *var* genes at the beginning of the infection, which could be expressed later to maintain infections in the long run (Coleman et al., 2014; Rovira-Graells et al., 2012). In this context, *var* group C has already been suggested to become important later in the course of infections (Bachmann et al. 2016).

Here, we are able to demonstrate for the first time, that the parasites indeed withhold the entire subset of C-type *var* genes for expression at later infection time points as shown by a representative non-controller in Figure 16 D. Quantification of this effect from all non-controllers revealed that parasites dominantly express C-type *var* genes only at the end of the infection before the individuals clear the infection (Figure 17 A). In our analysis, parasites from more immune controllers dominantly express C-type *var* genes approximately three weeks earlier than parasites from less immune non-controllers (Figure 17 B), suggesting that the parasites gradually shift from B-type to C-type *var* genes while adopting to the increasing host immunity (Figure 15 C). Hence, depending on the level of anti-PfEMP1 immunity at baseline, the parasites alternate more or less quickly through their PfEMP1 repertoire by expressing C-type *var* genes after B-type *var* genes. One explanation for the shift to centrally located C-type *var* genes might be linked to their relatively low “off-rates” compared to telomeric B-type and A-type *var* genes with higher “on” and “off-rates” (Frank et al. 2007). Thus, the expression differences from early and later infection time-points might be orchestrated by an epigenetically controlled ‘*position effect*’ including a flexible activation and silencing of subtelomeric located genes at the infection onset (Michel-Todó et al., 2023). At late infection stages, when the antigenic repertoire is however more

exhausted, central located C-type genes, which are less likely to be switched off are potentially the only remaining variants to maintain the infection (Frank et al., 2007; Wichers-Misterek et al., 2023).

Since another study suggested expression differences of parasites in response to environmental changes e.g., during the dry season, to protect the host from severe disease episodes and to resume transmission during the subsequent wet season (Andrade et al., 2020), we tested whether there is a correlation between expression of C-type *var* genes and the seasons (Figure 17 D). As this was not the case, we hypothesize that all *P. falciparum* strains exhibit a similar *var* expression program with mild-malaria linked C-type *var* genes expressed at late infection stages. This program is accompanied by a decreased parasitemia towards the end of infection, possibly due to fewer cytoadhesive parasites while the individuals' immune status rises (Figure 14, Figure 18). Thus, it is possible that the higher rate of asymptomatic infections observed during dry seasons solely relies on long-term infections originated in a previous wet season (Andrade et al., 2020; Fogang et al., 2024).

Parasite kinetics from individual volunteers determined by TBS show subsequent rise and fall of parasitemia with clearly delineated waves as observed in earlier studies with malaria-infected neurosyphilis patients or prisoners (Miller 1994, Eyles, Young 1951, Bruce-Chwatt 1963). Based on this indication, it has already hypothesized that antigenic variation is the main driver of *P. falciparum* malaria chronicity, where the parasite population gradually cycles through an antigen repertoire during the course of infection, similar to other organisms such as *P. knowlesi* or *T. brucei* (Galinski et al., 2018; Horn, 2014; MacGregor et al., 2012; McCulloch et al., 2017). Indeed, we were able to proof this antigenic variation hypothesis for *P. falciparum*, by showing that *P. falciparum* parasites maintain infections by expressing only a single or few *var* gene variants per delineated parasitemia wave (Figure 16 D, Supplementary Figure 3, Supplementary Figure 4). The only exception from this rule is the first parasitemia wave, during which the parasites express a more heterogenous *var* gene pattern as discussed earlier.

So far, only a single longitudinal study has been published investigating *var* gene expression by parasites isolated from a cohort of eleven asymptomatic children in Papua New Guinea (Kaestli et al., 2004). The study compared *var* gene expression of samples collected either bimonthly or, for three individuals, every fifth day over a period of four months and found that expression of several *var* gene variants reoccurred at multiple time points. Since the genomic sequences for the highly polymorphic *var* gene sequences are unknown in field isolates, Kaestli et al. 2004 used degenerated *var* primers targeting only selected upstream regions and N-terminal DBL α , CIDR α and DBL β domains for RT-PCR and TOPO cloning coupled to Sanger sequencing to compare the *var* gene transcript pattern over time. Although this approach was state-of-the-art at the time, due to primer biases presumably only a sub-proportion of the full *var* gene repertoire of these strains were amplified and sequenced. Moreover, sampling was not connected to parasitemia leading to a comparison between samples from different phases of parasite *in vivo* growth. Nevertheless, a dynamic picture of *var* gene expression was observed, which is largely in agreement with our data from comparable time points.

Moreover, a preliminary analysis measuring anti-PfEMP1 antibodies for 27 different NF54/3D7 PfEMP1 domains (plex 11, Table 14) revealed that during the course of infection, the host accumulates antibodies to PfEMP1 variants which were highly expressed in previous parasitemia waves (Figure 16 E). Thus, in response to highly expressed PfEMP1s, the host can accumulate functional antibodies targeting these PfEMP1 variants. Of note, this also depends on the parasitemia, which determines the level of antigen exposure to the host. This variant-specific response is presumably longer lasting, as the expression of variants, that were once highly expressed during a parasitemia wave do not reoccur in the parasite population of the respective volunteer (Figure 16 D, Supplementary Figure 3, Supplementary Figure 4). This idea is also supported by findings from other studies, showing that PfEMP1 antibodies can be detected up to 100 days after a single infection and that anti-VSA specific antibodies are increasing and maintained upon a change of the antigenic phenotype (Krause et al., 2007; Staalsoe et al., 2002). According to a mathematical model from Recker et al. 2004, long-lasting, variant-specific immunity in combination with a rather short-lived cross-protective immunity acquired from earlier infections shapes antigenic variation over time and presumably orchestrates the characteristic rise and fall of parasitemia during the infection (Recker and Gupta 2006; Mario Recker et al. 2004). Thus, only more divergent variants with a lower degree of shared epitopes compared to other isolates or strains can form new parasitemia waves which is in line with findings from this study suggesting that especially low sequence conserved B-type *var* genes are expressed at the infection onset or later during the infection before C-type expression becomes more dominant (Figure 13, Figure 16, Figure 17). Therefore, it is likely that the major driver of infection are variant specific growth rates while other factors including for example *var* gene switching is required for the continuous generation of diverse *var* gene expression in the parasite population (personal communication with Mario Recker).

Var gene switching can occur during the asexual replication cycle when progeny of an earlier parasite generation do not inherit the previous *var* gene expression and instead express another variant from the repertoire (Dzikowski & Deitsch, 2008, 2009; Epp et al., 2009; Frank et al., 2006). It is described that *var* gene switching is dependent on *var2csa*, which may represent a “switching node” from which a parasite population exhibiting an altered *var* expression can emerge (Dzikowski & Deitsch, 2009; Zhang et al., 2022). Uniquely for *var2csa*, expression is initiated slightly earlier in the ring stage than the other *var* gene variants (Petersen et al., 2021), in theory, allowing these parasites to switch from the *var2csa* “node” to another variant within a few hours during the same ring stage generation. Such “switching nodes” presumably represent a crucial factor for the longitudinal maintenance of infection granting the parasite enough flexibility to interchangeably switch expression from single variants to a more diverse parasite population expressing multiple variants (so-called, single-many-single (sms) mechanism) (Recker, Al-Bader, and Gupta 2005; Mario Recker et al. 2011; Mario Recker, Arinaminpathy, and Buckee 2008). Mathematical modelling demonstrated that this semi-coordinated mechanism has several advantages over other possible switching mechanisms. For example, a highly uncoordinated (random) switching would lead to a rapid exhaustion of the antigenic repertoire while a highly coordinated (one variant after the other) switching mechanism could be easily interrupted e.g., through the application of a treatment making reinfections unlikely to take place *in vivo* (Recker et al., 2008).

Since the expressed *var* gene pattern clearly changes across delineated parasitic waves, we suggest that if *var* gene switching occurs it is most likely occurring in the “background”, more precisely in a proportion of parasites which are flying under the radar of the immune response. In parasitemia ‘valleys’ the parasitemia frequently falls below the level of detection for microscopy-based diagnostics like TBS (Delley et al., 2000; Giudice et al., 1988; Hergott et al., 2024; Okell et al., 2009). Even though the sampling strategy did not include the collection of TBS negative samples in the parasitemia valleys, the analysis of samples collected a) during the wave’s incline once the infection becomes microscopically detectable and b) until the parasitemia falls below the TBS detection limit during the wave’s decline provided insights into the role of these ‘valleys’ for the maintenance of infection. Unexpectedly, we observed that *var2csa* expression was low during the parasitemia ‘valleys’ and was not elevated significantly at any time point during the trial, suggesting a rather minor role of *var2csa* mediated switching for maintaining malaria chronicity. Still, we cannot exclude that *var2csa* switching can occur in the ‘background’ parasite population to select for parasites expressing PfEMP1s with better sequestration abilities.

Interestingly, instead of *var2csa*, a higher proportion of parasites expressed severity-linked A-type *var* genes was found in some of the in- and decline phases of the parasitemia waves (Figure 16 D, F, Supplementary Figure 3, Supplementary Figure 4). Since A-type *var* genes are located at the subtelomeric end of the chromosomes, they were shown to have higher off-rates and a more dynamic switching pattern (Horrocks et al. 2004, Dzikowski and Deitsch 2008). Thus, it is possible that the parasites quickly switch from A-type *var* gene expression to a more diverse parasite population from which new variants with the potential to form new parasitemia waves can emerge. Apart from mediating *var* gene switching, the parasites expressing A-type PfEMP1s, might rescue the parasite population at low parasitemia levels potentially due to their ability to statically bind to the EPCR receptor expressed on brain endothelial cells (Jensen, A. R.; Adams, Y.; Hviid, 2020; Turner et al., 2013). Within this niche, parasites might hide from immune recognition while parasites expressing other PfEMP1s mostly binding to CD36 quickly accumulate at various endothelial tissues and are omnipresent in the circulation (Bachmann et al., 2022; Gazzinelli et al., 2014; Walker & Rogerson, 2023). Although A-type PfEMP1s appear to be more immunogenic and their recognition by the immune system is acquired early in life in people living in endemic areas, they might not be recognized in submicroscopic parasitemia “valleys”, as indicated by a recent study showing that immunity is rarely activated at the transcriptomic level in asymptomatic cases (Prah et al., 2023).

Characteristics of B and C-type waves

To better understand how the parasites mediates the shift from expressing in particular, B-type *var* genes at the infection onset to the expression of a single or few C-type *var* genes at the end of the infection, we compared the transcriptomics of parasites from both time points. However, our transcriptomic analysis is rather preliminary due to difficulties with the library preparation and sequencing at the sequencing facility. Although we observed a high overlap for the *var* gene expression pattern from samples simultaneously tested with our RT-qPCR and RNA-seq approach

(Supplementary Figure 6 A), we are currently resequencing the samples from the current analysis next to a larger sample cohort with additional time points at greater sequencing depth. Nevertheless, for the preliminary transcriptomic analysis we utilized a pre-established bioinformatic pipeline for analyzing *ex vivo* *falciparum* malaria samples (Tonkin-Hill et al., 2018). As one of the first steps, the pipeline includes an estimation of parasite stages from the transcriptomic profile of each sample to correct for differences in stage distribution and thus gene expression between different samples. Interestingly, we observed that samples exhibiting a dominant C-type expression showed a higher proportion of parasites with a schizont-like transcriptomic profile (median 0.23% of the total parasites) indicating that older parasite stages were circulating in the blood of these volunteers (Figure 18). Unfortunately, we were not able to retrieve blood smears from the study site to verify this result on a microscopic level. Even if blood smears were available, it would have been very difficult to quantify given the low abundance of parasites with the schizont-like expression profile. Usually, schizonts sequester at endothelial membranes and can only occasionally be observed in the blood circulation at very high parasitemia (Gazzinelli et al., 2014; Walker & Rogerson, 2023; Wiser, 2023).

In contrast, our data suggest that C-type expressing parasites bind less tightly to endothelial receptors, resulting in a small proportion of schizonts being found in the peripheral circulation before being cleared by the spleen. Given the fact, that both B and C-type encode PfEMP1s with N-terminal CIDRa2-6 domains mediating binding to the CD36 receptor, it is surprising that C-type PfEMP1s might have weaker sequestration capabilities. Possible explanations for this could be: (i) differences in *var* gene expression or translation, (ii) reduced C-type PfEMP1 display on the surface of the iRBC due to insufficient trafficking, or (iii) different overall protein structures, e.g., due to posttranslational protein modifications. Interestingly, we observed higher levels of total *var* gene expression for parasites expressing C-type *var* genes at the end of the infection (Supplementary Figure 6 B), which might suggest that the parasites compensate their weaker sequestration abilities by elevating *var* gene expression. Also, GO-term analysis showed a higher level of upregulated genes with the encoded proteins being involved in cell adhesion in late infection stages compared to earlier time points (Figure 19, Figure 20) indicating that the parasite in general upregulates biological mechanisms to increase cytoadhesion. *In vitro*, binding assays with genetically engineered parasites lines expressing a single *var* gene variant of choice could be used to quantify differences in protein surface exposure impacting on the parasite's binding abilities (Cronshagen et al. 2024).

In addition, differential expression analysis of B and C-type *var*-expressing parasites revealed that the latter express significantly lower levels of *rif* genes (Figure 21 B, Table 19). In parasites expressing B-type *var* genes, the expression of telomeric genes appears to be generally switched on, as the majority of *rif* expression is derived from those genes that are in close chromosomal proximity to telomeric B-type *var* genes (Figure 21 A, C). RIFINs were already shown to be involved in the formation of rosettes (Goel et al., 2015; Niang et al., 2014) as well as the suppression of NK, B and T-cells (Harrison et al., 2020; Yokoyama et al., 2018). Both processes have been linked to parasites virulence, suggesting that NF54 parasites at later infection stages use a different strategy to maintain persistence and immune

evasion than parasites at the early onset of blood stage infection. B-type *var* gene expression is indirectly linked to telomeric *rif* expression by a position effect and severity-linked A-type *var* genes as well as mild-malaria linked C-type *var* genes are directly co-regulated with their neighboring *rif* gene presumably via a shared promotor sequence (Figure 21 F, Claessens et al. 2012; Lavstsen et al. 2003). These strategies might be beneficial for the parasite to establish the infection and simultaneously suppress excessive and harmful immune responses endangering the host at selected time points during the infection (Gazzinelli et al., 2014).

Antigenic variation can also be observed in natural malaria infection settings

In the recent years, cohort studies with regular sampling of asymptomatic malaria cases looking at host immunity and/or *var* gene expression profiles are on the rise (Andrade et al., 2020; Collins et al., 2022; Fogang et al., 2024; Nyarko & Claessens, 2021; Stadler et al., 2023). Even though the L2 study was a CHMI study, in 25 volunteers (about 44 %) infections with local parasite strains were detected at the onset of the trial, which enabled us to longitudinally analyze *var* gene expression in parasites from these volunteers in addition to the simultaneously collected CHMI samples. After genotyping, the study was therefore retrospectively divided into two sample cohorts: a longitudinal ‘CHMI-study’ with all NF54 or 7G8 infections and a ‘NI-study’ of mosquito-borne infections with locally circulating parasites (Figure 9, Figure 22). The frequency of natural malaria infections was high, as no treatment was carried out before the start of the study and many volunteers carried submicroscopic infections into the trial, which became microscopically positive at later time points, indicated by two volunteers L2-32.14A and L2-32.16B described (Figure 9). Interestingly, volunteers from sequence A, who underwent treatment at day 17 during the first CHMI infection period were more likely to be CHMI-positive after the next NF54 challenge (14/28 volunteers: 50 %) than untreated volunteers from sequence B (11/28: 39 %) (Figure 9). Thus, inducing a malaria infection on top of an already existing infection seem to be more challenging as also indicated by the relatively low number of three detectable 7G8 infections (discussed earlier) or 7/25 (28 %) of so-called mixed infections with NF54 and locally circulating parasite genotypes. Further, this is supported by the fact, that the volunteers who were initially infected with NF54 parasites only became infected with local parasite genotypes after the NF54 infection had resolved (Figure 9).

To accurately compare the findings from the ‘CHMI-study’ to results from the natural infections, we would need a precise separation of volunteers into more and less immune individuals as illustrated in Figure 11 B. For our current approach, the exact day post infection when parasites become visible in the blood must be known (Figure 9), which is challenging to estimate in endemic settings due to frequent mosquito bites. Currently, a more accurate assessment of the parasitemia via RT-qPCR (Kamau et al., 2011; Mordmüller et al., 2017) and genotyping (MSP1, MSP2, GLURP; Falk et al. 2006) is ongoing in Tübingen. Results from these analyses will provide valuable insights into the date of infection onset, the infection multiplicity and changes of parasite genotypes during the courses of volunteer infections. Moreover, systems serology is performed with L2 plasma samples and will be compared to our *var* entropy-based measurement of semi-immunity, and can be ultimately used for a volunteer

classification. Thus, we suspended the classification of volunteers and the detailed analysis until further results are available.

Nevertheless, we already analyzed the longitudinal *var* gene profiles of Gabonese parasite isolates in four volunteers to validate the CHMI data on parasites antigenic variation. For this, we pursued an expressed sequence tag (EST) approach, which involved the amplification of a 350–500 bp long fragment of the DBL α sequence from cDNA by PCR and subsequent sequencing on a MiSeq device (Mackenzie et al., 2022; Stucke et al., 2019; Wichers et al., 2021). Overall, we observed a high degree of overlap between the CHMI and NI data sets: In each parasitemia wave, at most one or two *var* genes are dominantly expressed and these variants differ between individual parasitemia waves, suggesting that the antigenic repertoire is gradually exhausted over time. However, the DBL α -tag dataset has some limitations compared to the RT-qPCR dataset from the ‘CHMI-study’. First, the prediction tool (Varia) can only predict the connected full-length *var* sequences if a highly similar DBL α -tag sequence is found within *varDB*, leading to 11% DBL α -tag sequences without prediction for this study. This is similar to a study from Wichers et al. 2021 who reported incorrect domain compositions for about 15 % of the *var* sequences. Second, the inter-strain conserved variants, *var1*, *var2csa* and *var3*, cannot be accurately amplified by the degenerated primer pairs due to their different and unique domain compositions, so that occasional clusters with these sequences were manually excluded (section 2.2.18). However, these variants are also rarely expressed *in vivo* according to the longitudinal *var* gene expression data from the ‘CHMI-study’, suggesting that the additional coverage of these sequences has only limited additive value. Third, the EST approach is prone to PCR chimeras, which we indeed observed for DBL α -tag sequences from a single sample with NF54 parasites for which a reference genome exists. The extent to which these PCR chimeras occur is complicated to assess especially in samples from natural infections for which a reference genome does not exist. Fourth, the DBL α -EST approach does not allow the discrimination between B and C-type *var* genes encoding PfEMP1s with the same NTSB-DBL α -CIDR α 2-6 head structure (Rask et al., 2010).

Therefore, we infused another recently developed prediction tool called ‘*cUps*’ (Tan et al., 2023) to the Varia analysis pipeline, to verify whether parasites from natural infections also shift from B to C-type expression over time. The tool translates DBL α -tag cluster sequences into an amino acid sequence code, that is error-prone due to PCR or sequencing errors resulting to frameshifts and requires manual curation of the dataset. This curation step was skipped for time reasons and therefore the tool was unable to provide *var* group predictions for all DBL α sequences. For the remaining, annotated sequence clusters our data suggests that also in a natural infection setting, C-types are more preferably expressed with increasing duration of infection (Figure 17, Figure 24, Supplementary Figure 3, Supplementary Figure 4, Supplementary Figure 9). However, this data needs to be looked at cautiously since the tool currently annotates only about 70 % of translated C-type and 50 % of translated B-type sequences correctly, meaning that further validation steps will be required in the future.

5. Outlook

Results from the L2 study will contribute significantly to our understanding of how *P. falciparum* blood stage infections are established and maintained over time. But even though the clinical trial has been completed, blood fractions are currently being analyzed further at various partner institutions. Colleagues from Tübingen are currently performing a highly sensitive RT-qPCR with all collected samples to quantify sub-microscopic parasitemia as well as a genotyping approach for parasite-positive samples. This will provide more accurate information about the actual parasitemia levels during the trial and more precisely define the infection duration of the individuals. Additional genotyping data allow the identification of possible, yet unknown co-infections with local *P. falciparum* strains in the 'CHMI-study' sample cohort and the more accurate estimation of the infection onset in the 'NI-study' sample cohort. In addition, a longitudinal analysis similar to Kaestli et al. 2004, will be possible including an assessment of how the multiplicity of infection affect chronicity of *P. falciparum* infections.

To systematically analyze the correlation between parasitemia, gene expression and the occurrence of variant-specific PfEMP1 antibodies, we extend our serological analysis by including more extracellularly exposed PfEMP1 domains of NF54 parasites and investigate their recognition by antibodies. Currently, in collaboration with Eizo Takashima and Takafumi Tsuboi (Ehime University, Japan) our plasma samples are analyzed by AlphaScreen® including 274 PfEMP1 domains (Hassan et al. 2023; Kanoi et al. 2018; Takashima et al. 2022) and 80 selected control proteins expressed during the liver stage, in merozoites and gametocytes. These control proteins will enable us also to assess e.g., if liver stage immunity may also be involved in the delay of infection onset by releasing fewer parasites with lower *var* expression entropy. In a next step, antibody levels targeting the other VSA families including RIFIN, STEVOR and SURFIN will also be analyzed using AlphaScreen® (Hassan et al. 2023; Kanoi et al. 2018). These data need to be correlated with the genome-wide transcriptomic data and therefore we are currently repeating RNA-seq with all samples at greater sequencing depth including samples from additional time points.

In addition, longitudinal EST-based *var* gene expression data from only four individuals were presented in this study. The dataset will be expanded to the entire cohort of 49 (or more) volunteers who, according to our current genotyping approach, showed infections with local parasite strains at least once during the trial's study frame of 48 weeks. Similarly to samples from the 'CHMI-study', high parasitemia are currently processed for RNA-seq and *var* gene expression will be assessed according to Andradi-Brown et al. 2024, including a *de novo* assembly of *var* gene transcripts.

Finally, in collaboration with Mario Recker (University of Exeter, UK), we fit our *var* expression data set together with parasitemia and serology data from our 'CHMI-study' into a mathematical model (Recker et al., 2011) assess factors favoring chronic malaria infections.

6. Conclusion

In conclusion, we provide, for the first time, a concise longitudinal analysis of *var* gene expression dynamics in repeated CHMI infections. The obtained knowledge can be easily transferred to chronic asymptomatic *P. falciparum* infections to improve our understanding of long-term persistence in the human host. Moreover, also general mechanisms *P. falciparum* uses to establish blood stage infections in hosts with varying degree of immunity are now more solid and based on a larger sample size. We were able to correlate a highly diverse *var* gene expression and an early detectable blood stage parasitemia with (a) lower anti-PfEMP1 immunity levels at baseline, (b) higher parasitemia levels at early infection onset, and (c) a longer infection duration. With increasing infection duration and immunity, parasitemia levels and expressed *var* gene diversity are declining. Since higher anti-PfEMP1 immunity affected both, the infection duration and the parasite's ability to diversify its *var* gene pattern over time, we suggest that the degree of preestablished strain-specific immunity is a crucial indicator of persistence of infection. The course of infection is characterized by subsequent rise and fall of parasitemia with parasites mainly expressing a single *var* gene variant in clearly delineated parasitemia waves. Unlike described for other organisms, during the first wave of parasitemia at infection onset parasites express a highly diverse *var* gene pattern not dominated by a single variant. Over time the parasite population alternates through its PfEMP1 repertoire starting the infection with telomeric located B-type variants and, to some extent A-type variants, ending the infection with central located C-type variants, which potentially possess weaker sequestration capacities. The identification of factors accelerating the exhaustion of the antigen repertoire from B to C-type *var* genes, reducing the parasite's ability to release a highly diverse parasite population into the blood, to undergo *var* expression switching, or to survive in parasitemia 'valleys', represent valuable targets for future intervention and transmission control.

7. References

- Abdi, A. I., Warimwe, G. M., Muthui, M. K., Kivisi, C. A., Kiragu, E. W., Fegan, G. W., & Bull, P. C. (2016). Global selection of *Plasmodium falciparum* virulence antigen expression by host antibodies. *Scientific Reports*, 6(January). <https://doi.org/10.1038/srep19882>
- Achan, J., Reuling, I. J., Yap, X. Z., Dabira, E., Ahmad, A., Cox, M., Nwakanma, D., Tetteh, K., Wu, L., Bastiaens, G. J. H., Abebe, Y., Manoj, A., Kaur, H., Miura, K., Long, C., Billingsley, P. F., Kim Lee Sim, B., Hoffman, S. L., Drakeley, C., ... D'Alessandro, U. (2020). Serologic markers of previous malaria exposure and functional antibodies inhibiting parasite growth are associated with parasite kinetics following a *Plasmodium falciparum* controlled human infection. *Clinical Infectious Diseases*, 70(12), 2544–2552. <https://doi.org/10.1093/cid/ciz740>
- Achtman, A. H., Bull, P. C., Stephens, R., & Langhorne, J. (2005). Longevity of the immune response and memory to blood-stage malaria infection. *Current Topics in Microbiology and Immunology*, 297, 71–102. https://doi.org/10.1007/3-540-29967-x_3
- Agarwal, S., Kern, S., Halbert, J., Przyborski, J. M., Baumeister, S., Dandekar, T., Doerig, C., & Pradel, G. (2011). Two nucleus-localized CDK-like kinases with crucial roles for malaria parasite erythrocytic replication are involved in phosphorylation of splicing factor. *Journal of Cellular Biochemistry*, 112(5), 1295–1310. <https://doi.org/10.1002/jcb.23034>
- Aitken, E. H., Mahanty, S., & Rogerson, S. J. (2020). Antibody effector functions in malaria and other parasitic diseases: a few needles and many haystacks. *Immunology and Cell Biology*, 98(4), 264–275. <https://doi.org/10.1111/imcb.12320>
- Almelli, T., Nuel, G., Bischoff, E., Aubouy, A., Elati, M., Wang, C. W., Dillies, M. A., Coppée, J. Y., Ayissi, G. N., Basco, L. K., Rogier, C., Ndam, N. T., Deloron, P., & Tahar, R. (2014). Differences in gene transcriptomic pattern of *Plasmodium falciparum* in children with cerebral malaria and asymptomatic carriers. *PLoS ONE*, 9(12), 1–23. <https://doi.org/10.1371/journal.pone.0114401>
- Amit-Avraham, I., Pozner, G., Eshar, S., Fastman, Y., Kolevzon, N., Yavin, E., & Dzikowski, R. (2015). Antisense long noncoding RNAs regulate var gene activation in the malaria parasite *Plasmodium falciparum*. *Proceedings of the National Academy of Sciences of the United States of America*, 112(9), E982–E991. <https://doi.org/10.1073/pnas.1420855112>
- Amulic, B., Salanti, A., Lavstsen, T., Nielsen, M. A., & Deitsch, K. W. (2009). An upstream open reading frame controls translation of var2csa, a gene implicated in placental malaria. *PLoS Pathogens*, 5(1). <https://doi.org/10.1371/journal.ppat.1000256>
- Andrade, C. M., Fleckenstein, H., Thomson-Luque, R., Doumbo, S., Lima, N. F., Anderson, C., Hibbert, J., Hopp, C. S., Tran, T. M., Li, S., Niangaly, M., Cisse, H., Doumtabe, D., Skinner, J., Sturdevant, D., Ricklefs, S., Virtaneva, K., Asghar, M., Homann, M. V., ... Portugal, S. (2020). Increased circulation time of *Plasmodium falciparum* underlies persistent asymptomatic infection in the dry season. *Nature Medicine*, 26(12), 1929–1940. <https://doi.org/10.1038/s41591-020-1084-0>
- Andradi-Brown, C., Wichers-Misterek, J. S., von Thien, H., Höppner, Y. D., Scholz, J. A. M., Hansson, H., Hocke, E. F., Gilberger, T. W., Duffy, M. F., Lavstsen, T., Baum, J., Otto, T. D., Cunningham, A. J., & Bachmann, A. (2024). A novel computational pipeline for var gene expression augments the discovery of changes in the *Plasmodium falciparum* transcriptome during transition from in vivo to short-term in vitro culture. *ELife*, 13, 1–43. <https://doi.org/10.7554/eLife.87726>
- Aoki, S., Li, J., Itagaki, S., Okech, B. A., Egwang, T. G., Matsuoka, H., Palacpac, N. M. Q., Mitamura, T., & Horii, T. (2002). Serine repeat antigen (SERA5) is predominantly expressed among the SERA multigene family of *Plasmodium falciparum*, and the acquired antibody titers correlate with serum inhibition of the parasite growth. *Journal of Biological Chemistry*, 277(49), 47533–47540. <https://doi.org/10.1074/jbc.M207145200>
- Arya, A., Kojom Foko, L. P., Chaudhry, S., Sharma, A., & Singh, V. (2021). Artemisinin-based combination therapy (ACT) and drug resistance molecular markers: A systematic review of clinical studies from two malaria endemic regions – India and sub-Saharan Africa. *International Journal for Parasitology: Drugs and Drug Resistance*, 15(November 2020), 43–56. <https://doi.org/10.1016/j.ijpddr.2020.11.006>
- Ashley, E. A., Pyae Phy, A., & Woodrow, C. J. (2018). Malaria. *The Lancet*, 391(10130), 1608–1621. [https://doi.org/10.1016/S0140-6736\(18\)30324-6](https://doi.org/10.1016/S0140-6736(18)30324-6)
- Ashley, E. A., & White, N. J. (2014). The duration of *Plasmodium falciparum* infections. *Malaria Journal*, 13(1). <https://doi.org/10.1186/1475-2875-13-500>
- Auburn, S., Campino, S., Clark, T. G., Djimde, A. A., Zongo, I., Pinches, R., Manske, M., Mangano, V., Alcock, D., Anastasi, E., Maslen, G., MacInnis, B., Rockett, K., Modiano, D., Newbold, C. I., Doumbo, O. K., Ouedraogo, J. B., & Kwiatkowski, D. P. (2011). An effective method to purify *Plasmodium falciparum* dna directly from clinical blood samples for whole genome high-throughput sequencing. *PLoS ONE*, 6(7), 4–11. <https://doi.org/10.1371/journal.pone.0022213>
- Avraham, I., Schreier, J., & Dzikowski, R. (2012). Insulator-like pairing elements regulate silencing and mutually exclusive expression in the malaria parasite *Plasmodium falciparum*. *Proceedings of the National Academy of Sciences of the United States of America*, 109(52). <https://doi.org/10.1073/pnas.1214572109>
- Avril, M., Brazier, A. J., Melcher, M., Sampath, S., & Smith, J. D. (2013). DC8 and DC13 var Genes Associated with Severe Malaria Bind Avidly to Diverse Endothelial Cells. *PLoS Pathogens*, 9(6), 1–14.

- <https://doi.org/10.1371/journal.ppat.1003430>
- Ayres Pereira, M., Mandel Clausen, T., Pehrson, C., Mao, Y., Resende, M., Daugaard, M., Riis Kristensen, A., Spliid, C., Mathiesen, L., E. Knudsen, L., Damm, P., G. Theander, T., R. Hansson, S., A. Nielsen, M., & Salanti, A. (2016). Placental Sequestration of *Plasmodium falciparum* Malaria Parasites Is Mediated by the Interaction Between VAR2CSA and Chondroitin Sulfate A on Syndecan-1. *PLoS Pathogens*, 12(8). <https://doi.org/10.1371/journal.ppat.1005831>
- Babiker, H. A., Abdel-Muhsin, A. M. A., Ranford-Cartwright, L. C., Satti, G., & Walliker, D. (1998). Characteristics of *Plasmodium falciparum* parasites that survive the lengthy dry season in eastern Sudan where malaria transmission is markedly seasonal. *American Journal of Tropical Medicine and Hygiene*, 59(4), 582–590. <https://doi.org/10.4269/ajtmh.1998.59.582>
- Bachmann, A., Bruske, E., Krumkamp, R., Turner, L., Wichers, J. S., Petter, M., Held, J., Duffy, M. F., Sim, B. K. L., Hoffman, S. L., Kremsner, P. G., Lell, B., Lavstsen, T., Frank, M., Mordmüller, B., & Tannich, E. (2019). Controlled human malaria infection with *Plasmodium falciparum* demonstrates impact of naturally acquired immunity on virulence gene expression. *PLoS Pathogens*, 15(7), 1–24. <https://doi.org/10.1371/journal.ppat.1007906>
- Bachmann, A., Esser, C., Petter, M., Predehl, S., von Kalckreuth, V., Schmiedel, S., Bruchhaus, I., & Tannich, E. (2009). Absence of erythrocyte sequestration and lack of multicopy gene family expression in *Plasmodium falciparum* from a splenectomized malaria patient. *PLoS ONE*, 4(10). <https://doi.org/10.1371/journal.pone.0007459>
- Bachmann, A., Metwally, N. G., Allweier, J., Cronshagen, J., del Pilar Martinez Tauler, M., Murk, A., Roth, L. K., Torabi, H., Wu, Y., Gutsmann, T., & Bruchhaus, I. (2022). CD36 – A Host Receptor Necessary for Malaria Parasites to Establish and Maintain Infection. *Microorganisms*, 10(12), 1–16. <https://doi.org/10.3390/microorganisms10122356>
- Bachmann, A., Petter, M., Krumkamp, R., Esen, M., Held, J., Scholz, J. A. M., Li, T., Sim, B. K. L., Hoffman, S. L., Kremsner, P. G., Mordmüller, B., Duffy, M. F., & Tannich, E. (2016). Mosquito Passage Dramatically Changes var Gene Expression in Controlled Human *Plasmodium falciparum* Infections. *PLoS Pathogens*, 12(4). <https://doi.org/10.1371/journal.ppat.1005538>
- Bachmann, A., Petter, M., Tilly, A. K., Biller, L., Uliczka, K. A., Duffy, M. F., Tannich, E., & Bruchhaus, I. (2012). Temporal Expression and Localization Patterns of Variant Surface Antigens in Clinical *Plasmodium falciparum* Isolates during Erythrocyte Schizogony. *PLoS ONE*, 7(11). <https://doi.org/10.1371/journal.pone.0049540>
- Bachmann, A., Scholz, J. A. M., Janßen, M., Klinkert, M. Q., Tannich, E., Bruchhaus, I., & Petter, M. (2015). A comparative study of the localization and membrane topology of members of the RIFIN, STEVOR and PfMC-2TM protein families in *Plasmodium falciparum*-infected erythrocytes. *Malaria Journal*, 14(1), 1–18. <https://doi.org/10.1186/s12936-015-0784-2>
- Batinovic, S., McHugh, E., Chisholm, S. A., Matthews, K., Liu, B., Dumont, L., Charnaud, S. C., Schneider, M. P., Gilson, P. R., De Koning-Ward, T. F., Dixon, M. W. A., & Tilley, L. (2017). An exported protein-interacting complex involved in the trafficking of virulence determinants in *Plasmodium*-infected erythrocytes. *Nature Communications*, 8(May), 1–14. <https://doi.org/10.1038/ncomms16044>
- Bengtsson, A., Joergensen, L., Rask, T. S., Olsen, R. W., Andersen, M. A., Turner, L., Theander, T. G., Hviid, L., Higgins, M. K., Craig, A., Brown, A., & Jensen, A. T. R. (2013). A Novel Domain Cassette Identifies *Plasmodium falciparum* PfEMP1 Proteins Binding ICAM-1 and Is a Target of Cross-Reactive, Adhesion-Inhibitory Antibodies. *The Journal of Immunology*, 190(1), 240–249. <https://doi.org/10.4049/jimmunol.1202578>
- Bennett, B. J., Thompson, J., & Coppel, R. L. (1995). Identification of *Plasmodium falciparum* histone 2B and histone 3 genes. *Molecular and Biochemical Parasitology*, 70(1–2), 231–233. [https://doi.org/10.1016/0166-6851\(95\)00030-5](https://doi.org/10.1016/0166-6851(95)00030-5)
- Berger, S. S., Turner, L., Wang, C. W., Petersen, J. E. V., Kraft, M., Lusingu, J. P. A., Mmbando, B., Marquard, A. M., Bengtsson, D. B. A. C., Hviid, L., Nielsen, M. A., Theander, T. G., & Lavstsen, T. (2013). *Plasmodium falciparum* Expressing Domain Cassette 5 Type PfEMP1 (DC5-PfEMP1) Bind PECAM1. *PLoS ONE*, 8(7), 1–14. <https://doi.org/10.1371/journal.pone.0069117>
- Bernabeu, M., Howard, C., Zheng, Y., & Smith, J. D. (2021). Bioengineered 3D Microvessels for Investigating *Plasmodium falciparum* Pathogenesis. *Trends in Parasitology*, 37(5), 401–413. <https://doi.org/10.1016/j.pt.2020.12.008>
- Bhardwaj, I., Nyarko, P. B., Ashn, A. B., Cohen, C., Ceesay, S., Achan, J., Dabira, E., Nakajima, R., Jain, A., Taghavian, O., & Jasinskas, A. (2024). Diverse and weakly immunogenic var gene expression facilitates malaria infection. 1–31.
- Boddey, J. A., & Cowman, A. F. (2013). *Plasmodium* nesting: Remaking the erythrocyte from the inside out. *Annual Review of Microbiology*, 67, 243–269. <https://doi.org/10.1146/annurev-micro-092412-155730>
- Boddey, J. A., O'Neill, M. T., Lopaticki, S., Carvalho, T. G., Hodder, A. N., Nebl, T., Wawra, S., Van West, P., Ebrahimzadeh, Z., Richard, D., Flemming, S., Spielmann, T., Przyborski, J., Babon, J. J., & Cowman, A. F. (2016). Export of malaria proteins requires co-translational processing of the PEXEL motif independent of phosphatidylinositol-3-phosphate binding. *Nature Communications*, 7(May 2015). <https://doi.org/10.1038/ncomms10470>
- Bouyou-Akoté, M. K., M'Bondoukwé, N. P., & Mawili-Mboumba, D. P. (2015). Genetic polymorphism of

- merozoite surface protein-1 in *Plasmodium falciparum* isolates from patients with mild to severe malaria in Libreville, Gabon. *Parasite*, 22. <https://doi.org/10.1051/parasite/2015012>
- Brewster, D. R., Kwiatkowski, D., & White, N. J. (1996). Neurological sequelae of cerebral malaria [4]. *Lancet*, 348(9042), 1658–1659. [https://doi.org/10.1016/S0140-6736\(05\)65721-2](https://doi.org/10.1016/S0140-6736(05)65721-2)
- Bruce-Chwatt, Leonard Jan, Black, Robert Hughes, Canfield, Craig J, Clyde, David F, Peters, W. et al. (1986). Chemotherapy of malaria / L. J. Bruce-Chwatt, editor ; [authors], R. H. Black ... [et al.], rev. 2nd ed. World Health Organization. <https://iris.who.int/handle/10665/38605>
- Briggs, J., Teyssier, N., Nankabirwa, J. I., Rek, J., Jagannathan, P., Arinaitwe, E., Bousema, T., Drakeley, C., Murray, M., Crawford, E., Hathaway, N., Staedke, S. G., Smith, D., Rosenthal, P. J., Kamya, M., Dorsey, G., Rodriguez-Barraquer, I., & Greenhouse, B. (2020). Sex-based differences in clearance of chronic *Plasmodium falciparum* infection. *ELife*, 9, 1–14. <https://doi.org/10.7554/eLife.59872>
- CDC (Centers of Disease Control). (2022). Laboratory Diagnosis of malaria “*Plasmodium falciparum*.” *Centre for Diseases Controle and Prevention*, 1–4. https://www.cdc.gov/malaria/about/biology/index.html%0Ahttps://www.cdc.gov/dpdx/resources/pdf/benchAids/malaria/Pfalciparum_benchaidV2.pdf
- Cham, G. K. K., Kurtis, J., Lusingu, J., Theander, T. G., Jensen, A. T. R., & Turner, L. (2008). A semi-automated multiplex high-throughput assay for measuring IgG antibodies against *Plasmodium falciparum* erythrocyte membrane protein 1 (PfEMP1) domains in small volumes of plasma. *Malaria Journal*, 7, 1–8. <https://doi.org/10.1186/1475-2875-7-108>
- Cham, G. K. K., Turner, L., Lusingu, J., Vestergaard, L., Mmbando, B. P., Kurtis, J. D., Jensen, A. T. R., Salanti, A., Lavstsen, T., & Theander, T. G. (2009). Sequential, Ordered Acquisition of Antibodies to *Plasmodium falciparum* Erythrocyte Membrane Protein 1 Domains . *The Journal of Immunology*, 183(5), 3356–3363. <https://doi.org/10.4049/jimmunol.0901331>
- Chan, J. A., Fowkes, F. J. I., & Beeson, J. G. (2014). Surface antigens of *Plasmodium falciparum*-infected erythrocytes as immune targets and malaria vaccine candidates. *Cellular and Molecular Life Sciences : CMLS*, 71(19), 3633–3657. <https://doi.org/10.1007/s00018-014-1614-3>
- Chan, J. A., Howell, K. B., Reiling, L., Ataide, R., Mackintosh, C. L., Fowkes, F. J. I., Petter, M., Chesson, J. M., Langer, C., Warimwe, G. M., Duffy, M. F., Rogerson, S. J., Bull, P. C., Cowman, A. F., Marsh, K., & Beeson, J. G. (2012). Targets of antibodies against *Plasmodium falciparum*-infected erythrocytes in malaria immunity. *Journal of Clinical Investigation*, 122(9), 3227–3238. <https://doi.org/10.1172/JCI62182>
- Chappell, L., Ross, P., Ross, P., Orchard, L., Russell, T. J., Otto, T. D., Otto, T. D., Berriman, M., Rayner, J. C., Rayner, J. C., & Llinás, M. (2020). Refining the transcriptome of the human malaria parasite *Plasmodium falciparum* using amplification-free RNA-seq. *BMC Genomics*, 21(1), 1–19. <https://doi.org/10.1186/s12864-020-06787-5>
- Chen, I., Clarke, S. E., Gosling, R., Hamainza, B., Killeen, G., Magill, A., O’Meara, W., Price, R. N., & Riley, E. M. (2016). “Asymptomatic” Malaria: A Chronic and Debilitating Infection That Should Be Treated. *PLoS Medicine*, 13(1), 1–11. <https://doi.org/10.1371/journal.pmed.1001942>
- Chêne, A., Gangnard, S., Dechavanne, C., Dechavanne, S., Srivastava, A., Tétard, M., Hundt, S., Leroy, O., Havelange, N., Viebig, N. K., & Gamain, B. (2018). Down-selection of the VAR2CSA DBL1-2 expressed in *E. coli* as a lead antigen for placental malaria vaccine development. *Npj Vaccines*, 3(1). <https://doi.org/10.1038/s41541-018-0064-6>
- Cheng, Q., Cloonan, N., Fischer, K., Thompson, J., Waite, G., Lanzer, M., & Saul, A. (1998). *stevor* and *rif* are *Plasmodium falciparum* multicopy gene families which potentially encode variant antigens. *Molecular and Biochemical Parasitology*, 97(1–2), 161–176. [https://doi.org/10.1016/S0166-6851\(98\)00144-3](https://doi.org/10.1016/S0166-6851(98)00144-3)
- Chotivanich, K., Udomsangpetch, R., McGready, R., Proux, S., Newton, P., Pukrittayakamee, S., Looareesuwan, S., & White, N. J. (2002). Central Role of the Spleen in Malaria Parasite Clearance. *The Journal of Infectious Diseases*, 185, 1538–1541. <https://academic.oup.com/jid/article/185/10/1538/837204>
- Claessens, A., Adams, Y., Ghumra, A., Lindergard, G., Buchan, C. C., Andisi, C., Bull, P. C., Mok, S., Gupta, A. P., Wang, C. W., Turner, L., Arman, M., Raza, A., Bozdech, Z., & Rowe, J. A. (2012). A subset of group A-like var genes encodes the malaria parasite ligands for binding to human brain endothelial cells. *Proceedings of the National Academy of Sciences of the United States of America*, 109(26). <https://doi.org/10.1073/pnas.1120461109>
- Coban, C., Lee, M. S. J., & Ishii, K. J. (2018). Tissue-specific immunopathology during malaria infection. *Nature Reviews Immunology*, 18(4), 266–278. <https://doi.org/10.1038/nri.2017.138>
- Coleman, B. I., Skillman, K. M., Jiang, R. H. Y., Childs, L. M., Altenhofen, M., Ganter, M., Leung, Y., Goldowitz, I., Kafsack, B. F. C., Marti, M., Llinás, M., Buckee, C. O., & Duraisingh, M. T. (2014). A *Plasmodium falciparum* Histone Deacetylase Regulates Antigenic Variation and Gametocyte Conversion. *Cell Host and Microbe*, 16(2), 177–186. <https://doi.org/10.1016/j.chom.2014.06.014>
- Collins, K. A., Ceesay, S., Drammeh, S., Jaiteh, F. K., Guery, M. A., Lanke, K., Grignard, L., Stone, W., Conway, D. J., D’Alessandro, U., Bousema, T., & Claessens, A. (2022). A Cohort Study on the Duration of *Plasmodium falciparum* Infections During the Dry Season in The Gambia. *Journal of Infectious Diseases*, 226(1), 128–137. <https://doi.org/10.1093/infdis/jiac116>
- Colwill, K., Pawson, T., Andrews, B., Prasad, J., Manley, J. L., Bell, J. C., & Duncan, P. I. (1996). The Clk/Sty protein kinase phosphorylates SR splicing factors and regulates their intranuclear distribution. *EMBO Journal*, 15(2), 265–275. <https://doi.org/10.1002/j.1460-2075.1996.tb00357.x>

- Cooke, B. M., Mohandas, N., & Coppel, R. L. (2001). The malaria-infected red blood cell: Structural and functional changes. *Advances in Parasitology*, 50, 1–86. [https://doi.org/10.1016/S0065-308X\(01\)50029-9](https://doi.org/10.1016/S0065-308X(01)50029-9)
- Coughlan, C., Jäger, H. R., Brealey, D., Carletti, F., Hyare, H., Pattnaik, R., Sahu, P. K., Mohanty, S., Logan, S., Hoffmann, A., Wassmer, S. C., & Checkley, A. M. (2024). Adult Cerebral Malaria: Acute and Subacute Imaging Findings, Long-term Clinical Consequences. *Clinical Infectious Diseases*, 78(2), 457–460. <https://doi.org/10.1093/cid/ciad651>
- Cowman, A. F., & Crabb, B. S. (2006). Invasion of red blood cells by malaria parasites. *Cell*, 124(4), 755–766. <https://doi.org/10.1016/j.cell.2006.02.006>
- Crompton, P. D., Kayala, M. A., Traore, B., Kayentao, K., Ongoiba, A., Weiss, G. E., Molina, D. M., Burk, C. R., Waisberg, M., Jasinskas, A., Tan, X., Doumbo, S., Doumtabe, D., Kone, Y., Narum, D. L., Liang, X., Doumbo, O. K., Miller, L. H., Doolan, D. L., ... Pierce, S. K. (2010). A prospective analysis of the Ab response to Plasmodium falciparum before and after a malaria season by protein microarray. *Proceedings of the National Academy of Sciences of the United States of America*, 107(15), 6958–6963. <https://doi.org/10.1073/pnas.1001323107>
- Cronshagen, J., Allweier, J., Mesén-ramírez, P., Stäcker, J., Vaaben, V., Ramón-zamorano, G., Naranjo, I., Ofori, S., Jansen, P. W. T. C., Hornebeck, J., Kieferle, F., Murk, A., Martin, E., Castro-Peña, C., Bártfai, R., Lavstsen, T., Bruchhaus, I., Spielmann, T., (2024). A system for functional studies of the major virulence factor of malaria parasites. *bioRxiv*, <https://doi.org/10.1101/2024.04.30.591946>
- Cui, L., Mharakurwa, S., Ndiaye, D., Rathod, P. K., & Rosenthal, P. J. (2015). Antimalarial drug resistance: Literature review and activities and findings of the ICEMR network. *American Journal of Tropical Medicine and Hygiene*, 93(Suppl 3), 57–68. <https://doi.org/10.4269/ajtmh.15-0007>
- Cunnington, A. J.; Walther, M.; Riley, E. M. (2013). Piecing Together the Puzzle of Severe Malaria. *Science Translational Medicine*, 5(211), 10–39.
- Cunnington, A. J., Bretscher, M. T., Nogaro, S. I., Riley, E. M., & Walther, M. (2013). Comparison of parasite sequestration in uncomplicated and severe childhood Plasmodium falciparum malaria. *Journal of Infection*, 67(3), 220–230. <https://doi.org/10.1016/j.jinf.2013.04.013>
- Cunnington, A. J., Riley, E. M., & Walther, M. (2013). Stuck in a rut? Reconsidering the role of parasite sequestration in severe malaria syndromes. *Trends in Parasitology*, 29(12), 585–592. <https://doi.org/10.1016/j.pt.2013.10.004>
- Dahlbäck, M., Lavstsen, T., Salanti, A., Hviid, L., Arnot, D. E., Theander, T. G., & Nielsen, M. A. (2007). Changes in var gene mRNA levels during erythrocytic development in two phenotypically distinct Plasmodium falciparum parasites. *Malaria Journal*, 6, 1–11. <https://doi.org/10.1186/1475-2875-6-78>
- Datoo, M. S., Natama, H. M., Somé, A., Bellamy, D., Traoré, O., Rouamba, T., Tahita, M. C., Ido, N. F. A., Yameogo, P., Valia, D., Millogo, A., Ouedraogo, F., Soma, R., Sawadogo, S., Sorgho, F., Derra, K., Rouamba, E., Ramos-Lopez, F., Cairns, M., ... Tinto, H. (2022). Efficacy and immunogenicity of R21/Matrix-M vaccine against clinical malaria after 2 years' follow-up in children in Burkina Faso: a phase 1/2b randomised controlled trial. *The Lancet Infectious Diseases*, 22(12), 1728–1736. [https://doi.org/10.1016/S1473-3099\(22\)00442-X](https://doi.org/10.1016/S1473-3099(22)00442-X)
- Datoo, M. S., Natama, M. H., Somé, A., Traoré, O., Rouamba, T., Bellamy, D., Yameogo, P., Valia, D., Tegner, M., Ouedraogo, F., Soma, R., Sawadogo, S., Sorgho, F., Derra, K., Rouamba, E., Orindi, B., Ramos Lopez, F., Flaxman, A., Cappuccini, F., ... Tinto, H. (2021). Efficacy of a low-dose candidate malaria vaccine, R21 in adjuvant Matrix-M, with seasonal administration to children in Burkina Faso: a randomised controlled trial. *The Lancet*, 397(10287), 1809–1818. [https://doi.org/10.1016/S0140-6736\(21\)00943-0](https://doi.org/10.1016/S0140-6736(21)00943-0)
- Davison, B. B., Kaack, M. B., Rogers, L. B., Rasmussen, K. K., Rasmussen, T. A., Henson, E. W., Henson, M. C., Parekh, F. K., & Krogstad, D. J. (2006). The role of soluble tumor necrosis factor receptor types I and II and tumor necrosis factor- α in malaria during pregnancy. *Journal of Infectious Diseases*, 194(1), 123–132. <https://doi.org/10.1086/504694>
- Day, K. P., Artzy-Randrup, Y., Tiedje, K. E., Rougeron, V., Chen, D. S., Rask, T. S., Rorick, M. M., Migot-Nabias, F., Deloron, P., Luty, A. J. F., & Pascual, M. (2017). Evidence of strain structure in Plasmodium falciparum var gene repertoires in children from Gabon, West Africa. *Proceedings of the National Academy of Sciences of the United States of America*, 114(20), E4103–E4111. <https://doi.org/10.1073/pnas.1613018114>
- De Koning-Ward, T. F., Gilson, P. R., Boddey, J. A., Rug, M., Smith, B. J., Papenfuss, A. T., Sanders, P. R., Lundie, R. J., Maier, A. G., Cowman, A. F., & Crabb, B. S. (2009). A newly discovered protein export machine in malaria parasites. *Nature*, 459(7249), 945–949. <https://doi.org/10.1038/nature08104>
- Delley, V., Bouvier, P., Breslow, N., Doumbo, O., Sagara, I., Diakite, M., Mauris, A., Dolo, A., & Rougemont, A. (2000). What does a single determination of malaria parasite density mean? A longitudinal survey in Mali. *Tropical Medicine and International Health*, 5(6), 404–412. <https://doi.org/10.1046/j.1365-3156.2000.00566.x>
- Dimonte, S., Bruske, E. I., Hass, J., Supan, C., Salazar, C. L., Held, J., Tschan, S., Esen, M., Flötenmeyer, M., Koch, I., Berger, J., Bachmann, A., Sim, B. K. L., Hoffman, S. L., Kremsner, P. G., Mordmüller, B., & Frank, M. (2016). Sporozoite Route of Infection Influences In Vitro var Gene Transcription of Plasmodium falciparum Parasites from Controlled Human Infections. *Journal of Infectious Diseases*, 214(6), 884–894. <https://doi.org/10.1093/infdis/jiw225>
- Djimé, A., & Lefèvre, G. (2009). Understanding the pharmacokinetics of Coartem®. *Malaria Journal*, 8(SUPPL. 1), 1–8. <https://doi.org/10.1186/1475-2875-8-S1-S4>
- Drakeley, C. J., Corran, P. H., Coleman, P. G., Tongren, J. E., McDonald, S. L. R., Carneiro, I., Malima, R., Lusingu,

- J., Manjurano, A., Nkya, W. M. M., Lemnge, M. M., Cox, J., Reyburn, H., & Riley, E. M. (2005). Estimating medium- and long-term trends in malaria transmission by using serological markers of malaria exposure. *Proceedings of the National Academy of Sciences of the United States of America*, 102(14), 5108–5113. <https://doi.org/10.1073/pnas.0408725102>
- Duffy, F., Bernabeu, M., Babar, P. H., Kessler, A., Wang, C. W., Vaz, M., Chery, L., Mandala, W. L., Rogerson, S. J., Taylor, T. E., Seydel, K. B., Lavstsen, T., Gomes, E., Kim, K., Lusingu, J., Rathod, P. K., Aitchison, J. D., & Smith, J. D. (2019). Meta-analysis of plasmodium falciparum var signatures contributing to severe Malaria in African children and Indian adults. *MBio*, 10(2). <https://doi.org/10.1128/MBIO.00217-19>
- Duffy, M. F., Tang, J., Sumardy, F., Nguyen, H. H. T., Selvarajah, S. A., Josling, G. A., Day, K. P., Petter, M., & Brown, G. V. (2017). Activation and clustering of a Plasmodium falciparum var gene are affected by subtelomeric sequences. *FEBS Journal*, 284(2), 237–257. <https://doi.org/10.1111/febs.13967>
- Duffy, P. E., & Patrick Gorres, J. (2020). Malaria vaccines since 2000: progress, priorities, products. *Npj Vaccines*, 5(1), 1–9. <https://doi.org/10.1038/s41541-020-0196-3>
- Duraisingh, M. T., Voss, T. S., Marty, A. J., Duffy, M. F., Good, R. T., Thompson, J. K., Freitas, L. H., Scherf, A., Crabb, B. S., & Cowman, A. F. (2005). Heterochromatin silencing and locus repositioning linked to regulation of virulence genes in Plasmodium falciparum. *Cell*, 121(1), 13–24. <https://doi.org/10.1016/j.cell.2005.01.036>
- Dzikowski, R., & Deitsch, K. W. (2008). Active Transcription is Required for Maintenance of Epigenetic Memory in the Malaria Parasite Plasmodium falciparum. *Journal of Molecular Biology*, 382(2), 288–297. <https://doi.org/10.1016/j.jmb.2008.07.015>
- Dzikowski, R., & Deitsch, K. W. (2009). Genetics of antigenic variation in Plasmodium falciparum. *Current Genetics*, 55(2), 103–110. <https://doi.org/10.1007/s00294-009-0233-2>
- Dzikowski, R., Frank, M., & Deitsch, K. (2006). Mutually exclusive expression of virulence genes by malaria parasites is regulated independently of antigen production. *PLoS Pathogens*, 2(3), 0184–0194. <https://doi.org/10.1371/journal.ppat.0020022>
- Elmakki, E. E. (2012). Hyper-reactive Malarial Splenomegaly Syndrome (HMSS): Review article. *Cureus*, 4(11), 1–5. <https://doi.org/10.7759/cureus.72>
- Epp, C., Li, F., Howitt, C. A., Chookajorn, T., & Deitsch, K. W. (2009). Chromatin associated sense and antisense noncoding RNAs are transcribed from the var gene family of virulence genes of the malaria parasite Plasmodium falciparum. *Rna*, 15(1), 116–127. <https://doi.org/10.1261/rna.1080109>
- Epstein, J. E., Paolino, K. M., Richie, T. L., Sedegah, M., Singer, A., Ruben, A. J., Chakravarty, S., Stafford, A., Ruck, R. C., Eappen, A. G., Li, T., Billingsley, P. F., Manoj, A., Silva, J. C., Moser, K., Nielsen, R., Tosh, D., Cicatelli, S., Ganeshan, H., ... Hoffman, S. L. (2017). Protection against Plasmodium falciparum malaria by PfSPZ Vaccine. *JCI Insight*, 2(1), 0–14. <https://doi.org/10.1172/jci.insight.89154>
- Esmon, C. T. (2004). Structure and functions of the endothelial cell protein C receptor. *Critical Care Medicine*, 32(5 Suppl), 298–301. <https://doi.org/10.1097/01.ccm.0000126128.64614.81>
- Eyles, D.E., Young, M.D., 1951. The duration of untreated or inadequately treated Plasmodium falciparum infections in the human host. *J. Nat. Mal. Soc.* 10, 327–336.
- Falk, N., Maire, N., Sama, W., Owusu-Agyei, S., Smith, T., Beck, H. P., & Felger, I. (2006). Comparison of PCR-RFLP and genescan-based genotyping for analyzing infection dynamics of Plasmodium falciparum. *American Journal of Tropical Medicine and Hygiene*, 74(6), 944–950. <https://doi.org/10.4269/ajtmh.2006.74.944>
- Falkenhorst, G., Enkelmann, J., Frank, C., Lachmann, R., Faber, M., Pörtner, K., & Stark, K. (2020). Reiseassoziierte Krankheiten 2019. In *Epidemiologisches Bulletin*.
- Favuzza, P., de Lera Ruiz, M., Thompson, J. K., Triglia, T., Ngo, A., Steel, R. W. J., Vavrek, M., Christensen, J., Healer, J., Boyce, C., Guo, Z., Hu, M., Khan, T., Murgolo, N., Zhao, L., Penington, J. S., Reaksudsan, K., Jarman, K., Dietrich, M. H., ... Cowman, A. F. (2020). Dual Plasmepsin-Targeting Antimalarial Agents Disrupt Multiple Stages of the Malaria Parasite Life Cycle. *Cell Host and Microbe*, 27(4), 642–658.e12. <https://doi.org/10.1016/j.chom.2020.02.005>
- Febbraio, M., Hajjar, D. P., & Silverstein, R. L. (2001). CD36: A class B scavenger receptor involved in angiogenesis, atherosclerosis, inflammation, and lipid metabolism. *Journal of Clinical Investigation*, 108(6), 785–791. <https://doi.org/10.1172/JCI14006>
- Florini, F., Visone, J. E., Hadjimichael, E., Malpotra, S., Nötzel, C., Kafsack, B. F. C., & Deitsch, K. W. (2024). Transcriptional plasticity of virulence genes provides malaria parasites with greater adaptive capacity for avoiding host immunity. *Preprint*.
- Flueck, C., Bartfai, R., Volz, J., Niederwieser, I., Salcedo-Amaya, A. M., Alako, B. T. F., Ehlgen, F., Ralph, S. A., Cowman, A. F., Bozdech, Z., Stunnenberg, H. G., & Voss, T. S. (2009). Plasmodium falciparum heterochromatin protein 1 marks genomic loci linked to phenotypic variation of exported virulence factors. *PLoS Pathogens*, 5(9). <https://doi.org/10.1371/journal.ppat.1000569>
- Fogang, B., Lellouche, L., Ceesay, S., Drammeh, S., Jaiteh, F. K., Guery, M. A., Landier, J., Haanappel, C. P., Froberg, J., Conway, D., D'Alessandro, U., Bousema, T., & Claessens, A. (2024). Asymptomatic Plasmodium falciparum carriage at the end of the dry season is associated with subsequent infection and clinical malaria in Eastern Gambia. *Malaria Journal*, 23(1), 1–12. <https://doi.org/10.1186/s12936-024-04836-y>
- Frank, M., Dzikowski, R., Amulic, B., & Deitsch, K. (2007). Variable switching rates of malaria virulence genes are associated with chromosomal position. *Molecular Microbiology*, 64(6), 1486–1498. <https://doi.org/10.1111/j.1365-2958.2007.05736.x>

- Frank, M., Dzikowski, R., Costantini, D., Amulic, B., Berdough, E., & Deitsch, K. (2006). Strict pairing of var promoters and introns is required for var gene silencing in the malaria parasite *Plasmodium falciparum*. *Journal of Biological Chemistry*, 281(15), 9942–9952. <https://doi.org/10.1074/jbc.M513067200>
- Franklin, B. S., Parroche, P., Ataíde, M. A., Lauw, F., Ropert, C., De Oliveira, R. B., Pereira, D., Tada, M. S., Nogueira, P., Da Silva, L. H. P., Bjorkbacka, H., Golenbock, D. T., & Gazzinelli, R. T. (2009). Malaria primes the innate immune response due to interferon- γ induced enhancement of toll-like receptor expression and function. *Proceedings of the National Academy of Sciences of the United States of America*, 106(14), 5789–5794. <https://doi.org/10.1073/pnas.0809742106>
- Freitas, L. H., Hernandez-Rivas, R., Ralph, S. A., Montiel-Condado, D., Ruvalcaba-Salazar, O. K., Rojas-Meza, A. P., Mancio-Silva, L., Leal-Silvestre, R. J., Gontijo, A. M., Shorte, S., & Scherf, A. (2005). Telomeric heterochromatin propagation and histone acetylation control mutually exclusive expression of antigenic variation genes in malaria parasites. *Cell*, 121(1), 25–36. <https://doi.org/10.1016/j.cell.2005.01.037>
- Fried, M., Domingo, G. J., Gowda, C. D., Mutabingwa, T. K., & Duffy, P. E. (2006). *Plasmodium falciparum*: Chondroitin sulfate A is the major receptor for adhesion of parasitized erythrocytes in the placenta. *Experimental Parasitology*, 113(1), 36–42. <https://doi.org/10.1016/j.exppara.2005.12.003>
- Friedman-Klabanoff, D. A. J., Laurens, M. B., Berry, A. A., Travassos, M. A., Adams, M., Strauss, K. A., Shrestha, B., Levine, M. M., Edelman, R., & Lyke, K. E. (2019). The controlled human malaria infection experience at the University of Maryland. *American Journal of Tropical Medicine and Hygiene*, 100(3), 556–565. <https://doi.org/10.4269/ajtmh.18-0476>
- Fruh, K., Doumbo, O., Muller, H. M., Koita, O., McBride, J., Crisanti, A., Toure, Y., & Bujard, H. (1991). Human antibody response to the major merozoite surface antigen of *Plasmodium falciparum* is strain specific and short-lived. *Infection and Immunity*, 59(4), 1319–1324. <https://doi.org/10.1128/iai.59.4.1319-1324.1991>
- Galinski, M. R., Lapp, S. A., Peterson, M. S., Ay, F., Joyner, C. J., Le Roch, K. G., Fonseca, L. L., & Voit, E. O. (2018). *Plasmodium knowlesi*: A superb in vivo nonhuman primate model of antigenic variation in malaria. *Parasitology*, 145(1), 85–100. <https://doi.org/10.1017/S0031182017001135>
- Gamain, B., Miller, L. H., & Baruch, D. I. (2001). The surface variant antigens of *Plasmodium falciparum* contain cross-reactive epitopes. *Proceedings of the National Academy of Sciences of the United States of America*, 98(5), 2664–2669. <https://doi.org/10.1073/pnas.041602598>
- Gardner, M. J., Hall, N., Fung, E., White, O., Berriman, M., Hyman, R. W., Carlton, J. M., Pain, A., Nelson, K. E., Bowman, S., Paulsen, I. T., James, K., Eisen, J. A., Rutherford, K., Salzberg, S. L., Craig, A., Kyes, S., Chan, M. S., Nene, V., ... Barrell, B. (2002). Genome sequence of the human malaria parasite *Plasmodium falciparum*. *Nature*, 419(6906), 498–511. <https://doi.org/10.1038/nature01097>
- Gardner, M. J., Tettelin, H., Carucci, D. J., Cummings, L. M., Aravind, L., Koonin, E. V., Shallom, S., Mason, T., Yu, K., Fujii, C., Pederson, J., Shen, K., Jing, J., Aston, C., Lai, Z., Schwartz, D. C., Perte, M., Salzberg, S., Zhou, L., ... Hoffman, S. L. (1998). Chromosome 2 Sequence of the Human Malaria Parasite *Plasmodium falciparum*. *Science*, 282(5391), 1126–1132. <https://doi.org/10.1126/science.282.5391.1126>
- Garnham, P. C. C. of S. and T. (1981). The myth of quartan malaria. *Transactions of The Royal Society of Tropical Medicine and Hygiene, Volume 75, Issue 4, 1981, Pages 616–617, 75(4)*.
- Gazzinelli, R. T., Kalantari, P., Fitzgerald, K. A., & Golenbock, D. T. (2014). Innate sensing of malaria parasites. *Nature Reviews Immunology*, 14(11), 744–757. <https://doi.org/10.1038/nri3742>
- Ghebrehiwet, B., & Peerschke, E. I. B. (1998). Structure and function of gC1q-R: A multiligand binding cellular protein. *Immunobiology*, 199(2), 225–238. [https://doi.org/10.1016/S0171-2985\(98\)80029-6](https://doi.org/10.1016/S0171-2985(98)80029-6)
- Ginsburg, H., Krugliak, M., Eidelman, O., & Ioav Cabantchik, Z. (1983). New permeability pathways induced in membranes of *Plasmodium falciparum* infected erythrocytes. *Molecular and Biochemical Parasitology*, 8(2), 177–190. [https://doi.org/10.1016/0166-6851\(83\)90008-7](https://doi.org/10.1016/0166-6851(83)90008-7)
- Giudice, G. Del, Dayal-Drager, R., McGregor, S. J., McLaughlin, G., Mendis, N., Lanka, S., Perrin, L., Centre, B. T., Hospital, C., Picq, J. J., Armees, S., Scaife, J. G., Wenner, T., Verhave, J. P., Wirth, D., & Health, T. (1988). Malaria diagnosis: Memorandum from a WHO Meeting. *Bulletin of the World Health Organization*, 66(5), 575–594.
- Goel, S., Palmkvist, M., Moll, K., Joannin, N., Lara, P., R Akhouri, R., Moradi, N., Öjemalm, K., Westman, M., Angeletti, D., Kjellin, H., Lehtiö, J., Blixt, O., Idestrom, L., Gahmberg, C. G., Storry, J. R., Hult, A. K., Olsson, M. L., Von Heijne, G., ... Wahlgren, M. (2015). RIFINs are adhesins implicated in severe *Plasmodium falciparum* malaria. *Nature Medicine*, 21(4), 314–321. <https://doi.org/10.1038/nm.3812>
- Goel, S., Valiyaveetil, M., Achur, R. N., Goyal, A., Mattei, D., Salanti, A., Trenholme, K. R., Gardiner, D. L., & Gowda, D. C. (2010). Dual stage synthesis and crucial role of cytoadherence-linked asexual gene 9 in the surface expression of malaria parasite var proteins. *Proceedings of the National Academy of Sciences of the United States of America*, 107(38), 16643–16648. <https://doi.org/10.1073/pnas.1002568107>
- Gonzales, S. J., Reyes, R. A., Braddom, A. E., Batugedara, G., Bol, S., & Bunnik, E. M. (2020). Naturally Acquired Humoral Immunity Against *Plasmodium falciparum* Malaria. *Frontiers in Immunology*, 11(October), 1–15. <https://doi.org/10.3389/fimmu.2020.594653>
- Harrison, T. E., Mørch, A. M., Felce, J. H., Sakoguchi, A., Reid, A. J., Arase, H., Dustin, M. L., & Higgins, M. K. (2020). Structural basis for RIFIN-mediated activation of LILRB1 in malaria. *Nature*, 587(7833), 309–312. <https://doi.org/10.1038/s41586-020-2530-3>
- Hassan, I., Kanoi, B. N., Nagaoka, H., Sattabongkot, J., Udomsangpetch, R., Tsuboi, T., & Takashima, E. (2023). High-Throughput Antibody Profiling Identifies Targets of Protective Immunity against *P. falciparum*

- Malaria in Thailand. *Biomolecules*, 13(8), 1–13. <https://doi.org/10.3390/biom13081267>
- Hawking, F., Wilson, M., & Kenneth, G. (1971). TRANSACTIONS OF THE ROYAL SOCIETY OF IN a. *Tropical Medicine*, 65(5), 549–559.
- Henry, B., Roussel, C., Carucci, M., Brousse, V., Ndour, P. A., & Buffet, P. (2020). The Human Spleen in Malaria: Filter or Shelter? *Trends in Parasitology*, 36(5), 435–446. <https://doi.org/10.1016/j.pt.2020.03.001>
- Hergott, D. E. B., Owalla, T. J., Staubus, W. J., Seilie, A. M., Chavtur, C., Balkus, J. E., Apio, B., Lema, J., Cemer, B., Akileng, A., Chang, M., Egwang, T. G., & Murphy, S. C. (2024). Assessing the daily natural history of asymptomatic Plasmodium infections in adults and older children in Katakwi, Uganda: a longitudinal cohort study. *The Lancet Microbe*, 5(1), e72–e80. [https://doi.org/10.1016/S2666-5247\(23\)00262-8](https://doi.org/10.1016/S2666-5247(23)00262-8)
- Hidalgo, J., Arriaga, P., & Concejo, B. A. (2020). Highly Infectious Diseases in Critical Care. *Highly Infectious Diseases in Critical Care*, 213–234. <https://doi.org/10.1007/978-3-030-33803-9>
- Hiller, L. N., Bhattacharjee, S., van Ooij, C., Liolios, K., Harrison, T., Lopez-Estraño, C., & Halder, K. (2007). A Host-Targeting Signal in Virulence Proteins Reveals a Secretome in Malaria Infection. *Science*, 6(1), 51–66. <http://repositorio.unan.edu.ni/2986/1/5624.pdf%0Ahttp://fiskal.kemenkeu.go.id/ejournal%0Ahttp://dx.doi.org/10.1016/j.cirp.2016.06.001%0Ahttp://dx.doi.org/10.1016/j.powtec.2016.12.055%0Ahttps://doi.org/10.1016/j.jifatique.2019.02.006%0Ahttps://doi.org/10.1>
- Hoeijmakers, W. A. M., Salcedo-Amaya, A. M., Smits, A. H., François, K. J., Treeck, M., Gilberger, T. W., Stunnenberg, H. G., & Bártfai, R. (2013). H2A.Z/H2B.Z double-variant nucleosomes inhabit the AT-rich promoter regions of the Plasmodium falciparum genome. *Molecular Microbiology*, 87(5), 1061–1073. <https://doi.org/10.1111/mmi.12151>
- Hollin, T., & Le Roch, K. G. (2020). From Genes to Transcripts, a Tightly Regulated Journey in Plasmodium. *Frontiers in Cellular and Infection Microbiology*, 10(December), 1–13. <https://doi.org/10.3389/fcimb.2020.618454>
- Horn, D. (2014). Antigenic variation in African trypanosomes. *Molecular and Biochemical Parasitology*, 195(2), 123–129. <https://doi.org/10.1016/j.molbiopara.2014.05.001>
- Horrocks, P., Pinches, R., Christodoulou, Z., Kyes, S. A., & Newbold, C. I. (2004). Variable var transition rates underlie antigenic variation in malaria. *Proceedings of the National Academy of Sciences of the United States of America*, 101(30), 11129–11134. <https://doi.org/10.1073/pnas.0402347101>
- Howland, S. W., Poh, C. M., Gun, S. Y., Claser, C., Malleret, B., Shastri, N., Ginhoux, F., Grotenbreg, G. M., & Rénia, L. (2013). Brain microvessel cross-presentation is a hallmark of experimental cerebral malaria. *EMBO Molecular Medicine*, 5(7), 984–999. <https://doi.org/10.1002/emmm.201202273>
- Hui, G., & Hashimoto, C. (2007). Plasmodium falciparum anti-MSP1-19 antibodies induced by MSP1-42 and MSP1-19 based vaccines differed in specificity and parasite growth inhibition in terms of recognition of conserved versus variant epitopes. *Vaccine*, 25(5), 948–956. <https://doi.org/10.1016/j.vaccine.2006.08.041>
- Hviid, L., Lopez-Perez, M., Larsen, M. D., & Vidarsson, G. (2022). No sweet deal: the antibody-mediated immune response to malaria. *Trends in Parasitology*, 38(6), 428–434. <https://doi.org/10.1016/j.pt.2022.02.008>
- Idro, R., Jenkins, N. E., & Newton, C. R. J. (2005). Pathogenesis, clinical features, and neurological outcome of cerebral malaria. *Lancet Neurology*, 4(12), 827–840. [https://doi.org/10.1016/S1474-4422\(05\)70247-7](https://doi.org/10.1016/S1474-4422(05)70247-7)
- Informal consultation organized by the Medicines for Malaria Venture and cosponsored by the World Health Organization. (2006). *METHODS AND TECHNIQUES ANTIMALARIAL DRUG EFFICACY: genotyping to identify parasite populations*. In: 29–31 May 2007, Amsterdam, The Netherlands. 5(1), 127.
- Jeffery G. M., Young M. D., Eyles D. E. 1956. The treatment of Plasmodium falciparum infection with chloroquine, with a note on infectivity to mosquitoes of primaquine- and pyrimethamine-treated cases. *Am. J. Hyg.* (London) 64:1–11
- Jensen, A. R.; Adams, Y.; Hviid, L. (2020). Cerebral Plasmodium falciparum malaria: The role of PfEMP1 in its pathogenesis and immunity, and PfEMP1-based vaccines to prevent it. *Immunological Reviews Wiley*, 293, 230–252.
- Jespersen, J. S., Wang, C. W., Mkumbaye, S. I., Minja, D. T., Petersen, B., Turner, L., Petersen, J. E., Lusingu, J. P., Theander, T. G., & Lavstsen, T. (2016a). Plasmodium falciparum var genes expressed in children with severe malaria encode CIDR α1 domains. *EMBO Molecular Medicine*, 8(8), 839–850. <https://doi.org/10.15252/emmm.201606188>
- Jeyaprasasam, N. K., Liew, J. W. K., Low, V. L., Wan-Sulaiman, W. Y., & Vythilingam, I. (2020). Plasmodium knowlesi infecting humans in southeast asia: What's next? *PLoS Neglected Tropical Diseases*, 14(12), 1–16. <https://doi.org/10.1371/journal.pntd.0008900>
- Joannin, N., Abhiman, S., Sonnhammer, E. L., & Wahlgren, M. (2008). Sub-grouping and sub-functionalization of the RIFIN multi-copy protein family. *BMC Genomics*, 9, 1–14. <https://doi.org/10.1186/1471-2164-9-19>
- Joice, R., Nilsson, S. K., Montgomery, J., Dankwa, S., Morahan, B., Seydel, K. B., Bertuccini, L., Alano, P., Kim, C., Duraisingh, M. T., Taylor, T. E., & Milner, D. A. (2014). Levels and changes of HDL cholesterol and apolipoprotein A-I in relation to risk of cardiovascular events among statin-treated patients; a meta-analysis. *Circulation*, 6(244), 1–16. <https://doi.org/10.1126/scitranslmed.3008882>
- Kaestli, M., Cortes, A., Lagog, M., Ott, M., & Beck, H. P. (2004). Longitudinal assessment of Plasmodium falciparum var gene transcription in naturally infected asymptomatic children in Papua New Guinea. *Journal of Infectious Diseases*, 189(10), 1942–1951. <https://doi.org/10.1086/383250>
- Kamau, E., Tolbert, L. D. S., Kortepeter, L., Pratt, M., Nyakoe, N., Muringo, L., Ogutu, B., Waitumbi, J. N., & Ockenhouse, C. F. (2011). Development of a highly sensitive genus-specific quantitative reverse

- transcriptase real-time PCR assay for detection and quantitation of plasmodium by amplifying RNA and DNA of the 18S rRNA genes. *Journal of Clinical Microbiology*, 49(8), 2946–2953. <https://doi.org/10.1128/JCM.00276-11>
- Kanoi, B. N., Nagaoka, H., Morita, M., White, M. T., Palacpac, N. M. Q., Ntege, E. H., Balikagala, B., Yeka, A., Egwang, T. G., Horii, T., Tsuboi, T., & Takashima, E. (2018a). Comprehensive analysis of antibody responses to *Plasmodium falciparum* erythrocyte membrane protein 1 domains. *Vaccine*, 36(45), 6826–6833. <https://doi.org/10.1016/j.vaccine.2018.08.058>
- Kanoi, B. N., Nagaoka, H., White, M. T., Morita, M., Palacpac, N. M. Q., Ntege, E. H., Balikagala, B., Yeka, A., Egwang, T. G., Horii, T., Tsuboi, T., & Takashima, E. (2020). Global Repertoire of Human Antibodies Against *Plasmodium falciparum* RIFINs, SURFINs, and STEVORs in a Malaria Exposed Population. *Frontiers in Immunology*, 11(May). <https://doi.org/10.3389/fimmu.2020.00893>
- Kapelski, S., Klockenbring, T., Fischer, R., Barth, S., & Fendel, R. (2014). Assessment of the neutrophilic antibody-dependent respiratory burst (ADRB) response to *Plasmodium falciparum*. *Journal of Leukocyte Biology*, 96(6), 1131–1142. <https://doi.org/10.1189/jlb.4a0614-283rr>
- Kapulu, M. C., Kimani, D., Njuguna, P., Hamaluba, M., Otieno, E., Kimathi, R., Tuju, J., Sim, B. K. L., Abdi, A. I., Abebe, Y., Bejon, P., Billingsley, P. F., Bull, P. C., de Laurent, Z., Hoffman, S. L., James, E. R., Kariuki, S., Kinyanjui, S., Kivisi, C., ... Williams, T. N. (2022). Controlled human malaria infection (CHMI) outcomes in Kenyan adults is associated with prior history of malaria exposure and anti-schizont antibody response. *BMC Infectious Diseases*, 22(1), 1–10. <https://doi.org/10.1186/s12879-022-07044-8>
- Kar, N. P., Kumar, A., Singh, O. P., Carlton, J. M., & Nanda, N. (2014). A review of malaria transmission dynamics in forest ecosystems. *Parasites and Vectors*, 7(1), 1–12. <https://doi.org/10.1186/1756-3305-7-265>
- Kaul, D. K., Roth, E. F., Nagel, R. L., Howard, R. J., & Handunnetti, S. M. (1991). Resetting of *Plasmodium falciparum*-infected red blood cells with uninfected red blood cells enhances microvascular obstruction under flow conditions. *Blood*, 78(3), 812–819. <https://doi.org/10.1182/blood.v78.3.812.bloodjournal783812>
- Kibwana, E., Kapulu, M., & Bejon, P. (2022). *Controlled Human Malaria Infection Studies in Africa – Past, Present, and Future*. https://doi.org/10.1007/82_2022_256
- Kimingi, H. W., Kinyua, A. W., Achieng, N. A., Wambui, K. M., Mwangi, S., Nguti, R., Kivisi, C. A., Jensen, A. T. R., Bejon, P., Kapulu, M. C., Abdi, A. I., & Kinyanjui, S. M. (2022). Breadth of Antibodies to *Plasmodium falciparum* Variant Surface Antigens Is Associated With Immunity in a Controlled Human Malaria Infection Study. *Frontiers in Immunology*, 13(May), 1–10. <https://doi.org/10.3389/fimmu.2022.894770>
- Knuepfer, E., Rug, M., Klonis, N., Tilley, L., & Cowman, A. F. (2005). Trafficking of the major virulence factor to the surface of transfected *P. falciparum*-infected erythrocytes. *Blood*, 105(10), 4078–4087. <https://doi.org/10.1182/blood-2004-12-4666>
- Kraemer, S. M., & Smith, J. D. (2003). Evidence for the importance of genetic structuring to the structural and functional specialization of the *Plasmodium falciparum* var gene family. *Molecular Microbiology*, 50(5), 1527–1538. <https://doi.org/10.1046/j.1365-2958.2003.03814.x>
- Krause, D. R., Gattton, M. L., Frankland, S., Eisen, D. P., Good, M. F., Tilley, L., & Cheng, Q. (2007). Characterization of the antibody response against *Plasmodium falciparum* erythrocyte membrane protein 1 in human volunteers. *Infection and Immunity*, 75(12), 5967–5973. <https://doi.org/10.1128/IAI.00327-07>
- Krief, S., Escalante, A. A., Pacheco, M. A., Mugisha, L., André, C., Halbwax, M., Fischer, A., Krief, J. M., Kasenene, J. M., Crandfield, M., Cornejo, O. E., Chavatte, J. M., Lin, C., Letourneur, F., Grüner, A. C., McCutchan, T. F., Rénia, L., & Snounou, G. (2010). On the diversity of malaria parasites in African apes and the origin of *Plasmodium falciparum* from bonobos. *PLoS Pathogens*, 6(2). <https://doi.org/10.1371/journal.ppat.1000765>
- Kwak, J. D., Young, J. J., Stuij, A. C., Koelewijn, R., van Hellemond, J. J., & van Genderen, P. J. J. (2021). A comparative study of *Plasmodium falciparum* histidine-rich protein 2 (PfHRP2) blood levels and peripheral blood parasitemia as parameters of disease severity in individuals with imported falciparum malaria. *Travel Medicine and Infectious Disease*, 42(April), 102076. <https://doi.org/10.1016/j.tmaid.2021.102076>
- Kyeremeh, R., Antwi-Baffour, S., Annani-Akollor, M., Adjei, J. K., Addai-Mensah, O., & Frempong, M. (2020). Comediation of Erythrocyte Haemolysis by Erythrocyte-Derived Microparticles and Complement during Malaria Infection. *Advances in Hematology*, 2020. <https://doi.org/10.1155/2020/1640480>
- Kyes, S. A., Christodoulou, Z., Raza, A., Horrocks, P., Pinches, R., Rowe, J. A., & Newbold, C. I. (2003). A well-conserved *Plasmodium falciparum* var gene shows an unusual stage-specific transcript pattern. *Molecular Microbiology*, 48(5), 1339–1348. <https://doi.org/10.1046/j.1365-2958.2003.03505.x>
- Kyes, S. A., Kraemer, S. M., & Smith, J. D. (2007). Antigenic variation in *Plasmodium falciparum*: Gene organization and regulation of the var multigene family. In *Eukaryotic Cell* (Vol. 6, Issue 9, pp. 1511–1520). <https://doi.org/10.1128/EC.00173-07>
- Langhorne, J., Ndungu, F. M., Sponaas, A. M., & Marsh, K. (2008). Immunity to malaria: More questions than answers. *Nature Immunology*, 9(7), 725–732. <https://doi.org/10.1038/nif.205>
- Lau, C. K. Y., Turner, L., Jespersen, J. S., Lowe, E. D., Petersen, B., Wang, C. W., Petersen, J. E. V., Lusingu, J., Theander, T. G., Lavstsen, T., & Higgins, M. K. (2015). Structural conservation despite huge sequence diversity allows EPCR binding by the pfemp1 family implicated in severe childhood malaria. *Cell Host and Microbe*, 17(1), 118–129. <https://doi.org/10.1016/j.chom.2014.11.007>
- Laurens, M. B. (2019). RTS,S/AS01 vaccine (Mosquirix™): an overview. *Human Vaccines and Immunotherapeutics*. <https://doi.org/10.1080/21645515.2019.1669415>
- Laurens, M. B., Berry, A. A., Travassos, M. A., Strauss, K., Adams, M., Shrestha, B., Li, T., Eappen, A., Manoj, A.,

- Abebe, Y., Murshedkar, T., Gunasekera, A., Richie, T. L., Lyke, K. E., Plowe, C. V., Kennedy, J. K., Potter, G. E., Deye, G. A., Sim, B. K. L., & Hoffman, S. L. (2019). Dose-Dependent Infectivity of Aseptic, Purified, Cryopreserved *Plasmodium falciparum* 7G8 Sporozoites in Malaria-Naive Adults. *Journal of Infectious Diseases*, 220(12), 1962–1966. <https://doi.org/10.1093/infdis/jiz410>
- Lavazec, C., Sanyal, S., & Templeton, T. J. (2006). Hypervariability within the Rifin, Stevor and Pfmc-2TM superfamilies in *Plasmodium falciparum*. *Nucleic Acids Research*, 34(22), 6696–6707. <https://doi.org/10.1093/nar/gkl942>
- Lavstsen, T., Magistrado, P., Hermesen, C. C., Salanti, A., Jensen, A. T. R., Sauerwein, R., Hviid, L., Theander, T. G., & Staalsoe, T. (2005). Expression of *Plasmodium falciparum* erythrocyte membrane protein 1 in experimentally infected humans. *Malaria Journal*, 4, 1–9. <https://doi.org/10.1186/1475-2875-4-21>
- Lavstsen, T., Salanti, A., Jensen, A. T. R., Arnot, D. E., & Theander, T. G. (2003). Sub-grouping of *Plasmodium falciparum* 3D7 var genes based on sequence analysis of coding and non-coding regions. *Malaria Journal*, 2(27), 1–14. <https://doi.org/10.1073/pnas.80.16.5075>
- Lee, W. C., Russell, B., & Rénia, L. (2019). Sticking for a cause: The falciparum malaria parasites cytoadherence paradigm. *Frontiers in Immunology*, 10(JUN), 1–15. <https://doi.org/10.3389/fimmu.2019.01444>
- Lell, B., & McCall, M. (2018). Clinical Trial Protocol Repeat direct venous inoculation of *Plasmodium falciparum* sporozoites, strain NF54 and clone 7G8, in healthy adult volunteers naturally exposed to malaria in Gabon: a randomized open-label study L2. In *Clinical Trial Protocol L2*.
- Lell, B., Mordmüller, B., Agobe, J. C. D., Honkpehedji, J., Zinsou, J., Boex Mengue, J., Loembe, M. M., Adegnika, A. A., Held, J., Lalremruata, A., Nguyen, T. T., Esen, M., Natasha, K. C., Ruben, A. J., Chakravarty, S., Sim, B. K. L., Billingsley, P. F., James, E. R., Richie, T. L., ... Kremsner, P. G. (2018). Impact of sickle cell trait and naturally acquired immunity on uncomplicated malaria after controlled human malaria infection in adults in Gabon. *American Journal of Tropical Medicine and Hygiene*, 98(2), 508–515. <https://doi.org/10.4269/ajtmh.17-0343>
- Lennartz, F., Bengtsson, A., Olsen, R. W., Joergensen, L., Brown, A., Remy, L., Man, P., Forest, E., Barfod, L. K., Adams, Y., Higgins, M. K., & Jensen, A. T. R. (2015). Mapping the Binding Site of a Cross-Reactive *Plasmodium falciparum* PfEMP1 Monoclonal Antibody Inhibitory of ICAM-1 Binding. *The Journal of Immunology*, 195(7), 3273–3283. <https://doi.org/10.4049/jimmunol.1501404>
- Lenz, T., Zhang, X., Charkraborty, A., Ardakany, A. R., Prudhomme, J., Ay, F., Deitsch, K., & Le Roch, K. G. (2024). Chromatin structure and var2csa – a tango in regulation of var gene expression in the human malaria parasite, *Plasmodium falciparum*? Chromatin structure and var2csa regulate var gene expression. *BioRxiv*.
- Liao, Y., Smyth, G. K., & Shi, W. (2013). The Subread aligner: Fast, accurate and scalable read mapping by seed-and-vote. *Nucleic Acids Research*, 41(10). <https://doi.org/10.1093/nar/gkt214>
- Liao, Y., Smyth, G. K., & Shi, W. (2019). The R package Rsubread is easier, faster, cheaper and better for alignment and quantification of RNA sequencing reads. *Nucleic Acids Research*, 47(8). <https://doi.org/10.1093/nar/gkz114>
- Looker, O., Blanch, A. J., Liu, B., Nunez-Iglesias, J., McMillan, P. J., Tilley, L., & Dixon, M. W. A. (2019). The knob protein KAHRP assembles into a ring-shaped structure that underpins virulence complex assembly. *PLoS Pathogens*, 15(5), 1–26. <https://doi.org/10.1371/journal.ppat.1007761>
- López-Barragán, M. J., Lemieux, J., Quiñones, M., Williamson, K. C., Molina-Cruz, A., Cui, K., Barillas-Mury, C., Zhao, K., & Su, X. zhuan. (2011). Directional gene expression and antisense transcripts in sexual and asexual stages of *Plasmodium falciparum*. *BMC Genomics*, 12. <https://doi.org/10.1186/1471-2164-12-587>
- Lopez-Rubio, J. J., Gontijo, A. M., Nunes, M. C., Issar, N., Hernandez Rivas, R., & Scherf, A. (2007). 5' Flanking Region of Var Genes Nucleate Histone Modification Patterns Linked To Phenotypic Inheritance of Virulence Traits in Malaria Parasites. *Molecular Microbiology*, 66(6), 1296–1305. <https://doi.org/10.1111/j.1365-2958.2007.06009.x>
- Lopez-Rubio, J. J., Mancio-Silva, L., & Scherf, A. (2009). Genome-wide Analysis of Heterochromatin Associates Clonally Variant Gene Regulation with Perinuclear Repressive Centers in Malaria Parasites. *Cell Host and Microbe*, 5(2), 179–190. <https://doi.org/10.1016/j.chom.2008.12.012>
- Lubiana, P., Bouws, P., Roth, L. K., Dörpinghaus, M., Rehn, T., Brehmer, J., Wichers, J. S., Bachmann, A., Höhn, K., Roeder, T., Thye, T., Gutschmann, T., Burmester, T., Bruchhaus, I., & Metwally, N. G. (2020). Adhesion between *P. falciparum* infected erythrocytes and human endothelial receptors follows alternative binding dynamics under flow and febrile conditions. *Scientific Reports*, 10(1), 1–14. <https://doi.org/10.1038/s41598-020-61388-2>
- MacGregor, P., Szöo'R, B., Savill, N. J., & Matthews, K. R. (2012). Trypanosomal immune evasion, chronicity and transmission: An elegant balancing act. *Nature Reviews Microbiology*, 10(6), 431–438. <https://doi.org/10.1038/nrmicro2779>
- Mackenzie, G., Jensen, R. W., Lavstsen, T., & Otto, T. D. (2022). Varia: a tool for prediction, analysis and visualisation of variable genes. *BMC Bioinformatics*, 23(1). <https://doi.org/10.1186/s12859-022-04573-6>
- Magallón-Tejada, A., Machevo, S., Cisteró, P., Lavstsen, T., Aide, P., Rubio, M., Jiménez, A., Turner, L., Valmaseda, A., Gupta, H., De Las Salas, B., Mandomando, I., Wang, C. W., Petersen, J. E. V., Muñoz, J., Gascón, J., Macete, E., Alonso, P. L., Chitnis, C. E., ... Mayor, A. (2016). Cytoadhesion to gC1qR through *Plasmodium falciparum* Erythrocyte Membrane Protein 1 in Severe Malaria. *PLoS Pathogens*, 12(11), 1–22. <https://doi.org/10.1371/journal.ppat.1006011>

- Maier, A. G., Rug, M., O'Neill, M. T., Brown, M., Chakravorty, S., Szesztak, T., Chesson, J., Wu, Y., Hughes, K., Coppel, R. L., Newbold, C., Beeson, J. G., Craig, A., Crabb, B. S., & Cowman, A. F. (2008). Exported Proteins Required for Virulence and Rigidity of Plasmodium falciparum-Infected Human Erythrocytes. *Cell*, 134(1), 48–61. <https://doi.org/10.1016/j.cell.2008.04.051>
- Marti, M., Good, R. T., Rug, M., Knuepfer, E., & Cowman, A. F. (2004). Targeting Malaria Virulence and Remodeling Proteins to the Host Erythrocyte. *Science*, 306, 1930–1933. <http://repositorio.unan.edu.ni/2986/1/5624.pdf%0Ahttp://fiskal.kemenkeu.go.id/ejournal%0Ahttp://dx.doi.org/10.1016/j.cirp.2016.06.001%0Ahttp://dx.doi.org/10.1016/j.powtec.2016.12.055%0Ahttps://doi.org/10.1016/j.ijfatigue.2019.02.006%0Ahttps://doi.org/10.1>
- Mastrokolias, A., den Dunnen, J. T., van Ommen, G. J. B., 't Hoen, P. A. C., & van Roon-Mom, W. M. C. (2012). Increased sensitivity of next generation sequencing-based expression profiling after globin reduction in human blood RNA. *BMC Genomics*, 13(1). <https://doi.org/10.1186/1471-2164-13-28>
- Mauri, M., Elli, T., Caviglia, G., Ubaldi, G., & Azzi, M. (2017). RAWGraphs: A visualisation platform to create open outputs. *ACM International Conference Proceeding Series, Part F1313*. <https://doi.org/10.1145/3125571.3125585>
- McCulloch, R., Cobbold, C. A., Figueiredo, L., Jackson, A., Morrison, L. J., Mugnier, M. R., Papavasiliou, N., Schnauffer, A., & Matthews, K. (2017). Emerging challenges in understanding trypanosome antigenic variation. *Emerging Topics in Life Sciences*, 1(6), 585–592. <https://doi.org/10.1042/ETLS20170104>
- McRobert, L., Preiser, P., Sharp, S., Jarra, W., Kaviratne, M., Taylor, M. C., Renia, L., & Sutherland, C. J. (2004). Distinct trafficking and localization of STEVOR proteins in three stages of the Plasmodium falciparum life cycle. *Infection and Immunity*, 72(11), 6597–6602. <https://doi.org/10.1128/IAI.72.11.6597-6602.2004>
- Mebius, R. E., & Kraal, G. (2005). Structure and function of the spleen. *Nature Reviews Immunology*, 5(8), 606–616. <https://doi.org/10.1038/nri1669>
- Melé, M., Ferreira, P. G., Reverter, F., DeLuca, D. S., Monlong, J., Sammeth, M., Young, T. R., Goldmann, J. M., Pervouchine, D. D., Sullivan, T. J., Johnson, R., Segrè, A. V., Djebali, S., Niarchou, A., Wright, F. A., Lappalainen, T., Calvo, M., Getz, G., Dermitzakis, E. T., ... Guigó, R. (2015). The human transcriptome across tissues and individuals. *Science*, 348(6235), 660–665. <https://doi.org/10.1126/science.aaa0355>
- Menendez, C., Ordi, J., Ismail, M. R., Ventura, P. J., Aponte, J. J., Kahigwa, E., Font, F., & Alonso, P. L. (2000). The impact of placental malaria on gestational age and birth weight. *Journal of Infectious Diseases*, 181(5), 1740–1745. <https://doi.org/10.1086/315449>
- Michel-Todó, L., Bancells, C., Casas-Vila, N., Rovira-Graells, N., Hernández-Ferrer, C., González, J. R., & Cortés, A. (2023). Patterns of Heterochromatin Transitions Linked to Changes in the Expression of Plasmodium falciparum Clonally Variant Genes. *Microbiology Spectrum*, 11(1). <https://doi.org/10.1128/spectrum.03049-22>
- Miller, L. (1994). Malaria pathogenesis. *Science*, 264(5167), 1878–1883. <https://doi.org/10.1101/cshperspect.a025569>
- Milne, K., Ivens, A., Reid, A. J., Lotkowska, M. E., O'toole, A., Sankaranarayanan, G., Sandoval, D. M., Nahrendorf, W., Regnault, C., Edwards, N. J., Silk, S. E., Payne, R. O., Minassian, A. M., Venkatraman, N., Sanders, M. J., Hill, A. V. S., Barrett, M., Berriman, M., Draper, S. J., ... Spence, P. J. (2021). Mapping immune variation and var gene switching in naive hosts infected with plasmodium falciparum. *ELife*, 10. <https://doi.org/10.7554/eLife.62800>
- Minkah, N. K., & Kappe, S. H. I. (2021). Malaria vaccine gets a parasite boost in the liver. *Nature*, 595, 173–174. <https://www.who.int/publications/i/item/9789240015791>
- Moll, K., Pettersson, F., Vogt, A. M., Jonsson, C., Rasti, N., Ahuja, S., Spångberg, M., Mercereau-Puijalon, O., Arnot, D. E., Wahlgren, M., & Chen, Q. (2007). Generation of cross-protective antibodies against Plasmodium falciparum sequestration by immunization with an erythrocyte membrane protein 1-duffy binding-like 1α domain. *Infection and Immunity*, 75(1), 211–219. <https://doi.org/10.1128/IAI.00749-06>
- Mordmüller, B., Sulyok, Z., Sulyok, M., Molnar, Z., Lalremruata, A., Calle, C. L., Bayon, P. G., Esen, M., Gmeiner, M., Held, J., Heimann, H. L., Woldearegai, T. G., Ibáñez, J., Flügge, J., Fendel, R., Kreidenweiss, A., Kc, N., Murshedkar, T., Chakravarty, S., ... Kremsner, P. G. (2022). A PfSPZ vaccine immunization regimen equally protective against homologous and heterologous controlled human malaria infection. *Npj Vaccines*, 7(1), 1–9. <https://doi.org/10.1038/s41541-022-00510-z>
- Mordmüller, B., Supan, C., Sim, K. L., Gómez-Pérez, G. P., Ospina Salazar, C. L., Held, J., Bolte, S., Esen, M., Tschan, S., Joanny, F., Lamsfus Calle, C., Löhr, S. J. Z., Lalremruata, A., Gunasekera, A., James, E. R., Billingsley, P. F., Richman, A., Chakravarty, S., Legarda, A., ... Kremsner, P. G. (2015). Direct venous inoculation of Plasmodium falciparum sporozoites for controlled human malaria infection: A dose-finding trial in two centres. *Malaria Journal*, 14(1). <https://doi.org/10.1186/s12936-015-0628-0>
- Mordmüller, B., Surat, G., Lagler, H., Chakravarty, S., Ishizuka, A. S., Lalremruata, A., Gmeiner, M., Campo, J. J., Esen, M., Ruben, A. J., Held, J., Calle, C. L., Mengue, J. B., Gebru, T., Ibáñez, J., Sulyok, M., James, E. R., Billingsley, P. F., Natasha, K., ... Kremsner, P. G. (2017). Sterile protection against human malaria by chemoattenuated PfSPZ vaccine. *Nature*, 542(7642), 445–449. <https://doi.org/10.1038/nature21060>
- Moser, K. A., Drábek, E. F., Dwivedi, A., Stucke, E. M., Crabtree, J., Dara, A., Shah, Z., Adams, M., Li, T., Rodrigues, P. T., Koren, S., Phillippy, A. M., Munro, J. B., Ouattara, A., Sparklin, B. C., Dunning Hotopp, J. C., Lyke, K. E., Sadzewicz, L., Tallon, L. J., ... Silva, J. C. (2020). Strains used in whole organism Plasmodium falciparum vaccine trials differ in genome structure, sequence, and immunogenic potential.

- Genome Medicine*, 12(1), 1–17. <https://doi.org/10.1186/s13073-019-0708-9>
- Musasia, F. K., Nkumama, I. N., Frank, R., Kipkemboi, V., Schneider, M., Mwai, K., Odera, D. O., Rosenkranz, M., Fürle, K., Kimani, D., Tuju, J., Njuguna, P., Hamaluba, M., Kapulu, M. C., Wardemann, H., Abdi, A. I., Abebe, Y., Bejon, P., Billingsley, P. F., ... Osier, F. H. A. (2022). Phagocytosis of *Plasmodium falciparum* ring-stage parasites predicts protection against malaria. *Nature Communications*, 13(1), 1–12. <https://doi.org/10.1038/s41467-022-31640-6>
- Nag, S., Dalgaard, M. D., Kofoed, P. E., Ursing, J., Crespo, M., Andersen, L. O. B., Aarestrup, F. M., Lund, O., & Alifrangis, M. (2017). High throughput resistance profiling of *Plasmodium falciparum* infections based on custom dual indexing and Illumina next generation sequencing-technology. *Scientific Reports*, 7(1), 1–13. <https://doi.org/10.1038/s41598-017-02724-x>
- Nalinya, S., Musoke, D., & Deane, K. (2022). Malaria prevention interventions beyond long-lasting insecticidal nets and indoor residual spraying in low- and middle-income countries: a scoping review. *Malaria Journal*, 21(1), 1–13. <https://doi.org/10.1186/s12936-022-04052-6>
- Nasamu, A. S., Polino, A. J., Istvan, E. S., & Goldberg, D. E. (2020). Malaria parasite plasmepsins: More than just plain old degradative pepsins. *Journal of Biological Chemistry*, 295(25), 8425–8441. <https://doi.org/10.1074/jbc.REV120.009309>
- Nash, G., O'Brien, E., Gordon-Smith, E., & Dormandy, J. (1989). Abnormalities in the mechanical properties of red blood cells caused by *Plasmodium falciparum*. *Blood*, 74(2), 855–861. <https://doi.org/10.1182/blood.v74.2.855.855>
- Niang, M., Bei, A. K., Madnani, K. G., Pelly, S., Dankwa, S., Kanjee, U., Gunalan, K., Amaladoss, A., Yeo, K. P., Bob, N. S., Malleret, B., Duraisingh, M. T., & Preiser, P. R. (2014). STEVOR is a *Plasmodium falciparum* erythrocyte binding protein that mediates merozoite invasion and rosetting. *Cell Host and Microbe*, 16(1), 81–93. <https://doi.org/10.1016/j.chom.2014.06.004>
- Noble, R., Christodoulou, Z., Kyes, S., Pinches, R., Newbold, C. I., & Recker, M. (2013). The antigenic switching network of *Plasmodium falciparum* and its implications for the immuno-epidemiology of malaria. *eLife*, 2(13), 1–19. <https://doi.org/10.7554/eLife.01074>
- Nyarko, P. B., & Claessens, A. (2021). Understanding Host–Pathogen–Vector Interactions with Chronic Asymptomatic Malaria Infections. *Trends in Parasitology*, 37(3), 195–204. <https://doi.org/10.1016/j.pt.2020.09.017>
- O'Connell, M. J., Krien, M. J. E., & Hunter, T. (2003). Never say never. The NIMA-related protein kinases in mitotic control. *Trends in Cell Biology*, 13(5), 221–228. [https://doi.org/10.1016/S0962-8924\(03\)00056-4](https://doi.org/10.1016/S0962-8924(03)00056-4)
- Okell, L. C., Ghani, A. C., Lyons, E., & Drakeley, C. J. (2009). Submicroscopic infection in *Plasmodium falciparum*-endemic populations: A systematic review and meta-analysis. *Journal of Infectious Diseases*, 200(10), 1509–1517. <https://doi.org/10.1086/644781>
- Ortolan, L. S., Avril, M., Xue, J., Seydel, K. B., Zheng, Y., & Smith, J. D. (2022). *Plasmodium falciparum* Parasite Lines Expressing DC8 and Group A PfEMP1 Bind to Brain, Intestinal, and Kidney Endothelial Cells. *Frontiers in Cellular and Infection Microbiology*, 12(January), 1–10. <https://doi.org/10.3389/fcimb.2022.813011>
- Osier, F. H. A., Fegan, G., Polley, S. D., Murungi, L., Verra, F., Tetteh, K. K. A., Lowe, B., Mwangi, T., Bull, P. C., Thomas, A. W., Cavanagh, D. R., McBride, J. S., Lanar, D. E., Mackinnon, M. J., Conway, D. J., & Marsh, K. (2008). Breadth and magnitude of antibody responses to multiple *Plasmodium falciparum* merozoite antigens are associated with protection from clinical malaria. *Infection and Immunity*, 76(5), 2240–2248. <https://doi.org/10.1128/IAI.01585-07>
- Otto, T. D., Assefa, S. A., Böhme, U., Sanders, M. J., Kwiatkowski, D. P., Berriman, M., & Newbold, C. (2019a). Evolutionary analysis of the most polymorphic gene family in *Falciparum* malaria. *Wellcome Open Research*, 4, 1–29. <https://doi.org/10.12688/wellcomeopenres.15590.1>
- Oyola, S. O., Otto, T. D., Gu, Y., Maslen, G., Manske, M., Campino, S., Turner, D. J., MacInnis, B., Kwiatkowski, D. P., Swerdlow, H. P., & Quail, M. A. (2012). Optimizing illumina next-generation sequencing library preparation for extremely at-biased genomes. *BMC Genomics*, 13(1), 1. <https://doi.org/10.1186/1471-2164-13-1>
- Pandey, K. C., Singh, N., Arastu-Kapur, S., Bogyo, M., & Rosenthal, P. J. (2006). Falciparum, facilitates erythrocyte invasion. *PLoS Pathogens*, 2(11), 1031–1041. <https://doi.org/10.1371/journal.ppat.0020117>
- Petersen, J. E. V., Saelens, J. W., Freedman, E., Turner, L., Lavstsen, T., Fairhurst, R. M., Diakité, M., & Taylor, S. M. (2021). Sickletrait hemoglobin reduces adhesion to both CD36 and EPCR by *Plasmodium falciparum*-infected erythrocytes. *PLoS Pathogens*, 17(6). <https://doi.org/10.1371/journal.ppat.1009659>
- Petter, M., Bonow, I., & Klinkert, M. Q. (2008). Diverse expression patterns of subgroups of the rif multigene family during *Plasmodium falciparum* gametocytogenesis. *PLoS ONE*, 3(11). <https://doi.org/10.1371/journal.pone.0003779>
- Petter, M., Haeggström, M., Khattab, A., Fernandez, V., Klinkert, M. Q., & Wahlgren, M. (2007). Variant proteins of the *Plasmodium falciparum* RIFIN family show distinct subcellular localization and developmental expression patterns. *Molecular and Biochemical Parasitology*, 156(1), 51–61. <https://doi.org/10.1016/j.molbiopara.2007.07.011>
- Petter, M., Lee, C. C., Byrne, T. J., Boysen, K. E., Volz, J., Ralph, S. A., Cowman, A. F., Brown, G. V., & Duffy, M. F. (2011). Expression of *P. falciparum* var genes involves exchange of the histone variant H2A.Z at the promoter. *PLoS Pathogens*, 7(2). <https://doi.org/10.1371/journal.ppat.1001292>

- Petter, M., Selvarajah, S. A., Lee, C. C., Chin, W. H., Gupta, A. P., Bozdech, Z., Brown, G. V., & Duffy, M. F. (2013). H2A.Z and H2B.Z double-variant nucleosomes define intergenic regions and dynamically occupy var gene promoters in the malaria parasite *Plasmodium falciparum*. *Molecular Microbiology*, 87(6), 1167–1182. <https://doi.org/10.1111/mmi.12154>
- Pfaffl, M. W. (2004). Real-time RT-PCR: Neue Ansätze zur exakten mRNA Quantifizierung. *Biospektrum*, 01/04, 92–95.
- Plassmeyer, M. L., Reiter, K., Shimp, R. L., Kotova, S., Smith, P. D., Hurt, D. E., House, B., Zou, X., Zhang, Y., Hickman, M., Uchime, O., Herrera, R., Nguyen, V., Glen, J., Lebowitz, J., Jin, A. J., Miller, L. H., MacDonald, N. J., Wu, Y., & Narum, D. L. (2009). Structure of the *Plasmodium falciparum* circumsporozoite protein, a leading malaria vaccine candidate. *Journal of Biological Chemistry*, 284(39), 26951–26963. <https://doi.org/10.1074/jbc.M109.013706>
- Poespoprodjo, J. R., Douglas, N. M., Ansong, D., Kho, S., & Anstey, N. M. (2023). Malaria. *The Lancet*, 402(10419), 2328–2345. [https://doi.org/10.1016/S0140-6736\(23\)01249-7](https://doi.org/10.1016/S0140-6736(23)01249-7)
- Portugal, S., Tran, T. M., Ongoiba, A., Bathily, A., Li, S., Doumbo, S., Skinner, J., Doumtabe, D., Kone, Y., Sangala, J., Jain, A., Davies, D. H., Hung, C., Liang, L., Ricklefs, S., Homann, M. V., Felgner, P. L., Porcella, S. F., Färnert, A., ... Crompton, P. D. (2017). Treatment of chronic asymptomatic *Plasmodium falciparum* infection does not increase the risk of clinical malaria upon reinfection. *Clinical Infectious Diseases*, 64(5), 645–653. <https://doi.org/10.1093/cid/ciw849>
- Poti, K. E., Sullivan, D. J., Dondorp, A. M., & Woodrow, C. J. (2020). HRP2: Transforming Malaria Diagnosis, but with Caveats. *Trends in Parasitology*, 36(2), 112–126. <https://doi.org/10.1016/j.pt.2019.12.004>
- Prah, D. A., Dunican, C., Amoah, L. E., Marjaneh, M. M., Kaforou, M., Nordgren, A., Jones-Warner, W., Aniweh, Y., Awandare, G. ., & Cunington, A. J. (2023). Journal of Infection. *Journal Of Infection*, 87, 259–262. [https://www.journalofinfection.com/article/S0163-4453\(20\)30105-5/fulltext](https://www.journalofinfection.com/article/S0163-4453(20)30105-5/fulltext)
- Prudêncio, M., Rodriguez, A., & Mota, M. M. (2006). The silent path to thousands of merozoites: The *Plasmodium* liver stage. *Nature Reviews Microbiology*, 4(11), 849–856. <https://doi.org/10.1038/nrmicro1529>
- Quintana, M. del P., Ecklu-Mensah, G., Tcherniuk, S. O., Ditlev, S. B., Oleinikov, A. V., Hviid, L., & Lopez-Perez, M. (2019). Comprehensive analysis of Fc-mediated IgM binding to the *Plasmodium falciparum* erythrocyte membrane protein 1 family in three parasite clones. *Scientific Reports*, 9(1), 1–11. <https://doi.org/10.1038/s41598-019-42585-0>
- Rask, T. S., Hansen, D. A., Theander, T. G., Pedersen, A. G., & Lavstsen, T. (2010). *Plasmodium falciparum* erythrocyte membrane protein 1 diversity in seven genomes - divide and conquer. *PLoS Computational Biology*, 6(9). <https://doi.org/10.1371/journal.pcbi.1000933>
- Recker, M., Al-Bader, R., & Gupta, S. (2005). A mathematical model for a new mechanism of phenotypic variation in malaria. *Parasitology*, 131(2), 151–159. <https://doi.org/10.1017/S0031182005007481>
- Recker, M., Arinaminpathy, N., & Buckee, C. O. (2008). The effects of a partitioned var gene repertoire of *Plasmodium falciparum* on antigenic diversity and the acquisition of clinical immunity. *Malaria Journal*, 7, 1–11. <https://doi.org/10.1186/1475-2875-7-18>
- Recker, M., Buckee, C. O., Serazin, A., Kyes, S., Pinches, R., Christodoulou, Z., Springer, A. L., Gupta, S., & Newbold, C. I. (2011). Antigenic variation in *Plasmodium falciparum* malaria involves a highly structured switching pattern. *PLoS Pathogens*, 7(3). <https://doi.org/10.1371/journal.ppat.1001306>
- Recker, M., & Gupta, S. (2006). Conflicting immune responses can prolong the length of infection in *Plasmodium falciparum* malaria. *Bulletin of Mathematical Biology*, 68(4), 821–835. <https://doi.org/10.1007/s11538-005-9041-0>
- Recker, M., Nee, S., Bull, P. C., Kinyanjul, S., Marsh, K., Hewbold, C., & Gupta, S. (2004). Transient cross-reactive immune responses can orchestrate antigenic variation in malaria. *Nature*, 429(6991), 555–558. <https://doi.org/10.1038/nature02486>
- Reeder, J. C., Cowman, A. F., Davern, K. M., Beeson, J. G., Thompson, J. K., Rogerson, S. J., & Brown, G. V. (1999). The adhesion of *Plasmodium falciparum*-infected erythrocytes to chondroitin sulfate A is mediated by P. *falciparum* erythrocyte membrane protein 1. *Proceedings of the National Academy of Sciences of the United States of America*, 96(9), 5198–5202. <https://doi.org/10.1073/pnas.96.9.5198>
- Reyes, R. A., Raghavan, S. S. R., Hurlburt, N. K., Introini, V., Kana, I. H., Jensen, R. W., Martinez-Scholze, E., Gestal-Mato, M., Bau, C. B., Fernández-Quintero, M. L., Loeffler, J. R., Ferguson, J. A., Lee, W.-H., Martin, G. M., Theander, T. G., Ssewanyana, I., Feeney, M. E., Greenhouse, B., Bol, S., ... Lavstsen, T. (2024). Broadly inhibitory antibodies against severe malaria virulence proteins. *BioRxiv: The Preprint Server for Biology*, 1–36.
- Richard, D., MacRaild, C. A., Riglar, D. T., Chan, J. A., Foley, M., Baum, J., Ralph, S. A., Norton, R. S., & Cowman, A. F. (2010). Interaction between *Plasmodium falciparum* apical membrane antigen 1 and the rhoptry neck protein complex defines a key step in the erythrocyte invasion process of malaria parasites. *Journal of Biological Chemistry*, 285(19), 14815–14822. <https://doi.org/10.1074/jbc.M109.080770>
- Rivadeneira, E. M., Wassermann, M., & Espinal, C. T. (1983). Separation and Concentration of Schizonts of *Plasmodium falciparum* by Percoll Gradients. *The Journal of Protozoology*, 30(2), 185–456. <https://doi.org/10.1111/j.1550-7408.1983.tb02932.x>
- Robert, F., Ntoumi, F., Angel, G., Candito, D., Rogier, C., Fandeur, T., Sarthou, J. L., & Mercereau-Puijalon, O. (1996). Extensive genetic diversity of *Plasmodium falciparum* isolates collected from patients with severe malaria in Dakar, Senegal. *Transactions of the Royal Society of Tropical Medicine and Hygiene*, 90(6), 704–711. [https://doi.org/10.1016/S0035-9203\(96\)90446-0](https://doi.org/10.1016/S0035-9203(96)90446-0)

- Robinson, B. A., Welch, T. L., & Smith, J. D. (2003). Widespread functional specialization of Plasmodium falciparum erythrocyte membrane protein 1 family members to bind CD36 analysed across a parasite genome. *Molecular Microbiology*, 47(5), 1265–1278. <https://doi.org/10.1046/j.1365-2958.2003.03378.x>
- Rosenkranz, M., Nkumama, I. N., Ogwang, R., Kraker, S., Blickling, M., Mwai, K., Odera, D., Tuju, J., Fürle, K., Frank, R., Chepsat, E., & Kapulu, M. C. (2024). Full-length MSP1 is a major target of protective immunity after controlled human malaria infection. 7(8), 1–16. <https://doi.org/10.26508/lsa.202301910>
- Rossati, A., Bargiacchi, O., Kroumova, V., Zaramella, M., Caputo, A., & Garavelli, P. L. (2016). Climate, environment and transmission of malaria. *Infezioni in Medicina*, 24(2), 93–104.
- Rottmann, M., Lavstsen, T., Mugasa, J. P., Kaestli, M., Jensen, A. T. R., Müller, D., Theander, T., & Beck, H. P. (2006). Differential expression of var gene groups is associated with morbidity caused by Plasmodium falciparum infection in Tanzanian children. *Infection and Immunity*, 74(7), 3904–3911. <https://doi.org/10.1128/IAI.02073-05>
- Rovira-Graells, N., Gupta, A. P., Planet, E., Crowley, V. M., Mok, S., De Pouplana, L. R., Preiser, P. R., Bozdech, Z., & Cortés, A. (2012). Transcriptional variation in the malaria parasite Plasmodium falciparum. *Genome Research*, 22(5), 925–938. <https://doi.org/10.1101/gr.129692.111>
- Rubio, J. P., Thompson, J. K., & Cowman, A. F. (1996). The var genes of Plasmodium falciparum are located in the subtelomeric region of most chromosomes. *EMBO Journal*, 15(15), 4069–4077. <https://doi.org/10.1002/j.1460-2075.1996.tb00780.x>
- Rug, M., Prescott, S. W., Fernandez, K. M., Cooke, B. M., & Cowman, A. F. (2006). The role of KAHRP domains in knob formation and cytoadherence of P falciparum-infected human erythrocytes. *Blood*, 108(1), 370–378. <https://doi.org/10.1182/blood-2005-11-4624>
- Sahu, P. K., Duffy, F. J., Dankwa, S., Vishnyakova, M., Majhi, M., Pirpamer, L., Vigdorovich, V., Bage, J., Maharana, S., Mandala, W., Rogerson, S. J., Seydel, K. B., Taylor, T. E., Kim, K., Noah Sather, D., Mohanty, A., Mohanty, R. R., Mohanty, A., Pattnaik, R., ... Wassmer, S. C. (2021). Determinants of brain swelling in pediatric and adult cerebral malaria. *JCI Insight*, 6(18). <https://doi.org/10.1172/jci.insight.145823>
- Saito, F., Hirayasu, K., Satoh, T., Wang, C. W., Lusingu, J., Arimori, T., Shida, K., Palacpac, N. M. Q., Itagaki, S., Iwanaga, S., Takashima, E., Tsuboi, T., Kohyama, M., Suenaga, T., Colonna, M., Takagi, J., Lavstsen, T., Horii, T., & Arase, H. (2017). Immune evasion of Plasmodium falciparum by RIFIN via inhibitory receptors. *Nature*, 552(7683), 101–105. <https://doi.org/10.1038/nature24994>
- Salanti, A., Staalsoe, T., Lavstsen, T., Jensen, A. T. R., Sowa, M. P. K., Arnot, D. E., Hviid, L., & Theander, T. G. (2003). Selective upregulation of a single distinctly structured var gene in chondroitin sulphate A-adhering Plasmodium falciparum involved in pregnancy-associated malaria. *Molecular Microbiology*, 49(1), 179–191. <https://doi.org/10.1046/j.1365-2958.2003.03570.x>
- Salgado, C., Ayodo, G., Macklin, M. D., Gould, M. P., Nallandhighal, S., Odhiambo, E. O., Obala, A., O'Meara, W. P., John, C. C., & Tran, T. M. (2021). The prevalence and density of asymptomatic Plasmodium falciparum infections among children and adults in three communities of western Kenya. *Malaria Journal*, 20(1), 1–12. <https://doi.org/10.1186/s12936-021-03905-w>
- Sam-Yellowe, T. Y. (2009). The role of the Maurer's clefts in protein transport in Plasmodium falciparum. *Trends in Parasitology*, 25(6), 277–284. <https://doi.org/10.1016/j.pt.2009.03.009>
- Sauerwein, R. W., Roestenberg, M., & Moorthy, V. S. (2011). Experimental human challenge infections can accelerate clinical malaria vaccine development. *Nature Reviews Immunology*, 11(1), 57–64. <https://doi.org/10.1038/nri2902>
- Schofield, L., & Grau, G. E. (2005). Immunological processes in malaria pathogenesis. *Nature Reviews Immunology*, 5(9), 722–735. <https://doi.org/10.1038/nri1686>
- Sharma, L., & Shukla, G. (2017). Placental Malaria: A new insight into the pathophysiology. *Frontiers in Medicine*, 4(JUL), 1–6. <https://doi.org/10.3389/fmed.2017.00117>
- Shears, M. J., Nirujogi, R. S., Swearingen, K. E., Renuse, S., Mishra, S., Reddy, P. J., Moritz, R. L., Pandey, A., States, U., States, U., Seattle, N., & Park, I. T. (2020). HHS Public Access. 18(9), 3404–3418. <https://doi.org/10.1021/acs.jproteome.9b00324>
- Sheokand, P., Narwal, M., Thakur, V., & Mohammed, A. (2021). GlmS mediated knock-down of a phospholipase expedite alternate pathway to generate phosphocholine required for phosphatidylcholine synthesis in Plasmodium falciparum. *Biochemical Journal*, 478(18), 3429–3444. <https://doi.org/doi.org/10.1042/BCJ20200549>
- Silva, J. C., Dwivedi, A., Moser, K. A., Sissoko, M. S., Epstein, J. E., Healy, S. A., Lyke, K. E., Mordmüller, B., Kremsner, P. G., Duffy, P. E., Murshedkar, T., Sim, B. K. L., Richie, T. L., & Hoffman, S. L. (2022). Plasmodium falciparum 7G8 challenge provides conservative prediction of efficacy of PfNF54-based PfSPZ Vaccine in Africa. *Nature Communications*, 13(1), 1–9. <https://doi.org/10.1038/s41467-022-30882-8>
- Silverstein, R. L., & Febbraio, M. (2009). CD36, a Scavenger Receptor Involved in Immunity, Metabolism, Angiogenesis, and Behavior. *Science Signalling*, 2(72), 1–16. <https://doi.org/10.1126/scisignal.272re3>
- Singh, H., Madnani, K., Lim, Y. B., Cao, J., Preiser, P. R., & Lim, C. T. (2017). Expression dynamics and physiologically relevant functional study of STEVOR in asexual stages of Plasmodium falciparum infection. *Cellular Microbiology*, 19(6), 1–11. <https://doi.org/10.1111/cmi.12715>
- Singh, S., & Chitnis, C. E. (2012). Signalling mechanisms involved in apical organelle discharge during host cell invasion by apicomplexan parasites. *Microbes and Infection*, 14(10), 820–824. <https://doi.org/10.1016/j.micinf.2012.05.007>

- Smalley, M. E., Abdalla, S., & Brown, J. (1981). The distribution of plasmodium falciparum in the peripheral blood and bone marrow of gambian children. *Transactions of the Royal Society of Tropical Medicine and Hygiene*, 75(1), 103–105. [https://doi.org/10.1016/0035-9203\(81\)90019-5](https://doi.org/10.1016/0035-9203(81)90019-5)
- Smith, J. D., Rowe, J. A., Higgins, M. K., & Lavstsen, T. (2013). Malaria's deadly grip: Cytoadhesion of Plasmodium falciparum-infected erythrocytes. *Cellular Microbiology*, 15(12), 1976–1983. <https://doi.org/10.1111/cmi.12183>
- Spillman, N. J., Dalmia, V. K., & Goldberg, E. (2016). during Plasmodium falciparum Infection. 7(5), 1–13. <https://doi.org/10.1128/mBio.01538-16>
- Spring, M., Polhemus, M., & Ockenhouse, C. (2014). Controlled human malaria infection. *Journal of Infectious Diseases*, 209(SUPPL. 2). <https://doi.org/10.1093/infdis/jiu063>
- Spycher, C., Klonis, N., Spielmann, T., Kump, E., Steiger, S., Tilley, L., & Beck, H. P. (2003). MAHRP-1, a novel Plasmodium falciparum histidine-rich protein, binds ferriprotoporphyrin IX and localizes to the Maurer's clefts. *Journal of Biological Chemistry*, 278(37), 35373–35383. <https://doi.org/10.1074/jbc.M305851200>
- Spycher, C., Rug, M., Pachlatko, E., Hanssen, E., Ferguson, D., Cowman, A. F., Tilley, L., & Beck, H. P. (2008). The Maurer's cleft protein MAHRP1 is essential for trafficking of PfEMP1 to the surface of Plasmodium falciparum-infected erythrocytes. *Molecular Microbiology*, 68(5), 1300–1314. <https://doi.org/10.1111/j.1365-2958.2008.06235.x>
- Staalsoe, T., Hamad, A. A., Hviid, L., Elhassan, I. M., Arnot, D. E., & Theander, T. G. (2002). In vivo switching between variant surface antigens in human Plasmodium falciparum infection. *Journal of Infectious Diseases*, 186(5), 719–722. <https://doi.org/10.1086/342390>
- Stadler, E., Cromer, D., Ogunlade, S., Ongoiba, A., Doumbo, S., Kayentao, K., Traore, B., Crompton, P. D., Portugal, S., Davenport, M. P., & Khoury, D. S. (2023). Evidence for exposure dependent carriage of malaria parasites across the dry season: modelling analysis of longitudinal data. *Malaria Journal*, 22(1), 1–13. <https://doi.org/10.1186/s12936-023-04461-1>
- Stanisic, D. I., Fink, J., Mayer, J., Coghill, S., Gore, L., Liu, X. Q., El-Deeb, I., Rodriguez, I. B., Powell, J., Willemsen, N. M., De, S. L., Ho, M. F., Hoffman, S. L., Gerrard, J., & Good, M. F. (2018). Vaccination with chemically attenuated Plasmodium falciparum asexual blood-stage parasites induces parasite-specific cellular immune responses in malaria-naïve volunteers: A pilot study. *BMC Medicine*, 16(1), 1–16. <https://doi.org/10.1186/s12916-018-1173-9>
- Stucke, E. M., Niangaly, A., Berry, A. A., Bailey, J. A., Coulibaly, D., Ouattara, A., Lyke, K. E., Laurens, M. B., Dara, A., Adams, M., Pablo, J., Jasinskas, A., Nakajima, R., Zhou, A. E., Agrawal, S., Friedman-Klabanoff, D. A. J., Takala-Harrison, S., Kouriba, B., Kone, A. K., ... Travassos, M. A. (2019). Serologic responses to the PfEMP1 DBL-CIDR head structure may be a better indicator of malaria exposure than those to the DBL-α tag. *Malaria Journal*, 18(1), 1–8. <https://doi.org/10.1186/s12936-019-2905-9>
- Sulyok, Z., Fendel, R., Eder, B., Lorenz, F. R., Kc, N., Karnahl, M., Lalremruata, A., Nguyen, T. T., Held, J., Adjadi, F. A. C., Klockenbring, T., Flügge, J., Woldearegai, T. G., Lamsfus Calle, C., Ibáñez, J., Rodi, M., Egger-Adam, D., Kreidenweiss, A., Köhler, C., ... Kremsner, P. G. (2021a). Heterologous protection against malaria by a simple chemoattenuated PfSPZ vaccine regimen in a randomized trial. *Nature Communications*, 12(1), 1–10. <https://doi.org/10.1038/s41467-021-22740-w>
- Sutanto, I., Suprijanto, S., Kosasih, A., Dahlan, M. S., Syafruddin, D., Kusriastuti, R., Hawley, W. A., Lobo, N. F., & Ter Kuile, F. O. (2013). The effect of primaquine on gametocyte development and clearance in the treatment of uncomplicated falciparum malaria with dihydroartemisinin- piperazine in South Sumatra, Western Indonesia: An open-label, randomized, controlled trial. *Clinical Infectious Diseases*, 56(5), 685–693. <https://doi.org/10.1093/cid/cis959>
- Tadesse, F. G., Slater, H. C., Chali, W., Teelen, K., Lanke, K., Belachew, M., Menberu, T., Shumie, G., Shitaye, G., Okell, L. C., Graumans, W., Van Gemert, G. J., Kedir, S., Tesfaye, A., Belachew, F., Abebe, W., Mamo, H., Sauerwein, R., Balcha, T., ... Bousema, T. (2018). The Relative Contribution of Symptomatic and Asymptomatic Plasmodium vivax and Plasmodium falciparum Infections to the Infectious Reservoir in a Low-Endemic Setting in Ethiopia. *Clinical Infectious Diseases*, 66(12), 1883–1891. <https://doi.org/10.1093/cid/cix1123>
- Takashima, E., Kanoi, B. N., Nagaoka, H., Morita, M., Hassan, I., Palacpac, N. M. Q., Egwang, T. G., Horii, T., Gitaka, J., & Tsuboi, T. (2022). Meta-Analysis of Human Antibodies Against Plasmodium falciparum Variable Surface and Merozoite Stage Antigens. *Frontiers in Immunology*, 13(June), 1–11. <https://doi.org/10.3389/fimmu.2022.887219>
- Tan, M., Tiedje, K., Feng, Q., Zhan, Q., Pascual, M., Shim, H., Chan, Y., & Day, K. (2023). A paradoxical population structure of var DBLα 1 types in Africa. *BioRxiv*.
- Tham, W. H., Payne, P. D., Brown, G. V., & Rogerson, S. J. (2007). Identification of basic transcriptional elements required for rif gene transcription. *International Journal for Parasitology*, 37(6), 605–615. <https://doi.org/10.1016/j.ijpara.2006.11.006>
- Tibúrcio, M., Hitz, E., Niederwieser, I., Kelly, G., Davies, H., Doerig, C., Billker, O., Voss, T. S., & Treeck, M. (2021). A 39-Amino-Acid C-Terminal Truncation of GDV1 Disrupts Sexual Commitment in Plasmodium falciparum. *MSphere*, 6(3), 1–13. <https://doi.org/10.1128/msphere.01093-20>
- Tibúrcio, M., Niang, M., Deplaine, G., Perrot, S., Bischoff, E., Ndour, P. A., Silvestrini, F., Khattab, A., Milon, G., David, P. H., Hardeman, M., Vernick, K. D., Sauerwein, R. W., Preiser, P. R., Mercereau-Puijalon, O., Buffet, P., Alano, P., & Lavazec, C. (2012). A switch in infected erythrocyte deformability at the maturation and

- blood circulation of *Plasmodium falciparum* transmission stages. *Blood*, 119(24), 172–180.
<https://doi.org/10.1182/blood-2012-03-414557>
- Tompkins, A. M., & Ermert, V. (2013). A regional-scale, high resolution dynamical malaria model that accounts for population density, climate and surface hydrology. *Malaria Journal*, 12(1), 1–24.
<https://doi.org/10.1186/1475-2875-12-65>
- Tonkin-Hill, G. Q., Trianty, L., Noviyanti, R., Nguyen, H. H. T., Sebayang, B. F., Lampah, D. A., Marfurt, J., Cobbold, S. A., Rambhatla, J. S., McConville, M. J., Rogerson, S. J., Brown, G. V., Day, K. P., Price, R. N., Anstey, N. M., Papenfuss, A. T., & Duffy, M. F. (2018). The *Plasmodium falciparum* transcriptome in severe malaria reveals altered expression of genes involved in important processes including surface antigen-encoding var genes. *PLoS Biology*, 16(3). <https://doi.org/10.1371/journal.pbio.2004328>
- Tonkin, C. J., Carret, C. K., Duraisingh, M. T., Voss, T. S., Ralph, S. A., Hommel, M., Duffy, M. F., Da Silva, L. M., Scherf, A., Ivens, A., Speed, T. P., Beeson, J. G., & Cowman, A. F. (2009). Sir2 paralogs cooperate to regulate virulence genes and antigenic variation in *Plasmodium falciparum*. *PLoS Biology*, 7(4), 0771–0788.
<https://doi.org/10.1371/journal.pbio.1000084>
- Treutiger, C. J., Heddini, A., Fernandez, V., Muller, W. A., & Wahlgren, M. (1997). PECAM-1/CD31, an endothelial receptor for binding *Plasmodium falciparum*-infected erythrocytes. *Nature*, 387(6632), 1405–1408.
- Turner, L., Lavstsen, T., Berger, S. S., Wang, C. W., Petersen, J. E. V., Avril, M., Brazier, A. J., Freeth, J., Jespersen, J. S., Nielsen, M. A., Magistrado, P., Lusingu, J., Smith, J. D., Higgins, M. K., & Theander, T. G. (2013). Severe malaria is associated with parasite binding to endothelial protein C receptor. *Nature*, 498(7455), 502–505. <https://doi.org/10.1038/nature12216>
- Turner, L., Lavstsen, T., Mmbando, B. P., Wang, C. W., Magistrado, P. A., Vestergaard, L. S., Ishengoma, D. S., Minja, D. T. R., Lusingu, J. P., & Theander, T. G. (2015). IgG antibodies to endothelial protein C receptor-binding cysteine-rich interdomain region domains of *Plasmodium falciparum* erythrocyte membrane protein 1 are acquired early in life in individuals exposed to malaria. *Infection and Immunity*, 83(8), 3096–3103. <https://doi.org/10.1128/IAI.00271-15>
- Turner, L., Wang, C. W., Lavstsen, T., Mwakalinga, S. B., Sauerwein, R. W., Hermesen, C. C., & Theander, T. G. (2011). Antibodies against PfEMP1, RIFIN, MSP3 and GLURP are acquired during controlled *Plasmodium falciparum* malaria infections in naïve volunteers. *PLoS ONE*, 6(12), 1–8.
<https://doi.org/10.1371/journal.pone.0029025>
- Unwin, H. J. T., Sherrard-Smith, E., Churcher, T. S., & Ghani, A. C. (2023). Quantifying the direct and indirect protection provided by insecticide treated bed nets against malaria. *Nature Communications*, 14(1).
<https://doi.org/10.1038/s41467-023-36356-9>
- Vignali, M., Armour, C. D., Chen, J., Morrison, R., Castle, J. C., Biery, M. C., Bouzek, H., Moon, W., Babak, T., Fried, M., Raymond, C. K., & Duffy, P. E. (2011). NSR-seq transcriptional profiling enables identification of a gene signature of *Plasmodium falciparum* parasites infecting children. *Journal of Clinical Investigation*, 121(3), 1119–1129. <https://doi.org/10.1172/JCI43457>
- Voss, T. S., Healer, J., Marty, A. J., Duffy, M. F., Thompson, J. K., Beeson, J. G., Reeder, J. C., Crabb, B. S., & Cowman, A. F. (2006). A var gene promoter controls allelic exclusion of virulence genes in *Plasmodium falciparum* malaria. *Nature*, 439(7079), 1004–1008. <https://doi.org/10.1038/nature04407>
- Wahlgren, M., Goel, S., & Akhouri, R. R. (2017). Variant surface antigens of *Plasmodium falciparum* and their roles in severe malaria. *Nature Reviews Microbiology*, 15(8), 479–491.
<https://doi.org/10.1038/nrmicro.2017.47>
- Walker, I. S., & Rogerson, S. J. (2023). Pathogenicity and virulence of malaria: Sticky problems and tricky solutions. *Virulence*, 14(1). <https://doi.org/10.1080/21505594.2022.2150456>
- Wang, C. W., Lavstsen, T., Bengtsson, D. C., Magistrado, P. A., Berger, S. S., Marquard, A. M., Alifrangis, M., Lusingu, J. P., Theander, T. G., & Turner, L. (2012). Evidence for in vitro and in vivo expression of the conserved VAR3 (type 3) *plasmodium falciparum* erythrocyte membrane protein 1. *Malaria Journal*, 11, 1–11. <https://doi.org/10.1186/1475-2875-11-129>
- Warimwe, G. M., Fegan, G., Musyoki, J. N., Newton, C. R. J. C., Opiyo, M., Githinji, G., Andisi, C., Menza, F., Kitsao, B., Marsh, K., & Bull, P. C. (2012). Prognostic indicators of life-threatening malaria are associated with distinct parasite variant antigen profiles. *Science Translational Medicine*, 4(129).
<https://doi.org/10.1126/scitranslmed.3003247>
- White, N. J. (1998). Preventing antimalarial drug resistance through combinations. *Drug Resistance Updates*, 1(1), 3–9. [https://doi.org/10.1016/S1368-7646\(98\)80208-2](https://doi.org/10.1016/S1368-7646(98)80208-2)
- WHO. (2023). *World malaria World malaria report report*.
<https://www.wipo.int/amc/en/mediation/%0Ahttps://www.who.int/teams/global-malaria-programme/reports/world-malaria-report-2023>
- Wichers-Misterek, J. S., Krumkamp, R., Held, J., von Thien, H., Wittmann, I., Höppner, Y. D., Ruge, J. M., Moser, K., Dara, A., Strauss, J., Esen, M., Fendel, R., Sulyok, Z., Jenning, M. D., Kremsner, P. G., Sim, B. K. L., Hoffman, S. L., Duffy, M. F., Otto, T. D., ... Bachmann, A. (2023). The exception that proves the rule: Virulence gene expression at the onset of *Plasmodium falciparum* blood stage infections. *PLoS Pathogens*, 19(6 June), 1–27. <https://doi.org/10.1371/journal.ppat.1011468>
- Wichers, J. S., Scholz, J. A. M., Strauss, J., Witt, S., Lill, A., Ehnold, L.-I., Neupert, N., Liffner, B., Lühken, R., Petter, M., Lorenzen, S., Wilson, D. W., Löw, C., Lavazec, C., Bruchhaus, I., Tannich, E., Gilberger, T. W., & Bachmann, A. (2019). Dissecting the Gene Expression, Localization, Membrane Topology, and Function of

References

- the Plasmodium falciparum STEVOR Protein Family. *American Society for Microbiology*, 10(4). <https://doi.org/https://doi.org/10.1128/mBio.01500-19>.
- Wichers, J. S., Tonkin-Hill, G., Thye, T., Krumkamp, R., Kreuels, B., Strauss, J., Thien, H. von, Scholz, J. A. M., Hansson, H. S., Jensen, R. W., Turner, L., Lorenz, F. R., Schöllhorn, A., Bruchhaus, I., Tannich, E., Fendel, R., Otto, T. D., Lavstsen, T., Gilberger, T. W., ... Bachmann, A. (2021). Common virulence gene expression in adult first-time infected malaria patients and severe cases. *ELife*, 10, 1–30. <https://doi.org/10.7554/ELIFE.69040>
- Wickham, M. E., Rug, M., Ralph, S. A., Klonis, N., Mcfadden, G. I., Tilley, L., & Cowman, A. F. (2001). Trafficking and assembly of the cytoadherence complex in Plasmodium falciparum-infected human erythrocytes. *EMBO Journal*, 20(20), 5636–5649. <https://doi.org/10.1093/emboj/20.20.5636>
- Winter, G., Kawai, S., Haeggström, M., Kaneko, O., Von Euler, A., Kawazu, S. I., Palm, D., Fernandez, V., & Wahlgren, M. (2005). SURFIN is a polymorphic antigen expressed on Plasmodium falciparum merozoites and infected erythrocytes. *Journal of Experimental Medicine*, 201(11), 1853–1863. <https://doi.org/10.1084/jem.20041392>
- Wiser, M. F. (2023). Knobs, Adhesion, and Severe Falciparum Malaria. *Tropical Medicine and Infectious Disease*, 8(7). <https://doi.org/10.3390/tropicalmed8070353>
- Xie, Y., Li, X., Chai, Y., Song, H., Qi, J., & Gao, G. F. (2021). Structural basis of malarial parasite RIFIN-mediated immune escape against LAIR1. *Cell Reports*, 36(8), 109600. <https://doi.org/10.1016/j.celrep.2021.109600>
- Xu, X., Rao, G. S., Groh, V., Spies, T., Gattuso, P., Kaufman, H. L., Plate, J., & Prinz, R. A. (2011). Major histocompatibility complex class I-related chain A/B (MICA/B) expression in tumor tissue and serum of pancreatic cancer: Role of uric acid accumulation in gemcitabine-induced MICA/B expression.
- Yam, X. Y., Niang, M., Madnani, K. G., & Preiser, P. R. (2017). Three Is a Crowd – New Insights into Rosetting in Plasmodium falciparum. *Trends in Parasitology*, 33(4), 309–320. <https://doi.org/10.1016/j.pt.2016.12.012>
- Yamba, E. I., Fink, A. H., Badu, K., Asare, E. O., Tompkins, A. M., & Amekudzi, L. K. (2023). Climate Drivers of Malaria Transmission Seasonality and Their Relative Importance in Sub-Saharan Africa. *GeoHealth*, 7(2), 1–12. <https://doi.org/10.1029/2022GH000698>
- Yanik, S., Venkatesh, V., Parker, M. L., Ramaswamy, R., Diouf, A., Sarkar, D., Miura, K., Long, C. A., Boulanger, M. J., & Srinivasan, P. (2023). Structure guided mimicry of an essential P. falciparum receptor-ligand complex enhances cross neutralizing antibodies. *Nature Communications*, 14(1). <https://doi.org/10.1038/s41467-023-41636-5>
- Yman, V., White, M. T., Asghar, M., Sundling, C., Sonden, K., Draper, S. J., Osier, F. H. A., & Färnert, A. (2019). Antibody responses to merozoite antigens after natural Plasmodium falciparum infection: Kinetics and longevity in absence of re-exposure. *BMC Medicine*, 17(1), 1–14. <https://doi.org/10.1186/s12916-019-1255-3>
- Yokoyama, W. M., Hughes, H., Arora, G., Hart, G. T., Manzella-Lapeira, J., Doritchamou, J. Y., Narum, D. L., Thomas, L. M., Brzustowski, J., Rajagopalan, S., Doumbo, O. K., Traore, B., Miller, L. H., Pierce, S. K., Duffy, P. E., Crompton, P. D., Desai, S. A., & Long, E. O. (2018). NK cells inhibit Plasmodium falciparum growth in red blood cells via antibody-dependent cellular cytotoxicity. *ELife*, 7, 1–20. <https://doi.org/10.7554/eLife.36806.001>
- Zakama, A. K., Ozarslan, N., & Gaw, S. L. (2020). Placental Malaria. *Current Tropical Medicine Reports*, 7(4), 162–171. <https://doi.org/10.1007/s40475-020-00213-2>
- Zayed, A., Moustafa, M., Tageldin, R., & Harwood, J. F. (2023). Effects of Seasonal Conditions on Abundance of Malaria Vector Anopheles stephensi Mosquitoes, Djibouti, 2018–2021. *Emerging Infectious Diseases*, 29(4), 801–805. <https://doi.org/10.3201/eid2904.220549>
- Zhang, X., Florini, F., Visone, J. E., Lionardi, I., Gross, M. R., Patel, V., & Deitsch, K. W. (2022). A coordinated transcriptional switching network mediates antigenic variation of human malaria parasites. *ELife*, 11, 1–25. <https://doi.org/10.7554/ELIFE.83840>

8. Publication list and conferences

Manuscript in preparation:

Höppner, Y. D., Adamou R., Krumkamp, R., Zinsou, J. F., von Thien, H., Recker, M., Takashima, E., Fendel R., Turner, L., Lorenz, F., Ruge, J. M., Adegbite, B. R., Adegnika, A. A., Hoffman, S. L., Sim, B. K. B., Otto, T. D., Kremsner, B. G., Lavstsen, T., Tsuboi, T., Gilberger, T. W., Petter, M., Mordmüller, B., McCall, M., Bachmann A., **Antigenic variation of malaria parasites counteracts the host immune system – manuscript in preparation** (note: after consultation with the trial team/collaborators in Tübingen/Nijmegen/Gabon: since the trial document for L2 is not yet published (planned to be published by the end 2024 beginning of 2025), data from this study can currently not be published).

Paper contributions/Co-authorships:

Wichers-Misterek, J. S., Krumkamp, R., Held, J., von Thien, H., Wittmann, I., Höppner, Y. D., Ruge, J. M., Moser, K., Dara, A., Strauss, J., Esen, M., Fendel, R., Sulyok, Z., Jeninga, M. D., Kremsner, P. G., Sim, B. K. L., Hoffman, S. L., Duffy, M. F., Otto, T. D., Gilberger, T. W., ... Bachmann, A. (2023). The exception that proves the rule: **Virulence gene expression at the onset of *Plasmodium falciparum* blood stage infections**. *PLoS pathogens*, 19(6), e1011468. <https://doi.org/10.1371/journal.ppat.1011468>

Andradi-Brown, C., Wichers-Misterek, J. S., von Thien, H., Höppner, Y. D., Scholz, J. A. M., Hansson, H. S., Hocke, E. F., Gilberger, T. W., Duffy, M. F., Lavstsen, T., Baum, J., Otto, T. D., Cunningham, A. J., Bachmann, A. (2023). **A novel computational pipeline for *var* gene expression augments the discovery of changes in the *Plasmodium falciparum* transcriptome during transition from in vivo to short-term in vitro culture**. *eLife*, 12:RP87726. <https://doi.org/10.7554/eLife.87726.1>

Conferences and meetings:

MAM24, Lorne; Australia (2024): Abstract submitted, oral presentation: **Antigenic variation of malaria parasites counteracts the host immune system**. Talk summary published here: Longley, R. J., Malinga, J., Hesping, E., Sutanto, E., DonVito, S. M., Kucharski, M., ... & Mwikali, K. (2024). MAM 2024: Malaria in a changing world. *Trends in Parasitology*. <https://doi.org/10.1016/j.pt.2024.03.007>

BioMalPar XIX, Heidelberg; Germany (2023): Abstract submitted, poster presentation: **Impact of longitudinally acquired immunity on *P. falciparum var* gene expression (3rd poster prize)**.

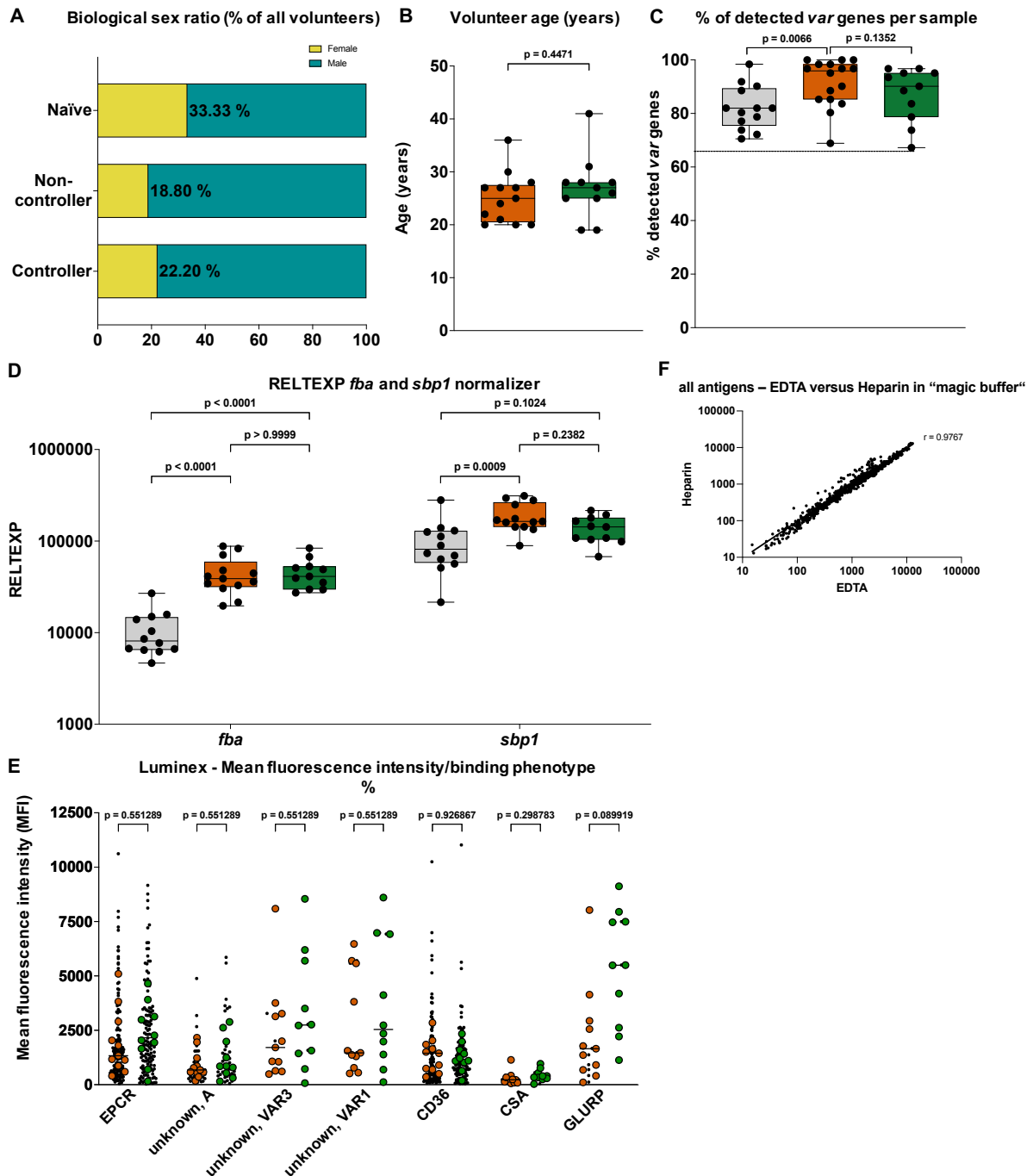
Malaria meeting, Hamburg; Germany (2023); Abstract submitted, oral presentation: **Impact of increasing host immunity on *P. falciparum var* gene expression**

9. Supplementary data

Per volunteer, the infection scheme (sequence A or B), the challenges in which they turned TBS+ for the 1st time, route of administration and amount of sporozoites injected, biological sex, age and the volunteer classification were registered. Independently established infections e.g., when volunteers underwent a treatment were considered as separate infections, therefore selected volunteers occur multiple time in the list. Furthermore, detailed information about the 1st day of TBS positivity including parasitemia, as well as longitudinal information e.g., on the amount of TBS+ samples collected per volunteer and whether the samples were included (blood and plasma) in specific analysis assays is shown. Volunteer animal sample information is depicted in the sample overview figures (Figure 9, Figure 22).

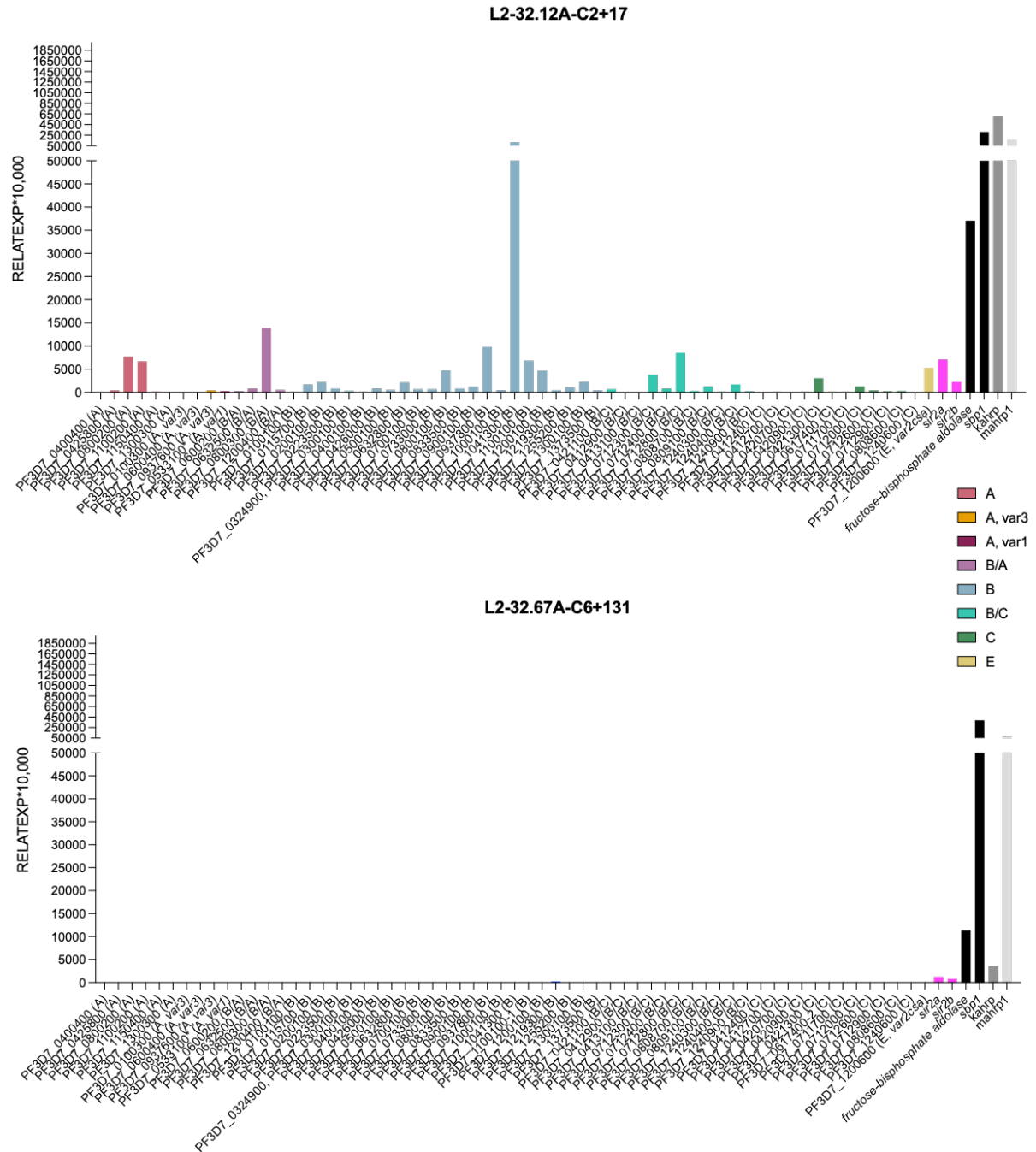
[illegible]

Supplementary data



Supplementary Figure 1.: Control variables and extended data for the CHMI studies, the Luminex, and RT-qPCR assays.

A) Biological sexes across the volunteer groups from the different trials shows a strong male recruitment bias but no overall sex biases among the groups (% females in the respective groups as indicated; malaria-naïve (n=12), non-controller (n=13), controller (n=11)) B) Age comparison of non-controller (n=13) and controller (n= only 11) from the L1 and L2 study shows an equal age distribution across both groups. C) Percent of detected var genes from the NF54 var repertoire (n=61) as a quality measurement for RT-qPCR accuracy showing that reduced parasitemia by controller (Figure 11 E) does not lead to a reduced detection of var genes for the naïve (n=12), non-controller (n=13) and controller (n=11) groups. Samples were included if they showed amplicons for >2/3 of all var genes and a Ct (Arginyl-tRNA-Synthetase (normalizer) < 31 (Mann-Whitney-U-test). D) RELTEXP measured by RT-qPCR for fructose-bisphosphate aldolase (*fba*) and skeleton binding protein 1 (*sbp1*) shows lower overall transcript amount for samples from malaria naïve individuals but equal levels in samples from non-controller and controller. E) Luminex assay for PfEMP domains with distinct binding phenotype (EPCR, unknown A, unknown var3, unknown var1, CD36 and CSA) shows higher reactivity of plasma samples from controller, however not significant (Mann-Whitney-U-tests, corrected for multiple testing). F) Accurate correlation of detected mean fluorescence intensity (MFI) in the Luminex-plex assay for blood samples collected in either EDTA or Heparin tubes using the LowCross-Buffer® vs. the commonly used ABE buffer. Non-controller and controller as indicated in dark orange dark green, respectively. Significance levels assessed with Mann-Whitney U-tests corrected for multiple tested using the Bonferroni method.



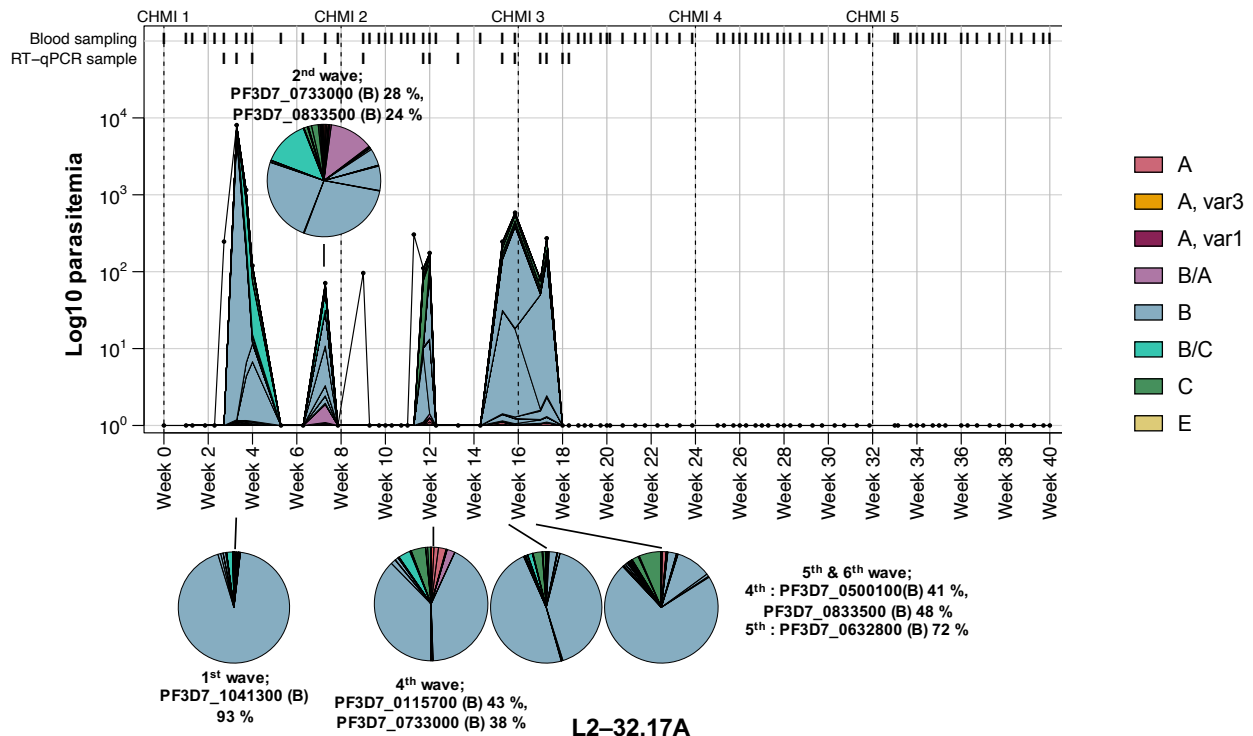
Supplementary Figure 2.: Var gene specific RT-qPCR results for infections with NF54 parasites and naturally occurring infections.

NF54 var gene specific RT-qPCR results for NF54 (top panel) and locally circulating parasite background (lower panel). Expression is measured as the $\delta\delta C_i$ value $\times 10.000$ for all NF54 var genes and core genes (sir2a, sir2b, fructose-bisphosphate aldolase, sbp1, kahrp and mahrp) normalized against expression of the housekeeping gene arginyl-tRNA-synthetase, calibrated against NF54 gDNA. Color-code (var genes): A-types (red), A; var3, (orange), A; var1 (dark red), B/A-types (purple), B-types (blue), C-types (green), E-type; var2csa (yellow). Sample IDs combine volunteer ID (e.g., L2-32.12A) with the respective sampling date (C2+17:2nd challenge and 17 days post infection).

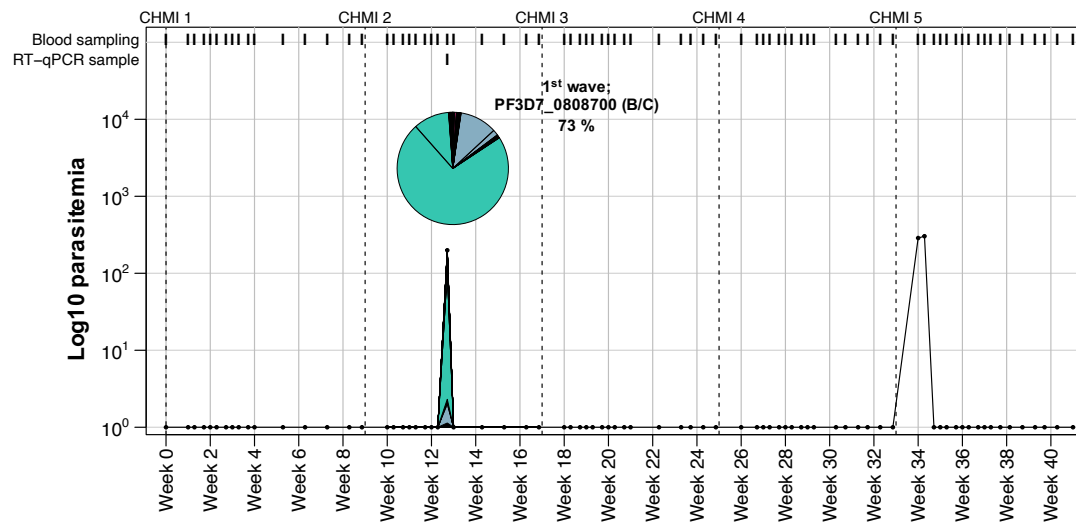
Supplementary data

Controller:

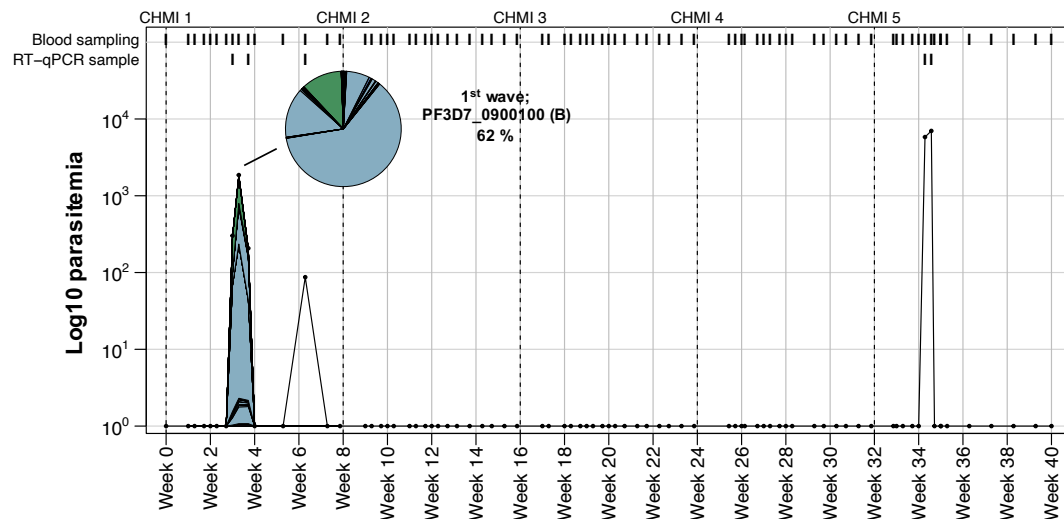
L2-32.42A



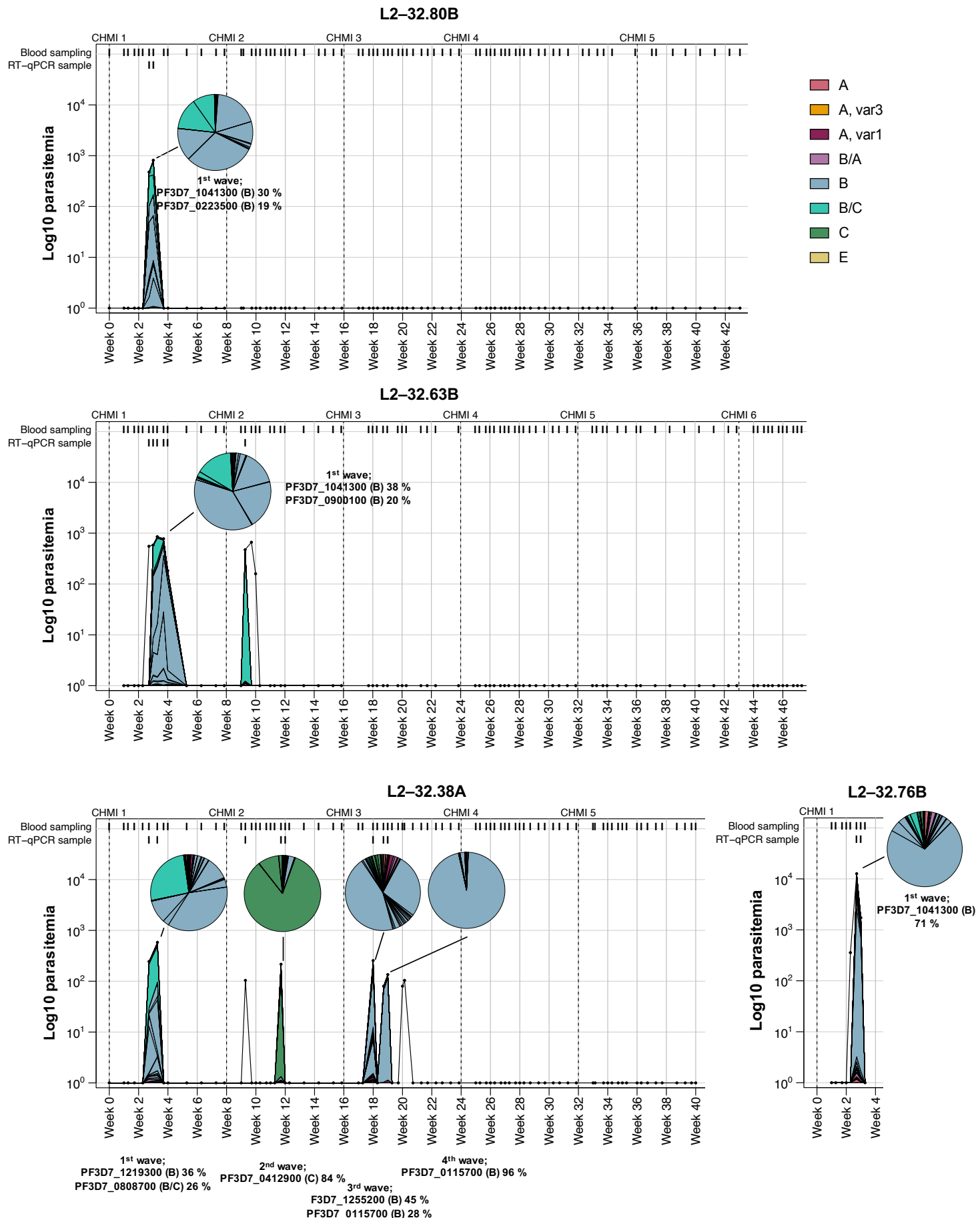
L2-32.17A



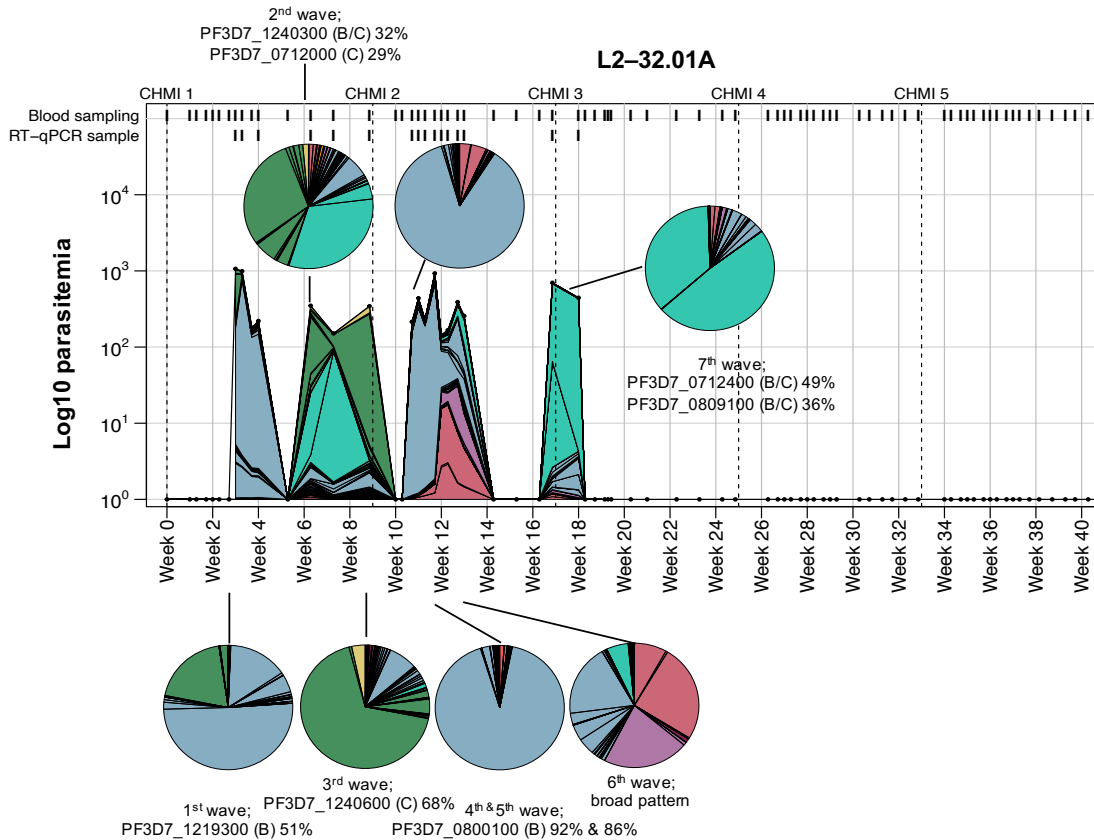
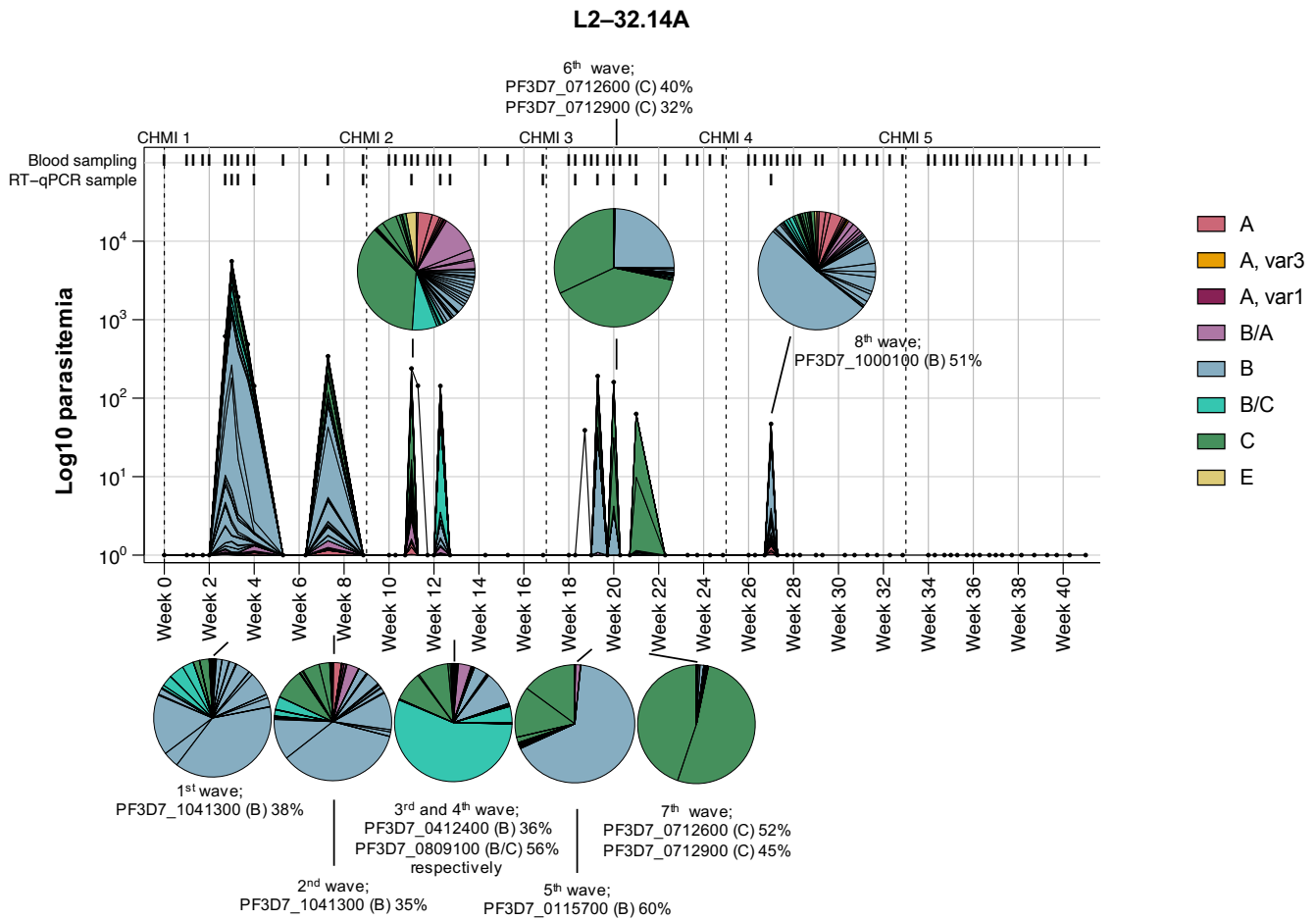
L2-32.66A



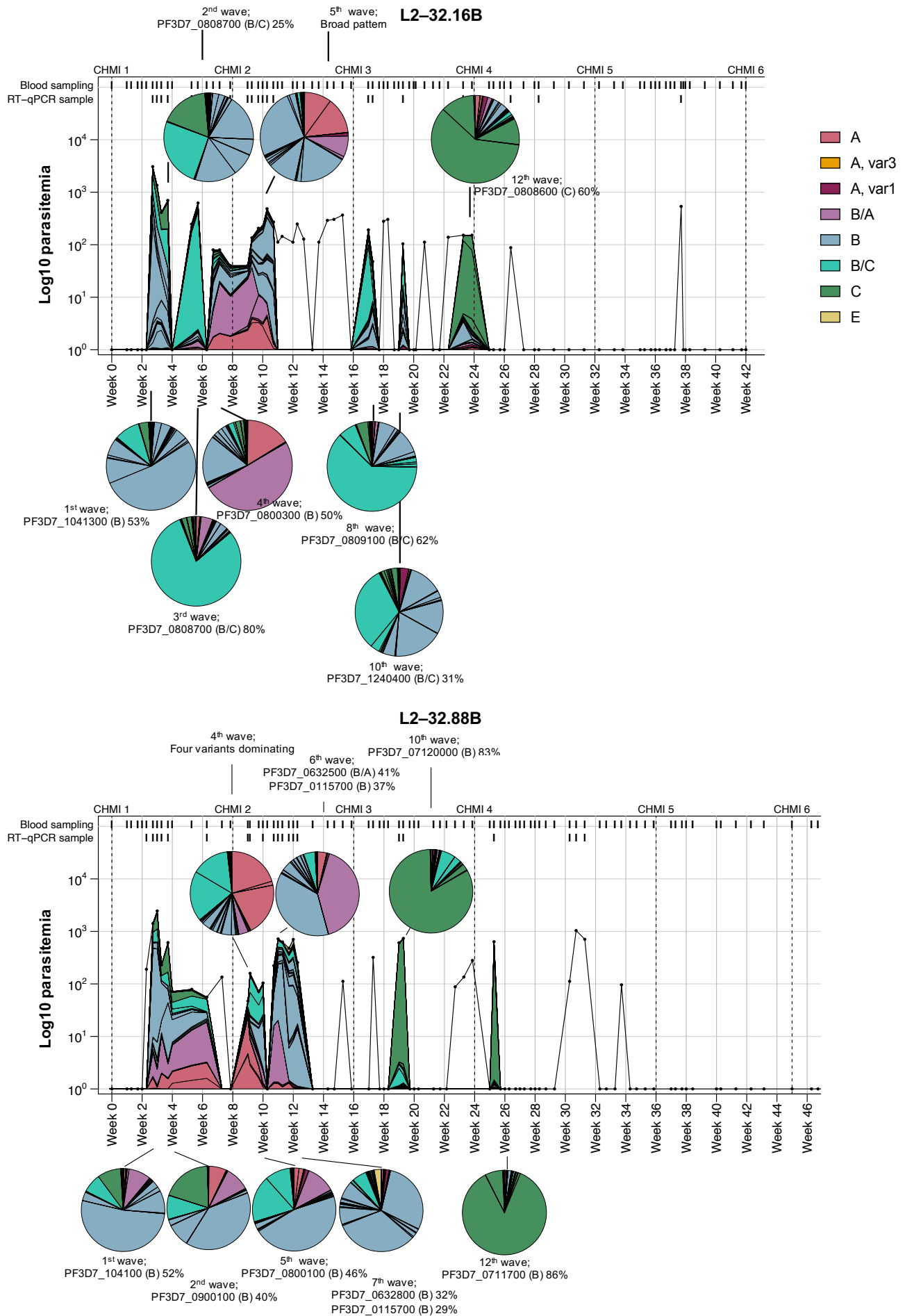
Supplementary data



Supplementary data



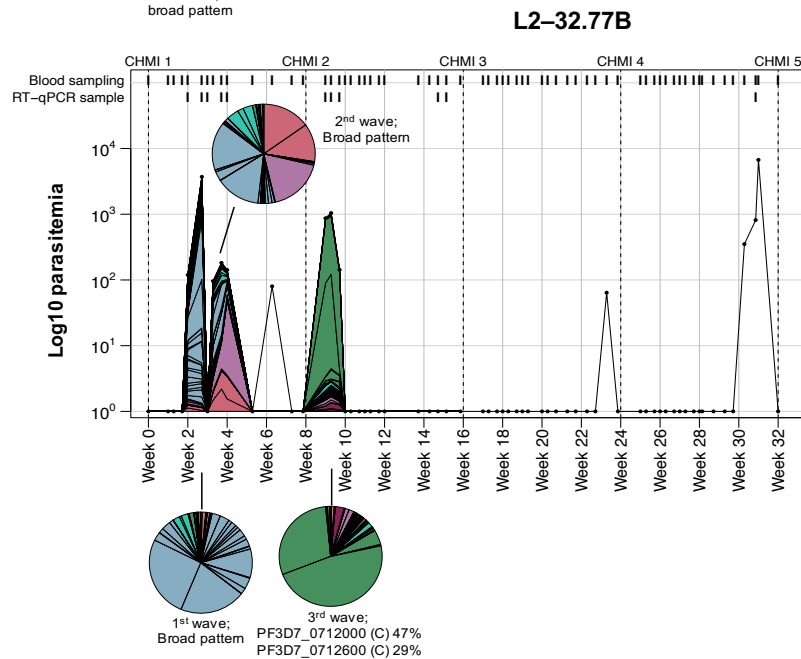
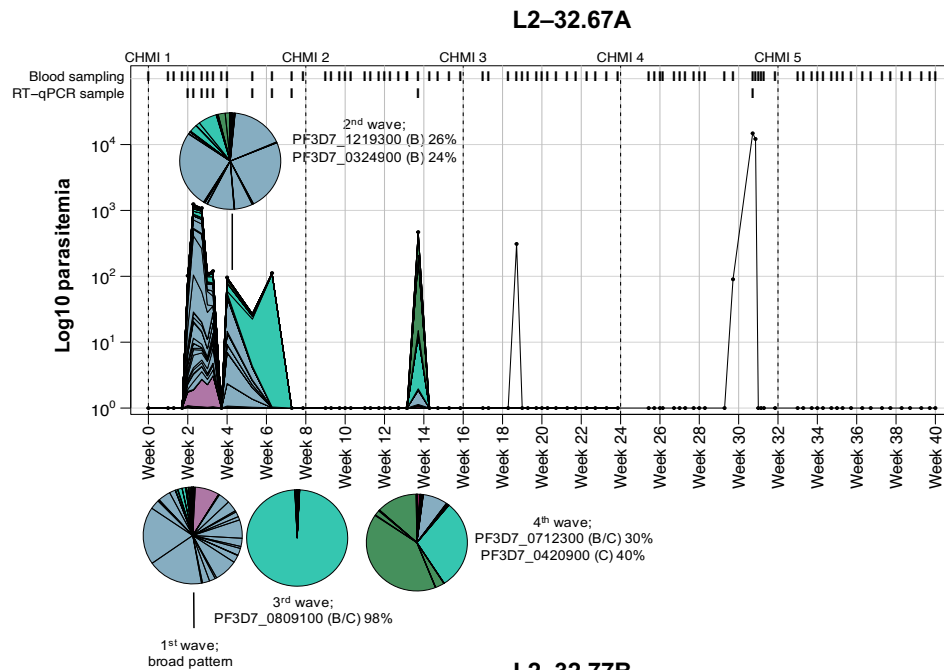
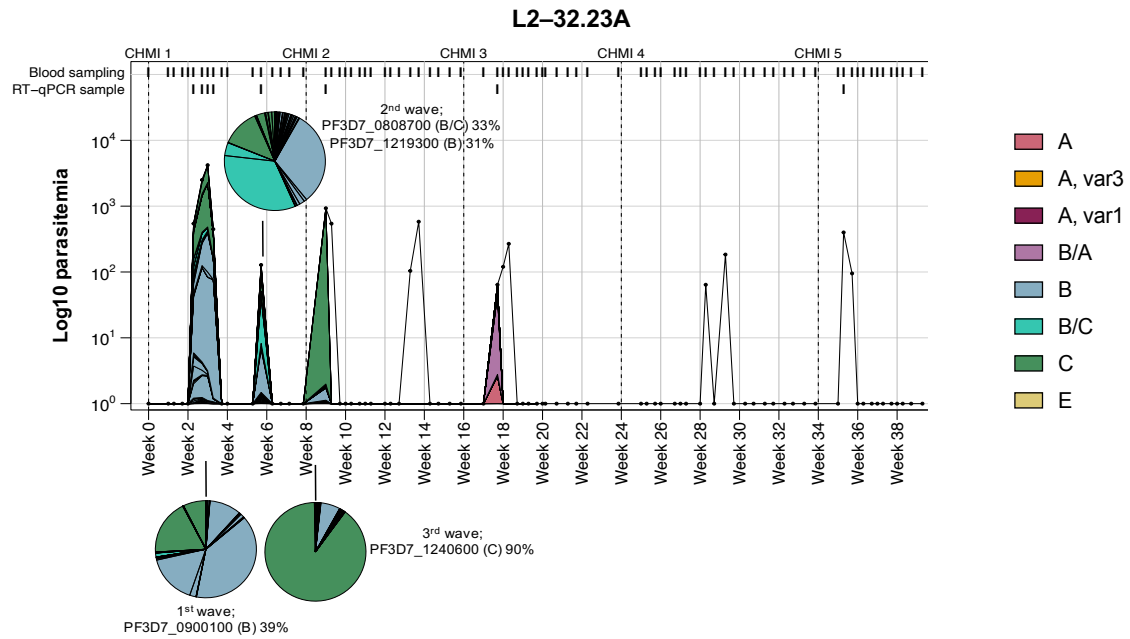
Supplementary data



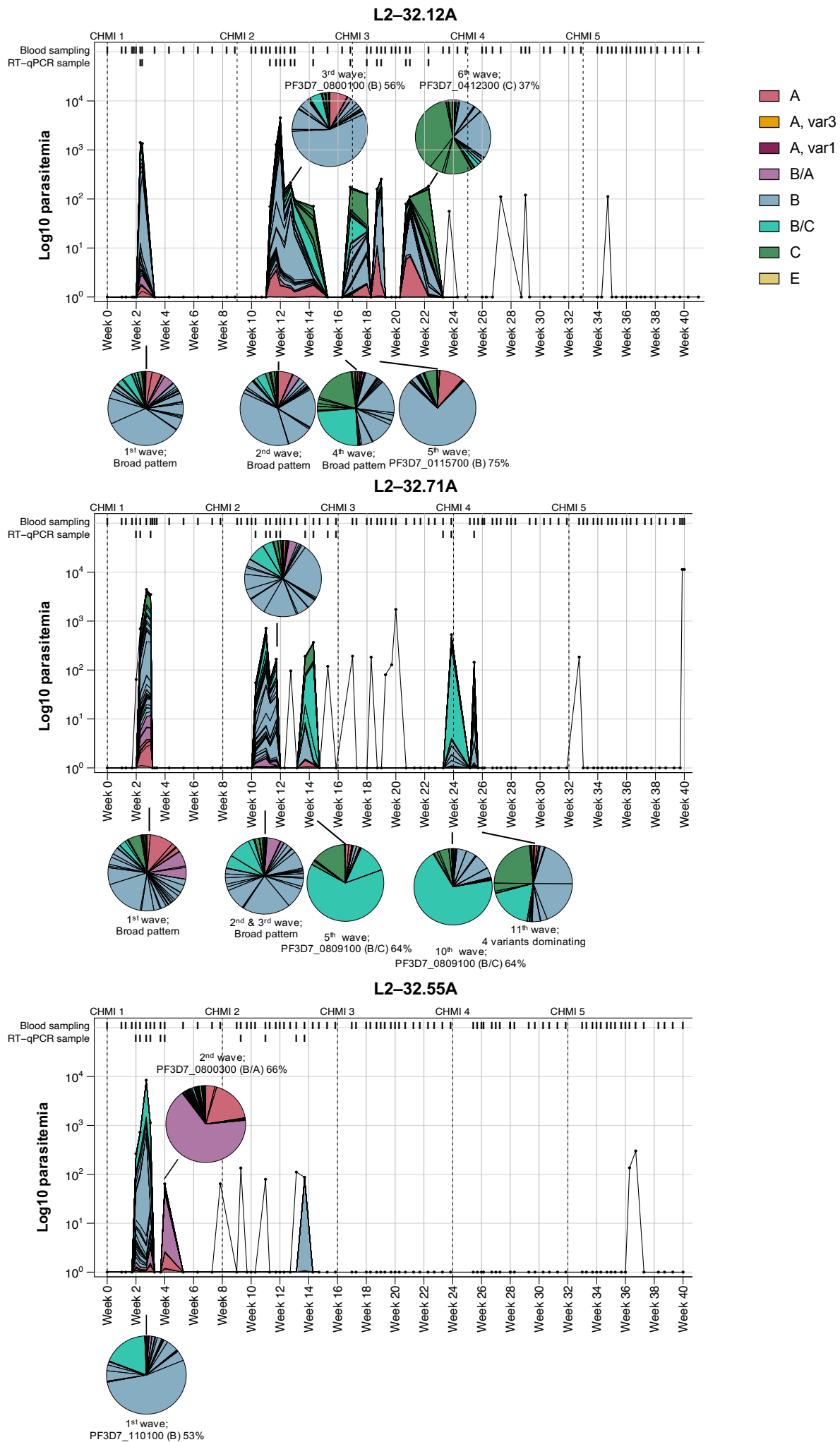
Supplementary Figure 3.: Longitudinal var gene expression in regards to the parasitemia for controllers.

Antigenic variation dynamics depicted for $n=11$ controllers showing that individual waves are dominated by a single or few variants only. For some waves high proportion of A-type var genes are detected similarly to Figure 16 D, and Figure 24 A. Var gene group coloring as indicated: A-types in light red, var3 genes in orange, var1 gene in dark red, B/C-type genes in purple, B-type genes in light blue, B/C-type genes in turquoise, C-type genes in dark green, E-type gene in yellow. Sample intervals are indicated above of the respective volunteer plot and if no samples were collected the time points were left blank.

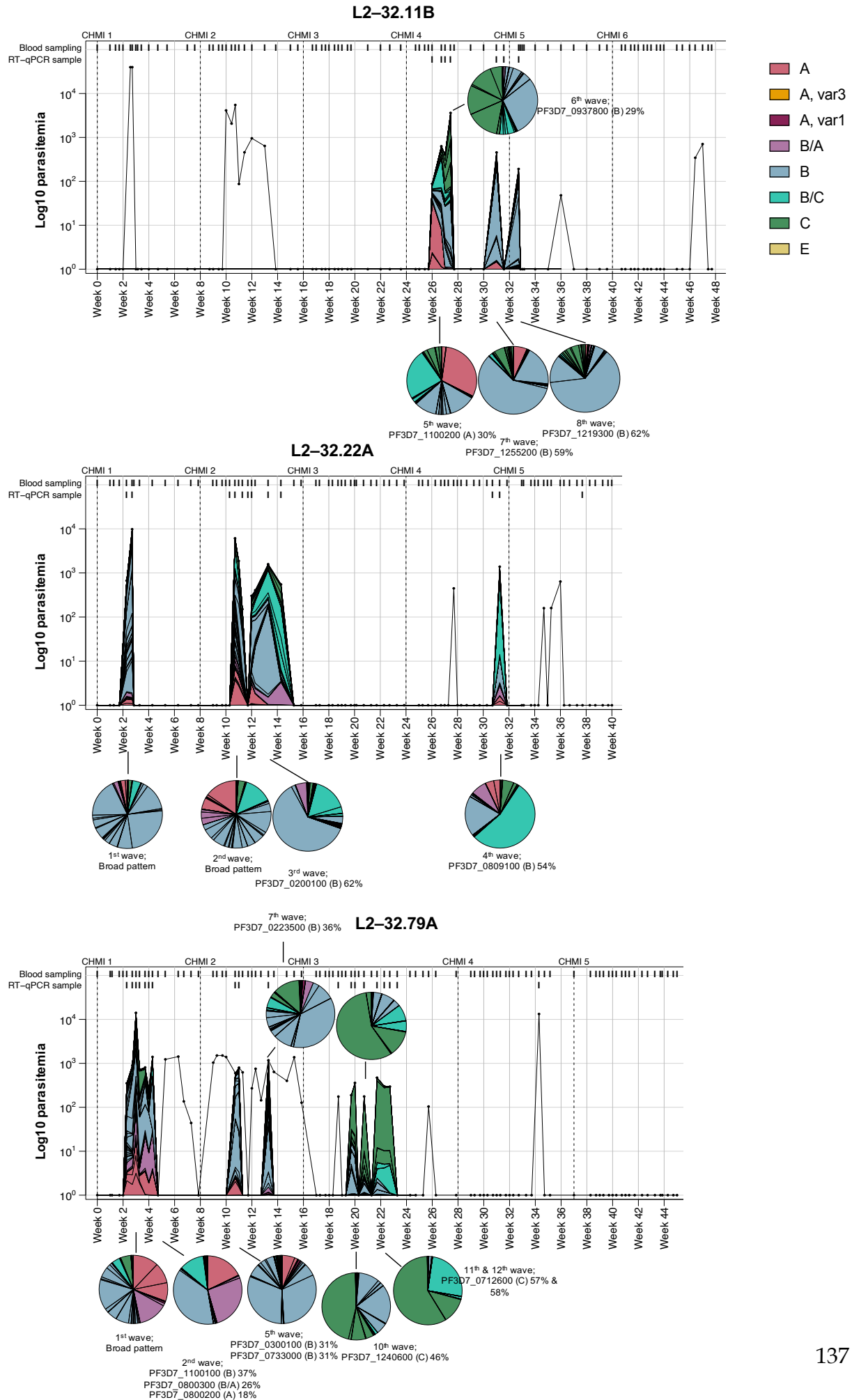
Supplementary data



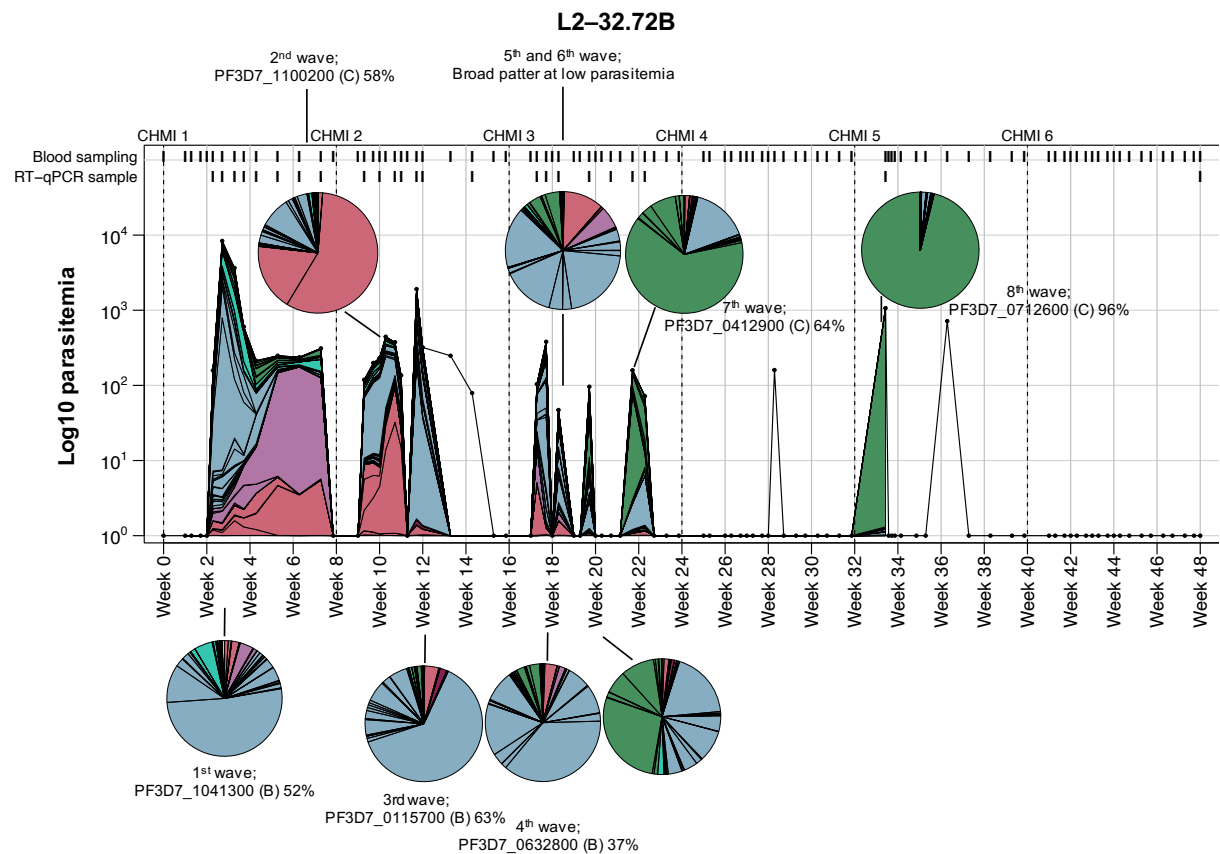
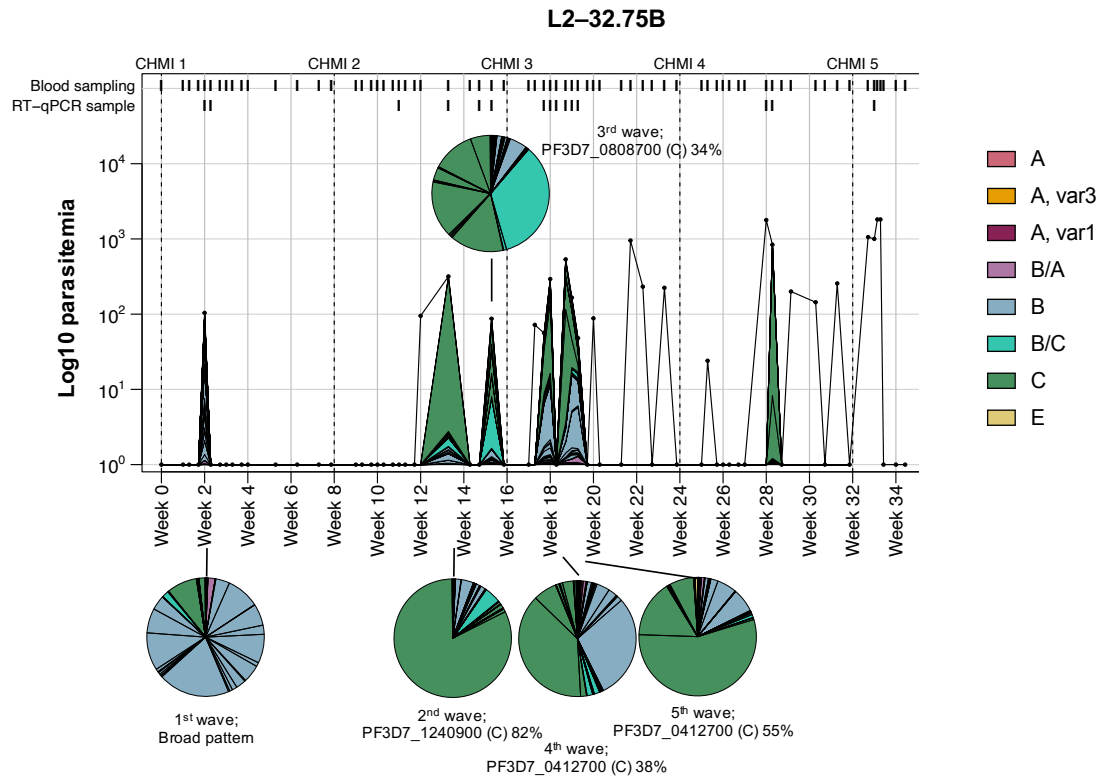
Supplementary data



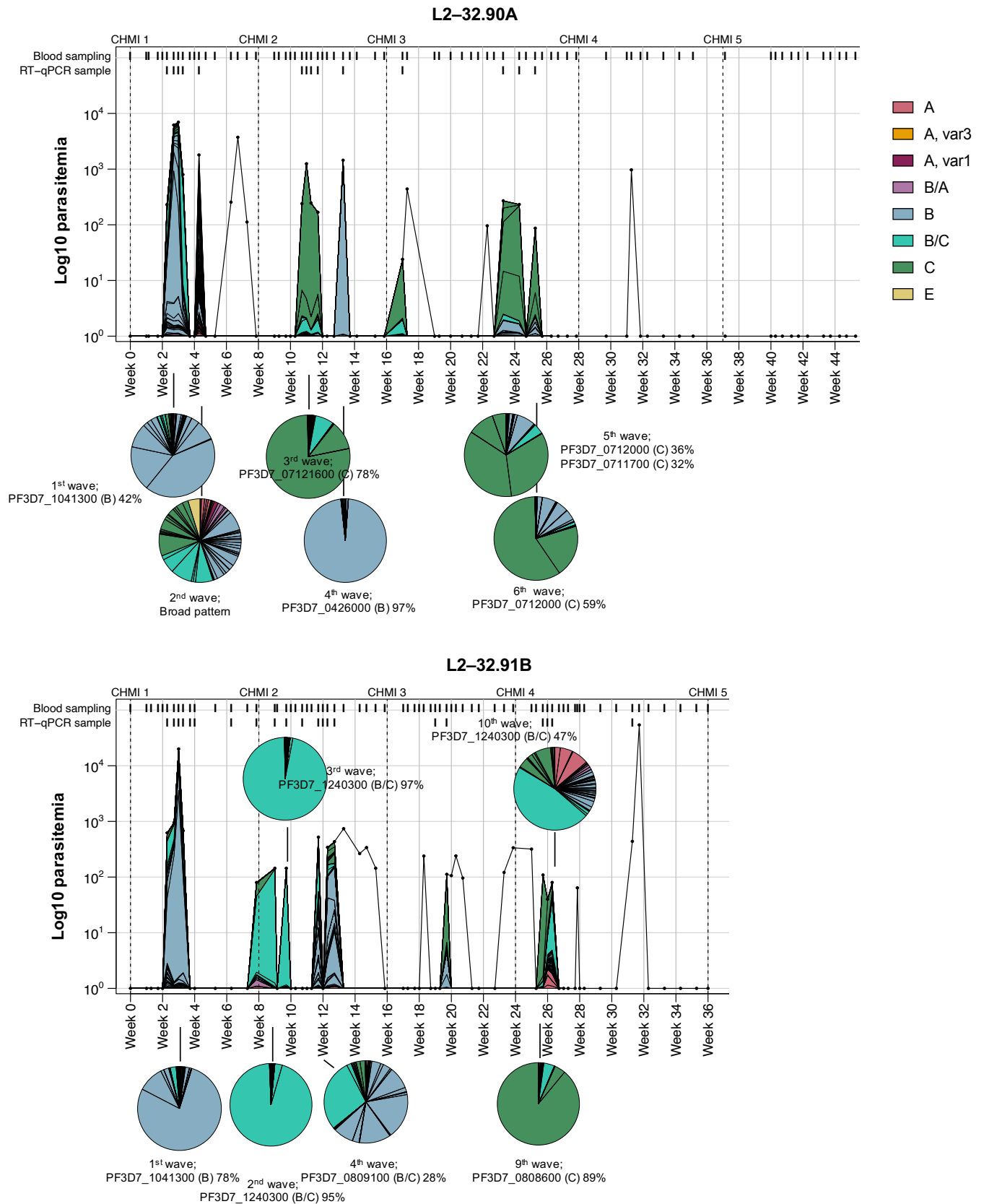
Supplementary data



Supplementary data



Supplementary data



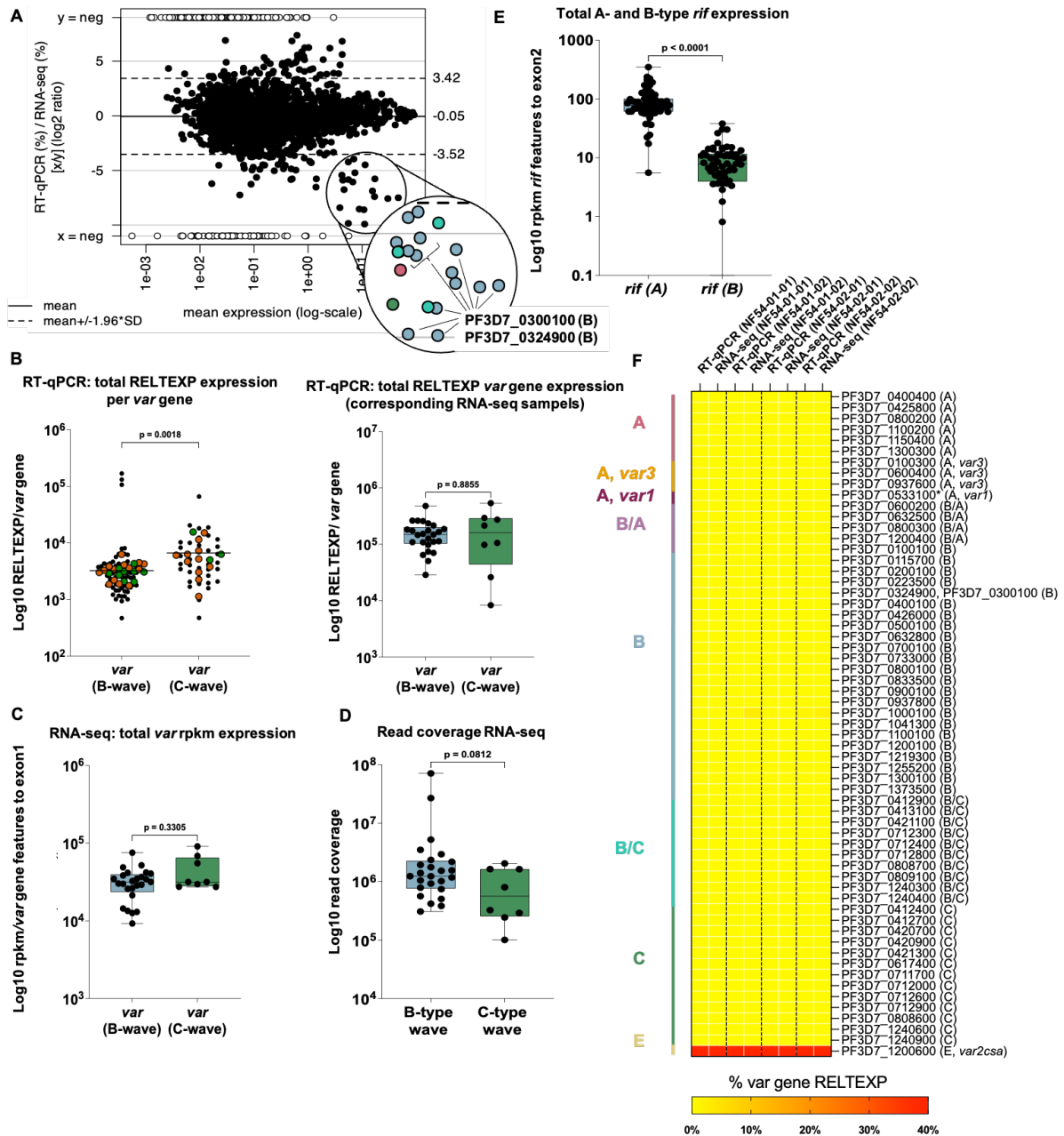
Supplementary Figure 4: Longitudinal var gene expression in regards to the parasitemia for noon-controllers.
Antigenic variation dynamics depicted for $n=13$ controllers showing that individual waves are dominated by a single or few variants only. For some waves high proportion of A-type var genes are detected similarly to Figure 16 D, and Figure 24 A. Var gene group coloring as indicated: A-types in light red, var3 genes in orange, var1 gene in dark red, B/C-type genes in purple, B-type genes in light blue, B/C-type genes in turquoise, C-type genes in dark green, E-type gene in yellow. Sample intervals are indicated above of the respective volunteer plot and if no samples were collected the time points were left blank.

Supplementary data

Malaria-naïve			Non-controller			Controller		
ID		peak	ID		peak	ID		peak
PF3D7_0632800 (B)		11.0868823	PF3D7_1041300 (B)		17.7911506	PF3D7_1041300 (B)		35.2318612
PF3D7_0400100 (B)		7.04210762	PF3D7_1100100 (B)		15.0128889	PF3D7_0808700 (B/C)		13.9338646
PF3D7_0937800 (B)		6.92608353	PF3D7_0900100 (B)		6.50034558	PF3D7_0900100 (B)		9.86257546
PF3D7_0733000 (B)		6.74189691	PF3D7_1255200 (B)		4.77294508	PF3D7_1219300 (B)		8.5963607
PF3D7_0400400 (A)		5.32731779	PF3D7_0800100 (B)		4.63990287	PF3D7_0412400 (C)		4.38121165
PF3D7_0800100 (B)		4.16172916	PF3D7_0808700 (B/C)		4.29218823	PF3D7_1255200 (B)		2.85958478
PF3D7_0100100 (B)		4.02741628	PF3D7_0937800 (B)		3.42861533	PF3D7_0223500 (B)		2.36889344
PF3D7_1255200 (B)		3.93944728	PF3D7_0412400 (C)		3.32098689	PF3D7_1100100 (B)		2.23367611
PF3D7_0223500 (B)		3.59919764	PF3D7_1200100 (B)		2.95522713	PF3D7_0733000 (B)		2.03227349
PF3D7_1373500 (B)		3.24194475	PF3D7_0425800 (A)		2.67812827	PF3D7_0100100 (B)		2.02539695
PF3D7_0115700 (B)		3.12922515	PF3D7_0100100 (B)		2.41710778	PF3D7_1200100 (B)		1.97075736
PF3D7_0900100 (B)		3.02237824	PF3D7_1300100 (B)		2.29816026	PF3D7_1240300 (B/C)		1.88866711
PF3D7_1041300 (B)		2.84622108	PF3D7_0800300 (B/A)		2.1610289	PF3D7_0800100 (B)		1.37385958
PF3D7_0426000 (B)		2.59362784	PF3D7_0115700 (B)		2.074447	PF3D7_0400100 (B)		1.24488266
PF3D7_1300100 (B)		2.56971951	PF3D7_0223500 (B)		2.06668384	PF3D7_1300100 (B)		1.11943227
PF3D7_0425800 (A)		2.56407939	PF3D7_0324900 (B)		1.77068365	PF3D7_0800300 (B/A)		1.10752876
PF3D7_0632500 (B/A)		2.51402144	PF3D7_0300100 (B)		1.70120416	PF3D7_0115700 (B)		0.82390804
PF3D7_0633500 (B)		2.14474614	PF3D7_1373500 (B)		1.65429312	PF3D7_0712400 (B/C)		0.66563686
PF3D7_1200100 (B)		2.03680033	PF3D7_0632500 (B/A)		1.6504559	PF3D7_0300100 (B)		0.62659589
PF3D7_0712300 (B/C)		1.79941705	PF3D7_1219300 (B)		1.64321957	PF3D7_0937800 (B)		0.56913409
PF3D7_0421100 (B/C)		1.6116113	PF3D7_0400100 (B)		1.35271959	PF3D7_0632800 (B)		0.46802102
PF3D7_0200100 (B)		1.27146062	PF3D7_0600200 (B/A)		1.31869334	PF3D7_0421300 (C)		0.42170083
PF3D7_1100100 (B)		1.22524309	PF3D7_0733000 (B)		1.28467843	PF3D7_0533100* (A, var1)		0.37472378
PF3D7_0800300 (B/A)		1.20753751	PF3D7_0712400 (B/C)		1.09556304	PF3D7_0809100 (B/C)		0.32741678
PF3D7_1100200 (A)		1.14436751	PF3D7_0800200 (A)		1.04082917	PF3D7_0200100 (B)		0.29445893
PF3D7_0324900 (B)		0.99838709	PF3D7_0632600 (B)		0.88042159	PF3D7_0900200 (A)		0.27505866
PF3D7_0300100 (B)		0.855135	PF3D7_0400400 (A)		0.74080956	PF3D7_1240900 (C)		0.23379015
PF3D7_1000100 (B)		0.81783857	PF3D7_1100200 (A)		0.70723436	PF3D7_0700100 (B)		0.19551171
PF3D7_0712800 (B/C)		0.75363183	PF3D7_0500100 (B)		0.69685116	PF3D7_0426000 (B)		0.19174431
PF3D7_0421300 (C)		0.72338743	PF3D7_1240900 (C)		0.6381202	PF3D7_0426000 (B)		0.18755115
PF3D7_0700100 (B)		0.67370912	PF3D7_0426000 (B)		0.61226402	PF3D7_1373500 (B)		0.17248334
PF3D7_0500100 (B)		0.61529048	PF3D7_0200100 (B)		0.60563633	PF3D7_0632500 (B/A)		0.17248334
PF3D7_0712400 (B/C)		0.5992141	PF3D7_1240300 (B/C)		0.54451339	PF3D7_0712000 (C)		0.13867006
PF3D7_1200600 (E, var2c5a)		0.59673227	PF3D7_0421300 (C)		0.53144278	PF3D7_1200600 (E, var2c5a)		0.12539462
PF3D7_1300300 (A)		0.59169343	PF3D7_1300300 (A)		0.49300046	PF3D7_0500100 (B)		0.1166002
PF3D7_1200400 (B/A)		0.59054711	PF3D7_0809100 (B/C)		0.47732354	PF3D7_0712300 (B/C)		0.11488653
PF3D7_0712000 (C)		0.53021663	PF3D7_0700100 (B)		0.27959627	PF3D7_0425800 (A)		0.09804009
PF3D7_0600200 (B/A)		0.38104575	PF3D7_0712000 (C)		0.27220382	PF3D7_1200400 (B/A)		0.08833179
PF3D7_0712600 (C)		0.37336264	PF3D7_0833500 (B)		0.21606962	PF3D7_0712600 (C)		0.07632215
PF3D7_0420700 (C)		0.33321894	PF3D7_0533100* (A, var1)		0.18768577	PF3D7_0833500 (B)		0.06776029
PF3D7_0808700 (B/C)		0.30547033	PF3D7_0712600 (C)		0.14686747	PF3D7_0600200 (B/A)		0.0656466
PF3D7_1219300 (B)		0.26562287	PF3D7_1200600 (E, var2c5a)		0.14036724	PF3D7_0937600 (A, var3)		0.05973749
PF3D7_1240400 (B/C)		0.24997514	PF3D7_1000100 (B)		0.12946193	PF3D7_1100200 (A)		0.05250047
PF3D7_1240900 (C)		0.24997514	PF3D7_0711700 (C)		0.11827353	PF3D7_1000100 (B)		0.04588733
PF3D7_0808600 (C)		0.23602931	PF3D7_0712800 (B/C)		0.10596906	PF3D7_0412900 (C)		0.04552789
PF3D7_1150400 (A)		0.22749872	PF3D7_1200400 (B/A)		0.10297814	PF3D7_0808600 (C)		0.04529916
PF3D7_0711700 (C)		0.20713639	PF3D7_0412900 (C)		0.07334818	PF3D7_0400400 (A)		0.044484
PF3D7_0809100 (B/C)		0.20406731	PF3D7_1150400 (A)		0.07157976	PF3D7_1240600 (C)		0.03918601
PF3D7_0533100* (A, var1)		0.17268985	PF3D7_0712300 (B/C)		0.05470618	PF3D7_0711700 (C)		0.03804118
PF3D7_1240300 (B/C)		0.1239675	PF3D7_0937800 (A, var3)		0.04824573	PF3D7_0420900 (C)		0.0375627
PF3D7_0937600 (A, var3)		0.12175886	PF3D7_1240400 (B/C)		0.03150535	PF3D7_0617400 (C)		0.03304199
PF3D7_1240600 (C)		0.11915473	PF3D7_0100300 (A, var3)		0.02815817	PF3D7_0712900 (C)		0.03288131
PF3D7_0412400 (C)		0.11733488	PF3D7_1240600 (C)		0.02211495	PF3D7_1240400 (B/C)		0.03267129
PF3D7_0712900 (C)		0.08748132	PF3D7_0420900 (C)		0.02156157	PF3D7_1150400 (A)		0.02480121
PF3D7_0617400 (C)		0.04860165	PF3D7_0712900 (C)		0.02107887	PF3D7_0712800 (B/C)		0.02355913
PF3D7_0600400 (A, var3)		0.03199058	PF3D7_0808600 (C)		0.01987179	PF3D7_0412900 (C)		0.02149405
PF3D7_0420900 (C)		0.01034154	PF3D7_0617400 (C)		0.01793866	PF3D7_0412700 (C)		0.01613224
PF3D7_0412700 (C)		0.00539733	PF3D7_0412700 (C)		0.01297598	PF3D7_0600400 (A, var3)		0.01414804
PF3D7_0100300 (A, var3)		0	PF3D7_0600400 (A, var3)		0.01287079	PF3D7_0420700 (C)		0.01234257
PF3D7_0412900 (B/C)		0	PF3D7_0420700 (C)		0.01049375	PF3D7_0100300 (A, var3)		0.00556433
PF3D7_0413100 (B/C)		0	PF3D7_0421100 (B/C)		0.00424358	PF3D7_0413100 (B/C)		0.00541356
			PF3D7_0413100 (B/C)			PF3D7_0421100 (B/C)		0.00438377

Supplementary Figure 5.: Overlap of var gene variants expressed >1% by parasites from malaria-naïves, non-controllers and controllers at the 1st parasitemia peak.

A high overlap was observed for variants >1% of the total RELTEXP among parasites isolated from malaria-naïves (n=11), non-controllers (n=13) and controllers (n=11). The pattern of the non-controllers served as a reference. Compared to parasites from non-controllers, a large proportion of B-type var genes (n=11, n=1 B/A variant) is expressed by parasites of all three volunteer groups. As expected, the diversity of var genes expressed at a higher level is reduced by parasites from controllers (n=16 variants reaching >1% of the total expression) compared to parasites from non-controller (n=26 variants reaching >1% of the total expression) and malaria-naïve individuals (n=25 variants reaching >1% of the total expression). In particular, A and B/A-type var genes expressed >1% of the total RELTEXP in non-controller parasites are expressed at a lower degree by controller parasites.

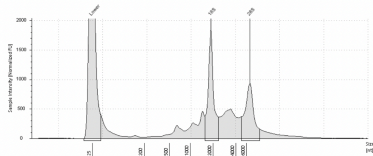


Supplementary Figure 6.: Validation of RNA-seq and RT-qPCR expression data.

A) Blant-Altman plot shows high agreement of individual var gene expression level determined with RNA-seq and RT-qPCR. For this, log10 mean expression data was linked to the ratio of % RELTEXP of var genes (RT-qPCR) and % rpkm for var genes measured with RT-qPCR or RNA-seq, respectively on a log2 scale (Mean -0.05% difference; +3.42 % (1.96*SD), -3.52 % (-1.96*SD). Open-circles indicate genes either not expressed in RNA-seq (x=neg) or not expressed in RT-qPCR (y=neg). Two genes PF3D7_0300100, PF3D7_0324900 were more profoundly expressed in RNA-seq and not in our RT-qPCR approach across all samples. In total 42 ex vivo samples and five in vitro samples were included (Table 15, Table 18). B) Super Plot indicating a higher RELTEXP by parasites from late infection stages ('C-type wave'; n=39 samples from late stage parasitemia peaks from n=13 non-controller (orange) and n=10 controller (green)) than from early infection stages ('B-type wave'; n=78 samples from the 1st waves from n=12 non-controller (orange) and n=3 controller (green)). RELTEXP is normalized to the number of expressed var genes (RELTEXP/var gene) (left) but not for the sample subset of sequenced samples which all have a parasitemia > 1000 pf/μL (right). C) RNA-seq processed samples, isolated from B and C-type waves which underwent transcriptomic stage comparison (Figure 18) also showed no higher rpkm expression per var gene difference. D) The same samples revealed no difference in sequencing read coverage (total reads mapped with STAR). E) In vivo samples overall show a significantly higher rate of A-type rif genes than B-type rifs. F) Heatmap showing in vitro samples tested with RT-qPCR and RNA-seq. RELTEXP and rpkm feature counts data for corresponding samples show high similarity and parasites almost exclusively express var2csa. From five included culture samples, 1x was removed due to <100,000 mapped P.falciparum reads. B- and C-type waves in blue and green as indicated. Significance levels were assessed with a Mann-Whitney-U-test.

Supplementary data

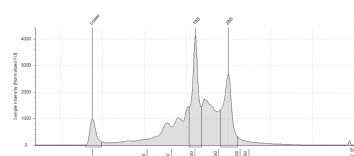
Tapestation electropherograms (Sequencing facility Bonn)



Well	80%	20% (SOL)	Cont. Input	Sample Description	Alert	Observations
A1	7.2	1.4	3070			Control Input Spectra Gap Detected

Size (bp)	Calibrated Conc. (ng/μl)	Assigned Conc. (ng/μl)	Peak Molarity (μM)	% Integrated Area	Peak Comment	Observations
121	40.0	40.0	2.00	24.53		Cont. Molar
201	2.9	-	1.28	1.6		125
441	8.08	-	3.08	34.47		125

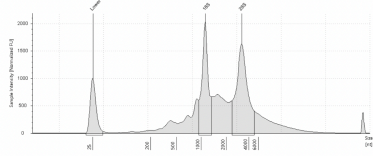
L2-32.01A C2+21



Well	80%	20% (SOL)	Cont. Input	Sample Description	Alert	Observations
B1	8.0	0.9	4000			Control Input Spectra Gap Detected

Size (bp)	Calibrated Conc. (ng/μl)	Assigned Conc. (ng/μl)	Peak Molarity (μM)	% Integrated Area	Peak Comment	Observations
121	1.28	1.28	1.28	23.30		Cont. Molar
201	2.9	-	1.28	1.6		125
441	8.0	-	3.08	34.47		125

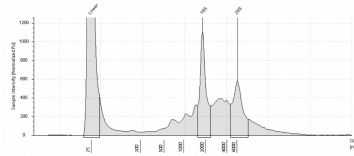
L2-32.12A C3+21



Well	80%	20% (SOL)	Cont. Input	Sample Description	Alert	Observations
A1	7.2	1.4	3070			Control Input Spectra Gap Detected

Size (bp)	Calibrated Conc. (ng/μl)	Assigned Conc. (ng/μl)	Peak Molarity (μM)	% Integrated Area	Peak Comment	Observations
121	40.0	40.0	2.00	24.53		Cont. Molar
201	2.9	-	1.28	1.6		125
441	8.08	-	3.08	34.47		125

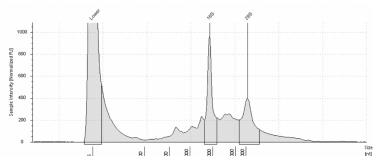
L2-32.01A C2+23



Well	80%	20% (SOL)	Cont. Input	Sample Description	Alert	Observations
B1	7.2	1.4	3070			Control Input Spectra Gap Detected

Size (bp)	Calibrated Conc. (ng/μl)	Assigned Conc. (ng/μl)	Peak Molarity (μM)	% Integrated Area	Peak Comment	Observations
121	40.0	40.0	2.00	24.53		Cont. Molar
201	2.9	-	1.28	1.6		125
441	8.08	-	3.08	34.47		125

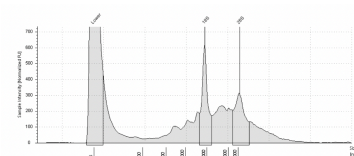
L2-32.14A C2+21



Well	80%	20% (SOL)	Cont. Input	Sample Description	Alert	Observations
C1	7.2	1.4	3070			Control Input Spectra Gap Detected

Size (bp)	Calibrated Conc. (ng/μl)	Assigned Conc. (ng/μl)	Peak Molarity (μM)	% Integrated Area	Peak Comment	Observations
121	40.0	40.0	2.00	24.53		Cont. Molar
201	2.9	-	1.28	1.6		125
441	8.08	-	3.08	34.47		125

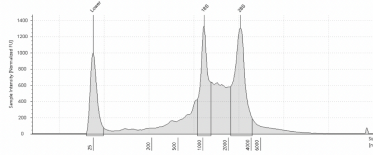
L2-32.01A C2+58



Well	80%	20% (SOL)	Cont. Input	Sample Description	Alert	Observations
A2	7.2	1.4	3070			Control Input Spectra Gap Detected

Size (bp)	Calibrated Conc. (ng/μl)	Assigned Conc. (ng/μl)	Peak Molarity (μM)	% Integrated Area	Peak Comment	Observations
121	40.0	40.0	2.00	24.53		Cont. Molar
201	2.9	-	1.28	1.6		125
441	8.08	-	3.08	34.47		125

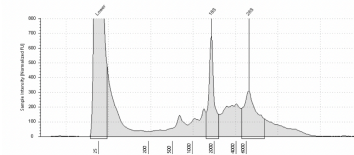
L2-32.14A C2+23



Well	80%	20% (SOL)	Cont. Input	Sample Description	Alert	Observations
B1	7.2	1.4	3070			Control Input Spectra Gap Detected

Size (bp)	Calibrated Conc. (ng/μl)	Assigned Conc. (ng/μl)	Peak Molarity (μM)	% Integrated Area	Peak Comment	Observations
121	40.0	40.0	2.00	24.53		Cont. Molar
201	2.9	-	1.28	1.6		125
441	8.08	-	3.08	34.47		125

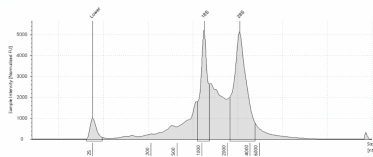
L2-32.11B C4+21



Well	80%	20% (SOL)	Cont. Input	Sample Description	Alert	Observations
B1	7.2	1.4	3070			Control Input Spectra Gap Detected

Size (bp)	Calibrated Conc. (ng/μl)	Assigned Conc. (ng/μl)	Peak Molarity (μM)	% Integrated Area	Peak Comment	Observations
121	40.0	40.0	2.00	24.53		Cont. Molar
201	2.9	-	1.28	1.6		125
441	8.08	-	3.08	34.47		125

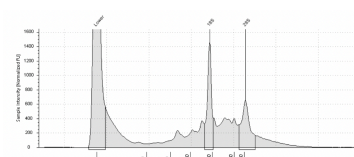
L2-32.16B C2+19



Well	80%	20% (SOL)	Cont. Input	Sample Description	Alert	Observations
C1	7.2	1.4	3070			Control Input Spectra Gap Detected

Size (bp)	Calibrated Conc. (ng/μl)	Assigned Conc. (ng/μl)	Peak Molarity (μM)	% Integrated Area	Peak Comment	Observations
121	40.0	40.0	2.00	24.53		Cont. Molar
201	2.9	-	1.28	1.6		125
441	8.08	-	3.08	34.47		125

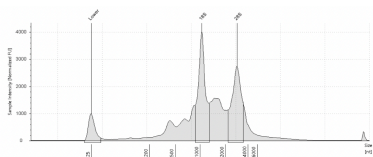
L2-32.11B C4+26



Well	80%	20% (SOL)	Cont. Input	Sample Description	Alert	Observations
C2	7.2	1.4	3070			Control Input Spectra Gap Detected

Size (bp)	Calibrated Conc. (ng/μl)	Assigned Conc. (ng/μl)	Peak Molarity (μM)	% Integrated Area	Peak Comment	Observations
121	40.0	40.0	2.00	24.53		Cont. Molar
201	2.9	-	1.28	1.6		125
441	8.08	-	3.08	34.47		125

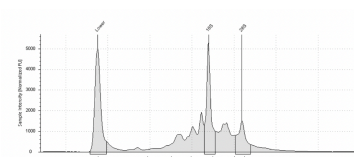
L2-32.16B C2+21



Well	80%	20% (SOL)	Cont. Input	Sample Description	Alert	Observations
D1	7.2	1.4	3070			Control Input Spectra Gap Detected

Size (bp)	Calibrated Conc. (ng/μl)	Assigned Conc. (ng/μl)	Peak Molarity (μM)	% Integrated Area	Peak Comment	Observations
121	40.0	40.0	2.00	24.53		Cont. Molar
201	2.9	-	1.28	1.6		125
441	8.08	-	3.08	34.47		125

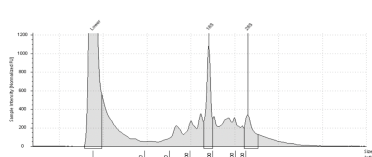
L2-32.12A C2+16



Well	80%	20% (SOL)	Cont. Input	Sample Description	Alert	Observations
D1	7.2	1.4	3070			Control Input Spectra Gap Detected

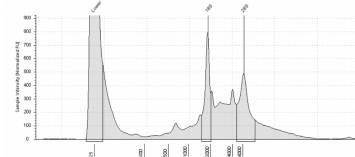
Size (bp)	Calibrated Conc. (ng/μl)	Assigned Conc. (ng/μl)	Peak Molarity (μM)	% Integrated Area	Peak Comment	Observations
121	40.0	40.0	2.00	24.53		Cont. Molar
201	2.9	-	1.28	1.6		125
441	8.08	-	3.08	34.47		125

L2-32.22A C2+19



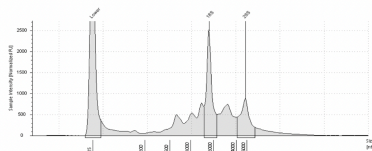
Well	RNA	Cont. Log2(I)	Sample Description	Alert
------	-----	---------------	--------------------	-------

Size (Å)	Calibrated Conc. (mg/dL)	Assigned Conc. (mg/dL)	Peak Molarly (mg/dL)	% Integrated Area	Peak Comment	Observations
25	40.0	40.0	4710	-		Lower Marker
1774	3.15	-	3.22	63.40		HS



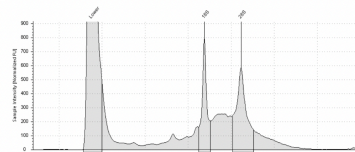
Well	Rf%	Cent. (mg/dl)	Sample Description	Alert
C7	8.6	13.6		▲

Size [a0]	Calibrated Conc. [mg/L]	Assigned Conc. [mg/L]	Peak Velocity [mm/s]	% Integrated Area	Peak Comment	Observations
25	40.0	40.0	4733	-		Lower Marker
1516	7.49	-	5.09	41.0%		185



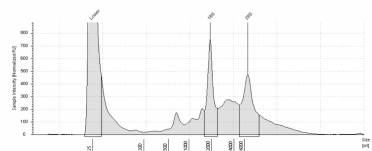
Well	RTs	Conc. (ng/l)	Sample Description	Alert
------	-----	--------------	--------------------	-------

Size [nm]	Calibrated Conc. [mg/dl]	Assigned Conc. [mg/dl]	Peak Molarly [nmol/l]	% Integrated Area	Peak Comment	Observations
35	40.0	-	47.15	-		Lower Marker
1750	11.2	-	18.8	62.82		105



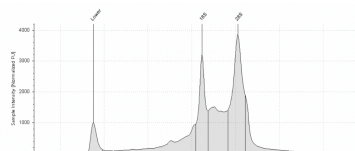
Sample Table

Size (nt)	Calibrated Conc. (μg/ml)	Assigned Conc. (μg/ml)	Peak Molarity (mole/L)	% Integrated Area	Peak Comment	Observations
25	40.0	40.0	4710	-		Lower Marker
1716	2.43	-	4.17	38.92		185



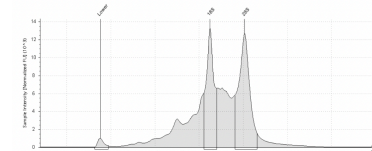
Well	RTS	Cont. (ng/ml)	Sample Description	Alert
------	-----	---------------	--------------------	-------

Size (µm)	Calibrated Conc. (µg/ml)	Assigned Conc. (µg/ml)	Peak Mass (amu)	% Integrated Area	Peak Comment	Observations
25	40.0	40.0	431.0	-		Lower Molar
1924	3.34	-	3.00	47.0%		185
680	3.76	-	4.4	57.6%		185



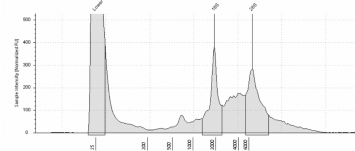
XX-01	0100%	240-500 (Ages)	Class: Level I	Example Description	Short	Observation
-------	-------	----------------	----------------	---------------------	-------	-------------

Size [µm]	Calibrated Conc.	Assigned Conc.	Peak Molarity	% Integrated Area	Peak Comment	Observation
25	750	750	82400	-		Lower Marker
1048	898	-	2520	35.00		



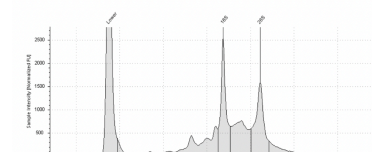
Well	RD%	28S/18S (Area)	Conc. (pg/μl)	Sample Description	Alert	Observations
F1	6.1	1.4	21300	IC		Cauton! Expir! Item Type device; Sample concentration outside recommended

Size [nt]	Calibrated Conc. [pmol/l]	Assigned Conc. [pmol/l]	Peak Melicity [pmol/l]	% Integrated Area	Peak Comment	Observations
25	700	700	8240	-		Lower Melicity
1599	4400	-	12400	41.96		185



Well	RfPc	Cont. (mg/L)	Sample Description	Alert
------	------	--------------	--------------------	-------

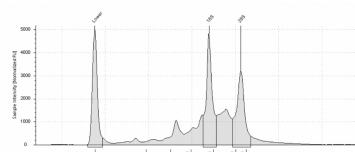
Size [Å]	Calibrated Conc. [mg/dl]	Assigned Conc. [mg/dl]	Peak Molarly [kDa]	% Integrated Area	Peak Comment	Observed
74	40.0	40.0	411.0			Lower Molar
101.8	2.07	-	2.33	64.48		185
163	2.07	-	64.63	785		



Sample Table

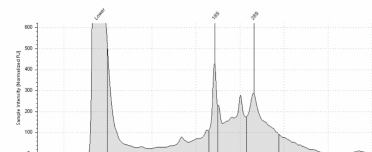
Category	Item	Value	Unit	Notes
Electronics	Smartphone	1200	USD	Latest model
	Laptop	800	USD	Business class
Clothing	Jeans	50	USD	Denim
	Shirts	30	USD	Cotton
Food	Apples	1.50	USD/lb	Organic
	Bananas	0.50	USD/lb	Local

Size (Å)	Calibrated Conc. (mg/mL)	Assigned Conc. (mg/mL)	Peak Molarity (mol/L)	% Integrated Area	Peak Comment	Observations
25	40.0	40.0	4710	-		Lower Molar



Well	RfPo	Cont. (ng/dl)	Sample Description	Alert
01	8.3	99.7		

Size (Å)	Calculated Conc. (mg/L)	Assigned Conc. (mg/L)	Peak Molarity (mol/L)	% Integrated Area	Peak Comment	Observation
25	40.0	40.0	4710	-		lower Molar
175	25.3	-	39.2	52.16		185
460	21.4	-	12.9	47.84		205

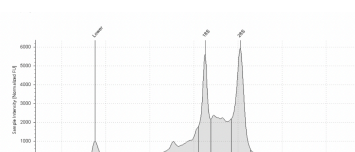


Sample Table


R0	7.9	12.1				
----	-----	------	--	--	--	--

Peak Table

Size (u)	Calibrated Conc. [mg/L]	Assigned Conc. [mg/L]	Peak Molarity [mmol/L]	%Integrated Area	Peak Comment	Observation
15	40.0	40.0	4310	-		Lower Molar



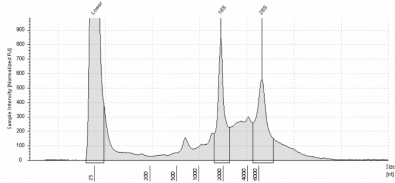
Sample Table

HI	7.2	1.5	7179	HS		Customer: Export Screen Type device
----	-----	-----	------	----	---	-------------------------------------

Peak Table

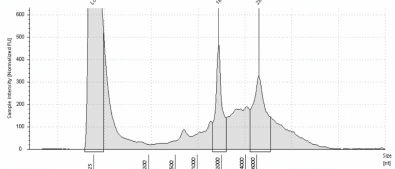
Size [nt]	Calibrated Conc. [mg/ml]	Assigned Conc. [mg/ml]	Peak Molarity [mol/l]	% Integrated Area	Peak Comment	Observations
34						

Supplementary data



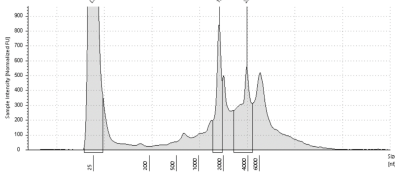
Sample Table					
Well	RP%	Conc. (µg/mL)	Sample Description	Alert	
A4	8.7	17.9			

Peak Table						
Size (µl)	Calibrated Conc. (µg/mL)	Assigned Conc. (µg/mL)	Peak Molarity (µmol/L)	%Integrated Area	Peak Comment	Observations
25	4810	4810	4710	1.87		
1883	1.50	-	1.46	47.51		Lower Marker
4812	1.86	-	1.87	52.49		185



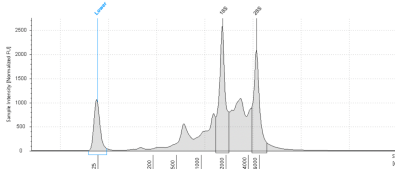
Sample Table					
Well	RP%	Conc. (µg/mL)	Sample Description	Alert	
B6	8.7	11.2			

Peak Table						
Size (µl)	Calibrated Conc. (µg/mL)	Assigned Conc. (µg/mL)	Peak Molarity (µmol/L)	%Integrated Area	Peak Comment	Observations
25	4810	4810	4710	1.67		
1883	1.86	-	1.87	41.49		Lower Marker
4812	2.38	-	1.87	58.51		185



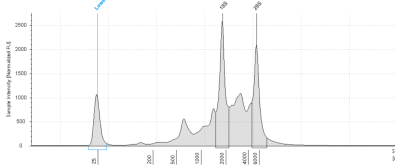
Sample Table					
Well	RP%	Conc. (µg/mL)	Sample Description	Alert	
B8	8.8	11.8			

Peak Table						
Size (µl)	Calibrated Conc. (µg/mL)	Assigned Conc. (µg/mL)	Peak Molarity (µmol/L)	%Integrated Area	Peak Comment	Observations
25	4810	4810	4710	1.67		
1883	2.36	-	1.87	41.50		Lower Marker
3955	1.50	-	2.61	58.71		185



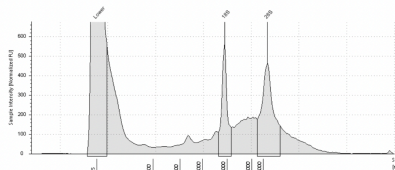
Sample Table					
Well	RP%	200/300 (Area)	Conc. (µg/mL)	Sample Description	Alert
B8	7.4	11.9	2640	13.4551 (2+21)	

Peak Table						
Size (µl)	Calibrated Conc. (µg/mL)	Assigned Conc. (µg/mL)	Peak Molarity (µmol/L)	%Integrated Area	Peak Comment	Observations
25	700	700	6340	1.46		calcd Lower Marker
1883	1.50	-	1.46	55.50		185
3553	1.59	-	299	48.10		185



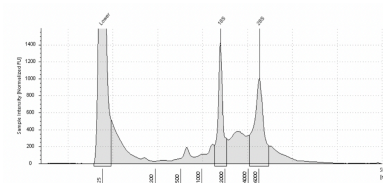
Sample Table					
Well	RP%	200/300 (Area)	Conc. (µg/mL)	Sample Description	Alert
B8	8.8	11.8	2640	13.4551 (2+21)	

Peak Table						
Size (µl)	Calibrated Conc. (µg/mL)	Assigned Conc. (µg/mL)	Peak Molarity (µmol/L)	%Integrated Area	Peak Comment	Observations
25	700	700	6340	1.46		calcd Lower Marker
1883	1.50	-	1.46	55.50		185
3553	1.59	-	299	48.10		185



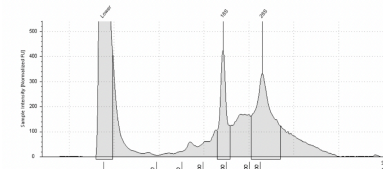
Sample Table					
Well	RP%	Conc. (µg/mL)	Sample Description	Alert	
D4	8.7	16.0			

Peak Table						
Size (µl)	Calibrated Conc. (µg/mL)	Assigned Conc. (µg/mL)	Peak Molarity (µmol/L)	%Integrated Area	Peak Comment	Observations
25	4810	4810	4710	2.29		
1873	1.79	-	1.82	32.57		185
7012	3.17	-	1.82	68.43		185



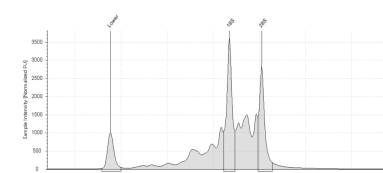
Sample Table					
Well	RP%	Conc. (µg/mL)	Sample Description	Alert	
E4	8.7	21.9			

Peak Table						
Size (µl)	Calibrated Conc. (µg/mL)	Assigned Conc. (µg/mL)	Peak Molarity (µmol/L)	%Integrated Area	Peak Comment	Observations
25	4810	4810	4710	1.86		
1792	4.35	-	2.26	41.76		185
6706	1.86	-	1.86	58.31		185



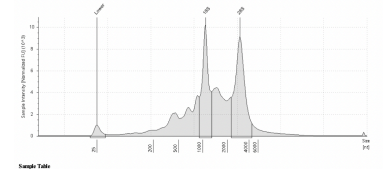
Sample Table					
Well	RP%	Conc. (µg/mL)	Sample Description	Alert	
F4	8.7	12.4			

Peak Table						
Size (µl)	Calibrated Conc. (µg/mL)	Assigned Conc. (µg/mL)	Peak Molarity (µmol/L)	%Integrated Area	Peak Comment	Observations
25	4810	4810	4710	1.86		
1811	1.86	-	1.86	32.81		Lower Marker
6368	3.77	-	1.86	68.09		185



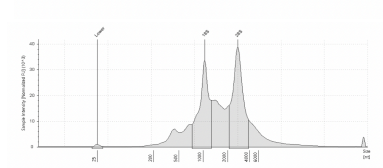
Sample Table					
Well	RP%	200/300 (Area)	Conc. (µg/mL)	Sample Description	Alert
E2	7.1	8.8	12.497 (2+21)		

Peak Table						
Size (µl)	Calibrated Conc. (µg/mL)	Assigned Conc. (µg/mL)	Peak Molarity (µmol/L)	%Integrated Area	Peak Comment	Observations
25	700	700	6340	1.50		Lower Marker
1883	6.75	-	1.50	55.75		185
3735	697	-	285	48.92		185



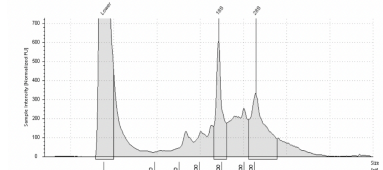
Sample Table					
Well	RP%	200/300 (Area)	Conc. (µg/mL)	Sample Description	Alert
A7	6.4	1.1	15306	14	

Peak Table						
Size (µl)	Calibrated Conc. (µg/mL)	Assigned Conc. (µg/mL)	Peak Molarity (µmol/L)	%Integrated Area	Peak Comment	Observations
25	700	700	6340	1.50		Lower Marker
2440	2700	-	2700	57.50		185



Sample Table					
Well	RP%	200/300 (Area)	Conc. (µg/mL)	Sample Description	Alert
B0	6.4	1.1	16400	14	

Peak Table						
Size (µl)	Calibrated Conc. (µg/mL)	Assigned Conc. (µg/mL)	Peak Molarity (µmol/L)	%Integrated Area	Peak Comment	Observations
25	700	700	6340	1.50		Lower Marker
2440	2700	-	2700	57.50		185



Sample Table					
Well	RP%	Conc. (µg/mL)	Sample Description	Alert	
D5	8.7	11.7			

Peak Table						
Size (µl)	Calibrated Conc. (µg/mL)	Assigned Conc. (µg/mL)	Peak Molarity (µmol/L)	%Integrated Area	Peak Comment	Observations
25	4810	4810	4710	1.87		
1824	2.29	-	1.87	42.57		Lower Marker
4443	1.12	-	1.87	57.51		185

L2-32.67A C2+19

L2-32.44B C3+19

L2-32.67A C2+51

L2-32.44B C3+21

L2-32.71A C2+21

L2-32.44B C3+51

L2-32.72B C+19

L2-32.55A C2+19

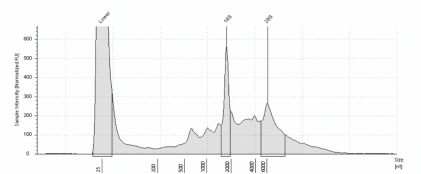
L2-32.72B C+23

L2-32.55A C2+21

L2-32.72B C2+26

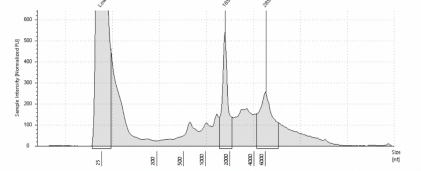
L2-32.67A C2+16

Supplementary data



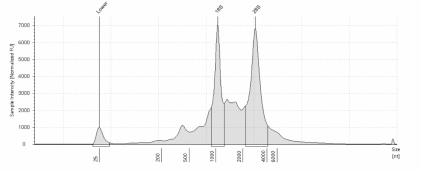
Well	RT	RT%	Conc. (µg/mL)	Sample Description	Alert
C2	12.1	9.8	1.2		

Size [µL]	Calibrated Conc. [µg/mL]	Assigned Conc. [µg/mL]	Peak Molarity [µmol/L]	% Integrated Area	Peak Comment	Observations
25	40.0	40.0	4.710	2.6		
179	1.9	-	2.6	1.48	Lower Molar	
479	2.49	-	3.78	21.81		



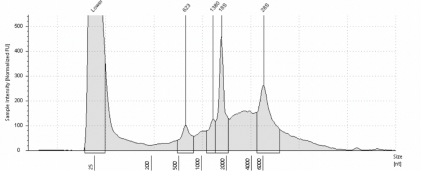
Well	RT	RT%	Conc. (µg/mL)	Sample Description	Alert
C3	12.1	9.8	1.2		

Size [µL]	Calibrated Conc. [µg/mL]	Assigned Conc. [µg/mL]	Peak Molarity [µmol/L]	% Integrated Area	Peak Comment	Observations
25	40.0	40.0	4.710	2.6		
179	1.9	-	2.6	1.48	Lower Molar	
6271	2.49	-	3.78	21.81		



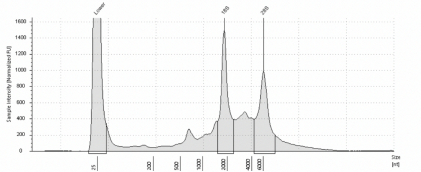
Well	RT	RT%	Conc. (µg/mL)	Sample Description	Alert	Observations
C2	12.1	9.8	1.5			

Size [µL]	Calibrated Conc. [µg/mL]	Assigned Conc. [µg/mL]	Peak Molarity [µmol/L]	% Integrated Area	Peak Comment	Observations
25	40.0	40.0	4.710	2.6		
179	1.9	-	2.6	1.48	Lower Molar	
2879	2.49	-	3.78	21.81		



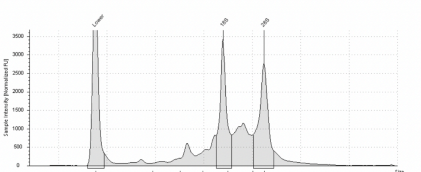
Well	RT	RT%	Conc. (µg/mL)	Sample Description	Alert
C2	12.1	9.8	1.5		

Size [µL]	Calibrated Conc. [µg/mL]	Assigned Conc. [µg/mL]	Peak Molarity [µmol/L]	% Integrated Area	Peak Comment	Observations
25	40.0	40.0	4.710	12.63		
633	0.533	-	0.64	0.36		
179	1.9	-	2.6	1.48	Lower Molar	
174	1.47	-	1.77	1.01		
6252	1.89	-	2.27	1.35		



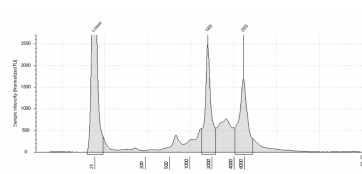
Well	RT	RT%	Conc. (µg/mL)	Sample Description	Alert
C2	12.1	9.8	1.5		

Size [µL]	Calibrated Conc. [µg/mL]	Assigned Conc. [µg/mL]	Peak Molarity [µmol/L]	% Integrated Area	Peak Comment	Observations
25	40.0	40.0	4.710	51.32		
179	1.9	-	2.6	46.6	Lower Molar	
175	1.87	-	2.25	1.35		



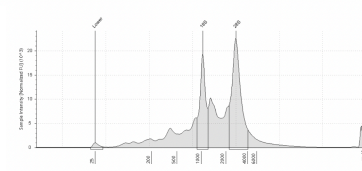
Well	RT	RT%	Conc. (µg/mL)	Sample Description	Alert
C2	12.1	9.8	1.5		

Size [µL]	Calibrated Conc. [µg/mL]	Assigned Conc. [µg/mL]	Peak Molarity [µmol/L]	% Integrated Area	Peak Comment	Observations
25	40.0	40.0	4.710	46.71	Lower Molar	
179	1.9	-	2.6	53.29		
1095	19.1	-	22.9	1.01		



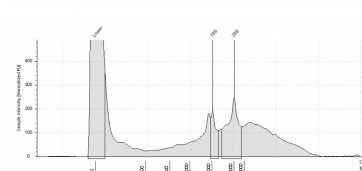
Well	RT	RT%	Conc. (µg/mL)	Sample Description	Alert
C2	12.1	9.8	40.0		

Size [µL]	Calibrated Conc. [µg/mL]	Assigned Conc. [µg/mL]	Peak Molarity [µmol/L]	% Integrated Area	Peak Comment	Observations
25	40.0	40.0	4.710	2.6		
179	1.9	-	2.6	1.48	Lower Molar	
1095	19.1	-	22.9	1.01		



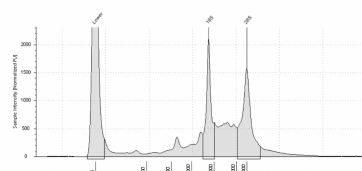
Well	RT	RT%	Conc. (µg/mL)	Sample Description	Alert	Observations
C2	12.1	9.8	1.8			

Size [µL]	Calibrated Conc. [µg/mL]	Assigned Conc. [µg/mL]	Peak Molarity [µmol/L]	% Integrated Area	Peak Comment	Observations
25	40.0	40.0	4.710	2.6		
1095	19.1	-	22.9	1.01		
2879	2.49	-	3.78	21.81		



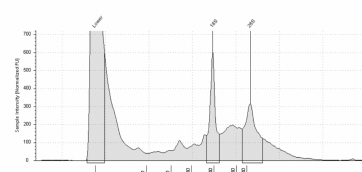
Well	RT	RT%	Conc. (µg/mL)	Sample Description	Alert
C2	12.1	9.8	1.5		

Size [µL]	Calibrated Conc. [µg/mL]	Assigned Conc. [µg/mL]	Peak Molarity [µmol/L]	% Integrated Area	Peak Comment	Observations
25	40.0	40.0	4.710	2.6		
179	1.9	-	2.6	1.48	Lower Molar	
633	0.533	-	0.64	0.36		



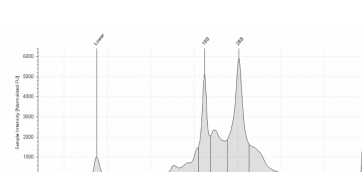
Well	RT	RT%	Conc. (µg/mL)	Sample Description	Alert
C2	12.1	9.8	34.8		

Size [µL]	Calibrated Conc. [µg/mL]	Assigned Conc. [µg/mL]	Peak Molarity [µmol/L]	% Integrated Area	Peak Comment	Observations
25	40.0	40.0	4.710	2.6		
179	1.9	-	2.6	1.48	Lower Molar	
681	9.77	-	11.73	58.82		



Well	RT	RT%	Conc. (µg/mL)	Sample Description	Alert
C2	12.1	9.8	11.7		

Size [µL]	Calibrated Conc. [µg/mL]	Assigned Conc. [µg/mL]	Peak Molarity [µmol/L]	% Integrated Area	Peak Comment	Observations
25	40.0	40.0	4.710	2.6		
179	1.9	-	2.6	1.48	Lower Molar	
681	9.77	-	11.73	58.82		



Well	RT	RT%	Conc. (µg/mL)	Sample Description	Alert	Observations
C2	12.1	9.8	1.8			

Size [µL]	Calibrated Conc. [µg/mL]	Assigned Conc. [µg/mL]	Peak Molarity [µmol/L]	% Integrated Area	Peak Comment	Observations
25	40.0	40.0	4.710	2.6		
1095	19.1	-	22.9	1.01		
2879	2.49	-	3.78	21.81		

L2-32.77B C2+9

L2-32.72B C2+28

L2-32.79A C2+19

L2-32.75B C4+28

L2-32.79A C2+21

L2-32.76B C+19

L2-32.79A C2+26

L2-32.76B C+21

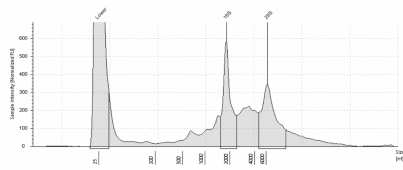
L2-32.79A C2+30

L2-32.77B C+19

L2-32.79A C3+21

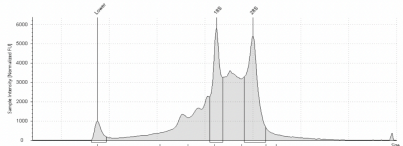
L2-32.77B C+21

Supplementary data



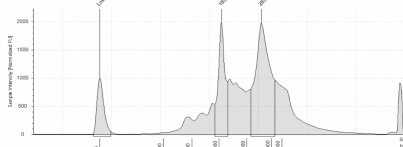
Sample Table		Well	RT%	Comp. Inj. (µl)	Sample Description	Alert
		F5	8.2	2.2		▲

Peak Table		Size (µl)	Calibrated Conc. (µg/ml)	Assigned Conc. (µg/ml)	Peak Molarity (mmol/l)	%Integrated Area	Peak Comment	Observations
21	40.0	40.0	47.0					Lower Molar
184	1.9	-	1.45	47.20				185
6322	3.12	-	1.45	31.80				185



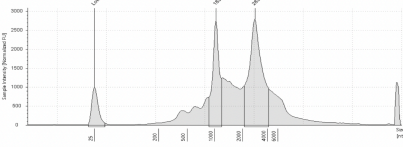
Sample Table		Well	RT%	280-380 (Area)	Comp. Inj. (µl)	Sample Description	Alert	Observations
		F2	6.8	1.5	9.00	66	▲	Current Injection System 7 ago device

Peak Table		Size (µl)	Calibrated Conc. (µg/ml)	Assigned Conc. (µg/ml)	Peak Molarity (mmol/l)	%Integrated Area	Peak Comment	Observations
15	15.00	15.00	15.00	42.18				Lower Molar
1077	1.00	-	1.00	1.00				185
2742	2.00	-	2.00	70.62				185



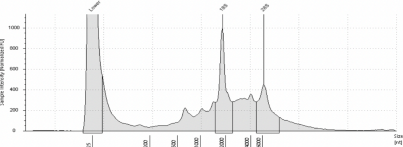
Sample Table		Well	RT%	280-380 (Area)	Comp. Inj. (µl)	Sample Description	Alert	Observations
		G2	7.2	2.1	3.00	86	▲	Current Injection System 7 ago device

Peak Table		Size (µl)	Calibrated Conc. (µg/ml)	Assigned Conc. (µg/ml)	Peak Molarity (mmol/l)	%Integrated Area	Peak Comment	Observations
25	10.00	10.00	10.00	67.43				Lower Molar
3053	1.10	-	1.10	1.10				185
3053	1.10	-	1.10	67.43				185



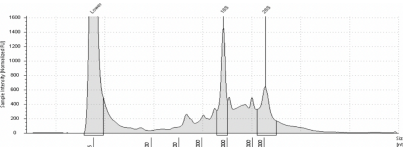
Sample Table		Well	RT%	280-380 (Area)	Comp. Inj. (µl)	Sample Description	Alert	Observations
		H0	7.8	2.0	9.00	67	▲	Current Injection System 7 ago device

Peak Table		Size (µl)	Calibrated Conc. (µg/ml)	Assigned Conc. (µg/ml)	Peak Molarity (mmol/l)	%Integrated Area	Peak Comment	Observations
15	15.00	15.00	15.00	53.32				Lower Molar
1028	1.00	-	1.00	1.00				185
2827	1.10	-	1.10	60.68				185



Sample Table		Well	RT%	Comp. Inj. (µl)	Sample Description	Alert
		H7	7.8	15.0		▲

Peak Table		Size (µl)	Calibrated Conc. (µg/ml)	Assigned Conc. (µg/ml)	Peak Molarity (mmol/l)	%Integrated Area	Peak Comment	Observations
15	15.00	15.00	15.00	46.84				Lower Molar
1070	1.00	-	1.00	1.00				185
2671	1.00	-	1.00	45.50				185



Sample Table		Well	RT%	Comp. Inj. (µl)	Sample Description	Alert
		G7	8.2	21.0		▲

Peak Table		Size (µl)	Calibrated Conc. (µg/ml)	Assigned Conc. (µg/ml)	Peak Molarity (mmol/l)	%Integrated Area	Peak Comment	Observations
15	15.00	15.00	15.00	37.05				Lower Molar
1070	1.00	-	1.00	1.00				185
2671	1.00	-	1.00	45.50				185

L2-32.79A C3+37

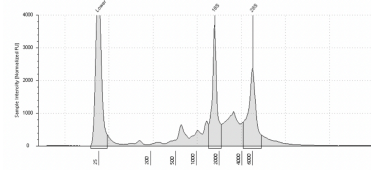
L2-32.88B C+19

L2-32.88B C+21

L2-32.88B C4+47

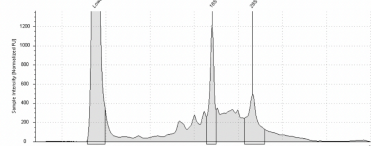
L2-32.90A C2+19

L2-32.90A C2+21



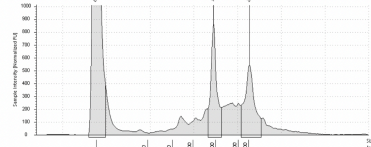
Sample Table		Well	RT%	Comp. Inj. (µl)	Sample Description	Alert
		G7	8.8	15.0		▲

Peak Table		Size (µl)	Calibrated Conc. (µg/ml)	Assigned Conc. (µg/ml)	Peak Molarity (mmol/l)	%Integrated Area	Peak Comment	Observations
15	40.0	40.0	47.0					Lower Molar
1347	11.0	-	11.0	40.11				185
6322	3.12	-	3.12	31.80				185



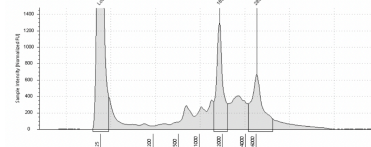
Sample Table		Well	RT%	Comp. Inj. (µl)	Sample Description	Alert
		E7	10.0	15.0		▲

Peak Table		Size (µl)	Calibrated Conc. (µg/ml)	Assigned Conc. (µg/ml)	Peak Molarity (mmol/l)	%Integrated Area	Peak Comment	Observations
15	40.0	40.0	47.0					Lower Molar
1700	1.00	-	1.00	51.97				185
6327	3.11	-	3.11	40.05				185



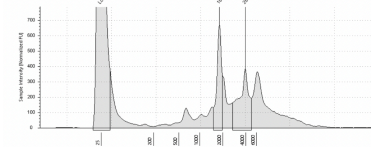
Sample Table		Well	RT%	Comp. Inj. (µl)	Sample Description	Alert
		F7	8.2	15.2		▲

Peak Table		Size (µl)	Calibrated Conc. (µg/ml)	Assigned Conc. (µg/ml)	Peak Molarity (mmol/l)	%Integrated Area	Peak Comment	Observations
25	40.0	40.0	47.0					Lower Molar
1481	1.00	-	1.00	42.02				185
6288	3.37	-	3.37	31.80				185



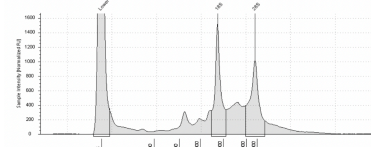
Sample Table		Well	RT%	Comp. Inj. (µl)	Sample Description	Alert
		G7	7.8	21.2		▲

Peak Table		Size (µl)	Calibrated Conc. (µg/ml)	Assigned Conc. (µg/ml)	Peak Molarity (mmol/l)	%Integrated Area	Peak Comment	Observations
25	40.0	40.0	47.0					Lower Molar
1441	1.00	-	1.00	42.02				185
6279	3.32	-	3.32	43.32				185



Sample Table		Well	RT%	Comp. Inj. (µl)	Sample Description	Alert
		H7	8.0	11.0		▲

Peak Table		Size (µl)	Calibrated Conc. (µg/ml)	Assigned Conc. (µg/ml)	Peak Molarity (mmol/l)	%Integrated Area	Peak Comment	Observations
15	15.00	15.00	15.00	40.34				Lower Molar
1077	1.00	-	1.00	1.00				185
2645	1.00	-	1.00	30.88				185



Sample Table		Well	RT%	Comp. Inj. (µl)	Sample Description	Alert
		H2	8.2	21.0		▲

Peak Table		Size (µl)	Calibrated Conc. (µg/ml)	Assigned Conc. (µg/ml)	Peak Molarity (mmol/l)	%Integrated Area	Peak Comment	Observations
15	15.00	15.00	15.00	40.34				Lower Molar
1077	1.00	-	1.00	1.00				185
2645	1.00	-	1.00	30.88				185

L2-32.88B C4+47

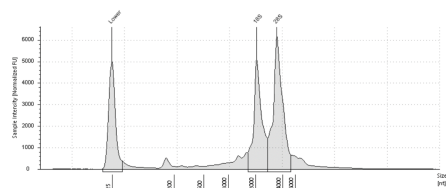
L2-32.90A C2+19

L2-32.90A C2+21

L2-32.90A C3+37

L2-32.91B C+19

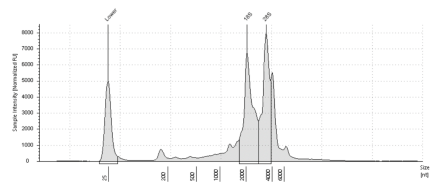
L2-32.91B C2+28

Tapestation electropherograms (Sequencing facility Bonn) – *in vitro*

NF54

Sample Table		Well	RNA	Conc. (ng/μl)	Sample Description	Alert
		12	54	74.1		

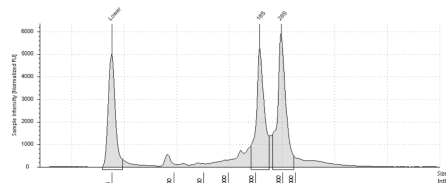
Size [nt]	Calibrated Conc. [ng/μl]	Assigned Conc. [ng/μl]	Peak Molarity [pmol/l]	%Integrated Area	Peak Comment	Observations
25	40.0	40.0	4710	42.34		Lower Marker
200	24.7	-	33.4	46.96		185
3406	33.8	-	28.7	87.76		285



NF54

Sample Table		Well	RNA	Conc. (ng/μl)	Sample Description	Alert
		12	54	8.8		

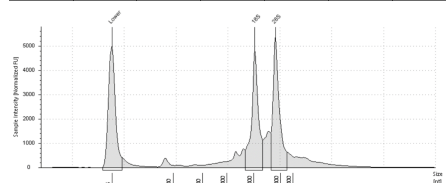
Size [nt]	Calibrated Conc. [ng/μl]	Assigned Conc. [ng/μl]	Peak Molarity [pmol/l]	%Integrated Area	Peak Comment	Observations
25	40.0	40.0	4710	42.34		Lower Marker
200	31.7	-	33.4	81.02		185
3407	31.1	-	28.7	46.96		285



NF54

Sample Table		Well	RNA	Conc. (ng/μl)	Sample Description	Alert
		12	54	74.1		

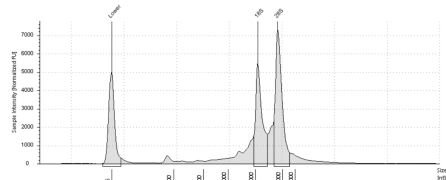
Size [nt]	Calibrated Conc. [ng/μl]	Assigned Conc. [ng/μl]	Peak Molarity [pmol/l]	%Integrated Area	Peak Comment	Observations
25	40.0	40.0	4710	42.34		Lower Marker
200	23.8	-	33.4	45.81		185
3872	28.1	-	21.3	54.19		285



NF54

Sample Table		Well	RNA	Conc. (ng/μl)	Sample Description	Alert
		12	54	62.4		

Size [nt]	Calibrated Conc. [ng/μl]	Assigned Conc. [ng/μl]	Peak Molarity [pmol/l]	%Integrated Area	Peak Comment	Observations
25	40.0	40.0	4710	42.37		Lower Marker
2000	30.8	-	26.9	48.17		185



NF54

Sample Table		Well	RNA	Conc. (ng/μl)	Sample Description	Alert
		12	54	40.1		

Size [nt]	Calibrated Conc. [ng/μl]	Assigned Conc. [ng/μl]	Peak Molarity [pmol/l]	%Integrated Area	Peak Comment	Observations
25	40.0	40.0	4710	42.85		Lower Marker
2135	24.9	-	34.3	42.85		185
2581	33.2	-	27.5	87.15		285

Supplementary Figure 7: Tapestation electropherograms for RNA samples.

Electropherograms conducted at the sequencing facility in Bonn prior to sequencing or all 60x *in vivo* and 5x *in vitro* RNA-seq samples. The degree of degradation was low and all samples were included for RNA-seq. RIN value for samples with RNA from two or more species is less reliable since, in particular, the human 28S rRNA is substantially larger (4.7-5.0 kb) than the *P. falciparum* 28S rRNA (4.1 kb) introducing a double peak which affects RIN value calculation.

Rsubread 2.12.3

```

Input files : 33 BAM files

B-L2-001_C2_21.bam
B-L2-012_C2_16.bam
B-L2-012_C3_21.bam
B-L2-014_C2_21.bam
B-L2-014_C2_23.bam
B-L2-016_C2_21.bam
B-L2-023_C2_19.bam
B-L2-042_C2_23.bam
B-L2-044_C_14.bam
B-L2-044_C_19.bam
B-L2-044_C_21.bam
B-L2-055_C2_19.bam
B-L2-055_C2_21.bam
B-L2-067_C2_16.bam
B-L2-067_C2_19.bam
B-L2-072_C_19.bam
B-L2-072_C_23.bam
B-L2-076_C_19.bam
B-L2-077_C_19.bam
B-L2-077_C_21.bam
B-L2-079_C2_19.bam
B-L2-079_C2_21.bam
B-L2-088_C_21.bam
B-L2-090_C2_19.bam
B-L2-091_C_21.bam
C-L2-011_C4_26.bam
C-L2-044_C3_19.bam
C-L2-044_C3_21.bam
C-L2-044_C3_51.bam
C-L2-077_C2_9.bam
C-L2-090_C2_30.bam
C-L2-090_C3_21.bam
C-L2-090_C3_23.bam

Paired-end : yes
Count read pairs : yes
Annotation : PlasmoDB-62_Pfalciparum3D7.gff (GTF)
Dir for temp files : .
Threads : 1
Level : meta-feature level

```

```

||      Multimapping reads : counted      ||
|| Multi-overlapping reads : not counted  ||
||      Min overlapping bases : 1          ||
||                                         ||
||=====||
||//===== Running =====\\
||                                         ||
|| Load annotation file PlasmoDB-62_Pfalciparum3D7.gff ... ||
||      Features : 15097                  ||
||      Meta-features : 5720              ||
||      Chromosomes/contigs : 16          ||
||                                         ||
|| Process BAM file B-L2-001_C2_21.bam... ||
||      Paired-end reads are included.    ||
||      Total alignments : 877788         ||
||      Successfully assigned alignments : 867327 (98.8%) ||
||      Running time : 0.05 minutes       ||
||                                         ||
|| Process BAM file B-L2-012_C2_16.bam... ||
||      Paired-end reads are included.    ||
||      Total alignments : 12977328       ||
||      Successfully assigned alignments : 4795060 (36.9%) ||
||      Running time : 0.97 minutes       ||
||                                         ||
|| Process BAM file B-L2-012_C3_21.bam... ||
||      Paired-end reads are included.    ||
||      Total alignments : 2706649        ||
||      Successfully assigned alignments : 2671207 (98.7%) ||
||      Running time : 0.12 minutes       ||
||                                         ||
|| Process BAM file B-L2-014_C2_21.bam... ||
||      Paired-end reads are included.    ||
||      Total alignments : 1017409        ||
||      Successfully assigned alignments : 1000024 (98.3%) ||
||      Running time : 0.05 minutes       ||
||                                         ||
|| Process BAM file B-L2-014_C2_23.bam... ||
||      Paired-end reads are included.    ||
||      Total alignments : 3442147        ||
||      Successfully assigned alignments : 3389945 (98.5%) ||
||      Running time : 0.19 minutes       ||
||                                         ||
|| Process BAM file B-L2-016_C2_21.bam... ||
||      Paired-end reads are included.    ||
||      Total alignments : 946871         ||
||      Successfully assigned alignments : 915220 (96.7%) ||
||      Running time : 0.06 minutes       ||
||                                         ||
|| Process BAM file B-L2-023_C2_19.bam... ||

```

Supplementary data

```
|| Paired-end reads are included.
|| Total alignments : 1918120
|| Successfully assigned alignments : 1899668 (99.0%)
|| Running time : 0.10 minutes
||
|| Process BAM file B-L2-042_C2_23.bam...
|| Paired-end reads are included.
|| Total alignments : 1454343
|| Successfully assigned alignments : 1433050 (98.5%)
|| Running time : 0.07 minutes
||
|| Process BAM file B-L2-044_C_14.bam...
|| Paired-end reads are included.
|| Total alignments : 459924
|| Successfully assigned alignments : 453427 (98.6%)
|| Running time : 0.02 minutes
||
|| Process BAM file B-L2-044_C_19.bam...
|| Paired-end reads are included.
|| Total alignments : 3788029
|| Successfully assigned alignments : 3734838 (98.6%)
|| Running time : 0.18 minutes
||
|| Process BAM file B-L2-044_C_21.bam...
|| Paired-end reads are included.
|| Total alignments : 1420587
|| Successfully assigned alignments : 1401102 (98.6%)
|| Running time : 0.07 minutes
||
|| Process BAM file B-L2-055_C2_19.bam...
|| Paired-end reads are included.
|| Total alignments : 82148356
|| Successfully assigned alignments : 81241368 (98.9%)
|| Running time : 7.85 minutes
||
|| Process BAM file B-L2-055_C2_21.bam...
|| Paired-end reads are included.
|| Total alignments : 32240137
|| Successfully assigned alignments : 31903328 (99.0%)
|| Running time : 2.34 minutes
||
|| Process BAM file B-L2-067_C2_16.bam...
|| Paired-end reads are included.
|| Total alignments : 641367
|| Successfully assigned alignments : 633633 (98.8%)
|| Running time : 0.03 minutes
||
|| Process BAM file B-L2-067_C2_19.bam...
|| Paired-end reads are included.
|| Total alignments : 549064
```

Supplementary data

```
|| Successfully assigned alignments : 542541 (98.8%)
|| Running time : 0.03 minutes
||
|| Process BAM file B-L2-072_C_19.bam...
|| Paired-end reads are included.
|| Total alignments : 1949849
|| Successfully assigned alignments : 1921962 (98.6%)
|| Running time : 0.10 minutes
||
|| Process BAM file B-L2-072_C_23.bam...
|| Paired-end reads are included.
|| Total alignments : 2558777
|| Successfully assigned alignments : 2501689 (97.8%)
|| Running time : 0.13 minutes
||
|| Process BAM file B-L2-076_C_19.bam...
|| Paired-end reads are included.
|| Total alignments : 1605576
|| Successfully assigned alignments : 1574714 (98.1%)
|| Running time : 0.10 minutes
||
|| Process BAM file B-L2-077_C_19.bam...
|| Paired-end reads are included.
|| Total alignments : 790001
|| Successfully assigned alignments : 779714 (98.7%)
|| Running time : 0.06 minutes
||
|| Process BAM file B-L2-077_C_21.bam...
|| Paired-end reads are included.
|| Total alignments : 640354
|| Successfully assigned alignments : 631104 (98.6%)
|| Running time : 0.04 minutes
||
|| Process BAM file B-L2-079_C2_19.bam...
|| Paired-end reads are included.
|| Total alignments : 2116096
|| Successfully assigned alignments : 2083764 (98.5%)
|| Running time : 0.11 minutes
||
|| Process BAM file B-L2-079_C2_21.bam...
|| Paired-end reads are included.
|| Total alignments : 1826993
|| Successfully assigned alignments : 1695733 (92.8%)
|| Running time : 0.10 minutes
||
|| Process BAM file B-L2-088_C_21.bam...
|| Paired-end reads are included.
|| Total alignments : 1508280
|| Successfully assigned alignments : 1474975 (97.8%)
|| Running time : 0.09 minutes
||
```

```

|| Process BAM file B-L2-090_C2_19.bam...
||   Paired-end reads are included.
||   Total alignments : 1223931
||   Successfully assigned alignments : 1205544 (98.5%)
||   Running time : 0.06 minutes
||
|| Process BAM file B-L2-091_C_21.bam...
||   Paired-end reads are included.
||   Total alignments : 1224419
||   Successfully assigned alignments : 1200006 (98.0%)
||   Running time : 0.06 minutes
||
|| Process BAM file C-L2-011_C4_26.bam...
||   Paired-end reads are included.
||   Total alignments : 1830881
||   Successfully assigned alignments : 1791724 (97.9%)
||   Running time : 0.09 minutes
||
|| Process BAM file C-L2-044_C3_19.bam...
||   Paired-end reads are included.
||   Total alignments : 2399433
||   Successfully assigned alignments : 2316742 (96.6%)
||   Running time : 0.12 minutes
||
|| Process BAM file C-L2-044_C3_21.bam...
||   Paired-end reads are included.
||   Total alignments : 983474
||   Successfully assigned alignments : 942011 (95.8%)
||   Running time : 0.05 minutes
||
|| Process BAM file C-L2-044_C3_51.bam...
||   Paired-end reads are included.
||   Total alignments : 1973036
||   Successfully assigned alignments : 1883119 (95.4%)
||   Running time : 0.09 minutes
||
|| Process BAM file C-L2-077_C2_9.bam...
||   Paired-end reads are included.
||   Total alignments : 738122
||   Successfully assigned alignments : 732137 (99.2%)
||   Running time : 0.03 minutes
||
|| Process BAM file C-L2-090_C2_30.bam...
||   Paired-end reads are included.
||   Total alignments : 682641
||   Successfully assigned alignments : 670038 (98.2%)
||   Running time : 0.03 minutes
||
|| Process BAM file C-L2-090_C3_21.bam...

```

```

|| Paired-end reads are included.
|| Total alignments : 475401
|| Successfully assigned alignments : 457151 (96.2%)
|| Running time : 0.02 minutes
||
|| Process BAM file C-L2-090_C3_23.bam...
|| Paired-end reads are included.
|| Total alignments : 156810
|| Successfully assigned alignments : 152670 (97.4%)
|| Running time : 0.01 minutes
||
|| Write the final count table.
|| Write the read assignment summary.
||
\\=====//

```

Hide

```

t <- fc_counts_CHMI$counts
fc_counts_CHMI$counts <- t
x <- DGEList(counts=fc_counts_CHMI$counts, genes=fc_counts_CHMI$annotation)

```

Hide

```

DfSamples <- c("B-L2-001_C2_21", "B-L2-012_C2_16", "B-L2-012-C3_21", "B-L2-014_C2_
21", "B-L2-014_C2_23", "B-L2-016_C2_21", "B-L2-023_C2_19", "B-L2-042_C2_23", "B-L2
-044_C_14", "B-L2-044_C_19", "B-L2-044_C_21", "B-L2-055_C2_19", "B-L2-055_C2_21",
"B-L2-067_C2_16", "B-L2-067_C2_19", "B-L2-072_C_19", "B-L2-072_C_23", "B-L2-076_C
19", "B-L2-077_C_19", "B-L2-077_C_21", "B-L2-079_C2_19", "B-L2-079_C2_21", "B-L2-0
88_C_21", "B-L2-090_C2_19", "B-L2-091_C_21", "C-L2-011_C4_26", "C-L2-044_C3_19", "
C-L2-044_C3_21", "C-L2-044_C3_51", "C-L2-077_C2_9", "C-L2-090_C2_30", "C-L2-090_C3
_21", "C-L2-090_C3_23")
head(DfSamples)
gene_counts_list<- DGEList(counts = fc_counts_CHMI$counts, samples = DfSamples, ge
nes = fc_counts_CHMI$annotation)

head(gene_counts_list)

```

#We next filter out genes that do not have sufficient coverage across our samples for reliable estimates to be made.

Hide

```

before <- nrow(gene_counts_list)
keep <- rowSums(cpm(gene_counts_list$counts)>2) >= 6
gene_counts_list2 <- gene_counts_list[keep,,keep.lib.sizes=FALSE]
x <- x[keep,,keep.lib.sizes=FALSE]
head(gene_counts_list2)

```

Hide

```

bplot <- melt(colSums(gene_counts_list2$counts))

```

Warning: The melt generic in data.table has been passed a numeric and will attempt to redirect to the relevant reshape2 method; please note that reshape2 is deprecated, and this redirection is now deprecated as well. To continue using melt methods from reshape2 while both libraries are attached, e.g. melt.list, you can prepend the namespace like reshape2::melt(colSums(gene_counts_list2\$counts)). In the next version, this warning will become an error.

```
bplot <- melt(colSums(gene_counts_list2$counts))
```

Warning: The melt generic in data.table has been passed a numeric and will attempt to redirect to the relevant reshape2 method; please note that reshape2 is deprecated, and this redirection is now deprecated as well. To continue using melt methods from reshape2 while both libraries are attached, e.g. melt.list, you can prepend the namespace like reshape2::melt(colSums(gene_counts_list2\$counts)). In the next version, this warning will become an error.

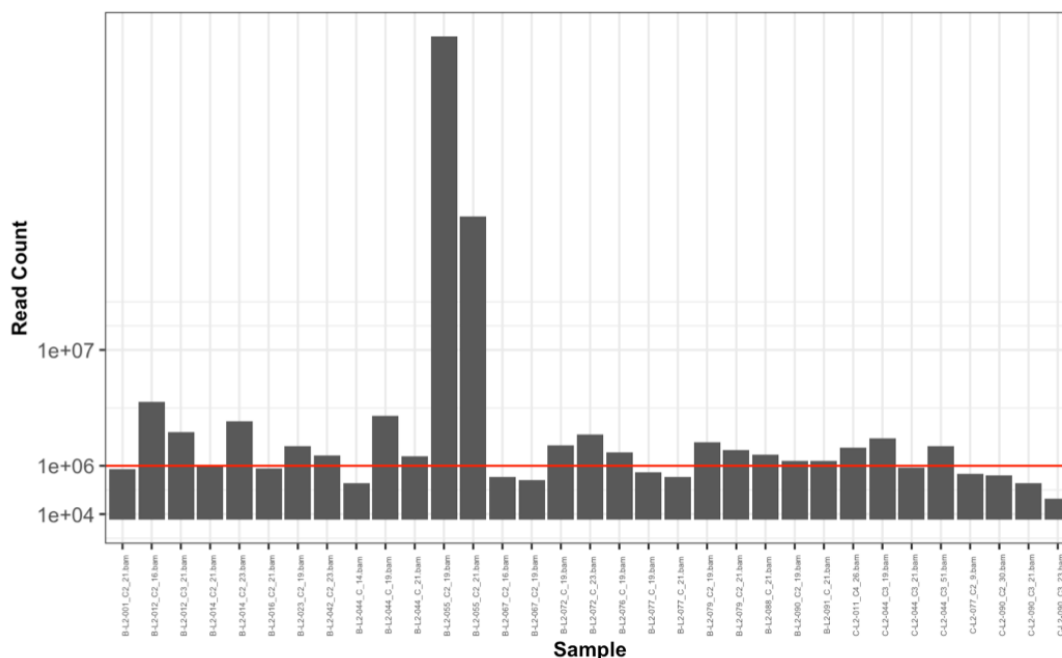
Hide

```
colnames(bplot) <- c("Read.Counts")
bplot$Sample <- rownames(bplot)

gg <- ggplot(bplot, aes(x=factor(Sample), y=Read.Counts)) + geom_bar(stat = "identity")
gg <- gg + theme_bw() + scale_y_sqrt(breaks=c(10000,1000000,10000000,100000000,1000000000))
gg <- gg + theme(axis.text.x = element_text(size=4, angle = 90),
  axis.text.y = element_text(size=10, angle = 0),
  axis.title=element_text(size=10,face="bold"))
gg <- gg + labs(x='Sample', y='Read Count')
gg <- gg + geom_hline(aes(yintercept=1000000), col="red")

filt.annotation <- fc_counts_CHMI$annotation[fc_counts_CHMI$annotation$GeneID %in% rownames(x$counts),]
dge <- DGEList(counts=x$counts, genes=filt.annotation)

plot(gg)
```



Supplementary data

#calculate rpkm and create file

Hide

```
our_log_rpkm <- rpkm(gene_counts_list2)
our_log_rpkm <- log2(1+our_log_rpkm)
rpkm_genes_log <- our_log_rpkm
write.csv(our_log_rpkm, "~/Desktop/BvsC-rpkm.txt")
```

#now load in transcriptomic data im using for comparison, from Lopez_B dataset, must first remove ookinete and then reorganise the data frame, then finally also log transform

Hide

```
su_rpkm <- read.csv(file="~/Desktop/B-vs-C/rpkm_7SexualAndAsexualLifeStages_sueta
1.csv", header = TRUE, sep = ",")

su_rpkm$Ookinete <- NULL
rownames(su_rpkm) <- su_rpkm$ID
su_rpkm$ID <- NULL
su_rpkm_log <- log2(1 +su_rpkm)
su_log_rpkm <-su_rpkm_log
```

#now everything set up run as per Gary's pipeline

Hide

```
findMix <- function(Y, X){
  X[is.na(X)] <- t(replicate(ncol(X), apply(X,1,mean, na.rm=T)))[is.na(X)]
  Rinv <- solve(chol(t(X) %*% X))
  C <- cbind(rep(1,ncol(X)), diag(ncol(X)))
  b <- c(1,rep(0,ncol(X)))
  d <- t(Y) %*% X
  qp <- solve.QP(Dmat = Rinv, factorized = TRUE, dvec = d, Amat = C, bvec = b, meq=
1)
  sol <- qp$solution
  sol[sol<1e-10] <- 0
  return(sol)
}

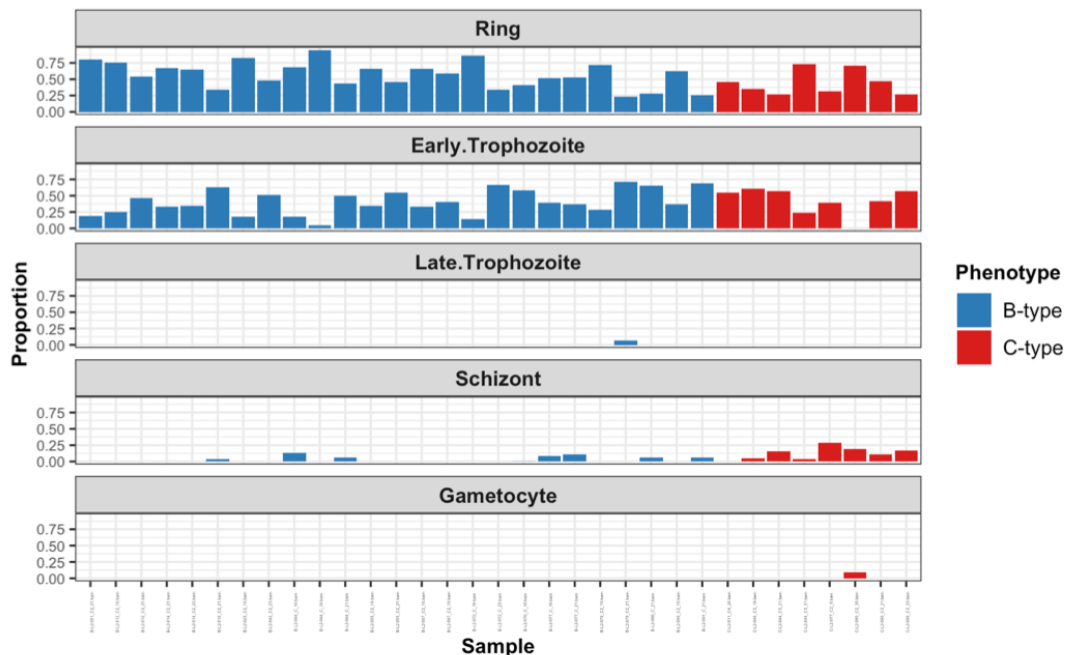
###Calculate Sample Life-Cycle Profiles
#We fit this mixture model to each of our samples in turn. The results are then pl
otted. A column represents each sample in the plot below. As we are fitting propor
tion parameters each columns values must add to 1 over the 5 stages. Note that we
have also combined the estimated proportions for the gametocyte samples into one g
ametocyte variable. The columns are coloured by phenotype.
#First get the intersection of the genes for the two datasets and order them by ro
wname.
inter <- intersect(rownames(rpkm_genes_log), rownames(su_log_rpkm))

O <- rpkm_genes_log[rownames(rpkm_genes_log) %in% inter, ]
O <- O[order(rownames(O)),]
S <- su_log_rpkm[rownames(su_log_rpkm) %in% inter, ]
S <- S[order(rownames(S)), ]

#Now lets fit some samples!
ourPlotData <- data.frame()
for (i in 1:ncol(O)){
  mix <- findMix(O[,i], as.matrix(S))
  ourPlotData <- rbind(ourPlotData, data.frame(sample=rep(colnames(O)[i], ncol(
S)), stage=colnames(S), proportion=mix))
}
```

```
#Organise the results.
ourPlotData$stage <- gsub("Gametocyte.*", "Gametocyte", ourPlotData$stage)
ourPlotData <- aggregate(proportion~sample+stage, data=ourPlotData, FUN=sum)
ourPlotData <- within(ourPlotData, stage <- factor(stage, levels=c("Ring", "Early.
Trophozoite", "Late.Trophozoite", "Schizont", "Gametocyte")))
ourPlotData$phenotype <- ifelse(substring(ourPlotData$sample, 1, 2)=="B-", "B-type", "
C-type")

#Make a pretty plot.
gg <- ggplot(ourPlotData, aes(x=factor(sample), y=proportion, fill=factor(phenotyp
e))) + geom_bar(stat="identity")
gg <- gg + scale_fill_manual(values = c("B-type"= "#2c7bb6", "C-type"="#d7191c"))
gg <- gg + facet_wrap(~ stage, ncol = 1)
gg <- gg + theme_bw()
gg <- gg + theme(axis.text.x = element_text(size=2, angle = 90)
, axis.text.y = element_text(size=7, angle = 0)
, axis.title=element_text(size=10, face="bold")
, strip.text.x = element_text(size = 10, face="bold"))
gg <- gg + labs(x='Sample', y='Proportion', fill='Stage')
gg <- gg + theme(legend.text=element_text(size=10))
gg <- gg + theme(legend.key.size = unit(0.25, "in"))
gg <- gg + theme(legend.title = element_text(size=10, face="bold"))
gg <- gg + guides(fill=guide_legend(title="Phenotype"))
print(gg)
```



##Investigate Differential Expression We now perform the Voom transformation on our count matrix. Prior to the transformation we use TMM normalisation to account for the different library sizes present in our sample. TMM was chosen as it is more robust to outliers.

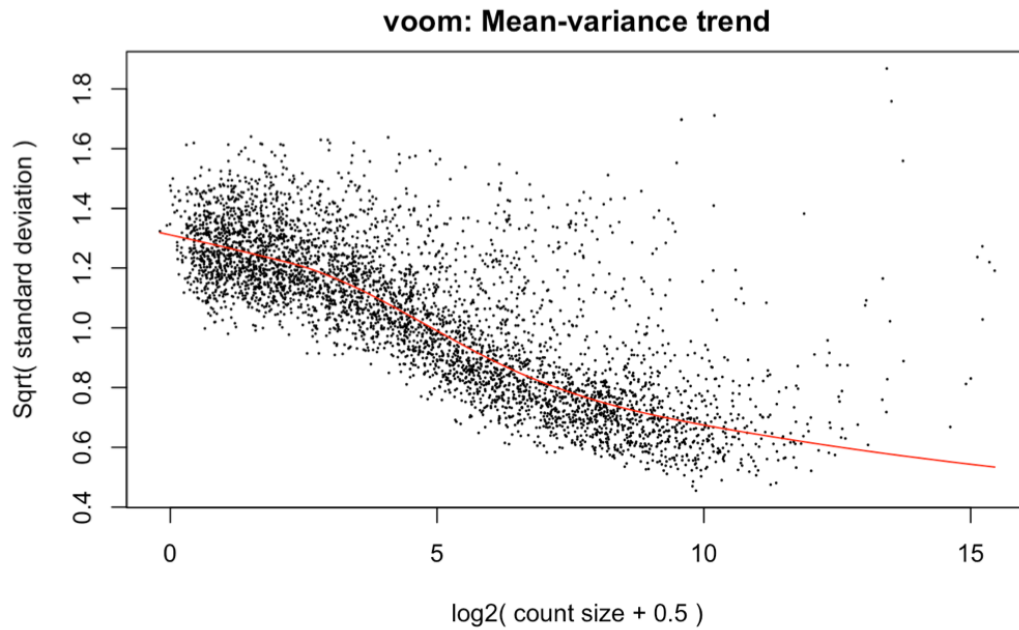
From the Voom variance trend it is evident that there are a number of genes that have both high variability and high expression. After looking at some of the main offenders these were identified to be influenced by staging in the parasite. Consequently it is important to account for life-cycle stage when conducting the differential expression analysis.

Hide

Supplementary data

```
categories<- as.factor(substring(rownames(dge$samples),1,2))
DGE_norm <- calcNormFactors(gene_counts_list2, method="TMM")
DGE_norm$samples$group <- categories
design <- model.matrix(~group, data=DGE_norm$samples)

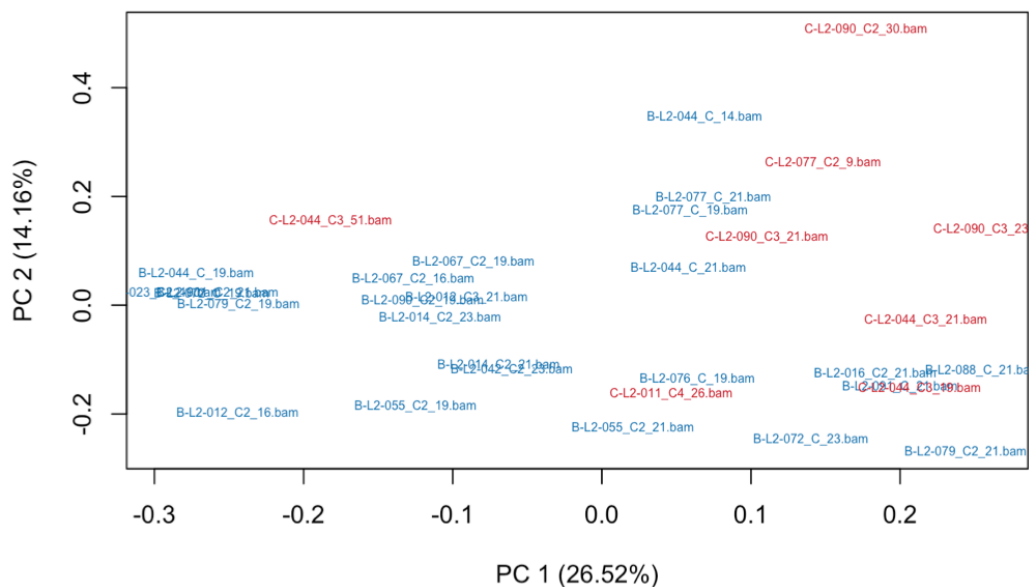
voom_object <- voom(DGE_norm, design=design, plot=TRUE)
```



###The PCA plot below indicates that accounting for library size alone does not cope with the impact of life-cycle stages.

Hide

```
plotPCA(voom_object$E, col=colors[categories], cex=0.5, isLog=TRUE)
```



Hide

```
plotVoomRLE <- function(E, colours){
  mn <- apply(E, 1, median)
  rle <- data.frame(sweep(E, MARGIN=1, STATS=mn, FUN='-'))
  boxplot(rle,col=colours, outline=FALSE, las=2, ylim=c(-7,7))
  abline(h = 0, col = "black")
}
plotVoomRLE(voom_object$E, colors[categories])
```

###PCA Normalising for Library Size and Ring Stage Effects

We then investigate the impact of only accounting for the Ring stage parameter in the model. This gives us more power with which to identify differential expression related to severe disease.

Hide

```
covs <- data.frame(voom_object$design[,2])
ourPlotData$phenotype <- NULL
c <- dcast(ourPlotData, sample ~ ..., value.var = "proportion")
covs <- merge(covs, c, by.x=0, by.y="sample")

colnames(covs) <- c("sample", "disease", colnames(c)[2:ncol(c)])
rownames(covs) <- covs$sample
covs$sample <- NULL
covs <- covs[match(colnames(voom_object$E), rownames(covs)),]
stopifnot(colnames(voom_object$E)==rownames(covs))

#head(covs)
covs <- covs[,c(1,2,5,6)]

mod = model.matrix(
  as.formula(paste("~", paste(colnames(covs), collapse=" + "), sep="")), data=cov
s)

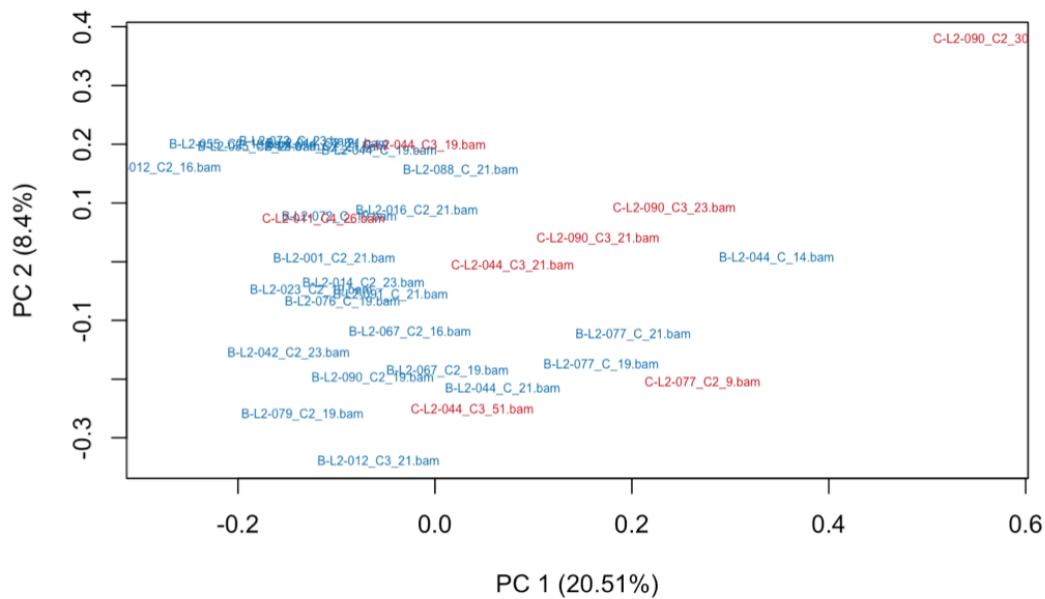
norm_counts_ring <- removeBatchEffect(voom_object$E, covariates=mod[,3:ncol(mod)],
design=mod[,1:2])
plotPCA(norm_counts_ring, col=colors[categories], cex=0.5, isLog=TRUE)
plotVoomRLE(norm_counts_ring, col=colors[categories])
```

Hide

```
covs <-covs[,c(1,2)]
mod = model.matrix(
  as.formula(paste("~", paste(colnames(covs), collapse=" + "), sep="")), data=cov
s)

norm_counts_ring <- removeBatchEffect(voom_object$E, covariates=mod[,3:ncol(mod)],
design=mod[,1:2])
plotPCA(norm_counts_ring, col=colors[categories], cex=0.5, isLog=TRUE)
```

Supplementary data



We are however able to identify differentially expressed genes in this less parameterised model. The summary of results accounting only for the Ring stage variable are given below.

Hide

```
stopifnot(colnames(DGE_norm)==rownames(mod))
v2 <- voom(DGE_norm, design=mod, plot=FALSE)
fit <- lmFit(v2, mod)
fit <- eBayes(fit, robust=TRUE)

summary(de1<-decideTests(fit, adjust.method="BH", p.value=0.05))
```

	(Intercept)	disease	Ring
Down	34	16	1260
NotSig	803	4371	2224
Up	3610	60	963

#this gave vvv genes up regulated and vvv down (different numbers to without) will print table out for interests sake

Hide

```
top_DEG_ring_norm <- topTable(fit, coef = 2, p.value = 0.05, sort.by = "p", number
= Inf, adjust.method = "BH", confint = TRUE)
write.table(top_DEG_ring_norm, file = "~/Desktop/B-vs-C-diff.txt", sep = "\t")
```

For our data just correcting for rings seems to reduce variation enough based on RLE and PCA however Gary thought the RUV based correction was better as it will also remove unwanted variation not identified. This requires a control set of genes. For initial run I will use the one Gary used but not 100% sure if this is appropriate for my data. #correction using RUV.4

Supplementary data

Hide

```
ctrl_genes_vignali <- read.table("~/Desktop/B-vs-C/ctrl_genes_vignali.txt", qu
ote="\")

geneID_mappings <- fread("~/Desktop/B-vs-C/geneID_mappings.txt", data.table = FALS
E, stringsAsFactors = FALSE, header = TRUE)

trim <- function (x) gsub("^\\ss+|\\ss+$", "", x)
ss <- str_split(as.character(geneID_mappings$`Previous ID(s)`), ',')
geneID_mappings <- data.frame(current=rep(geneID_mappings$`Gene ID`, sapply(ss,
FUN=length)), old=unlist(ss))
geneID_mappings$old <- str_trim(geneID_mappings$old)

ctrl_vignali <- geneID_mappings$current[geneID_mappings$old %in% ctrl_genes_vign
ali$V1]
length(ctrl_vignali)
```

```
[1] 1009
```

Hide

```
empirical_controls <- ctrl_vignali[0:length(ctrl_vignali)]
empirical_controls <- rownames(voom_object$E) %in% empirical_controls

categoriesRUV <- categories
categoriesRUV <- data.matrix(as.numeric(categoriesRUV))
#this is slightly different from how Gerry had it but based on tutorial https://gi
thub.com/johanngb/ruv-useR2018/tree/master/session2/Differential_Expression_with_R
UV4 i think it provides the correct info 1: RSA71, 2 C580Y parental
ring <- data.matrix(mod[,c(1,3)])
genes <- data.matrix(t(voom_object$E))

ruv <- RUV4(genes, categoriesRUV, empirical_controls, 2, Z=ring)

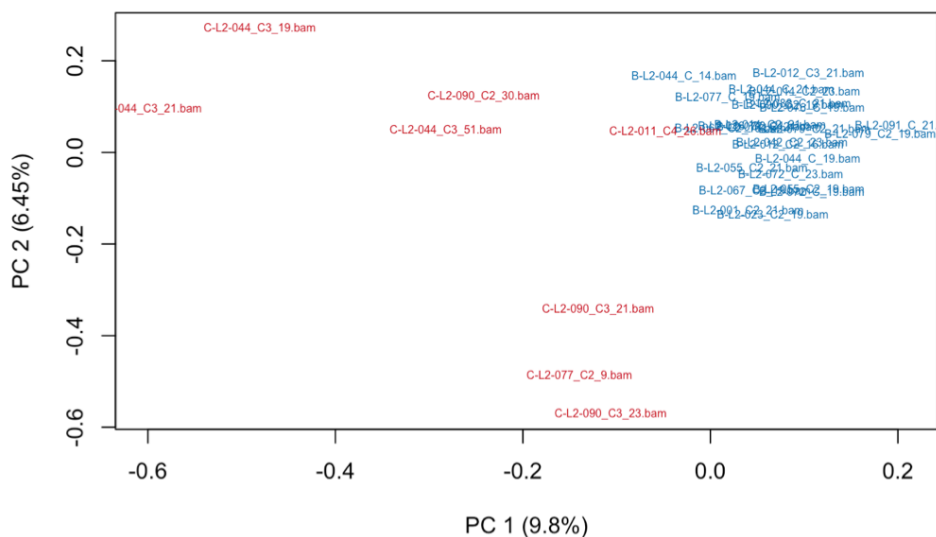
modRUV = cbind(mod, ruv$W)

norm_counts_ring_ruv <- removeBatchEffect(voom_object$E, covariates=modRUV[,3:ncol
(modRUV)], design=modRUV[,1:2])
```

The PCA plot below looks nice

Hide

```
plotPCA(norm_counts_ring_ruv, col=colors[categories], cex=0.5, isLog=TRUE)
```



Hide

```
plotVoomRLE(norm_counts_ring_ruv, colors[categories])
```

###Identify DE Genes using Limma and Voom We now use the limma-voom pipeline, with the robust eBayes option which handles dispersion outliers. This was done to further ensure our results were less likely to be affected by outlier samples. Multiple testing correction was performed using the Benjamini-Hochberg approach.

Hide

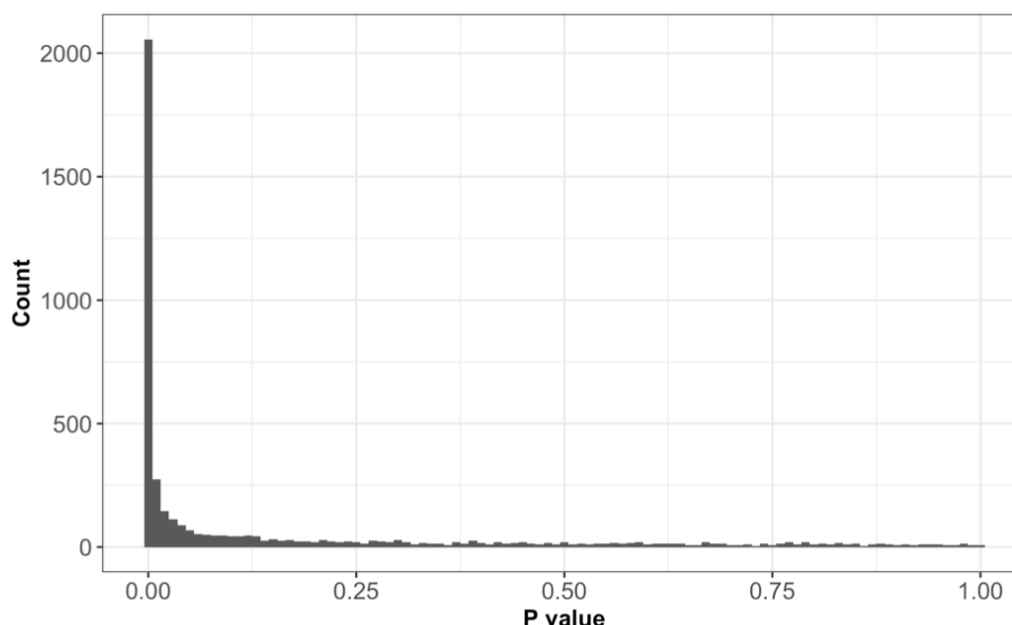
```
stopifnot(colnames(DGE_norm)==rownames(modRUV))
voom_rings_ruv <- voom(DGE_norm, design=modRUV, plot=F)
fit <- lmFit(voom_rings_ruv, modRUV)
fit <- eBayes(fit, robust=TRUE)
sum_DGE_ruv_rings <- summary(de_ruv_rings<-decideTests(fit, adjust.method="BH", p.
value=0.05))
sum_DGE_ruv_rings
```

	(Intercept)	disease	Ring		
Down	33	12	1430	809	432
NotSig	684	4396	1938	2958	3312
Up	3730	39	1079	680	703

A good check for validity of our model it to look at the distribution of the resulting p-values. If everything is okay we would expect a uniform distribution except near $p = 0$ where we would hope to see a spike. The barplot below indicates this is what we see which is helpful in affirming that we have done okay in removing unwanted variation without negatively impacting on the variation due to the variable of interest (disease severity).

Hide

```
top_ring_ruv <- topTable(fit, coef=2, p.value=0.05, sort.by="p", number=Inf, adjust.
method="BH", confint=TRUE)
hist<- data.frame(topTable(fit, coef=3, number=Inf))
gg <- ggplot(hist, aes(x=P.Value)) + geom_histogram(binwidth = 0.01)
gg <- gg + theme_bw()
gg <- gg + theme(axis.text.x = element_text(size=12)
, axis.text.y = element_text(size=12, angle = 0)
, axis.title=element_text(size=12,face="bold"))
gg <- gg + labs(x='P value', y='Count')
gg
```



Supplementary data

###Results table Below is a table of genes that were found to be differentially expressed, ordered by their respective p-values. The 95% confidence intervals are given with the estimated LFC as well as the BH adjusted p-values and the log-odds that the gene is differentially expressed.

Hide

```
#Load additional gene information
GeneAnnotationPlasmoDB <- fread("~/Desktop/B-vs-C/GeneAnnotationPlasmoDB.txt", header= TRUE, data.table = FALSE, na.strings = "N/A")

#First lets import some additional gene information to make a nicer table
GeneAnnotationPlasmoDB <- GeneAnnotationPlasmoDB[, colnames(GeneAnnotationPlasmoDB) %in% c("[Gene ID]", "[Product Description]", "[Gene Name or Symbol]")]
top_ring_ruv <- merge(top_ring_ruv, GeneAnnotationPlasmoDB, by.x=0, by.y="[Gene ID]", all.x=TRUE)
top_ring_ruv <- top_ring_ruv[with(top_ring_ruv, order(adj.P.Val)), ]

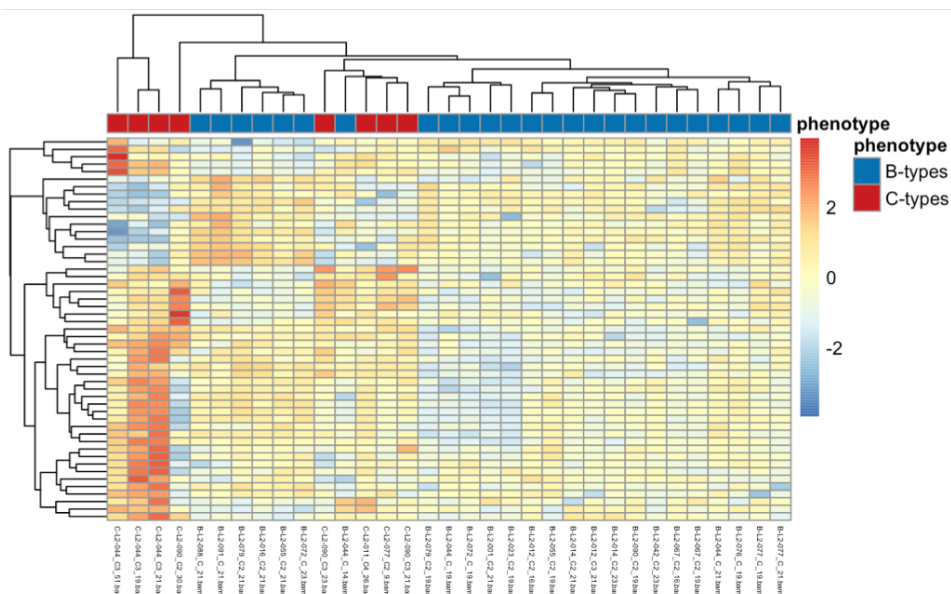
top_ring_ruv$P.Value <- format(top_ring_ruv$P.Value, scientific=TRUE, digits=3)
top_ring_ruv$adj.P.Val <- format(top_ring_ruv$adj.P.Val, scientific=TRUE, digits=3)
kable(top_ring_ruv[,c(2:4,6:ncol(top_ring_ruv))], digits=3)

#Now print the table
write.table(top_ring_ruv, file = "~/Desktop/B-vs-C/B-vs-C_ruv_corrected.txt", sep=
"\t")
```

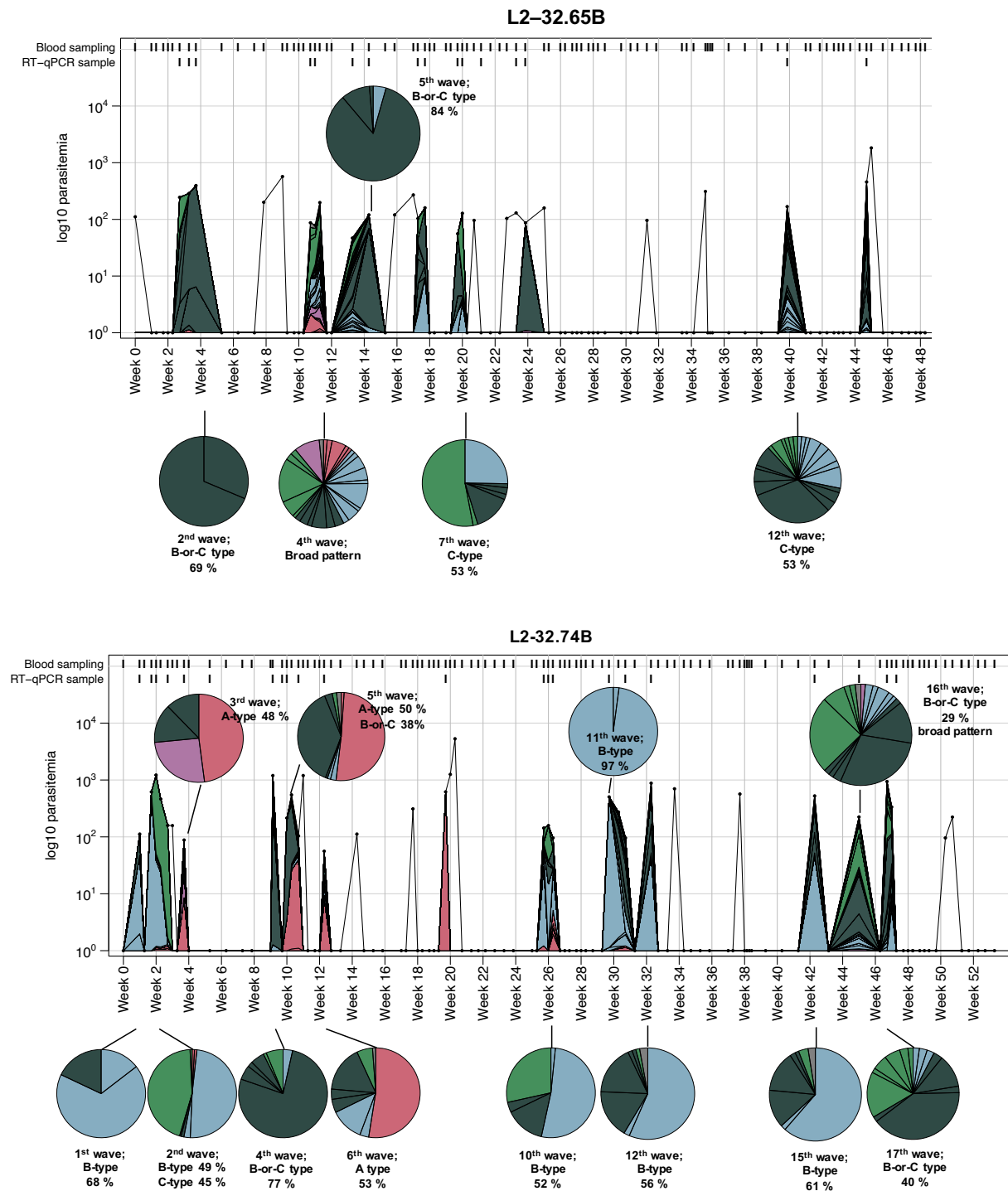
Hide

```
##Heatmap of deregulated genes
col_annot <- data.frame(row.names=colnames(voom_object$E), stringsAsFactors = F)
col_annot$phenotype[substring(colnames(voom_object$E),1,2)=="B-"] <- "B-types"
col_annot$phenotype[substring(colnames(voom_object$E),1,2)=="C-"] <- "C-types"
col_annot$phenotype <- as.factor(col_annot$phenotype)

pheatmap(voom_rings_ruv$E[rownames(voom_object$E) %in% top_ring_ruv$GeneID,],
, show_rownames = FALSE
, fontsize_col = 4
, scale = "row"
, annotation_col = col_annot
, annotation_colors = list(phenotype=c(`B-types`=colors[1], `C-types`=colors[2])))
```



Supplementary Figure 8.: R-scripted pipeline for the analysis of *in vivo* *P.falciparum* transcriptomic data (Tonkin-Hill et al. 2018).



Supplementary Figure 9.: Longitudinal var gene expression pattern of parasites isolated from volunteer infections with locally circulating parasite strains.

In addition to Figure 15, two representative examples of two longitudinally tracked volunteers across a study time frame of 48-52 weeks, showing restricted var gene pattern at the parasitemia peaks similar to infections tracked within the 'CHMI-study'. B-or-C-type var gene sequences were not definitely annotated into the B-type or the C-type group. B- or C-type var gene sequences could not be allocated to a particular var gene group, but are of type B or C due to their DBL α 0-encoding sequence. For these sequences, the Varia tool predicted a DBL α 0 domain, however the ups-based prediction approach was unable to certainly annotate a var gene group for these sequences. Similar to infections from volunteers in the CHMI-study, A-type var genes are occasionally expressed). Sample intervals are indicated above of the respective volunteer plot and if no samples were collected the time points were left blank. A-type var genes (red), B/A-type var genes with DBL α 2 sequence contained within DC8 (purple), B-type var genes (blue), B- or C-type var genes (petrol), C-type var genes (green) and inconclusive predictions (grey).